UNIVERSIDAD COMPLUTENSE DE MADRID

FACULTAD DE CIENCIAS FÍSICAS
Departamento de Física de la Tierra, Astronomía y Astrofísica II

STATISTICAL DOWNSCALING OF SURFACE WIND FIELD AND WIND ENERGY OVER A COMPLEX TERRAIN AREA.

MEMORIA PARA OPTAR AL GRADO DE DOCTOR

PRESENTADA POR

Elena García Bustamante

Bajo la dirección de los doctores

J. Fidel González Rouco
Jorge Navarro Montesinos

Madrid, 2011

ISBN: 978-84-694-2808-5

Statistical downscaling of surface wind field and wind energy over a complex terrain area

ELENA GARCÍA BUSTAMANTE

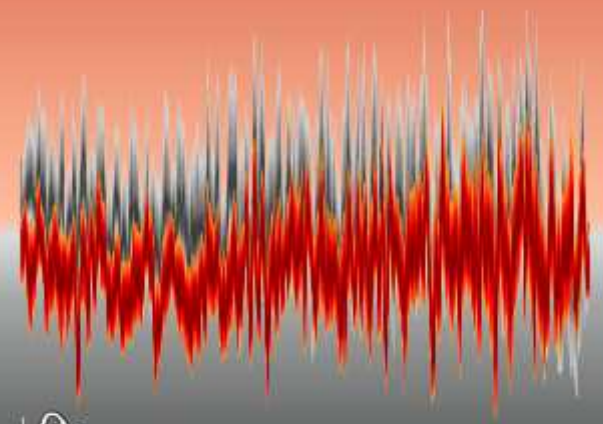

Statistical downscaling of surface wind field and wind energy over a complex terrain area

Estimación estadística del viento en superficie y de la energía eólica en una región de terreno complejo

Memoria que presenta

Elena García Bustamante

para optar al grado de

Doctor en Ciencias Físicas

Directores:

Dr. J. Fidel González Rouco
Dr. Jorge Navarro Montesinos

Departamento de Física de la Tierra, Astronomía y Astrofísica II
Facultad de Ciencias Físicas
Universidad Complutense de Madrid

II

Convienen los físicos en que el viento es un movimiento sensible del aire; y no es dudable, pues el simple movimiento que puede darle un abanico hace un viento bien perceptible. Puede este movimiento venir de qualquiera parte, así pueden ser tantas las diferencias de los vientos, si se examinan físicamente, quanto son los puntos sensibles del Horizonte. [...] Sospecho que así como la luz excita al fuego, conmueve también al aire, y que muchos efectos admirables que tenemos delante de los ojos, y ignoramos sus causas, nacen de las operaciones recíprocas de los elementos. Con esto se explica la formación de los vientos continuos, y periódicos que se observan en varios lugares. [...] Pueden los vapores excitar el viento empujando el aire y obligandole à ceder à su fuerza, y esta es la causa más común de los vientos. Finalmente el fuego puede causar los vientos, dilatando el aire, y aflojando sus muelles. [...] El Sol excita al fuego, levanta los vapores, y hace vibrar la luz; así pone en acción todas las causas próximas de los vientos, y sus mudanzas. [...] Hemos explicado las causa generales de los vientos, pero haciendo variar de muchos modos sus operaciones, la situación de los montes, valles, mares y otras muchas cosas propias del clima, es preciso explicarlas acomodándonos a estas particularidades. [...] Si estas causas se combinan de muchas maneras, pueden hacer mucha variedad en los vientos, que solamente podrán atinarse con la observación cuidadosa de los lugares y los tiempos.

Dr. A. Piquer. Física Moderna, Racional y Experimental, 1745.

Contents

Agradecimientos

Sentirse agradecido, dar las gracias, no es un mero formalismo. Agradecer significa sentirse afortunado de haber tenido la oportunidad de recibir algo bueno. También significa reconocerse limitado y, sin embargo, disfrutar de saber que donde uno no llega, llegan los demás. Es así como, de la mano de los que alguna o muchas veces nos la tendieron, se llega a donde uno piensa que merecía la pena llegar. El camino que he recorrido a lo largo de estos años de tesis ha sido una experiencia valiosa y esta es una ocasión bonita para expresarlo. Hay muchas personas a las que me gustara decir gracias por haber andado conmigo algún trecho de ese camino o buena parte de él. De todas ellas no quisiera dejar de mencionar a las siguientes:

A Elena, mi madre, quiero agradecerle su bondad infinita y fruto de ella, su comprensión sin límites. Además, su paciencia, su generosidad y desprendimiento, su discreción, su sencillez, su fuerza... podría seguir... me impresionan profundamente y son un referente para mi. Gracias por compartir conmigo todos esos viajes.

A Pedro, mi padre, quisiera darle gracias por su apoyo incondicional. Iguales pero distintos, hemos encontrado un espacio en el que aprender el uno del otro. Su vastísima cultura, sus ansias de saber y su curiosidad vital inclinan la balanza de su lado, sin duda quien más ha aprendido del otro he sido yo. A él y a su perenne mensaje *"persevera en aquello que tú creas que es bueno conseguir.. y disfrútalo.."*. Gracias por hacerme saber que siempre estabas ahí detrás, en la retaguardia, por si acaso...

A Bea, mi hermana, que me quiere tanto y me lo dice siempre, a su frescura y su naturalidad que no las he visto antes, a sus consejos de hermana mayor,

suya es la primera mano que recuerdo, a sus risas, a su instinto protector y a la sensación de seguridad que transmite, porque al lado de Bea todo parece ir bien.

A Fidel, mi maestro y mi amigo. Para agradecerle todo lo que me ha enseñado tendría que escribir otro libro con tantas páginas como este. Su generosidad hacia todos, sin distinciones, su humildad sin precedentes y su pasión por aprender debieran ser quizá objeto de algún estudio científico. Fidel es el artífice de este trabajo, el que hacía las cosas posibles cuando parecía que no lo eran. Con Fidel he aprendido infinitas cosas de valor incalculable, pero quiero resaltar el haber aprendido de él lo provechoso de un uso delicado del lenguage: para atreverse siempre a decir lo que uno piensa, para dar razones y argumentos, para dar forma a las ideas, para preguntar cuando surgen las dudas, usar el lenguaje para dar opciones, para acoger y respetar otras opiniones... no hablo sólo de ciencia. He disfrutado mucho de su amistad, a través de la cual he descubierto la increíble cantidad de dimensiones distintas que puede llegar a tener una persona, así es como conocí también al *dios de la semisatisfacción* y los intentos de conjurarlo... Gracias Fidel por no ponerle nunca precio a tu tiempo.

A Jorge, que me ha apoyado sin condiciones desde aquel primer día. Él me ha transmitido siempre su confianza en mi, no sólo con palabras, también cuidando cada detalle hasta el final, haciendo posible la continuidad del trabajo, asegurando la estabilidad más de mil veces. Sin Jorge nada de esto habría sido posible. Además él es la alegría en persona, sabe gestionar cada situación desde la creencia de que todo tiene solución, que las cosas pueden salir bien. ¡Qué suerte haberle encontrado! Gracias Jorge.

A Marisa, a la que admiro profundamente desde que la conocí. Marisa es una mujer irrepetible, una luchadora incansable, es justa como pocos, de esas personas que inspiran, cuando uno ve a Marisa hacer ciencia quiere imitarla. Ella piensa en todos y se preocupa por todos y a mi en concreto me ha ayudado en incontables ocasiones. No sé cómo habría sido esto sin Marisa.

A Pedro, mi compañero, al que aún no me he acostumbrado a no tener cerca. Comenzamos esta andanza como compañeros de fatigas y se convirtió también en un maestro para mi. Todo lo que fue aprendiendo me lo transmitió como hermano mayor. Pedro es un científico de lo clásicos, para él llegar a entender las cosas más sencillas supone un triunfo y una fiesta, siempre interpreté eso como un rasgo de su inteligencia. Todavía puedo verle observando fijamente la pantalla de su ordenador. Gracias por enseñarme a no tener prisa.

A Angela, el experimento: amiga desde hace años y ahora compañera en el trabajo. Nada de lo que diga aquí es suficiente para agradecerle su paciencia. Angela me aporta cosas siempre, todos los días, es creativa, es crítica, tiene ideas, organiza.. Y sobre todo, me cuida, cuida de mi constantemente. Angela

es mi familia. ¿Cómo puedo agradecerte todo eso amiga? Desde luego no parece posible con palabras, pero aún así quisiera decirlo, gracias por estar a mi lado.

A Juanpe, a su don para intercalar ciencia y alegría, que me enseñó a pacientemente a hacer integraciones con MM5, a mi y a tantos, que siempre está al otro lado del teléfono, no importa qué hora sea, con una opinión. Juanpe ha participado con constancia en todos y cada uno de los trabajos, en las tesis, en Global, en las publicaciones.. no recuerdo un sólo correo no contestado, siempre crítico, no es fácil sesgar a Juanpe. ¿Cuantas cervezas habremos compartido? ¿Cuantas ideas salieron de ellas? Todo un lujo y un placer ser de tu equipo.

A mis amigos del laboratorio: a Pablete y su sentido del humor refinado, siempre un juego de palabras a la orden del día ; a Laura, que cuando entra por la puerta es como si amaneciera; a Etor, auténtico y original, no hay nadie como Etor, gracias por tus quijotes "ilustrados"; a Rubén, siempre dipuesto a unas risas, cuanta sensatez se le adivina aún sin necesidad de hablar ¡lo que da San Martín de Valdeiglesias!; a Roland, que solía saberlo todo sobre linux y siempre quería saber más y que nos contaba con ilusión sus viajes; a Germán, tan sincero, que siempre me regaña cuando le doy las gracias, ¡gracias Germán!; a Jose, tan discreto y tan cariñoso; a Volker, sus libros y sus discos, gracias por compartirlos conmigo. A todos vosotros que habéis hecho posible un ambiente de trabajo único y que día tras día y, muchas veces, noche tras noche, os he visto sacar lo mejorcito de vosotros mismos, de todo corazón, gracias.

A Elena, a su efervescencia y a su espíritu infatigable. Elena no dudó en acogerme en su casa y en tratarme desde el primer día como a una amiga, como a una hermana y como a una hija, triple dimensión de cariño, casi inverosímil. No sólo me ha cuidado en lo personal, también ha cuidado de nuestro trabajo hasta la última palabra, participando en las discusiones, aportando ideas, leyéndonos, corrigiéndonos, planteando estrategias. Gracias Elena por todo esto y por las inolvidables noches de primavera suizas de vino y jazz. Y gracias a Juerg, *her beloved husband*, una persona cálida, acogedora al más puro estilo Xoplaki-Luterbacher, delicado en el trato con todos, sobre todo con sus estudiantes, alguien que se interesa por tus cosas al minuto de conocerte, de conversación fácil y agradable... vaya dos...

A Nacho, mi amigo, mi compañero de toda la vida, hemos visto pasar por nuestro lado toda clase de tormentas y tempestades y no hemos tenido miedo de explorar a donde nos llevaban todos esos vientos, los dos hemos crecido de la mano. Nacho lleva años preocupándose con ternura de las horas que duermo y de si bebo o no agua. Pero lo mejor de todo es cuanto me hace reir. Gracias por tu música, gracias por la bicicleta y gracias por ponerme en la catapulta, por conducirme a descubrir que uno puede ser y hacer cosas, muchas cosas...

A mis amigos, a la suerte de haberlos encontrado: Raquel, la eficiencia, que me enseña a buscar una actitud coherente y a cuestionar cosas viejas; a Miguel Ángel, el cuñao, a su vitalidad y su cultura de dimensiones desconocidas por el ser humano, a las cuerdas de su guitarra; a Laura, la pequeña, a su intuición que siempre acierta, a su ser sin prisas (¡qué bien haber llegado juntas a esto!); a Angela, a quien ya he nombrado y que merece ocupar también este puesto, a las risas juntas, esas noches de risas casi por los suelos, los viajes; a Estrella, la más antigua, con quien descubrí esta ciudad, que me dejaba sentarme a su ordenador cuando quería ordenar las ideas y me desvelaba las ventajas de pensar las cosas dos veces, en silencio o no, siempre a mi lado; a Marine y su espíritu positivo, ¡una valiente! Quisiera estar cerca de ellos siempre.

A M. Isabel, que me enseñó lo que significa la honradez en el trabajo entre tantas otras cosas y que me hizo disfrutar de las matemáticas, misteriosa habilidad la que ella tiene para mostrar el lado luminoso de las cosas, que me acercó a la física sin darse cuenta.

A Eugenia, Lucía y Antonio, por su disponibilidad todos los días, por su descomunal eficacia. A Paul, Nico, Miguel, Fernando y Jorge, por vuestra ayuda y los buenos ratos. A Paco, Alfonso, Ana, Carolina, Carmen, Pedro, David, Mariano, el Pive, Isabel y, en general, a todos los chicos de la facultad, me habéis hecho sentir como en casa.

List of acronyms

APC	Average Power Curve
β	Brier skill score
c	Weibull scale parameter
CCA	Canonical Correlation Analysis
CCA_{pow}	CCA with the wind power as predictand
$CCA_{pow-mod}$	wind module CCA and wind-wind power linear transfer
CCA_{pow-uv}	wind components CCA and wind-wind power linear transfer
$CCA_{pow-reg}$	wind module CCA and regional wind-wind power linear transfer
CFN	Comunidad Foral de Navarra
CIEMAT	Centro de Investigaciones Energéticas, Medioambientales y Tecnológicas
C_p	Power coefficient
D	data or observations
EA	East Atlantic pattern
EA/WR	East Atlantic/Western Russian pattern
ECMWF	European Center for Medium-range Weather Forecast
ENSO	EL Niño Southern Oscillation
EOF	Empirical Orthogonal Function
EPC	Effective Power Curve
ϕ_{850}	850 hPa geopotential height
ϕ_{850}	500 hPa geopotential height
$f(w_i)$	wind speed frequencies for the i class interval

GCM	General Circulation Model
F	Fisher distribution
HadSLP2	Hadley Centre SLP observations version 2
H_i	a prior hypothesis
IP	Iberian Peninsula
k	Weibull shape parameter
κ	Number of EOFs/CCAs retained in the statistical downscaling model (Ch. 7)
μ	Large scale domain size in the statistical downscaling model (Ch. 7)
MOS	Model Output Statistic
NAO	North Atlantic Oscillation
NCAR	National Center for Atmospheric Research
n_{eff}	Effective sampled size after corrections based on serial autocorrelation
P	actual power produced by a wind turbine
P_a	available power carried by the wind
PDF	Probability Density Function
$p(H_i)$	prior probability of the hypothesis
$p(D\|H_i)$	probability of obtaining data D, supposed H_i is true (likelihood)
$p(H_i\|D)$	marginal posterior probability of H_i
P_{Linear}	monthly linearly fitted power output
P_{Interp}	monthly interpolated power output
$p_{out}(w_i)$	transfer function for the power *vs.* wind speed relation for a given w_i
P_w	wind power generated by an ideal wind turbine
P(μ)	prior probability distribution of the large scale domain size
P(σ)	prior probability distribution of the predictor field(s) (Ch. 7)
P(κ)	prior probability distribution of the number of EOFs/CCAs patterns retained
P(θ)	prior probability distribution of the number of crossvalidation subset size
$p(\mu, \sigma, \rho, \theta\|D)$	joint marginal posterior distribution of the parameters μ, σ, ρ and θ
PFC	Polynomial Fit Curve
$r(\mu, \sigma, \rho, \theta)$	residual (obs. minus est.) for the combination of parameters μ, σ, ρ and θ
$\|\|r\|\|^2$	sum of square residuals for all time steps

$\|\|r_{min}\|\|^2$	minimum sum of square residuals
ρ	correlation skill score
RCM	Regional Circulation Model
R^2	statistic for the evaluation of the parameters rejection areas
R_{era40}	wind field reconstructions based on ERA-40 SLP
$R_{power-era40}$	wind energy reconstructions based on ERA-40 SLP
R_{had}	wind field reconstructions based on HadSLP2 observations
$R_{power-had2}$	Wind energy reconstructions based on HadSLP2 observations
R_{Luterb}	wind field reconstructions based on Luterb. *et al.* (2002) SLP recon.
R_{ncar}	wind field reconstructions based on NCAR SLP observations
$R_{power-ncar}$	wind energy reconstructions based on NCAR SLP observations
σ	predictor field(s) in the statistical downscaling (Ch. 7) model
SCAND	Scandinavian pattern
SLP	Sea level pressure
S_{w_m}	monthly mean wind speed standard deviation
S_{wE_m}	monthly mean wind energy standard deviation
TPC	Theoretical Power Curve
θ	crossvalidation sample size in the statistical (Ch. 7) downscaling model
U10	zonal component of the wind at 10 m
UCM	Universidad Complutense de Madrid
V10	meridional component of the wind at 10 m
w	wind speed
w_i	wind speed representative for the i class interval
$\overline{w}$	monthly mean wind speed
wE	wind energy
wE_{Linear}	total monthly wind energy from the monthly linear fit
wE_{Interp}	total monthly wind energy from the monthly interpolation

wE_{H-EPC_w}	total monthly wind energy from hourly wind speed using the EPC and the Weibull expected frequencies
wE_{H-APC}	total monthly wind energy from hourly wind speed using the APC
wE_{H-APC_w}	as the previous but with Weibull expected frequencies
wE_{H-PFC}	total monthly wind energy estimated from hourly wind speed using the PFC
wE_{H-ref}	total monthly wind energy estimated from hourly wind speed using the EPCs
wE_m	monthly mean wind energy
ξ_i	wind energy estimation error using the i method (Ch. 4)
$Z_{500-850}$	thickness between 500 and 850 hPa geopotential heights

Summary

The assessment of the wind field variability at the regional/local scale involves many challenging scientific questions concerning the multiple interactions between large and local scales that give rise to the large spatio-temporal variability of the wind field, especially over complex terrain regions. Additionally, the evaluation of the surface wind circulations entails interesting applications for society: insurance companies, air-quality or health oriented studies as well as wind energy production, that require accurate estimates from the short term predictions to the long term sustainability assessments. These are some examples that demand knowledge about the wind field circulation at the regional/local scales.

This work pursues two main objectives. One of them is the evaluation of the relation between wind and wind power. The second objective is the analysis of the coupled variability between the regional surface wind field and wind power production in the northeast of the Iberian Peninsula and the large scale circulation over the North Atlantic and Mediterranean areas. The results obtained in the first part of the work evidence a linear relationship between wind and wind power that supports the exploration of dependencies of both variables with the large scale circulation in the second part of the text.

Surface wind field observations for the period 1992-2005 are recorded at 29 meteorological stations homogeneously distributed around the target region (Comunidad Foral de Navarra; CFN). In addition, wind and wind power records are available at five wind farms within the region for the period 1999-2003. All observed series were subject to quality assurance processes to guarantee the quality of the observations that are the inputs in the different analyses.

The relation between wind and wind power is explored on the basis of the analysis of classical methodologies to estimate wind energy. The different contributions to the error in wind energy estimations are evaluated. Two main sources

of error are explored: the representation of the observed wind frequencies by a theoretical distribution and the contribution due to the assumed wind-wind power transfer function. It is shown that the typical Weibull assumption applied to estimate wind frequencies does not hold at every site or time step, however the resulting errors are not large due to a partial cancellation of residuals with different sign. The larger contribution to the errors arises from the use of transfer functions to translate wind into wind power values. Different alternatives were tested and a simpler linear relation between monthly wind-wind power values proves a good performance in estimating monthly wind energy compared to other more elaborated approaches. It also represents the basis to explore in the second part of the work the performance of a statistical downscaling technique applied to estimate wind power from changes in the large scale.

The connection between the variability of the wind field at the CFN and the large scale atmospheric circulation is investigated through the application of a statistical downscaling approach (Canonical Correlation Analysis). To a large extent, the variability of the wind at monthly timescales is found to be governed by the large scale circulation modulated by the particular orographic features of the area. The sensitivity of the downscaling methodology to the selection of the model parameter values is explored, in a second step, by performing a systematic sampling of the parameter space. This provides a metric for the uncertainty associated with the various possible model configurations. This uncertainty is considerably dependent on the spatial variability of the wind. While the sampling of the parameter space in the model set up moderately impacts estimations during the calibration period, the regional wind variability is very sensitive to the parameter selection at longer timescales. This fact illustrates that downscaling exercises based on a single configuration of parameters should be interpreted with extreme caution. The downscaling model is used to extend the estimations several centuries to the past using long datasets of sea level pressure, thereby illustrating the large temporal variability of the regional wind field from inter annual to multi centennial timescales.

Based on the linear relation between the wind and the wind power found in the first part of the text, the downscaling approach is extended to the case of the wind power as a non-meteorological variable. This can be ascribed to the context of impact oriented studies. It is shown that the variability of the wind power in the region is connected to variations of the large scale circulation over the North Atlantic areas. Alternative procedures that estimate first the wind over the region and then translate it into wind power estimates using the linearity between both variables, prove useful in practical situations where no wind power records are available. The uncertainty associated to the wind power estimations is identically explored herein as in the case of the wind field.

Finally, a probabilistic approach to evaluate the impact of each parameter of the model configuration on the wind field estimates is analysed. The treatment of uncertainties is based on the Bayesian theory and it consists in assigning weights to each parameter value depending on its ability to produce wind estimations in good agreement with observations. The ability of the method to identify the optimal model configurations or to detect parameters with a robust response to changes in the rest of the parameters is discussed.

This work provides therefore a description of a sequence of experiments posed from different, albeit connected, approaches targeting a better understanding of the variability of the wind and wind power over a region of complex terrain. In doing so, this text offers the reader not only improved knowledge on the nature of the wind power and wind variability changes in the region of interest but also how they relate to each other and how they are driven by large scale circulation changes. Also, and perhaps more importantly, this work provides an in depth and novel assessment of the uncertainties associated with the various methodologies used in this process. The results of this Thesis are therefore relevant both as a contribution to the knowledge of the variability of the wind field and related impact variables and, from a broader perspective, to the still scarcely explored uncertainty in the context of downscaling approaches. Readers with an interest in application studies may also find potential in the context of wind power resource exploration.

Resumen

El análisis de la variabilidad del campo de viento a escala regional es interesante, no sólo desde un punto de vista académico, si no también por su utilidad en múltiples aspectos relevantes para la sociedad. Como ejemplos de aplicación se pueden citar la predicción de rachas intensas de vientos asociados a tormentas o huracanes (Powell et al., 1991), estudios relacionados con la contaminación atmosférica (Jakobs et al., 1995), análisis de la influencia de la rugosidad del terreno en el viento en superficie (Grimenes and Thue-Hansen, 2004), el impacto de vientos extremos en el diseño de estructuras (Zhang et al., 2006) o la evaluación de la altura del oleaje (Caires and Sterl, 2004). Además, en el ámbito de la energía eólica, la cual ha experimentado un desarrollo notable en la últimas décadas, no son pocas las aplicaciones relevantes relacionadas con el análisis de la variabilidad del viento en distintas escalas temporales, desde la predicción a corto plazo de la producción de potencia eólica (Kariniotakis et al., 2004) hasta la evaluación, a más largo plazo, de la sostenibilidad del recurso eólico (Pryor et al., 2006). La aplicación de cualquier estrategia orientada a la estimación de energía eólica a partir del viento precisa del entendimiento de la relación existente entre ambos, la potencia producida y el viento que la genera. El análisis de errores derivados de las diversas hipótesis acerca de las funciones de transferencia entre ambas variables o sobre cómo representar el viento observado a través de una distribución teórica, no es trivial ya que puede originar desviaciones no despreciables en las estimaciones de energía eólica (Palutikof et al., 1987; Noorgard and Holttinen, 2004). La primera parte de este trabajo se centra en una evaluación de las particularidades de la relación viento-potencia así como de las desviaciones en la estimación de energía eólica a partir del viento.

El viento en superficie puede considerarse una respuesta a la circulación general de la atmósfera, que intenta compensar el exceso de radiación en el ecuador

transportándolo hacia los polos y, a su vez, está sujeta a los efectos de la rotación terrestre, que es responsable de los vientos promedio procedentes del oeste en latitudes medias y del este en latitudes bajas y altas (Lorentz, 1967; Holton, 2004). La heterogeneidad de la superficie terrestre es asimismo responsable en buena medida de la gran variabilidad espacio-temporal del campo de viento. De este modo, la interacción de la circulación atmosférica a gran escala con las particularidades de la orografía a escala regional y local, que genera forzamientos locales de caracter térmico, como la brisa marina o las circulaciones de valle (Wagner, 1938; Simpson, 1994; Bianco et al., 2006) o bien dinámico, tales como ascensos forzados, canalizaciones, etc. (Whiteman and Doran, 1993), confiere al campo de viento regional su gran variabilidad espacial y temporal característica.

Dada la compleja combinación de múltiples forzamientos, el análisis de las variaciones del viento en superficie a escala regional requiere el uso de estrategias específicamente diseñadas para integrar procesos que ocurren en distintas escalas espacio-temporales. El uso de observaciones *in situ* para el análisis de la variabilidad climática regional, está frecuentemente acotado por la calidad de las mismas y por la falta de disponibilidad de medidas, no solo en el tiempo (series cortas o periodos con ausencia de datos), sino también en el espacio, lo que conlleva ciertas limitaciones en la representacion de la realidad a través de los datos observados. Los modelos de circulación general (GCMs del inglés *General Circulation Models*) que han mostrado habilidad en reproducir aspectos generales de la variabilidad climática así como de la circulación atmosférica a gran escala (Stocker et al., 1992; Latif, 1998; McKendry et al., 2006), no pueden resolver de manera adecuada los procesos físicos característicos de escalas espaciales menores, dada su limitada resolución espacial (100-300 km). Por tanto, la alternativa al uso de GCMs es la aplicación de estrategias de aumento de resolución, también conocidas como técnicas de *downscaling* (von Storch, 1995; Wilby and Wigley, 1997). El concepto de downscaling o técnicas *crosescala* está ligado a la aparición, a comienzos de la década de los 60, de una serie de procedimientos diseñados para obtener clasificaciones de los distintos estados de la circulación atmosférica para luego establecer relaciones con observaciones locales de alguna variable climática, lo que sugiere una conexión entre downscaling y climatología sinóptica (Barry and Perry, 1973).

Las técnicas de downscaling se basan en hacer uso de la información disponible de la circulación atmosférica a gran escala para obtener estimaciones de una variable a escala regional o local. El procedimiento implica bien resolver explícitamente los procesos físicos mediante simulaciones numéricas con modelos regionales (downscaling dinámico) o bien identificar de manera empírica las asociaciones entre ambas escalas (downscaling estadístico). En ambos casos, es necesario aportar información acerca del estado de la circulación general de la atmósfera. Dicha información la pueden proporcionar observaciones en una malla regular (Zorita

et al., 1992; Zorita and von Storch, 1999), datos de reanálisis (Xoplaki et al., 2003a, 2004) o salidas de GCMs (Lenderink et al., 2007).

Los modelos regionales, también conocidos como modelos de área limitada (Black, 1994; Skamarock et al., 2005), fueron creados en su origen para proporcionar predicciones meteorológicas. Sus fundamentos físicos son análogos a aquellos por los que se rigen los GCMs con la diferencia de que los primeros generan estimaciones sobre una área concreta permitiendo así que las salidas alcancen una mayor resolución horizontal (entre 50 km y 10 km e incluso mayor). Con ello aumentan las posibilidades de capturar de manera más realista los procesos que son importantes para la variabilidad climática a escala regional. Sin embargo el coste computacional asociado no es desdeñable. Una alternativa menos costosa desde el punto de vista computacional, son las técnicas de downscaling estadístico. Con este tipo de metodologías se exploran las asociaciones entre los forzamientos procedentes de la gran escala que actúan como *predictores* y la respuesta regional a dicho forzamiento de la variable climática en cuestión o *predictando* (von Storch et al., 1993; Noguer, 1994; von Storch, 1995; González-Rouco et al., 2000; Xoplaki et al., 2004; Busuioc et al., 2008). Por lo tanto este tipo de metodología precisa de la existencia de datos históricos y, al igual que las técnicas de carácter dinámico, también proporcionan una interpretación de cuales son los mecanismos físicos responsables de la variabilidad a escala regional. Una cuestión clásica que atañe al uso de estrategias estadísticas es la no estacionariedad en las relaciones entre las distintas escalas espaciales. Una hipótesis que con frecuencia se asume al hacer uso de este tipo de métodos es que la relación entre la circulación a gran escala y la escala regional se mantiene en un clima futuro, perturbado por la emisión de gases de efecto invernadero (Benestad, 2002). Sin embargo, esta es una afirmación que no se puede garantizar. Una especulación razonable es que estados futuros del clima implicarán cambios en la intensidad, frecuencia de ocurrencia y persistencia de los patrones de circulación general (Hewitson and Crane, 1996). Esto supondrá un incremento de la incertidumbre asociada a las estimaciones regionales en escenarios de cambio climático, pero en principio no existen razones físicas de peso que sugieran que las relaciones empíricas entre escalas son más susceptibles de sufrir no-estacionariedades que, por ejemplo, las parametrizaciones que se usan en los modelos regionales para diagnosticar algunos procesos físicos.

La aplicación de técnicas de downscaling estadísticas es frecuente en el caso de variables como la precipitación (Zorita et al., 1992; González-Rouco et al., 2000) o la temperatura (Xoplaki et al., 2003a,b), sin embargo aplicaciones directas de este tipo de estrategias a la variabilidad del viento es escasa en la literatura. La segunda parte de este trabajo está dedicada a inspeccionar la habilidad de una de estas técnicas de caracter estadístico para estimar el campo de viento, así como su derivada, la producción de potencia eólica, en una región de terreno complejo,

la Comunidad Foral de Navarra, situada al noreste de la península ibérica (Fig. 2.1). Precisamente esta es una particularidad del estudio que contribuye a su caracter diferencial puesto que la variabilidad del campo de viento en regiones con orografía compleja es mayor y su estimación presenta a priori mayor dificultad.

El traspaso de información entre escalas espaciales está sujeto a distintos tipos de incertidumbre que se propaga desde la escala global hasta las escalas regionales/locales (Mitchell and Hulme, 1999; Schwierz et al., 2006). Estas incertidumbres en un contexto de cambio climático por ejemplo, podrían estar asociadadas a distintos tipos de forzamiento radiativo y se pueden estimar considerando diversos escenarios para obtener estimaciones de futuro (Nakicenovic et al., 2000; Denman et al., 2007) o bien usando una colección de GCMs que den cuenta de la variabilidad debida al uso de distintos modelos (Pryor et al., 2006; Najac et al., 2009). La selección de una estrategia específica para el ejercicio de downscaling implica cierto grado de subjetividad y por tanto representa una fuente adicional de incertidumbre. Igualmente, en el diseño de la configuración de un modelo participa un cierto número de juicios que comparten una componente de arbitrariedad (aunque también argumentos plausibles basados en la experiencia). Esto constituye el origen de incertidumbre adicional que se agrega a la cascada de incertidumbres asociadas a la estimaciones en escala regional. En el caso de los modelos regionales, por ejemplo, se puede explorar la sensibilidad de las estimaciones a cambios en la física (Zhang and Zheng, 2004) o en las condiciones iniciales (Weisse and Feser, 2003). Cuando se trata de métodos estadísticos, el cambio en los valores de ciertos parámetros que son importantes en la configuración del modelo, aún cuando no implique necesariamente un descenso de la habilidad en reproducir las observaciones, supone la aparición de incertidumbres que es interesante cuantificar. Así, es posible ilustrar la sensibilidad de las estimaciones a cambios en la configuración del modelo, lo que se conoce como *sensibilidad* o *incertidumbre metodológica*. Huth and Kyselý (2000) y Huth (2004) han contribuído en esta línea con trabajos que reflejan la sensibilidad de la temperatrua en centroeuropa a cambios en los campos predictores, aplicando metodologías de caracter estadístico. Dado que este tipo de ejercicio no es muy usual para el caso del campo de viento, parece apropiado elaborar aquí una estrategia de exploración de la incertidumbre metodológica.

Existe una alternativa a este tratamiento de la incertidumbre metodológica basado en inferencias de caracter probabilista que se fundamenta en la teoría bayesiana. Epstein (1962) fue el primero en discutir la aplicación de este tipo de técnicas probabilistas en el contexto de las predicciones meteorológicas. Desde entonces su uso se ha extendido en la estimación de incertidumbres asociadas a propiedades del sistema climático (Forest et al., 2000, 2002; Tebaldi et al., 2004a,b; Hegerl et al., 2006). El análisis de carácter bayesiano que se aplica aquí

a la incertidumbre asociada a las estimaciones del campo de viento regional persigue asociar a cada parámetro del modelo estadístico una distribución de probabilidad lo que permite identificar aquellos parámetros con los que se obtienen las estimaciones más realistas. Esto permite a su vez acotar la incertidumbre debida a distintas hipótesis en el espacio de los parámetros del modelo. Esta aproximación al estudio de la incertidumbre no es posible si se aplica una lógica frecuentista (Gelman et al., 2004). El análisis de tipo bayesiano que se plantea en este trabajo representa una extensión de la evaluación de la incertidumbre metodológica que no es muy frecuente en el caso de incertidumbres asociadas a la variabilidad regional del clima y no ha sido aplicado todavía en el contexto de downscaling estadístico del campo de viento. En general se puede decir que la evaluación de las distintas fuentes de incertidumbre a escala regional es un campo aún en desarrollo (Denman et al., 2007).

Un aspecto interesante de los métodos de downscaling estadístico es que permiten encontrar relaciones empíricas entre la circulación atmosférica y variables de impacto en ecosistemas naturales o de carácter humano, es decir, variables no atmosféricas cuya evolución depende en buen grado de la evolución del clima. Tal es el caso de la producción de energía eólica, cuya estimación a partir del viento implica aspectos interesantes desde el punto de vista físico e ingenieril, además de múltiples utilidades prácticas para la sociedad, relacionadas con la economía, ecología, etc. en un amplio espectro de escalas temporales, desde las predicciones meteorológicas horarias (Kariniotakis et al., 2004) hasta las proyecciones en escenarios de cambio climático (Palutikof et al., 1987; Pryor et al., 2005a).

Es en este contexto donde resulta relevante entender la relación entre el viento y la potencia eólica producida. Sin embargo, en la práctica, la falta de disponibilidad de observaciones, tanto de viento como de potencia, representa una limitación. Por ello, las estimaciones de potencia eólica se basan tradicionalmente en el uso de distribuciones teóricas de probabilidad a las que se ajustan las frecuencias observadas del viento. A partir de las propiedades de dichas distribuciones y de sus parámetros característicos se pueden obtener estimaciones de la densidad de energía que transporta el viento, como sustituto de la potencia eólica observada. La disponibilidad de datos medidos en los aerogeneradores (Weisser and Foxon, 2003; Akpinar and Akpinar, 2005a; Pryor and Schoof, 2005) permitiría enfocar el análisis de la variabilidad en la producción de la potencia eólica como respuesta a los forzamientos procedentes de la gran escala, desempeñando el papel de variable no meteorológica en estudios orientados a evaluación de impactos. Los análisis que se llevan a cabo en la primera parte del texto acerca de la relación entre el viento y la potencia tendrán relevancia en la segunda parte de este trabajo de tesis, en la que se presentará este tipo de tratamiento alternativo de la potencia como una variable derivada del viento y que se plantea en base

al mismo tipo de estrategia de downscaling que se aplica al caso del campo de viento.

Objetivos

El objetivo fundamental de esta tesis es profundizar en la comprensión de la variabilidad regional del campo de viento en superficie y de la potencia eólica así como proporcionar una estimación de la incertidumbre que acompaña al método de downscaling estadístico aplicado. La región de estudio, la Comunidad Foral de Navarra (CFN) al noreste de la península ibérica (IP, Fig. 2.1), presenta una considerable complejidad orográfica. Esta particularidad del area de estudio constituye un marco idóneo para explorar la habilidad de técnicas de downscaling estadístico en reproducir la variabilidad observada a escalas espaciales locales y/o regionales. Los datos observacionales del campo de viento que se utilizan en las distintas metodologías en el periodo comprendido entre 1992 y 2005 proceden de 29 estaciones meteorológicas distribuídas por toda la región de Navarra (círculos en Fig. 2.1). Estos datos fueron sometido a un meticuloso control de calidad (Jiménez et al., 2010a). Además, en cinco parques eólicos de la región (cuadrados en Fig. 2.1) hay disponibilidad de observaciones tanto de viento como de potencia generada (ver Tabla 2.1) en el periodo comprendido entre 1999 y 2003 (Capítulo 2).

El objetivo principal puede a su vez desgranarse en dos objetivos parciales, de modo que el texto está dividido en dos partes ligadas entre sí y de acuerdo a estos dos objetivos complementarios. El primero de ellos persigue explorar la relación existente entre el viento y la potencia producida en varios parques eólicos por su implicación en las estimaciones de potencia eólica a través de metodologías clásicas, cuyas fuentes de error fundamentales son analizadas durante este proceso. El segundo objetivo parcial de esta tesis consiste en identificar cuales son los forzamientos procedentes de la circulación atmosférica a gran escala responsables de las variaciones del viento en superficie y de la potencia eólica a escala regional. Uno de los aspectos más interesantes de la variabilidad climática regional radica en el hecho de que esta se encuentra afectada por toda la cascada de incertidumbres que se propagan en el traspaso de información desde la escala global hasta la escala regional o local. Por ello y dentro de los objetivos enmarcados en la segunda parte del trabajo, se investiga la sensibilidad metodológica asociada a las estimaciones de viento y potencia, atendiendo a posibles variaciones en la configuración de un método de downscaling específico y su impacto potencial en dichas estimaciones.

Ambos objetivos parciales están ligados a través del análisis de la variabilidad de la potencia eólica y su dependencia con la circulación a gran escala. Este tipo

de exploración se enmarca en el contexto de los llamados estudios de impacto y su aplicación en esta tesis se basa en la relación lineal entre el viento y la potencia eólica reflejada en la primera parte del trabajo.

Aproximación conceptual

Una de las maneras de aproximarse a entender la relación entre el viento y la potencia que este genera es evaluar el uso de las metodologías estándar que tradicionalmente se aplican a la estimación de producción de potencia eólica (Celik, 2003b,c, 2004) pues estas conllevan la definición de una función de transferencia entre el viento y la energía que de él se puede extraer (Seguro and Lambert, 2000; Akpinar and Akpinar, 2005a). Esto constituye una primera fuente de error que afecta a las estimaciones de potencia, pero no es la única. La limitación de observaciones disponibles implica que en los tratamientos clásicos de estimación de energía a partir del viento se haga uso de distribuciones teóricas de probabilidad (PDF, del inglés "*Probability Density Function*") para representar la variabilidad del viento en el lugar de interés (Li and Li, 2005b; Ramírez and Carta, 2006). La primera parte del trabajo se basa en una evaluación crítica de estas metodologías clásicas, la validez de las hipótesis que se asumen para compensar la falta de valores observados, como el ajuste a una cierta distribución para el viento o la selección de una determinada función de transferencia viento-potencia así como el impacto que ello produce en las estimaciones de energía.

El uso de la distribución Weibull (Hennesey, 1977; Tuller and Brett, 1984) se justifica por ser una de las PDF más empleadas en técnicas que proporcionan estimaciones de energía eólica (Chang et al., 2003; Celik, 2003a; Jaramillo and Borja, 2004; Pryor and Schoof, 2005), porque reproduce razonablemente las propiedades de las distribuciones en frecuencia del viento (por ejemplo, su asimetría positiva) y porque estudios anteriores muestran que resulta apropiada para representar el viento sobre la región de Navarra (García et al., 1998). Sin embargo en este trabajo (Capítulo 3) se muestra que en todos los emplazamientos el viento observado no se ajusta a una distribución Weibull. Como funciones de transferencia entre el viento y la potencia generada se exploran distintas posibilidades que implican distinto grado de complejidad (Capítulo 4). Cada una de ellas se evalua en base a una estimación de referencia que representa la situación ideal en la que se dispondría de datos observados pero lleva implícito el error metodológico y constituye un umbral para el error que se comete en la estimacion de energía. Alternativas a esta función de transferencia basada en observaciones son la curva de potencia del fabricante, que da cuenta del valor teórico esperado de potencia dado un valor de velocidad del viento, o bien curvas promedio o curvas de ajuste polinómico al cubo sobre los pares de valores viento-potencia observados. Estos

análisis, al igual que el análisis de los errores debidos al uso de una PDF teórica, se llevan a cabo en escalas horarias. Sin embargo, para obtener energía en escala mensual se puede pensar también en estrategias que operen directamente con valores mensuales de viento y de potencia. En esta dirección se exploran, de nuevo la curva teórica del fabricante y una simple relación lineal entre el viento y la potencia mensuales. Esta relación no es intuitiva pues debido a la energía cinética que transporta el viento en escalas temporales por debajo de la mensual, la potencia aumenta con el cubo de la velocidad del viento. A pesar de ello, en escalas mensuales se evidencia una relación empírica entre ambos que se puede aproximar mediante una recta. Este resultado proporciona un soporte argumental para, en la segunda parte del texto, explorar la variabilidad de la potencia eólica que está conectada con variaciones de la circulación a gran escala. Con ello la potencia recibe un tratamiento alternativo y novedoso como variable de impacto no atmosférica.

El segundo de los objetivos parciales descrito en la sección anterior implica la búsqueda de las asociaciones entre las variaciones del campo de viento en superficie y la circulación atmosférica a gran escala en la región del Atlántico Norte (Capítulo 5). Esta conexión se investiga en base a la aplicación de una técnica de downscaling estadístico (Análisis de Correlación Canónica; CCA del inglés *"Canonical Correlation Analysis"*). Para la región de estudio existen simulaciones del campo de viento basadas en el uso de modelos numéricos mesoscalares (Jiménez et al., 2010b). Sin embargo no existen en toda la IP aplicaciones de downscaling estadístico al estudio de la variabilidad del viento a escala regional. El CCA (Hotelling, 1936; Glahn, 1968; Levine, 1977) es una técnica lineal multivariante que consiste en encontrar pares de patrones (modos canónicos) de la gran escala y de la escala local para combinaciones de campos predictor(es) y predictando(s) y que permite expresar las variables originales como una combinación lineal de los modos canónicos encontrados. Esta técnica se ha empleado ampliamente con otras variables como la precipitación (Zorita et al., 1992; González-Rouco et al., 2000) y la temperatura (Xoplaki et al., 2003a,b) pero su uso aplicado al campo de viento es escaso (Kaas et al., 1996).

El diseño de la configuración del modelo estadístico se basa inicialmente en la exploración de distintas posibilidades y la selección de un *modelo de referencia*, una configuración que, sin ser necesariamente la óptima, es razonablemente representativa de la variabilidad acoplada entre predictor y predictando. Sin embargo, con el fin de ilustrar la incertidumbre metodológica, se explora en una segunda fase la sensibilidad de la estimaciones de viento a cambios en la configuración del modelo. Esta exploración de la sensibilidad metodológica, basada en el muestreo sistématico de distintas opciones en los parámetros que intervienen en la configuración del modelo (tamaño del dominio de la gran escala para los predic-

tores, número de modos canónicos que se retienen, etc.), se puede catalogar como perteneciente a la escuela frecuentista de inferencia estadística. La otra escuela tradicional es la probabilista, considerada una teoría robusta basada en la lógica bayesiana (Gregory, 2005). A su vez, una división clásica de las incertidumbres las agrupa en *aleatorias* o *epistémicas*. La primera es inherente al sistema y no se puede mitigar mientras que la segunda está basada en un conocimiento insuficiente del sistema y en cierto grado puede ser reducida (O'Hagan and Oakley, 2004). De hecho el tipo de análisis (frecuentista) de la sensibilidad metodológica que se ha planteado en este trabajo proporciona una medida de la varianza en las estimaciones ante cambios en los parámetros del modelo y esta varianza es epistémica por definición, pues procede de un conocimiento inexacto de la(s) configuración(es) óptima(s) o más adecuada(s) del modelo. Por tanto, puede decirse que una exploración probabilista de la sensibilidad metodológica se alinea más con la lógica de las incertidumbres de índole epistémica. Así, se plantea en este trabajo un ejercicio alternativo de análisis de incertidumbres basado en la teoría bayesiana. Con esta evaluación, que se expone en Capítulo 7, se obtienen distribuciones posteriores de probabilidad para cada uno de los parámetros importantes del modelo, es decir, se asignan pesos o probabilidades a los parámetros en función del grado de acuerdo entre las estimaciones que generan y las observaciones de viento (Gelman et al., 2004). La aplicación de esta aproximación al problema de las incertidumbres asociadas al método no es muy frecuente en el campo de la variabilidad climática regional. Asimismo no se conocen trabajos de este tipo enfocados a downscaling del campo de viento (Denman et al., 2007).

Uno de los usos interesantes de los métodos de downscaling estadísticos consiste en obtener, a bajo coste computacional, estimaciones de la variable de interés fuera del periodo observacional basándose en las relaciones encontradas entre predictores y predictando en el periodo de solapamiento y aprovechando la información proporcionada por predictores de la gran escala como reanálisis (Uppala et al., 2005), reconstrucciones basadas en datos proxy (Luterbacher et al., 2002) u observaciones históricas (por ejemplo de cambios de presión Uppala et al., 2005). Esta aplicación de lo métodos de downscaling facilita resolver preguntas relacionadas con la variabilidad regional del campo de viento en escalas temporales más largas (interdecadales o seculares). Este ejercicio se expone en los Capítulos 5 y 6 de esta tesis.

La relación lineal entre el viento y la potencia, fruto de los análisis en la primera parte del trabajo, invita a cuestionarse si un downscaling directo entre las variables predictoras de la gran escala y la potencia como predictando es posible de la misma manera en la que se ha aplicado al campo de viento. Por esta razón, en el Capítulo 6 se aplica la misma técnica estadística a la potencia generada en tres de los parques eólicos de la región (Fig. 2.1) para explorar la predictibilidad de la

potencia eólica en función de las variaciones de la circulación atmosférica sobre el área del Atlántico Norte. El planteamiento de esta aproximación con diferentes alternativas, como por ejemplo un downscaling de viento y el uso posterior de una función de transferencia viento-potencia, como la relación lineal, permitiría, a modo de aplicación práctica, estimar potencia eólica en ausencia de observaciones.

Aportaciones fundamentales

A continuación se detallan los objetivos específicos de cada capítulo así como los resultados más relevantes de esta tesis.

Parte I: Análisis de la relación entre el viento y la potencia eólica

- Capítulo 3: *Influencia del uso de la distribución Weibull en la estimación mensual de energía eólica*

  El objetivo de este capítulo consiste en comprender cual es la contribución al error en las estimaciones mensuales de energía eólica debido a asumir que el viento se ajusta a una distribución de probabilidad teórica: la distribución Weibull. Esta inspección en, cinco parques eólicos de la CFN, se realiza en el contexto de una evaluación crítica de las hipótesis tradicionalmente aceptadas en las metodologías clásicas que estiman energía a partir del viento (Eqs. 3.1 y 3.3).
  El análisis se basa en ajustar el viento observado en escala horaria a la distribución Weibull y obtener estimaciones de energía mensual a partir de la relación entre viento y potencia que proporcionan las observaciones. Con ello se aisla el efecto de asumir una PDF teórica. Los resultados son indicativos de que la distribución Weibull no reproduce las características del viento observado en todos los emplazamientos. Sin embargo, la falta de acuerdo entre las distribuciones de viento observada y teórica no produce un impacto considerable en el error al estimar energía (Figs. 3.6 y 3.7). Esto último se justifica debido a las cancelaciones de errores que tienen lugar en el cálculo de energía, la cual se basa en la contribución acumulada de los términos de frecuencia del viento pesada por términos de potencia para cada intervalo de viento (Figs. 3.10 y 3.11). A esta conclusión se llega a través de un análisis comparativo entre los errores en la estimación de energía y un parámetro representativo de la bondad de ajuste entre las distribuciones de viento observada y teórica (Figs. 3.8 y 3.12).

Los resultados más importantes de esta Sección de la Tesis han sido publicados en García-Bustamante et al. (2008)

- Capítulo 4: *Comparación de metodologías para la estimación mensual de energía eólica*

  El objetivo de esta sección de la tesis es evaluar el impacto en el error que se comete en la estimación de energía debido a asumir una determinada función de transferencia entre el viento y la potencia, es decir, el error debido a los términos de potencia (Eq. 4.1). Para ello se analiza el papel de distintas curvas viento-potencia en la estimación de energía eólica mensual. Se exploran diversas opciones de dicha relación viento-potencia tanto en escala horaria como directamente en escala mensual (Fig. 4.1). Se observa que métodos más sencillos, que requieren menos resolución temporal en los datos de entrada, en comparación con otros más elaborados, producen estimaciones en buen acuerdo con las observaciones de potencia en los parques. En general, todos los métodos explorados reproducen la variabilidad de la potencia observada (Fig. 4.5).
  En esta parte del análisis se pone de manifiesto la relación lineal existente entre el viento y la potencia en escalas mensuales (Fig. 4.3), cuando lo esperado en escalas temporales menores es que la potencia producida varíe con el cubo de la velocidad del viento. Esta evidencia de linealidad no documentada previamente en la literatura, demostrará tener aplicaciones relevantes en el estudio de la variabilidad de potencia relacionada con cambios en la circulación atmosférica. Se puede decir que la mayor contribución al error en la estimación de potencia se debe a las hipótesis relacionadas con los términos de potencia en comparación con las asociadas a la distribución en frecuencia del viento (Tabla 4.2).
  Los resultados más importantes de esta Sección de la Tesis han sido publicados en García-Bustamante et al. (2009)

Parte II: Relación del viento y la potencia eólica con la circulación atmosférica a gran escala

En esta segunda parte de la tesis se obtienen estimaciones del campo de viento y de la potencia en escala regional ilustrando la predictibilidad de estas dos variables de distinta naturaleza a través de la aplicación de una técnica de downscaling estadístico.

- Capítulo 5: *Relación entre la circulación atmosférica sobre el Atlántico Norte y el campo de viento superficial en el noreste de la península ibérica*

  Con objeto de entender la relación entre el campo de viento en superficie en varias estaciones de la CFN y la circulación atmosférica a gran escala se aplica un método de downscaling estadístico basado en CCA. Con este procedimiento se aislan los modos fundamentales de covariabilidad entre la escala regional y la escala global (Figs. 5.1 y 5.2). Esta inspección evidencia el papel que desempeña la orografía en combinación con la circulación a gran escala y que da lugar a los patrones de viento característicos de la región: circulaciones del NO (*Cierzo*) y del SE (*Bochorno*) a lo largo de la cuenca del Ebro y patrones más complejos debido a la orografía más abrupta en las zonas centrales y al norte de la CFN. Este tipo de análisis no se había aplicado previamente al campo de viento sobre la IP.
  Esta exploración se lleva a cabo usando una configuración de referencia del modelo estadístico con el fin de ilustrar las asociaciones entre escalas más importantes en la variabilidad del viento en superficie en la región. Sin embargo, con objeto de estimar la incertidumbre metodológica asociada a la técnica de downscaling aplicada, se exploran asimismo múltiples combinaciones de los parámetros que intervienen en la configuración del modelo (Apéndice A). Este tipo de exploración es poco frecuente en el caso de métodos de downscaling estadístico, especialmente en el caso del campo de viento.
  Se observa que la sensibilidad de las estimaciones a cambios en la configuración del modelo depende fuertemente de la variabilidad característica del campo de viento en cada emplazamiento. El abanico de estimaciones generadas con este procedimiento (*ca.* 60.000; Tabla 5.3) contiene a la mayoría de las observaciones a lo largo de todo el periodo de calibración, lo que es indicativo de la robustez del método a cambios en los parámetros importantes en su configuración (Fig. 5.8). Además no se pudo discriminar un impacto diferencial en las estimaciones de un parámetro con respecto a otro (Fig. 5.7). Esta evidencia es objeto de una exploración adicional en el Capítulo 7 con una orientación de caracter probabilista acerca del papel de cada parámetro en la generación de incertidumbres. Un ejercicio adicional en el que se investiga la influencia del uso de distintas bases de datos como predictores de la gran escala indica una influencia moderada en la incertidumbre metodológica debida a las diferencias entres los distintas bases de datos predictoras usadas (Fig. 5.10).
  En esta parte de la tesis se explora además la variabilidad a largo plazo del viento regional, desde escalas interanuales hasta multidecadales y seculares (Fig. 5.11). Esto es posible en base a la relación entre escalas encontrada du-

rante el periodo de calibración. El método permite obtener estimaciones de viento fuera del periodo observacional aprovechando la información de la gran escala disponible (fundamentalmente de presión a nivel de mar) en el pasado. Se aprecia una gran variabilidad del viento regional en escalas decadales e interdecadales pero no se observan en general tendencias pronunciadas a largo plazo. La variabilidad estimada del viento se puede interpretar en base a cambios en los modos de circulación más importantes encontrados en el periodo de calibración. Se estima la incertidumbre metodológica asociada a las reconstrucciones de viento en el pasado usando múltiples configuraciones del modelo de manera similar al procedimiento usado durante el periodo observacional. Se observa un impacto interesante en las estimaciones de viento a largo plazo debido a la selección de la configuración del modelo: cambios en uno de los parámetros (número de modos canónicos que se retienen en el análisis) produce una segregación de las estimaciones hacia anomalías de viento de signo opuesto en función del número de modos considerado (Fig. 5.13). Este impacto, que es ilustrativo de cierta variabilidad en la intensidad de las asociaciones entre los patrones de viento regionales y los modos de la gran escala, pone de manifiesto la importancia de estimar las incertidumbres y de interpretar cuidadosamente las estimaciones que se basan en una única configuración del modelo.
Los resultados más importantes de esta Sección de la Tesis están en proceso de revisión (García-Bustamante et al., 2010a).

- Capítulo 6: *Relación entre la circulación atmosférica sobre el Atlántico Norte y potencia eólica*

  El objetivo de este capítulo es extender el análisis de variabilidad del campo de viento regional mediante el uso de técnicas de downscaling al caso de la potencia eólica como predictando en un ejercicio que se puede enmarcar en los estudios de impacto con variables no atmosféricas. La exploración de la relación viento-potencia en la primera parte de la tesis anticipaba que las relaciones entre la circulación a gran escala y el viento regional son extensibles a la potencia, dada la linealidad entre ambas variables en escala mensual. Un análisis de downscaling similar al del caso del campo de viento se aplica al caso de la potencia como predictando local. El modo más importante de covariabiliad entre escalas para el caso de la potencia guarda semejanzas con el segundo modo canónico que se obtuvo al aplicar el CCA al campo de viento en superficie (Fig. 6.1). Esta similitud confiere robustez a ambos análisis. Se plantearon alternativas al downcaling directo de potencia, tales como obtener estimaciones del campo de viento a través de un CCA, como en el capítulo

anterior y generar finalmente estimaciones de potencia gracias a la relación lineal entre viento y potencia mensuales (Fig. 6.7). Este ejercicio es ilustrativo de las aplicaciones potenciales con bajo coste computacional para estimar energía en emplazamientos y periodos en los que no se dispone de potencia observada (Figs. 6.8, 6.9 y 6.10). La incertidumbre metodológica de la potencia estimada se exploró de manera similar al caso del viento mostrando que igualmente la mayoría de las observaciones permanecen dentro del area de incertidumbre que además preserva razonablemente la variabilidad observada (Figs. 6.3, 6.4 y 6.5).
Los resultados más importantes de esta Sección de la Tesis serán enviados en breve para su publicación como García-Bustamante et al. (2010b).

- Capítulo 7: *Análisis bayesiano de las incertidumbres asociadas a las estimaciones de viento*

  Alternativamente al tratamiento frecuentista de incertidumbres planteado en los Capítulos 5 y 6, se explora en el Capítulo 7 una técnica de carácter probabilista basada en el método bayesiano con el fin de ahondar en la compresión de la habilidad del método de downscaling dependiendo de los parámetros que se consideren en la configuración del mismo. En este proceso se presenta un planteamiento formal del procedimiento de obtención de las funciones de probabilidad que conforman el teorema de Bayes, a saber, una distribución de probabilidad que cifra el conocimiento a priori de las posibles configuraciones del modelo, más una distribución que penaliza aquellos parámetros los cuales generan estimaciones que se apartan más del comportamiento observado (Apéndice A).
  Los resultados de evaluar las distribuciones de probabilidad posteriores de cada parámetro del modelo ilustran la habilidad de algunos valores de cada parámetro para generar estimaciones cuyos residuos respecto a las observaciones son particularmente pequeños (Figs. 7.5 y 7.6). Esto se traduce en una asignación de probabilidades altas a dichos valores y al contrario, el resto de opciones de cada parámetro recibe probabilidades muy bajas. Sin embargo una inspección pormenorizada de dichos residuos (Figs. 7.3 y 7.4) muestra que existen otros valores de algunos de los parametros que, generando residuos también razonablemente pequeños, aunque algo mayores que el mínimo, muestran además un comportamiento estable en cuanto a la magnitud de los residuos para la mayoría de combinaciones de los demás parámetros. Paralelamente, se observa que aquellos valores de algunos parámetros con habilidad para generar residuos cercanos al mínimo, generan también residuos considerablemente mayores con otras muchas combinaciones de los demás

parámetros. Las probabilidades que el método bayesiano asigna a cada opción de los parámetros no discriminan este comportamiento. Por tanto la interpretación de los resultados a los que se llega con esta metodología debe llevarse a cabo cuidadosamente atendiendo a dos posibles maneras de razonar, es decir, si lo que se busca es el conjunto de configuraciones que optimizan las estimaciones o bien se busca encontrar qué valores de cada parámetro producen estimaciones en buen acuerdo con las observaciones independientemente de cuales sean los demás parámetros que intervienen. El método probabilista aplicado evidencia habilidad para discriminar las configuraciones óptimas pero no permite identificar comportamientos robustos a cambios en los parámetros.
Los resultados más importantes de esta Sección de la Tesis serán enviados en breve para su publicación como García-Bustamante et al. (2010c).

Conclusiones más relevantes

El trabajo desarrollado en esta tesis ha contribuído a comprender la relación existente entre el viento y la potencia eólica producida en distintas escalas temporales y sus implicaciones en la obtención de estimaciones de energía eólica de calidad con metodologías estándar. Se ha ilustrado como las cancelaciones de errores con distinto signo en las estimaciones puede mitigar el impacto de la falta de acuerdo entre la distribución de viento observada y teórica (Weibull). Se ha mostrado asimismo que en escalas mensuales la relación viento-potencia se puede asumir como lineal. Esto último ha demostrado implicaciones relevantes en un análisis alternativo de estimación de potencia eólica en el que se trata a esta variable no atmosférica como una variable de impacto, cuyas variaciones están asociadas a su vez a variaciones en la circulación atmosférica a gran escala.

Además esta tesis ha contribuído a entender la variabilidad del campo de viento en un región de terreno complejo como combinación de los forzamientos de la gran escala sobre el área del Atlántico Norte con las particularidades de la orografía de la región, como la presencia del Valle del Ebro. Es decir, se ha investigado la variabilidad a escala regional que es fruto de la interacción entre procesos característicos de distintas escalas espacio-temporales y se ha evidenciado que una proporción considerable de la varianza del campo de viento en estas escalas espaciales se puede explicar en función de la variabilidad de la circulación atmosférica a gran escala.

El análisis de sensibilidad metodológica que se ha planteado a lo largo de este trabajo permite cuantificar la incertidumbre asociada a las estimaciones regionales del campo de viento al aplicar técnicas de downscaling estadístico.

Esta es sólo una porción de la cascada de incertidumbres que afectan a la escala regional, sin embargo, esta exploración ha mostrado su relevancia, no sólo para analizar lo robusto del método antes posibles cambios en su configuración, si no también porque el tratamiento aplicado en esta tesis es informativo de los riesgos de considerar una única configuración del modelo seleccionado. Se han obtenido evidencias de la limitada fiabilidad de estimaciones en las que no se explora la varianza metodológica a través de un ejercicio en el que se discriminaba el impacto de cada parámtero en las incertidumbres estimadas para un periodo pasado que comprende los tres últimos siglos.

En una aplicación novedosa de downscaling estadístico a la potencia eólica como predictando no-atmosférico, se ha mostrado la predictibilidad de esta variable en base a su relación con la variabilidad de la atmosféra a gran escala. Este tratamiento presenta utilidades prácticas ventajosas para la estimación del recurso eólico incluso en ausencia de datos observados de potencia generada.

Se identificaron los parámetros más realistas del modelo de downscaling, ya que producen las estimaciones más fiables, en un análisis exploratorio de la incertidumbre asociada a las estimaciones regionales de viento basado en la lógica bayesiana. Este análisis ilustra la habilidad de este método probabilístico para detectar configuraciones óptimas y se ha discutido su capacidad para detectar los valores de aquellos parámetros que intervienen en la configuración del modelo y que generan estimaciones robustas ante cambios en los demás parámetros.

Publicaciones relacionadas con la Tesis en las que ha participado la autora

- García-Bustamante, E., J. F. González-Rouco, P. A. Jiménez, J. Navarro, and J. P. Montávez, 2008: The influence of the Weibull assumption in monthly wind energy estimation. *Wind Energy*, 11, 483-502.
- García-Bustamante, E., J. F. González-Rouco, P. A. Jiménez, J. Navarro, and J. P. Montávez, 2009: A comparison of methodologies for monthly wind energy estimations. *Wind Energy*, 12, 640-659.
- García-Bustamante, E., J. F. González-Rouco, J. Navarro, E. Xoplaki, P. A. Jiménez and J. P. Montávez, 2011a: North Atlantic atmospheric circulation and surface wind in the Northeast of the Iberian Peninsula: uncertainty and long term downscaled variability. *Clim. Dyn.* DOI 10.1007/s00382-010-0969-x.
- García-Bustamante, E., J. F. González-Rouco, J. Navarro, E. Xoplaki, P. A. Jiménez and J. P. Montávez, 2011b: Relationship between wind power production and North Atlantic atmospheric circulation: methods, associated uncertainty and long term downscaled variability. En preparación.

- García-Bustamante, E., J. F. González-Rouco, J. Sáenz, J. Navarro, E. Xoplaki, P. A. Jiménez and J. P. Montávez, 2011c: Bayesian uncertainty in downscaled wind field estimations. En preparación.
- Jiménez, P. A., J. F. González-Rouco, J. P. Montávez, J. Navarro, E. García-Bustamante, and F. Valero, 2008a: Surface wind regionalization in complex terrain. *J. Appl. Meteor. & Climatol.*, 47, 308-325.
- Jiménez, P. A., J. F. González-Rouco, J. P. Montávez, E. García-Bustamante, and J. Navarro, 2008b: Climatology of wind patterns in the northeast of the Iberian Peninsula. *Int. J. Climatol.*, 29, 501-525.
- Jiménez, P. A., J. F. González-Rouco, E. García-Bustamante, J. Navarro, J. P. Montávez, J. Vilà-Guerau de Arellano, J. Dudhia, and A. Roldán, 2010a: Surface wind regionalization over complex terrain: evaluation and analysis of a high resolution WRF numerical simulation. *J. Appl. Meteor. & Climatol.*, 49, 268-287.
- Jiménez, P. A., J. P. Montávez, E. García-Bustamante, J. Navarro, J. M. Jiménez-Gutiérrez, E. E. Lucio-Eceiza, and J. F. González-Rouco, 2009b: Diurnal surface wind variations over complex terrain. *Física de la Tierra*, 21, 79-91.
- Jiménez, P. A., J. F. González-Rouco, J. Navarro, J. P. Montávez, and E. García-Bustamante, 2011a: Quality control and bias correction of high resolution surface wind observations from automated weather stations, J. Atmos. Oceanic Technol. Oceanic Tech.-A, 27, 1101-1122.
- Jiménez, P. A., J. Vilà-Guerau de Arellano, J. F. González-Rouco, J. Navarro, J. P. Montávez, García-Bustamante, E. and J. Dudhia, 2011b: Influence of heatwaves and drought conditions on surface wind circulations. J. Climate. En revisión.

1

Introduction

The origin of the winds has been the focus of attention of numerous studies since the ancient times attempting an improved understanding of the mechanisms responsible for their different characteristics, their sources and their effects on human life. Therefore, many efforts implicitly oriented to the understanding of the general circulation of the atmosphere can be perceived since early in the human history. One of the classic contributions, *The situations and names of winds* (*Ventorum Situs*), is attributed to Aristotle and was written around the 3^{rd} century BC. In this treatise the origin of the winds was determined by the position of the sunrise and the sunset in the equinox which implied a varying position depending on the observer. Contemporary to that work is the construction in Athens of *The tower of winds* (between the 2^{nd} and the 1^{st} century BC) where a representation of the winds according to their origins was given, each one being characterized as a deity. Some examples of those winds are Boreas from the North, Eurus from the East or Notus and Zephyrus from the South and West, respectively. Zephyrus for instance, was represented as a *graceful young man, almost effeminate, wearing just a loose mantle with pleats full of flowers* (Arcimis, 1897). Galileo Galilei by 1600 attempted an explanation of the historically observed persistent westward winds based on an early perception of the rotation of the earth. Johannes Kepler (1571-1630) used similar arguments to explain the westward motion of the tropical oceans. The concepts of radiation heating and centrifugal force due to the earth rotation came for the first time to scene with Hadley (1735). Hadley contributed to the understanding of the atmospheric circulation on the basis of poleward motion at some level in height being compensated by equatorward movement at the surface to satisfy the conservation of mass and complemented this scheme by a combination of westward with eastward circulations at different latitudes in order to fulfill the conservation of angular

momentum. His theory would be criticized later as having assumed a too idealized atmosphere without oceans or continents and many other physical properties that would have changed the symmetry of his hypothesized circulation. However, the main objection to his theoretical considerations throughout the centuries was that he did not incorporate a meridional component of the Coriolis force which would have completed the arguments for an idealized correct atmospheric circulation. A hundred years gap existed between Hadley's efforts in elucidating the motion of the air masses in a physically consistent fashion and the description of the atmospheric currents deflection due to the rotation of the Earth by Coriolis (1835). Science has accepted and celebrated since then many contributions to the understanding of the meteorological phenomena and the motion of atmospheric fluids (Kant, 1756; Coriolis, 1835; Dove, 1837; Dalton, 1837; Ferrel, 1856; Brunt, 1934; Richardson, 1946). However, the scarceness of observations, that was overcome during the Second World War, hampered a precise knowledge of the atmospheric circulation. Lorentz (1967) raised a comprehensive explanation of the general circulation of the atmosphere with mathematical rigour, physically consistent equations and transparent scientific language: the atmosphere is responsible for the transport of the radiation energy exceedance from the equator to the poles and the mid latitudes westerly winds and the tropical easterlies compensate the angular momentum transfer. The so called primitive equations provide a hydrodynamical and thermodynamical description of the atmosphere accounting for the forces and their balances that drive the general movements of the air masses at large scales.

1.1 Nature of the cross-scales problem: assessing regional climate variability

Besides the radiative and rotational mechanisms that drive large scale circulation, winds are governed by processes of different nature and lifetime that aggregate their influence to picture the complicated behaviour of the wind field at smaller temporal and spatial scales. One of the main contributors to the complexity of wind variability is the orography that induces substantial variations to the geostrophic flow (Wagner, 1938; Smith, 1979). The presence of extensive geographical attributes like oceans, large mountain ranges and desserts or smaller scale terrain features like hills, valleys or urban settlements are responsible for thermally driven flows, momentum transport circulations caused by gravity waves or turbulent mixing and forced channellings of the wind (Whiteman and Doran, 1993). As the local scale becomes important, more physical processes are involved in the wind circulation. This is the case for instance, of boundary layer dynamics,

that enhance or hamper local flows depending on the effectiveness of the turbulent mixing. Other examples of local scale phenomena that are relevant for the wind field are the presence of land-sea contrasts (Simpson, 1994) or the changes of land use and thus, of roughness length and other surface physical properties, that produce significant effects in the vertical wind profiles (Wieringa, 1993).

The generalized definition of regional scale refers to a sub-continental scale with high heterogeneity in climatic features that are the product of interactions of phenomena at multiple timescales, from intra daily to multi centennial, combining mesoscale circulations and local forcings (Houghton et al., 2001). The need of assessing the regional climate variability can be thought of in terms of two different viewpoints. On one hand, from the academic perspective, the understanding of the multiple interactions of physical mechanisms playing a role in generating climatic variability at regional spatial scales can be still considered a challenge (Denman et al., 2007). On the other hand, from a more pragmatic point of view, mankind entails countless sociological, political, economical, environmental and cultural aspects that are very sensitive to climate variability (Gates, 1985; Robinson and Finkelstein, 1991; Bahn et al., 2006; Rosenzweig et al., 2007). Therefore, an improved understanding of climate at regional scales and how it interacts with diverse dimensions of the *human* ecosystems is of paramount importance.

The wind field, as explained above, can be loosely considered a local response to the large scale circulation. However, such a response also includes and is sometimes overridden by the effect of orography and a variety of factors such as vegetation, land-sea interactions or other thermally-driven phenomena (Bianco et al., 2006). This combination of large and smaller scale forcings imposes a high spatial as well as temporal variability on the surface wind field (Simpson, 1994). The large variability and the vectorial nature of this variable do not only introduce additional complexity to its diagnosis and prediction, but they also provide the topic with a valuable scientific interest. Exploring its variability at the regional scale involves practical applications that range from the short term wind forecasts to the assessment of climate change. Storms forecasting (Powell et al., 1991), air pollution research (Jakobs et al., 1995), surface roughness studies (Grimenes and Thue-Hansen, 2004), structures design related to extreme wind events (Zhang et al., 2006) or wave field evaluation (Caires and Sterl, 2004) are some of the applications of the wind speed analysis that are also relevant for many aspects of society.

Within this context, wind energy facilities have undergone considerable development in many regions of the world (Ackerman and Soder, 2002; Jager-Waldau and Ossenbrink, 2004; Flowers and Dougherty, 2004; Kenisarin et al., 2006; Hohmeyer and Trittin, 2008). Through the last decades renewable energies have been progressively established as a competitive and feasible energy resource

that can be used as an alternative to more problematic energy sources such as oil, carbon-based or nuclear technologies (DTI, 2006; Saidur et al., 2010). Wind energy assessment is therefore both a topic of scientific interest and an issue of relevance with ecological, economic and political implications for society. Efforts have been oriented to the analysis and understanding of wind energy variability at every timescale, from the short term wind power prediction (Kariniotakis et al., 2004; Pryor et al., 2009) to the medium/long term wind predictability evaluation applied to the resource assessment (Pryor et al., 2006). The application of every strategy oriented to estimate wind power production requires knowledge about its relation to wind variability. Understanding this relationship may have many implications in the quality of wind energy estimations. Errors may stem from various assumptions made on the process, both concerning hypotheses about the probability distributions of wind speed values and also the definitions of transfer functions to translate wind observations into wind power estimations. An evaluation of this scheme of potential errors involved in the estimation of wind power production and the analysis of the particularities of the wind-wind power relation will be the focus of the first part of this Thesis.

The complexity and multiplicity of the mechanisms involved at the regional scales calls for a wide spectrum of techniques and strategies that may be applied to gain insight into the regional climate problem. In practice no strategy can totally compensate the need for measurements to accurately describe the climate fields and their variations (Trenberth, 2008) and indeed many studies pursue an assessment of the surface wind field variability providing statistical descriptions of wind related variables based solely on observed records typically at the regional/local scale (Klink and Willmott, 1989; Klink, 2002; Archer and Jacobson, 2003, 2004, 2005; McVicar et al., 2008; Parish et al., 2008; Zhou et al., 2009). The quality of observations and the scarceness, both in space and time, of measurements are two factors that hamper the informative power of such assessments. The quality of observations is usually bounded by the presence in records of inhomogeneities, gaps, missing data or errors associated with a bad operation of sensors and data transmission (Gandin, 1988; Graybeal, 2006). The limited coverage of observations is often a problem in many regions to gain understanding of lower frequency variability for which longer records are needed. Such regional/local approaches can be complemented by analyses with a broader spatial perspective in which the regional/local variability is studied in terms of changes in the large scale circulation of the atmosphere. In fact, specific strategies can be designed to capture the interactions between large scale dynamics and the regional/local scale variability. These so called *downscaling* techniques (von Storch and Zwiers, 1999) can be exploited to deliver estimations and/or predictions of regional variability for different purposes.

The *downscaling* approaches employ large scale atmospheric circulation information to obtain estimations of variables at the regional/local scale by identifying the main statistical associations between both spatial scales (*statistical downscaling*) or explicitly resolving the physics involved using mesoscale models (*dynamical downscaling*). The large scale atmospheric state is provided by gridded observations (Zorita et al., 1992; Zorita and von Storch, 1999), reanalysis data (Xoplaki et al., 2003a, 2004) or general circulation model (GCM) outputs (Lenderink et al., 2007). One of the assets of the downscaling strategies is that they allow to overcome GCMs deficiencies in simulating the regional climate (von Storch et al., 1993; von Storch, 1995; McKendry et al., 2006). This lack of reliability arises because of their coarse spatial resolution (*ca.* 100 to 300 km) which does not allow to adequately resolve sub-grid scale processes that need to be parametrized (Müller and von Storch, 2004). The concept of *across-scales* or downscaling approach is already applied in the early 1960s when methods were designed to establish classifications of the large scale atmospheric states and then relate them to the local observed features of the climate. This suggests a closed connection between the notion of downscaling and synoptic climatology (Barry and Perry, 1973). During the subsequent decades *dynamical* and *statistical downscaling* strategies were adopted in order to satisfy the needs at regional and local scales (Hewitson and Crane, 1996).

The dynamical downscaling is based on the use of regional circulation models (RCMs) that solve the fundamental equations of the atmosphere yielding finer time-space simulations (Hong and Kalnay, 2000; Conil and Hall, 2006). These models that originally were used for numerical weather prediction issues are also called limited area models (LAMs; Giorgi and Bates, 1989; Giorgi and Mearns, 1991) and evolved as sophisticated versions of GCMs over a confined geographical area with typical spatial resolutions that range from the 50 km to 10 km or even higher (Jiménez et al., 2010b).

The use of RCMs may imply however relatively high computational resources. Thus, the empirical o statistical approaches stand as a practical procedure to explore connections between the large scale forcings or *predictors* and the regional/local response of a climatic variable or *predictands* (Zorita et al., 1992; von Storch et al., 1993; Noguer, 1994; von Storch, 1995; González-Rouco et al., 2000; Xoplaki et al., 2004; Busuioc et al., 2008). The computational demand is lower than in the case of RCMs and the implementation of the statistical model, although depending on the strategy selected, is to a great extent more straightforward than that of RCMs. Notwithstanding, statistical downscaling methods can provide also an understanding of the physical mechanisms responsible for the variability of regional fields. From a different perspective, they can also be applied within GCM simulations for validation purposes by assessing the ability

of the models in generating consistent large scale forcings in different regions of the globe as in van Loon and Rogers (1978). The statistical downscaling methods require training historical data of both predictand and predictor variables in order to identify the relationships between them. Some reviews and comparison of these statistical techniques can be found in Wilby and Wigley (1997), Wilby et al. (1998), Hanssen-Bauer et al. (2003), Wood et al. (2004), Haylock et al. (2006) and Schmidli et al. (2006).

The application of statistical downscaling techniques to variables like precipitation (e.g., Zorita et al., 1992; González-Rouco et al., 2000) or temperature (e.g., Xoplaki et al., 2003a,b) using the sea level pressure or other alternative large scale predictor fields is widespread in the literature. However studies of the wind field variability based on statistical approaches are relatively scarce. Some examples dealing with wind related variables will be discussed later in the text. Specifically, Part II of this work will show a novel application of such methodologies to wind related variables in a region of high orographic complexity in the northeastern Iberian Peninsula (IP).

It is worth to mention that some studies in the line of assessing the regional climate variability combine both types (dynamical and statistical) of downscaling strategies. These hybrid techniques are based on the use of some model that resolves the physics to provide estimations at the regional scale. Then, the simulation can be corrected from biases or systematic errors by means of a statistical approach, this last traditionally known as model output statistics (MOS) technique. For instance de Rooy and Kok (2004) reported several benefits in the estimation of the local wind due to the ability of the combination of both types of approach.

1.2 Uncertainty in downscaling estimations

Nonetheless, the transfer of information between spatial scales involves many sources of uncertainty that propagate from the global to the regional/local scale in downscaling exercises (Mitchell and Hulme, 1999; Schwierz et al., 2006). In the context of future climate projections, the uncertainties associated with the radiative forcing are accounted for by considering a variety of climate change scenarios (Nakicenovic et al., 2000; Denman et al., 2007) and by the use of a suite of GCMs to represent the intermodel variability. For instance, Pryor et al. (2006) studied the possible changes of surface winds in northern Europe through the downscaling of several GCM simulations under different scenarios. Najac et al. (2009) applied a statistical downscaling to wind observations over France within a multimodel strategy and estimated future changes of the wind field in a particular future climate scenario. The uncertainty associated with the use of a specific

model for the downscaling step can also be addressed. In the case of RCMs, the effect of changes in the discretization of the equations of motion or the different parametrizations can imply changes that contribute to uncertainty in the simulated regional field. Experiments that explore the sensitivity of the model to variations in the physics (Zhang and Zheng, 2004) or to changes in the initial conditions (Weisse and Feser, 2003) are designed to provide a measure of this type of uncertainty. In the case of statistical methods, the effect of applying different methodologies can also be examined (Zorita and von Storch, 1999; Matulla et al., 2003; Maurer and Hidalgo, 2007). Even in the case of using one specific downscaling method, uncertainties arise from a number of somewhat subjective decisions taken in the design of the statistical model. Usually such decisions are founded on good practise and lead to skillful estimations of the target regional variables (Hanssen-Bauer et al., 2005). However, introducing changes in the model configuration by changing parameter values, spatial domains, etc., would produce somewhat modified, though still skillful estimations. Even in the case of methods that provide probabilistic estimations of the regional targets (Furrer et al., 2007; Dibike et al., 2008) there are additionally unquantified uncertainties stemming from specific decisions in the model set up. These additional uncertainties are difficult to estimate, but they can at least be explored considering a variety of configuration designs in the downscaling approach. This path illustrates the sensitivity to changes in the model configuration, what can be regarded as a methodological variability or methodological uncertainty. Interesting works in this context are carried out by Huth (2000, 2004) who investigated the sensitivity of local downscaled temperatures in Central Europe to changes in the predictor variables. Nevertheless, this type of studies are rather uncommon in the case of wind related variables, thus an exploration of the methodological sensitivity of statistically downscaled wind field seems pertinent. Furthermore, the uncertainty may also arrive from potential inaccuracies of the GCMs or reanalysis as they provide the large scale information that feeds the downscaling models. For this reason, it is also interesting to explore the uncertainty that is associated to the use of different datasets as boundary and initial conditions in the case of the dynamical downscaling (Koukidis and Berg, 2009) or as predictors if dealing with statistical models. Part II of this thesis will complement the application of downscaling strategies with an assessment of this type of uncertainties.

The evaluation of the methodological uncertainty explained above to provide an insight into the model sensitivity can be regarded as a typical *frequentist* approach, since a systematic sampling is usually the strategy proposed to render a measure of uncertainty associated to the varying competing hypotheses. This is one of the two classical schools of statistical inference and it is based on assuming that probabilities are directly related to frequency of occurrence of a

random variable (in this case the model configuration). The other school incorporates probabilistic notions and it is considered a robust theory usually based on Bayesian logic (Gregory, 2005).

Classical definitions of uncertainties segregate them into *aleatory* and *epistemic* uncertainties. The first type, arriving from inherent system variability, cannot be reduced. In contrast the epistemic uncertainties are related to the imperfect knowledge about the system and to some extent they can be reduced (O'Hagan and Oakley, 2004). The analysis of sensitivity to changing model configurations explained above is based on a frequentist approach to explore the model output variance due to changes of the model parameters, but this variance is epistemic by definition as in its origin lies an inaccurate knowledge about optimal or potentially most suitable model configurations. In this sense the frequentist strategy is based to a great extent in aleatory statements, although the selection of possible model parameters may lean on reasonable arguments or experience. In contrast, the probabilistic Bayesian analysis is more aligned with the logic of epistemic uncertainties and it allows for computing probabilities, constrained by the observational evidence, of any parameter involved in the set up of the statistical method. The posterior probability distributions that this approach provides encompass the uncertainty about competing hypothesis on the model parameters allowing for sound interpretations where the frequentist approaches can not (Gelman et al., 2004). Thus, through the Bayesian approach inferences about the most suitable parameters of the model set up can be made. This probabilistic approach, that will be examined as an extension of the methodological sensitivity analysis in the second part of the text, is not yet extensively explored in the context of uncertainties associated to regional climate variability and to our knowledge, it has not been applied in the framework of statistical downscaling of the wind field. In general, it can be said that the evaluation of the different sources of uncertainty affecting the regional scale is an issue under development (Denman et al., 2007).

1.3 Impact oriented studies

An interesting benefit of statistical downscaling models lies in the fact that they may embrace studies dealing with biological or other environmental variables that are non-climatological but their evolution strongly depends on climate variability. Statistical tools allow for searching the relationships between atmospheric forcings and the sociological or ecosystem impact responses. An interesting example in this line is the wind power production in the context of renewable energy generation. Estimation of wind energy production from surface wind speed is not only interesting from a physical and engineering point of view. It also involves many

ecological, economic and political aspects relevant for society within a variety of timescales, ranging from hourly meteorological forecasts to long term climate prediction. Short term wind energy forecast (hourly to daily scales) is important for electricity system management, particularly in liberalized markets, in order to ensure stability in the energy market (Kariniotakis et al., 2004). Monthly and seasonal range prediction of wind energy can potentially allow electricity system operators to estimate the energy production availability from wind farms, and allows the electric network to conveniently adapt demand and resources (Weisser and Foxon, 2003). Future changes in the regional and local wind fields as a result of the climate evolution within those spatial scales, though subjected to large uncertainties, can plausibly have significant impacts on energy resources which are worth to be analyzed (Palutikof et al., 1987). Therefore, evaluating the potential availability of wind energy resources (Jamil et al., 1995; García et al., 1998; Mathew et al., 2002; Chang et al., 2003; Bechrakis et al., 2004), their predictability (Mengelkamp, 1999; de Rooy and Kok, 2004) and variations at different timescales (Palutikof et al., 1987; Pryor and Barthelmie, 2003; Pryor et al., 2006) is an issue of interest in the context of renewable energy.

An understanding of the relation between wind speed and and wind energy is desirable to attempt such evaluations and is often hampered in practical situations by the limited availability of historical power production records. Due to this limitation and as discussed in Section 1.1, the classic handling of wind power analyses was based on the use of a theoretical probability distribution function (PDF) that fits the frequency distribution of wind velocity observations (Justus et al., 1977; Conradsen and Nielsen, 1984; Weisser, 2003; Balouktsis et al., 2002; Celik, 2003a,c; Li and Li, 2005b). Subsequently the estimated parameters of the PDF can be used to provide an idea of the expected energy that is carried by the wind (Pryor et al., 2005b). Thus, using the wind speed PDFs and in the absence of available historical series of wind energy production, the relation between wind speed and wind energy is frequently established in terms of the associated wind energy *density* as a substitute of the real wind power generation

However, turbine outputs have recently become available (Weisser and Foxon, 2003; Akpinar and Akpinar, 2005a; Pryor and Schoof, 2005). Thus, the analysis of this variable as a response to the large scale circulation constitutes a new take on the topic with wind power production playing the role of a non-atmospheric variable. This is aligned with impact oriented type of studies where, in this case an understanding of the relationships between the power generation and its main driver, the wind, becomes of relevance. The analyses developed in Part I of this thesis concerning the wind-wind power relation and the quantification of errors in the estimation of wind energy will evidence some implications for the second part

of the report, where an alternative treatment to the wind power production as a wind derived variable will be explored in the context of a downscaling strategy.

1.4 Objectives and structure

This study aims at providing an understanding of the regional variability of the wind and the wind power production, together with the evaluation of the uncertainties associated with both variables that arrive as a consequence of using a specific downscaling method to estimate them. One of the most challenging issues in this study is the spatial focus of the assessment, a region of complex terrain in the northeastern IP that constitutes an ideal frame to test downscaling methodologies and provides the exercise with a special practical and academical interest. The work focuses on variability above monthly timescales. The data and a description of the target region, the Comunidad Foral de Navarra (*CFN*), will be described in detail in Chapter 2.5.

The objective of this study is twofold and the text is organized in two parts according with these main objectives. The first focus is to explore the relationships between the wind field and the wind power production, a non-climatological variable directly depending on the wind. Methods for energy estimation can be thought of on the basis of estimations of its main agent, the wind, in combination with an appropriate transfer function for translating wind speed into wind power. These methods are evaluated in this work and discussed in terms of the different sources of error and their relative contribution to the wind power estimates. First, an analysis of the assumptions involved in the representation of the observed wind by theoretical probability distributions is provided and its implications in the performance of traditionally accepted methodologies is discussed in Chapter 3. Another source of error in the wind energy estimation arises from the assumed transfer functions between wind and wind power. In this part of the work the rationale and methodologies to explore these relations are elaborated providing insight into the validity of typical assumptions that are made about the wind-wind power relations. New empirical relationships depicted between the wind, and its derivative, the wind power, will prove useful in their simplicity with regard to other conventional methodologies. These considerations are exposed in Chapter 4. The results of this part will support the conceptual approach that explores the wind power variability through the application of a downscaling technique in the second part of the Thesis.

A second primary interest of this thesis developed in the second part consists in identifying the more important large scale circulation features that are responsible for the observed wind (Chapter 5) and wind power (Chapter 6) variations

at the regional scale. A statistical downscaling model is applied in order to isolate the large scale circulation modes over the North Atlantic and Mediterranean areas that govern the monthly regional wind field in the CFN. The application of statistical downscaling approaches to the wind field and impact related variables over the IP is novel. The physical consistency of the coupled modes between the large and the regional scale is thoroughly analysed. The sensitivity associated to the various methodological aspects will be examined based on the argument that a single selection of the model set up does not permit to account for the uncertainty in estimations that arises in the downscaling step. The evaluation of this type of uncertainty provides confidence in the robustness of the model skill in reproducing the observed monthly wind and helps in discriminating whether certain parameters have a decisive influence in the quality of estimates. The parameters that are important for the configuration of the model (for instance, the predictor variables, the large scale domain selected for the search of the connections between atmospheric circulation and regional wind, etc.) are systematically sampled to provide a large ensemble of configuration set ups. The properties of the ensemble are investigated and the reasons for the selection of the parameter values are also discussed in Chapter 5.

The understanding of the mechanisms responsible for the temporal variations of the regional wind at inter decadal and centennial timescales is also a relevant issue since it allows for an analysis of the wind variability on a longer term perspective. Besides, uncertainty in estimations is expected to increase at longer timescales due for instance, to additional uncertainty in the large scale input data or changes in the frequency and intensity that the associations between large and regional scales are subject to. Nevertheless, this is hampered by the limited temporal length of the observational series since usually short periods are used for calibrating and validating models. The statistical methodology applied allows for obtaining estimates in the absence of observations by downscaling the available information from large scale circulation. Past projections of the wind climatology and its associated uncertainty are estimated several centuries backward using available datasets of large scale predictor variables. The long term variability of the regional wind (Chapter 5) and wind power production (Chapter 6) are interpreted in terms of the variations in sign and intensity of the main modes of the atmospheric circulation affecting the regional wind that were found during the observational period. This exercise provides a broader perspective of the regional wind variability in observations that may be of use in the context of comparison with climate change downscaling exercises. A robust assessment of the uncertainties derived from the downscaling step has many implications for the understanding of past and future estimations of the wind field. Through the evaluation of the methodological uncertainty at longer timescales, it will be

possible to discriminate why single estimations should be managed with care. Arguments in this line are constructed in the basis of results in Chapter 5. The two main points described above, i.e., the relationship between wind and wind power and the connection between regional wind and large scale circulation, lead in a natural manner to open questions regarding the relations between wind power production as a wind derivative variable and the atmospheric circulation. Thus, an outspread target of this work is investigating to what extent the wind power production may be also considered a response to the large scale forcings as in the case of the wind field. In this context of impact oriented studies there is space for examining these connections and the plausible applications and benefits this could involve. The uncertainties associated with the wind power estimations through the statistical downscaling model are also investigated in this step (Chapter 6) in a comparable approach to the case of the wind downscaling in Chapter 5.

The methodological sensitivity analysis described in Chapters 5 and 6 can be considered as a classical (frequentist) approach for the treatment of the uncertainties associated with the downscaled estimates. It is reasonable to consider that a certain degree of subjectivity is involved in the selection of possible values for the parameters of the model applied and more formal treatments may be explored. Alternatively, as introduced in Section 1.2, a more objective assessment of this type of methodological uncertainty can be attained by applying a probabilistic approach, as is the case of the Bayesian analyses. The procedure implies that prior knowledge in the model parameters can be updated by using the available observations during the calibration period. Thus, the optimal parameters and the uncertainty associated with the method are estimated based on the possible constraints imposed by the observations. It will be shown how a Bayesian treatment can assign weights (probabilities) to each possible combination of parameters discriminating which cases are more realistic according to the information provided by the observed fields. This alternative treatment of the methodological uncertainty is presented in Chapter 7, where the potentials and limitations of this methodology will be also discussed.

The features afore mentioned are some specific aspects of the case study proposed herein that highlight its distinctive character. Still another particularity of the present study may be emphasized. The foundations for this analysis are based on two variables, closely related to each other but different in nature, the wind field and the wind power production. One is a meteorological field and the other is a response variable, with technical and engineering aspects involved in its variability. Thus, two orientations coexist: the conceptual viewpoint of understanding the physical mechanisms influencing the behavior of the wind field and its derivatives and, on the other hand, certain parts of the study can be also

ascribed to the framework of impact studies, as the wind power can be regarded as an impact variable.

2

Observational datasets

This chapter contains a description of the geographical area of interest and the different datasets that have been used in the work. The next section presents the target region and highlights those particularities of the area that are relevant for the evaluation of the wind and wind power variability and predictability. The large scale circulation features affecting the IP that will show influence on the regional circulations over the target area are discussed. The Part I of this thesis deals with the assessment of methodologies to obtain wind power estimations allowing for the understanding of the relationships between wind speed and wind power production. The analysis in this part is based on the use of observations of both variables recorded at five wind farms in the CFN. Section 2.2 illustrates the availability of wind and wind power measurements at the wind farm locations.

Part II will use an extended dataset with wind speed and direction records at 29 meteorological stations distributed over the CFN to explore the influence of the large scale atmospheric circulation in the regional variability of the wind field. Section 2.3 presents this extended dataset of observed wind field over the CFN. The climatology of the wind is also explored in this section providing a description of the windiest areas and local circulations which are illustrative to a first approximation of the importance of orography. The large scale atmospheric fields required for the downscaling exercises are provided by several datasets (reanalysis, observations and a proxy-based reconstruction) that are enumerated in Section 2.4.

2.1 Climatology of the CFN

The large climate variability in the IP is a response to the combination of two effects, namely the synergy among air masses with different geographical origins

and properties and the variety of orographical features that spot the IP (Font, 2000).

The dominant mode of the large scale circulation is the semi-permanent subtropical high pressure centre over the Azores Islands (Sahsamanoglou, 1990). Its position and intensity largely determine the climate over the western part of the European continent since it produces a zonal transport of air masses from the Atlantic area. In general it determines the pathways of the cyclones that tend to travel northeastward and then merge with the subpolar Icelandic low (Seierstad et al., 2007). Due to the seasonality of the Azores high, during winter it tends to be centred at lower latitudes with respect to summer, where an expansion of the high pressure centre towards higher latitudes generates a partial blocking over the IP and the European continent (Davis et al., 1997). This background westerly circulations interact with other large scale modes as, for instance the Siberian high, which brings polar air masses to the peninsula, or the semipermanent Sahara low, contributing with tropical continental flow. These features and the location of the IP determine that, especially in winter, the peninsula is intersected by the Atlantic storm track and embedded in a region of large spatial (north to south) gradients and large temporal variability in precipitation, temperature and wind regimes. For instance, the precipitation is largely controlled by negative sea level pressure (SLP) over the North Atlantic and Mediterranean regions (González-Rouco et al., 2000; Trigo and Palutikof, 2001). The high summer temperatures in the peninsula are associated with positive SLP anomalies over the IP that combined with smaller lows between Portugal and Morocco generates advection of warm and dry air from the North of Africa (García-Herrera et al., 2005). Seneca, the famous philosopher from Córdoba (4 B.C. - 65 A.D.), in his *Naturales quaestiones* described the nature of the winds in the peninsula: *Levante*, *Poniente*, *Mediodia* and *Septentrion*. In broad terms, dominant winds are from the west in the Atlantic coast, mainland winds are from the north and in the Mediterranean area the origin of the prevailing winds encompass directions between the north and the south. In addition, the rich orography plays a significant role in the variety of different climate regimes in the peninsula.

The CFN in northeastern IP is a region of intricate orography surrounded by two large mountain ranges, the Pyrenees and the Cantabrian systems. Many other smaller geographical features give rise to the complex landscape of the region (Fig. 2.1). There are important climatic contrasts between the north and the rest of the region (García and Reija, 1994): the northern areas are characterized by a moist and warm flow advected from the Atlantic throughout most part of the year. However the more important geographical feature is the Ebro Valley, that passes across the two mountain ranges with a northwest-southeast direction and finally flows into the Mediterranean. Along the valley the winds are drier

and colder and the dominant orientation is NW-SE. The synoptic conditions responsible for cold northern winds are the same through the whole year but they tend to intensify in autumn and winter, since pressure gradients are stronger. The typical synoptic situation consists of anticyclonic circulations over the Biscay Bay and low pressures over the Balearic Islands and the Mediterranean areas. This generates a flow that is strongly channeled along the valley. This local wind is know as *Cierzo*, originally *Cercio* or *Circius* (Biel, 1952). The opposite direction wind is known as *Bochorno* and it is milder and moister. It tends to appear in situations characterized by high pressures over the Mediterranean and lower pressures over the Cantabrian sea (de Pedraza, 1985).

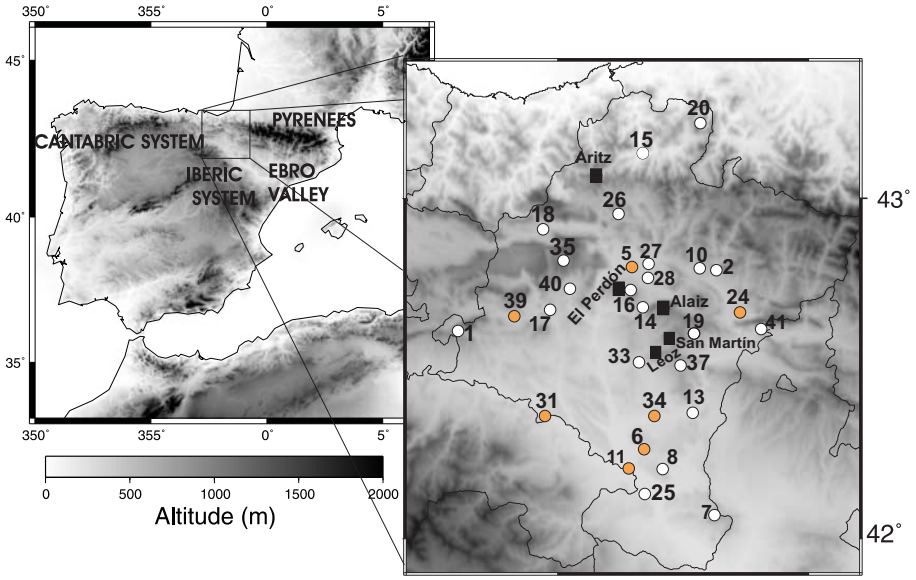

Fig. 2.1: The region under study: left panel shows the IP and the main geographical features surrounding the CFN. The right panel amplifies the region of the CFN and its orography (shading). Circles stand for the location of the wind stations. Coloured circles represent those stations with anemometers at 2 m while the rest are located at 10 m height (see Table 2.4 for sites description). Squares correspond to the wind farm locations: Alaiz, Aritz, El Perdón, Leoz and San Martín (see Table 2.1).

All geographical and synoptic features highlighted in the previous paragraphs will prove significant influence on the variability of the wind field and power production throughout the analyses that follows in Part II.

2.2 Observed wind speed and wind power at the wind farm locations

Part I of this thesis focuses on the evaluation of the wind speed empirical and theoretical distributions and the relation between the wind and the derived wind power generation. These assessments are important for the estimation of wind energy from wind and will prove useful in the second part of the work where direct estimations of wind power from atmospheric variables are examined. The analysis is based on the wind speed and wind power recorded at the several wind farms within the CFN. A description of the observations and the wind farm sites is provided in the following paragraphs.

The geographical location of the five wind farms, the wind sensor heights and dates with available observations are summarized in Table 2.1, the five wind farms, Alaiz, Aritz, El Perdón, Leoz and San Martín, are also marked with a square in Fig. 2.1. Original wind speed and wind power data have been subject to a basic quality control in order to mitigate possible disturbances due to erroneous records in the performance of the methods applied during the work. *Repeated values* (duplicated dates/hours), *missing* information (dates, wind speed,...), unrealistic negative values or observations larger than physical thresholds supported by the instrument were identified and replaced with a *missing* code. The observations were not subject to any other controls to filter out doubtful data like extreme wind speed or power production values (outliers). Thus, some dispersion in the representation of the hourly values can be expected as discussed below.

Hourly wind velocity measurements were collected by anemometers placed in meteorological masts at each wind farm (see Table 2.1 for details). For the particular case of the wind farm at Leoz, wind data were additionally available at each wind turbine at the hub height, this varying between 40 and 45 meters. Thus, in Leoz all the 30 wind speed time series (one series per wind turbine) were spatially averaged obtaining a single representative series for the whole wind farm. Wind speed mean values ($\overline{w}$) and deviations (S_w) for each site are shown in Table 2.2. All wind farms have similar $\overline{w}$ values, ranging from 7.4 ms^{-1} in San Martín to 7.9 ms^{-1} in Alaiz and Leoz, except for El Perdón, which is the windiest location (9.2 ms^{-1}). Its deviation is also the largest one (5.2 ms^{-1}). S_w values in the rest of the locations vary from 3.8 ms^{-1} to 4.8 ms^{-1}.

Fig. 2.2 illustrates the variability of the monthly frequency distribution of wind at each location. Frequency levels of occurrence (points) were calculated

Table 2.1: Geographical details, sensor height, dates with available observations and number and model type of turbines for the five wind farms considered in this study. The codes for the turbine model are 1 for G39-500, 2 for G42-500, 3 for G42-600, 4 for G44-600 and 5 for G47-660. See also Fig. 2.1.

	Lat (^{o})	Lon (^{o})	Sensor height (m)	Dates (yr/mon)	Turbines model (n^o)
Alaiz	42.679	-1.579	30	1999/12-2003/05	5(39)
Aritz	43.067	-1.847	40	2000/01-2003/05	3(32)
El Perdón	42.736	-1.735	40	1999/06-2003/05	1(26), 2(11), 3(3)
Leoz	42.549	-1.582	40-45	2000/11-2003/06	3(16), 4(13), 5(1)
San Martín	42.565	-1.548	30	2001/03-2002/12	3(21), 4(19)

Table 2.2: Monthly mean wind ($\overline{w}$) and wind energy ($\overline{wE}$) and their respective standard deviations (S_w and S_{wE}) at each wind farm.

	$\overline{w}$ (S_w)	$\overline{wE}$ (S_{wE})
	(ms^{-1})	(GWh)
Alaiz	7.9 (4.2)	3.4 (0.8)
Aritz	7.7 (4.8)	2.1 (0.8)
El Perdón	9.2 (5.2)	3.2 (0.7)
Leoz	7.9 (4.1)	2.2 (0.5)
San Martín	7.4 (3.8)	2.9 (0.7)

from the hourly observations and depicted for each month over a fixed array of 2 ms^{-1} width wind speed intervals, common to all months for each site. The range of variability of the monthly frequency of wind occurrence changes from site to site, subject to the particularities of the annual cycle and inter annual variability. For the purpose of illustration, the wind speed annual cycle is represented in Fig. 2.3 at each site: summer months are less windy than winter ones, except for El Perdón, which shows a less pronounced annual cycle with the minimum of the curve slightly displaced to the autumn months.

An estimation of a mean histogram is also provided in Fig. 2.2 through the average of all monthly frequency values for each wind interval. It is interesting to explore some properties of the frequency distributions, like their symmetry and kurtosis ranges as they are descriptive of the variability of the monthly PDFs that will be of relevance in Chapter 3. The overall tendency to present positive skewness (values larger than 0; Celik, 2003a) is evident from the average histograms. The most positively skewed distributions are found at Aritz and

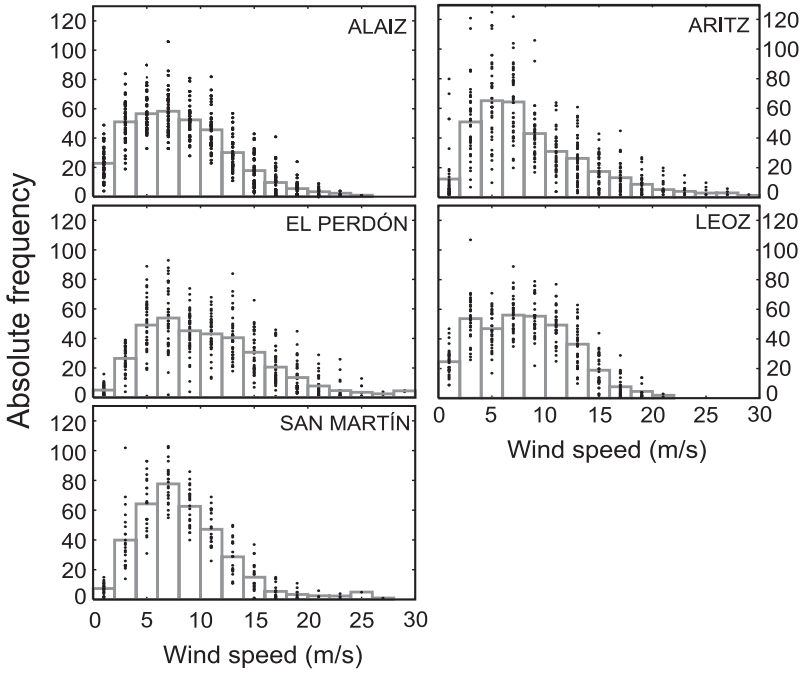

Fig. 2.2: Wind speed monthly histograms at each site. The monthly frequency levels for each representative wind value are indicated by points. Bars represent the average histogram for all available months. See text for details.

Alaiz with some monthly values that reach 1.57 and 0.96, respectively. Some examples of negatively skewed histograms are also found at some locations, with maximum values reaching -0.93 and -0.3 at El Perdón and Leoz, respectively. Most months show platykurtic (i.e. flatter than normal; kurtosis lower than 3) distributions with values typically between 2 and 3; minimum values of 1.8 are reached at El Perdón and Leoz. Leptykurtic distributions (i.e. more peaked than normal; kurtosis larger than 3), though less frequent, can also be found mainly at Aritz and San Martín, where maximum values reach 7.01 and 4.07, respectively. The values obtained in this study for the symmetry (skewness) of histograms can be considered moderate if compared, for instance, with those obtained by Torres et al. (1992) also for Navarra locations. There, the wind speed data were first divided into sectors according to wind direction and an extended sample was obtained, resulting in larger skewness values than the ones obtained in the

present work. In the case of kurtosis or the *peakedness*, they also suggested a typical flattening of the distribution when considering the dominant direction of the wind speed. Additionally, they found some cases with larger values than any of those found in the present study (some cases reached kurtosis values of 10).

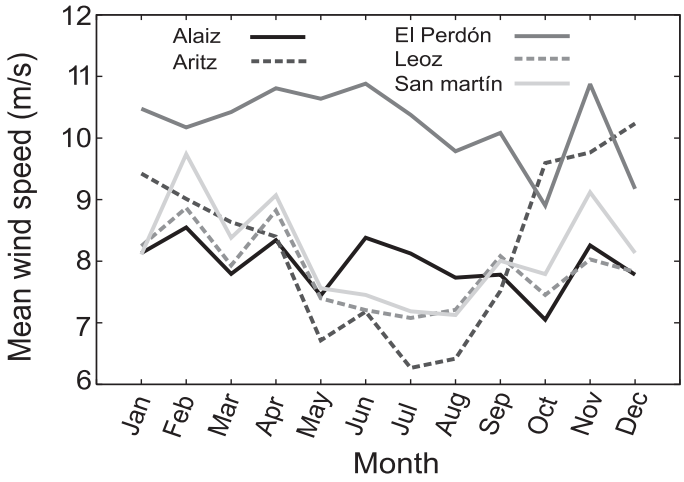

Fig. 2.3: Long term monthly mean wind speed for the period 1999/06 to 2003/06 at each wind farm.

A wind power production time series at each wind farm was obtained by spatially averaging the hourly power outputs from every wind turbine within the wind farm. Some of the wind farms incorporate more than one type of turbine model with different technical properties which also imply different power production. This is the case of El Perdón, Leoz and San Martín wind farms (see Table 2.1). El Perdón combines three types of turbines: G39-500, G42-500 and G42-600. The nomenclature GXX-YYY is related to the blade diameter in meters (XX) and the *rated* power (the power output under nominal operating conditions which are determined by the optimum rotor speed and the installed rated generator power; Hau, 2006) in kW (YYY). In the case of Leoz, three turbine types are installed: G42-600 kW, G44-600 kW and G47-660 kW. Finally, San Martín makes use of the types G42-600 kW and G44-600 kW. The types of machine described are angle pitch regulated (Hau, 2006). Since different models of turbine provide different power production for different wind speed levels, in the cases of wind farms with several turbine types a power production series was calculated for each type of wind. Hence, just one power production time series was calculated

to represent Alaiz and Aritz, whereas three series were obtained for El Perdón and Leoz and two in the case of San Martín. The number and types of wind turbines installed at each wind farm are shown in Table 2.1.

Additionally, the correlation values between the selected power production time series at each site in Table 2.3, present high values in the center of the CFN showing a similar evolution of wind power production variability. The production in Alaiz is strongly correlated with the other three wind farms (correlations of 0.8-0.9). El Perdón presents a correlation of 0.74 and 0.57 with Leoz and San Martín while these two locations present a 0.95 correlation coefficient. The exception is the most distant wind farm, Aritz, which presents a decoupled wind power production. The fact that power production in Aritz is uncorrelated with the rest can be attributed to its geographical situation to the north of the other four sites (Figure 2.1) that favors exposure to more Atlantic circulations while the others are more conditioned by the presence of the Ebro Valley. This will be discussed in Chapter 6 Some information regarding the circulation regimes that influence the regional wind and wind energy as well as the climate variability in the CFN can be found in Jiménez et al. (2008b,a).

Table 2.3: Correlation between the monthly power production time series at each wind farm (wind turbines are type G42-600 kW, except for Alaiz where the model G47-660 kW is used).

	Alaiz	Aritz	El Perdón	Leoz	San Martín
Alaiz	1.00	-0.03	0.91	0.90	0.77
Aritz	-0.03	1.00	-0.22	0.21	0.39
El Perdón	0.91	-0.22	1.00	0.74	0.57
Leoz	0.90	0.21	0.74	1.00	0.95
San Martín	0.77	0.39	0.57	0.95	1.00

To elude any perturbation caused by the different number of observations within each month on the analysis performed in Part I, 350 pairs of simultaneous hourly wind speed-wind power data (ca. 50% of observations) were selected from each month. The random selection is conditioned to follow a uniform distribution, that allows for each value to have equal probability of being chosen. This approach enables an homogeneous and representative sampling of the variability of both, wind speed and wind power, within every month in the dataset. The number of extractions (350) was selected as a balance between decimating excessively the dataset or, alternatively, using potentially non representative monthly mean values calculated from too few observations. Notwithstanding a sensitivity test

to the number of extractions at El Perdón was performed as an example. Wind speed and wind power production series with different percentages of retained data are represented in Fig. 2.4a,b, respectively. It is apparent that no large impacts in results may be expected due to a varying number of data included per month.

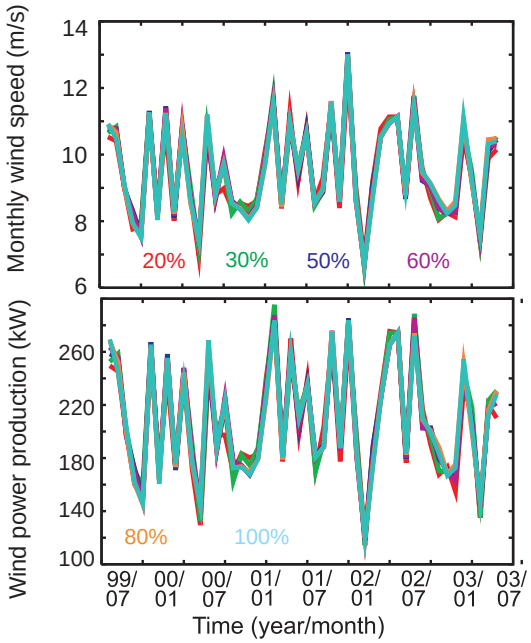

Fig. 2.4: Wind speed (top) and wind power production (bottom) time series at El Perdón with a variable number of data retained for the analysis (see legend).

Further details on the implications of assuming averaged series to represent the wind power production at the wind farms will be provided in the following chapter on the basis of its relation with the corresponding representative wind speed time series.

2.3 Observed wind field in the CFN

Wind velocity and direction observations over the CFN were measured at 29 meteorological stations from January 1992 to September 2005. Their geographical

distribution is represented in Fig. 2.1 and Table 2.4 provides information about their location data, sensor height and dates of the sensors installation. The original observations consist of 10-minutes wind speed (module) and wind direction data at 10 meters height over the surface, although there are also some stations at 2 meters. From these initial measurements the zonal (u) and meridional (v) components of the wind are computed and then monthly averaged for the specific purposes of the study herein. The monthly wind module (m) is obtained from $m = \sqrt{u^2 + v^2}$. In addition, observational data from 3 out of the 5 wind farms (squares in Figure 2.1) are also considered for the downscaling analyses that make use of this wind field dataset in the second part of the study. Wind data series at the wind farms span throughout the period between June 1999 and May 2003, for the longest series, as explained in the previous section. Thus two of them could not be included since their length was considered insufficient to calibrate a statistical downscaling method. However, the inclusion of the 3 wind farms with longest records in the analysis is interesting to illustrate the influence of the orography by comparing these wind farm records obtained at the hub height (between 30 and 40 meters) and usually at the top of a hill with the wind measured at the rest of stations, located closer to the surface (usually at 10 m and a few of them at 2 m).

This data were subject to quality control procedures that involve the detection of missing and repeated values and in general, the errors associated to the manipulation and storage of records as well as range checks to identify unrealistic values. Additionally, to guarantee temporal consistency, the higher/lower than normal variations of the wind values were examined. For further details on the data set and the quality control procedure the reader is addressed to Jiménez et al. (2008b, 2010a).

The analyses of the wind field variability and predictability in the second part of the report are focused on the most windy months, when the links between the atmospheric circulation and the regional wind field are stronger. As mentioned before (recall Section 2.1), the synoptic conditions that intensify the wind over the region are rather similar along the year. However, in autumn and winter the surface pressure gradient over the Ebro Valley is intensified and stronger winds are associated with an intense cold air advection from the Atlantic area (de Pedraza, 1985; Jiménez et al., 2008a). For this reason an extended *winter* season covering September to March is used in the analysis.

The climatology of the wind field in the region is described in the following paragraphs. Observed mean wind module (solid curves) and wind components (vectors) are represented in Figure 2.5. Notice that there is no direct relation between the vector length and its module in Figure 2.5 since the averages calculated over the wind components can neutralize each other with opposite signs

Table 2.4: Code of the meteorological station as in Fig. 2.1, name, latitude, longitude, sensor height above ground level and available dates (year/month).

Num.	Name	Lat. (^{o})	Lon. (^{o})	Sensor height (m)	Dates
1	Aguilar de Codés	42.614	-2.394	10	1992/03-2005/04
2	Aoiz-Agoitz	42.792	-1.369	10	1992/03-2005/05
3	Arazuri	42.801	-1.702	2	2000/02-2005/09
4	Bardenas-barranco salado	42.265	-1.654	2	1998/03-2004/01
5	Bardenas-loma negra	42.071	-1.375	10	1992/03-2005/05
6	Bardenas-Nstra Sra. Yugo	42.206	-1.582	10	1992/01-2005/05
7	Beortegi	42.796	-1.434	10	1997/05-2005/05
8	Cadreita-Riegos	42.209	-1.717	2	1998/03-2005/09
9	Carcastillo	42.372	-1.463	10	1992/03-2005/05
10	Carrascal	42.683	-1.660	10	1992/01-2005/05
11	Doneztebe	43.132	-1.660	10	1999/06-2005/05
12	Perdón	42.733	-1.709	10	1992/03-2005/05
13	Estella-Lizarra	42.676	-2.028	10	1992/03-2005/05
14	Etxarri-Aranatz	42.910	-2.057	10	1992/03-2005/05
15	Getadar	42.605	-1.457	10	2000/05-2005/05
16	Gorramendi	43.220	-1.432	10	1992/05-2005/05
17	Lumbier-Ilumberri	42.668	-1.275	2	2000/05-2005/09
18	Montes del Cierzo	42.133	-1.652	10	1998/07-2005/07
19	Oskotz	42.956	-1.756	10	1999/03-2005/05
20	Pamplona-Larrabide	42.810	-1.638	10	1997/01-2005/06
21	Pamplona-Noain	42.769	-1.639	10	1992/04-2005/09
22	Sartaguda-Riegos	42.363	-2.050	2	1998/03-2005/09
23	Tafalla	42.522	-1.676	10	1992/03-2005/06
24	Traibuenas	42.363	-1.614	2	1999/04-2005/09
25	Trinidad de Iturgoien	42.819	-1.975	10	1992/01-2005/07
26	Ujué	42.513	-1.510	10	1992/01-2005/07
27	Valdega	42.657	-2.172	2	2001/05-2005/09
28	Villanueva del Yerri	42.736	-1.949	10	1998/01-2005/05
29	Yesa	42.618	-1.190	10	1992/03-2005/06

and thus cancel each corresponding contribution to the resulting module. The mean flow in the CFN is from NW to SE and it is channeled from the northern valleys along the Ebro Valley (Jiménez et al., 2008a). As explained in Section 2.1, this corresponds to the characteristic cold and dry wind pattern known as *Cierzo* while the flow in the opposite direction (SE to NW) resulting from the advection of moist and warmer air from the Mediterranean is known as *Bochorno*. The dashed lines in Figure 2.5 show the standard deviation of the wind module.

The spatial variations of wind and its deviation are coincident to a good degree, which is a typical feature of positively defined variables like precipitation (Xoplaki et al., 2004). It is worth noting that some locations at the north and centre of the region reveal a higher mean wind than the rest of the sites. Some of these sites correspond to the wind farms, located at higher elevations, less influenced by smaller scale orographic features. Two of the wind farms show a more NE-SW flow in agreement with the mean direction at the surrounding stations while the other, more northerly located, presents a more SE-NW direction. In fact, the northern area in the CFN is exposed to a different large scale circulation regime than the central and southern sections of the region under study (Jiménez et al., 2008b).

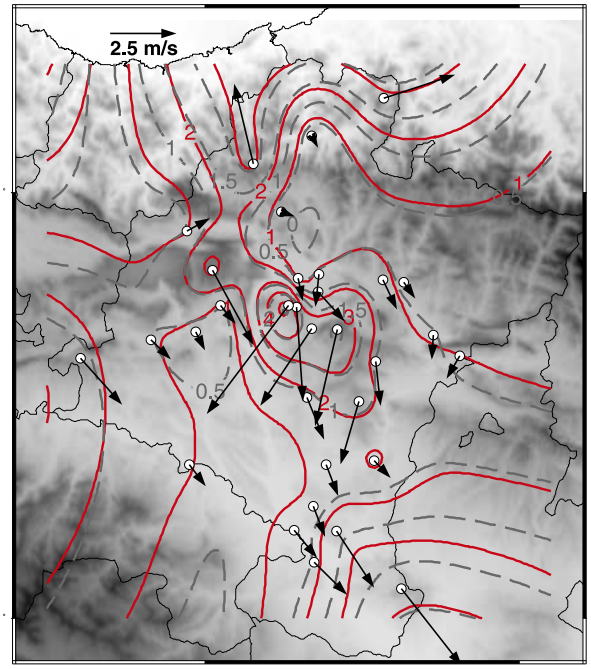

Fig. 2.5: Observed mean zonal and meridional wind components (vectors) and wind module (red solid contours). Dashed contours show the spatial variations of the wind module standard deviation.

The spatially averaged, hereafter the *regional*, time series of the zonal and meridional observed wind components and wind module are represented in Fig-

ure 2.6. It can be appreciated that, the wind component series present opposite sign throughout the whole period; their correlation value being -0.77. This suggests a conservation of the surface momentum at these timescales, i.e, the kinetic energy is transferred from one component to the other so that an increase (decrease) in the zonal (meridional) component entails a decrease (increase) in the meridional (zonal) one. As the prevailing direction of the mean flow in the region is established by the channeling effect of the Ebro Valley, this orographic axis acts as a physical constraint that favours a momentum transfer between both wind components. Changes in the wind module (Figure 2.6) present significant intra and inter annual variability which could be of great interest, e.g, in the context of wind energy and that will be better understand in Part II of this work, where this dataset will serve as the predictand field in downscaling exercises.

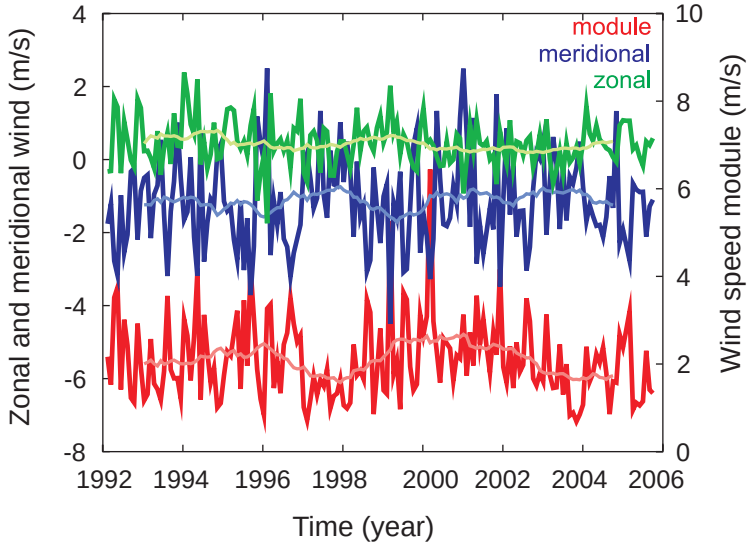

Fig. 2.6: Regional zonal (green) and meridional (blue) observed wind components and wind module (red) throughout the whole observational period. The corresponding three years moving average is also represented.

2.4 Large scale fields

Six gridded (2.5^o latitude x 2.5^o longitude) variables over the North Atlantic region and Europe are used as predictor fields for the CCA exercise: SLP, 850 hPa and 500 hPa geopotential heights (ϕ_{850} and $\phi 500$), 10-m height zonal (U10) and meridional (V10) wind components and 500-850 hPa thickness data ($Z_{500-850}$). These data will play the role of predictor field(s) in Part II of this work. Monthly mean values are calculated from the original 6-hour resolution time series. Data are taken from the ERA-40 reanalysis of the European Center for Medium-Range Weather Forecast (ECMWF; Uppala et al., 2005) from 1992 to 2002. Analyses from the ECMWF general model outputs are also used to complete the whole period of observations (2002 to 2005), however and for the sake of simplicity this database will be referred to as the ERA-40 fields from now on. The strategy of combining both ERA-40 and the ECMWF datasets has been used previously in other studies as in Fisher et al. (2007) or in Jiménez et al. (2010b). Jiménez et al. (2010b) performed a numerical simulation of the wind field using both datasets as initial and boundary conditions over the same target region and period. No evidences of inhomogeneities due to the use of the two forcing datasets were found, thus, it appears reasonable to use the same set up to overcome the lack of reanalysis data after 2002.

For two additional exercises that *i)* explore the uncertainty related to the use of different datasets as large scale predictors (Chapter 5) and *ii)* provide a wind field and wind power past reconstructions (Chapters 5 and 6), only one variable, the SLP from different sources with longer temporal coverage, is used. The datasets employed in these two parts of the work are: a) monthly SLP observations from 1899 to 2005 from the National Center for Atmospheric Research (NCAR; Trenberth and Paolino, 1980); b) an observational dataset provided by the Hadley Centre consisting of historical gridded monthly mean SLP (HadSLP2) for the period 1850-2004 (Allan and Ansell, 2006); and c) a SLP proxy-based reconstruction from 1659 by Luterbacher et al. (2002). This reconstruction is limited to a spatial domain ranging from 30^oW to 40^oE in longitude and from 30^oN to 70^oN in latitude and thus, all experiments including these datasets will be performed using that large scale domain with comparison purposes. This information regarding the large scale predictors used in the second part of work is summarized in Table 2.5.

Table 2.5: Characteristics of the datasets employed as large scale predictors: source and data type, variables considered within the dataset, period used for the analyses and spatial resolution.

Source	Type	Variables	period (yrs)	spat. res.
				(lat. x lon.)
ERA-40	Reana.	SLP,$\phi_{850,500}$,UV10,$Z_{500-850}$	1957-2005	2.5^o x 2.5^o
NCAR	Obs.	SLP	1899-2005	5^o x 5^o
Hadley Center	Obs.	SLP	1850-2005	5^o x 5^o
Luterbacher et al. (2002)	Recon.	SLP	1650-2005	5^o x 5^o

Part I

Relationship between wind speed and wind power

3

The influence of the Weibull assumption in monthly wind energy estimation*

Part I of this thesis is devoted to evaluate several methodologies that provide wind energy estimations. The implementation of these methodologies requires two sources of information: the probability distribution that the wind speed values follow and a transfer function for translating the wind velocities into wind power. Thus, this first part is divided into two chapters. In this one an estimation of the monthly wind energy output for the period 1999 to 2003 at the five wind farms described in Section 2.2 is provided. The methodology applied herein involves the use of an estimate of the wind probability distribution and the wind-wind power transfer function based on the observed average wind power *vs.* wind relation obtained from hourly data. The impact of assuming a theoretical PDF as a substitute of the actual histogram in the wind energy estimation is evaluated. Results reveal that the use of a Weibull probability distribution has a moderate impact in the energy calculation although the Weibull assumption is not strictly substantiated for most of the sites.

Section 3.2 presents and discusses the selection of representative wind and wind power series at each wind farm. Section 3.3 describes the methodology employed in the estimation of monthly wind energy as well as general aspects of the Weibull distribution, its empirical fit and the evaluation of the goodness of fit. Results are presented in Section 3.4. Finally, conclusions are presented in Section 3.5.

The next chapter will focus on the contribution to the errors in the estimation of wind energy due to the assumptions in the wind-wind power relationships.

* The main contents of this chapter are included in:
García-Bustamante, E., J. F. González-Rouco, P. A. Jiménez, J. Navarro and J. P. Montávez, 2008: The Influence of the Weibull Assumption in Monthly Wind Energy Estimation. *Wind Energ.*, **11**, 483-502.

3.1 Rationale: the need of assessing wind speed distributions

The use of alternative renewable energies has undergone a significant development through the last few decades in order to meet the increasing energy demand of industrialised countries and as an attempt of bringing new energy facilities to remote locations with little access to standard electrical networks (Ackerman and Soder, 2002; Jager-Waldau and Ossenbrink, 2004; Kenisarin et al., 2006). Wind energy has experienced a considerable expansion and the assessment of its resources and the variability they are subject to has become a relevant aspect from the economical, sociological and scientific points of view. Therefore, many efforts are focused on the analysis and understanding of the wind variability and its relation to wind energy production, as well as the determination and evaluation of potential local and regional wind energy resources.

Specifically, there has been an emphasis in improving the understanding of wind regimes and their variability at different timescales in order to assess the suitability of operating conditions, both to ensure quality in the generation of the electricity supply to the network and guidance in the long term management of large and small scale wind farms. The use and analysis of wind probability distributions have been some of the necessary lines of procedure due to its involvement in the computation of total available wind energy and wind energy distribution (wind power density). Numerous studies have paid attention to wind speed probability distributions in relation to a variety of topics such as wind energy development and sustainability (Jamil et al., 1995; Bechrakis et al., 2004; Ramírez and Carta, 2006), analysis of wind loads (Davenport, 1963; Holmes, 2002), studies of wave fields and surface roughness (Johannessen and Haver, 2002; Caires and Sterl, 2004; Beljaars, 1987), etc. The problems associated with these studies relate to an understanding of the wind, and often the wind power distributions. With this aim, a variety of theoretical probability distributions have been explored according to specific regions and site characteristics: Wentink (1974) investigated some methods of fitting the Planck distribution to explore the wind power potential in Alaska; both Baynes (1974) and Celik (2004) worked with the Rayleigh distribution, the former studied extreme winds which could affect structure design and the latter evaluated the suitability of this function to estimate wind energy; Sherlock (1951) used the Pearson Type III (gamma) family to describe wind speed distributions; García et al. (1998) employed the Lognormal and Weibull distributions to fit hourly wind speed data and to estimate wind energy production also in the CFN (IP), comparing it with experimental wind power production; Li and Li (2005b) and Ramírez and Carta (2006) analyzed the MEP-type distribution functions (a family of exponential probability distributions derived from the maximum entropy principle), and compared them with the Weibull distribution

in its ability to reproduce wind and wind power density. Of the above, the most frequently referred probability function is the Weibull distribution (Hennesey, 1977; Tuller and Brett, 1984; Palutikof et al., 1987; Jaramillo and Borja, 2004; Pérez et al., 2007).

The Weibull distribution has been employed using a number of different perspectives: on one hand, its suitability to reproduce some aspects of the wind speed frequency distribution (Conradsen and Nielsen, 1984; Dorvlo, 2002; Ramírez and Carta, 2005); on the other hand, the use of the Weibull function has been included in techniques that provide estimations of the available wind power (Celik, 2003a,b; Pryor and Schoof, 2005) and, from this perspective, it has been used to assess the suitability of specific locations to generate wind energy (Chang et al., 2003; Akpinar and Akpinar, 2005a).

Within the context described above, wind energy density is calculated through two main approaches: either using the parameters derived from the fitted theoretical distributions (Jamil et al., 1995; Weisser and Foxon, 2003; Pryor and Schoof, 2005) or through the calculation of the wind power density contribution from the particular range of wind speeds measured at a specific site (Celik, 2003b; Chang et al., 2003; Akpinar and Akpinar, 2005a; Mathew et al., 2002; Carta and Ramírez, 2007). The following is concerned with the second approach in which the wind energy estimation is obtained through the product of the power corresponding to each wind value by the probability of each wind speed (Celik, 2004, 2003a; Biswas et al., 1990). In practice, the relationship between wind power and wind is expressed in terms of a transfer function which relates both variables. This can be either a theoretical power curve (Frandsen et al., 2000; Bivona et al., 2003; Noorgard and Holttinen, 2004) provided by the manufacturer, or some specifically interpolated or fitted curve representing power *vs.* wind that expresses the effective relationship present in the actual data set (Celik, 2003c). In general, the errors in this approach will stem both from the approximations made to express the wind power *vs.* wind relationship and from those relative to the assumption of a given theoretical frequency distribution. This chapter is devoted to the latter source of error and efforts are made to illustrate and quantify the contribution to the error of the probability terms in estimating total wind energy. Chapter 4 will complete the analysis herein by extending the evaluation of potential errors in wind energy estimations derived from assuming a certain wind-wind power transfer function. For this purpose, monthly observations (see Section 2.2) of wind energy and estimations are compared herein. The analysis assumes an *a priori* selection of the Weibull function as a candidate to fit the experimental histograms. This choice was made on the basis of its extended use, since it is the most frequent probability density function in wind and wind energy studies (Pavia and Orien, 1986; Mathew et al., 2002; Bivona et al., 2003; Deaves

and Lines, 1997; Weisser, 2003; Pryor et al., 2005b). It additionally provides a good fit to the wind speed distribution (Conradsen and Nielsen, 1984; Lun and Lam, 2000), replicates its skewness well (Celik, 2003a) and provides a suitable estimation of the cube wind speed for wind power analyses (Celik, 2003b). The selection was based also on the fact that previous studies (García et al., 1998) have found this distribution appropriate for specific sites in the same area of the IP. However, the analysis will evidence that a Weibull distribution is not adequate for all sites and time steps. The impact that the quality of the fit of Weibull statistics to the observed values has on the final estimation of wind energy will be discussed. In doing so, an overall evaluation of the total error obtained using this approach (under the assumption of the Weibull statistics) is also provided. The study uses the data from five wind farms located in the CFN described in Section 2.2.

3.2 Preliminary aspects of the wind-wind power relation: analysis of observations

This section presents the rationale for the selection of the representative wind and wind power data at each site. The arguments for such a selection, especially for the case of the wind power production, are based in the consistency between wind velocity and turbine output records and incorporate some technical aspects that, to some extent, are relevant for the observed behavior of both variables at the wind farms.

The hourly power outputs from every wind turbine (presented in Section 2.2) were averaged to obtain the corresponding number of series (as many as turbine types installed, see Section 2.2) representative for the whole location. The alternative to the use of a single series at each wind farm would be to use the records at every wind turbine. This strategy could potentially improve the estimation, as the information from each mast would provide a more realistic wind speed-wind power relation at individual turbines. Nevertheless, this work leans on the use of single average wind power series per farm. Several reasons have favored this simplified approach, as for instance, a small variation of the wind power production from turbine to turbine or the constraining fact that in this case study four out of the five available wind farms have wind speed measurements available at only one location within the farm. This limitation is in practice not severe since changes in variability of power production among turbines are very small, particularly at monthly timescales as can be seen in Fig. 3.1, where the monthly power outputs from every wind turbine in Alaiz, as an example, are represented showing high temporal concordance among the whole set of wind turbines. In addition, the ultimate goal of this chapter is to explore the impacts

of the Weibull assumption in the calculation of monthly wind energy, rather than refining as much as possible our estimates and to illustrate, in a parsimonious rather than sophisticated approach, the advantages and disadvantages of various strategies to estimate monthly wind power production.

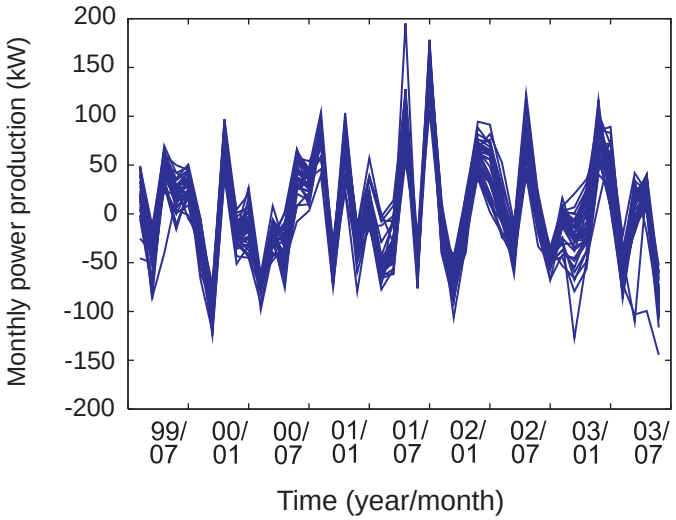

Fig. 3.1: Monthly mean wind power outputs from every wind turbine in Alaiz.

Nevertheless, the use of a pair of average time series as representative of the whole wind farm introduces some perturbations in the wind power *vs.* wind relation at hourly timescales. Fig. 3.2 illustrates this by showing, for each wind farm, the theoretical power curve (TPC) together with the dispersion diagram of the hourly wind-wind power pairs. For reasons of simplicity, in the cases of wind farms with several wind turbine models (El Perdón, Leoz and San Martín), diagrams include only hourly data from one model of turbine. The hourly pairs and the TPC shown in Fig. 3.2 correspond to the model G42-600 in all wind farms except for Alaiz (G47-660). The dispersion of points observed in Fig. 3.2 reveals that the actual production can deviate considerably from the TPC, either distributing around it for intermediate or low wind speeds or typically below the *rated power* at high wind velocity values (e.g. Alaiz, Aritz or San Martín). However, wind power values higher than the theoretical rated power can also be observed (El Perdón, Leoz). Thus, smaller than theoretically expected wind power values are present in most sites for high wind speeds and conversely larger

than expected power outputs are achieved for some small wind velocities. These deviations of the actual power outputs from the expected can be related to some extent to the methodological approach commented above, i. e., the average over the total set of turbines to obtain the total power production, together with other methodological issues like the fact that in some wind farms wind speeds are recorded at a meteorological mast instead of the exact turbine locations or the use of single pair of wind speed and wind power series to represent the whole wind farm. In addition, the hourly dispersion could stem from many factors such as manipulation of the turbine parameters to meet different operational conditions, shading effects of neighboring wind masts, the effect of turbulence on short timescales, or the influence of changes in air density could lead to deviations from the expected wind speed-wind power relationship.

Further, it is interesting to note the strong power reduction for some cases close to the *cutoff* wind value, particularly in Alaiz, Aritz and El Perdón, which is mainly due to the spatial averaging effect. Such patterns of behavior are related to the operational control management that forces some wind turbines to stop and thus, reduces the average wind power production relative to the expected values. This can happen for various reasons such as for technical assistance, breakdown or for instance, security reasons in order to avoid damages due to high aerodynamic loads. In the case of the latter a subset of wind turbines in the area of the highest intensity winds in the farm are switched off but at the same time other turbines within the wind farm may still generate power at high wind velocities. The average over all muted and operating turbines produces a power decrease for high wind speed values (Aubrun et al., 2005).

Regarding the averaging of wind speed records from each turbine at the hub height (in Leoz) *vs.* the use of a wind series recorded at each meteorological mast (the rest of wind farms), it is also worth to remark that in Leoz the hourly observations are less dispersed than in the rest of the locations. This evidence could point out that the power generated is sensitive to wind speed variations along distances within the wind farm dimensions and that using wind data from a single meteorological mast (i. e., less precise than measurements at each turbine location) could contribute to the mentioned scattering. The latter is illustrated in Fig. 3.3, where two variants of the hourly wind speed-wind power dispersion diagrams in Leoz are represented. The diagram in Fig. 3.3a is calculated by using the wind velocity and wind power recorded at a single turbine arbitrarily selected as an example, whereas for the one in Fig. 3.3b the wind speed corresponds to a meteorological mast in the wind farm and the power outputs are the average over the whole set of turbines. Thus, the diagram for Leoz in Fig. 3.2 represents an intermediate situation between considering the specific wind and wind power at a particular turbine (Fig. 3.3a) and considering a representative

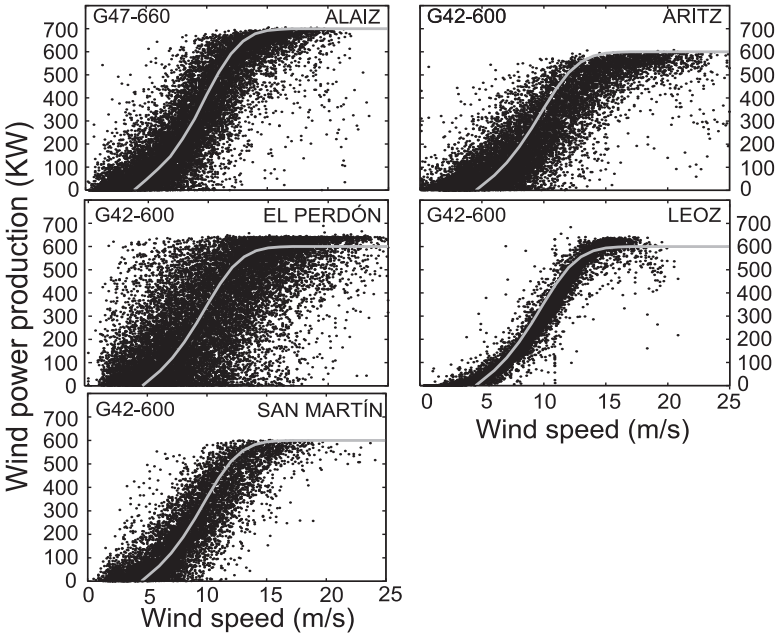

Fig. 3.2: Dispersion diagrams of wind and wind power hourly values (points) obtained at each of the wind farms. Theoretical power curves are also shown (lines) for comparison. For simplicity, only one type of turbine model and the corresponding hourly data are arbitrarily shown in farms with multiple turbines types (G42-600 kW turbine model is used as example in all locations except for the case of Alaiz, where the model used is the G47-660 kW).

wind and power series identically as in the rest of wind farms (Fig. 3.3b). The dispersion is substantially reduced in the first case while in the second variant the use of a reference wind series, instead of the average of the wind measured at each turbine, introduces additional dispersion of the hourly pairs. Therefore, potentially more elaborated schemes could incorporate the use of wind observations at each turbine. This approach would not necessarily suffer from turbulence effects since wind speed observations recorded with specific instrumentation at hub height (e.g. nacelle anemometers in the case of Leoz) incorporate corrections from possible distortions caused by shading or wake effects among turbines (Barthelmie et al., 2007). Nevertheless, the analysis of the potential sources of

scattering in the wind speed-wind power diagrams is of relevance since it helps to understand to what extent the TPC or any substitute of it is representative of the observations.

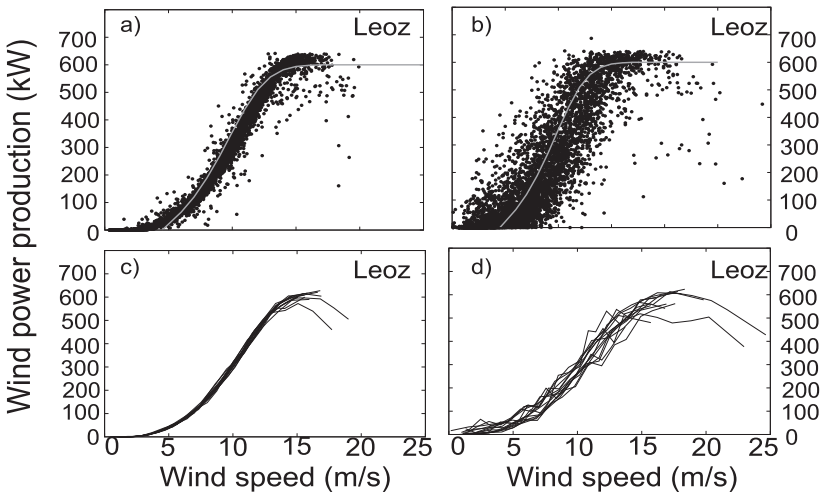

Fig. 3.3: Dispersion diagrams of wind and wind power hourly values (points) obtained at Leoz a) by using wind speed and power outputs from a particular turbine randomly selected for illustration and b) using the wind speed measured at a reference meteorological mast together with the average power outputs from every wind turbine (as in the rest of the wind farms). Theoretical power curves are also shown (lines) for comparison. G42-600 kW turbine model is used. c) and d) represent the effective power curves at Leoz in the same situations of a) and b), respectively.

Fig. 3.4 illustrates the variability in the monthly wind-wind power relation produced by the perturbations discussed in Fig. 3.2. Monthly *effective power curves* (EPCs) are obtained from the hourly values through the average of wind power measurements within each wind speed interval. As in the case of Fig. 3.2, to obtain the EPCs shown in this figure data corresponding only to one model of wind turbine has been used (G47-660 in Alaiz and G42-600 in the rest of wind farms). Aritz and El Perdón are the sites showing more month to month variability while Leoz and San Martín show less scattered wind-wind power pairs, a feature compatible with the standard deviation values in Table 2.2. In the case of Leoz the smallest dispersion of the EPCs can be influenced by the fact of having

wind measurements at each wind turbine. Therefore, the reduced variability of the EPCs at this site suggests that the average of mast specific wind values provides a better representation of the wind-wind power relation for the whole wind farm than using observations from a single meteorological station as in the other wind farms. To further illustrate this, the EPCs corresponding to the alternative situations of using measurements of the wind-wind power pairs at a particular turbine or using averaged power and reference wind records are also represented in Figs. 3.3c and 3.3d respectively, for comparison. The monthly dispersion of EPCs decreases (increases) in the first (second) case with respect to the scattering in Fig. 3.4 for Leoz, as expected.

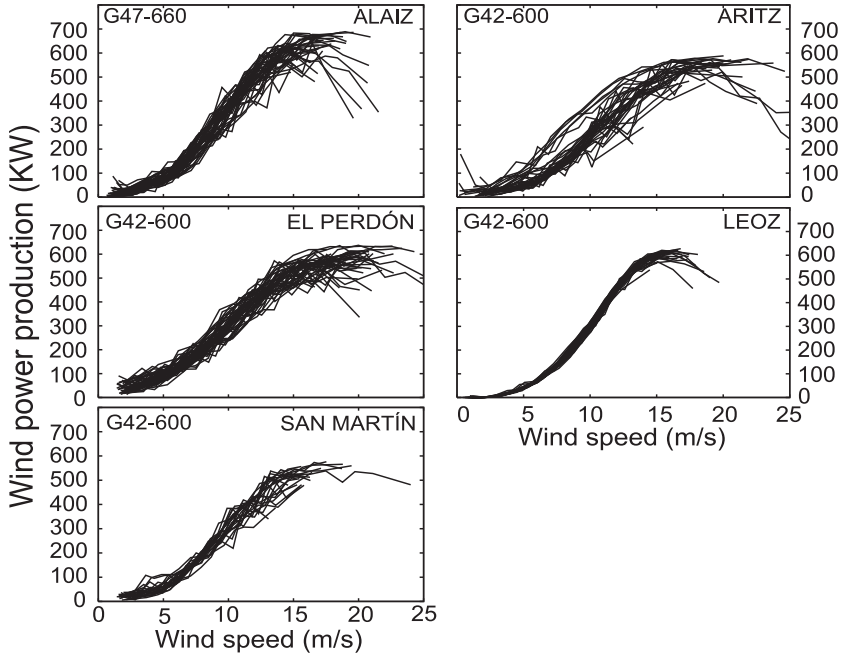

Fig. 3.4: Effective power curves at the different wind farms. Each curve depicts the observed wind power *vs.* wind relation for each month within the dataset. The data used to represent the EPCs correspond to the turbine model G47-660 kW in Alaiz while for the other sites the model G42-600 kW is employed.

The total monthly mean wE ($\overline{wE}$) and its corresponding standard deviation (S_m) are indicated in the second column of Table 2.2. The final total production depends on the balance between the number of wind turbines available (see Table 2.1) and the rated power. The maximum monthly energy production is achieved in Alaiz, where the most powerful turbines of the type G47-660 kW, are installed. Aritz is the location with less energy production stemming both from a lower rated power and fewer turbines.

Correlations between the monthly power production series corresponding to the different turbine models are larger than 0.9 at El Perdón, Leoz and San Martín. For this reason, results concerning only one type of turbine (G42-600 kW) will be shown in the three sites for simplicity from here on.

3.3 Methodology

The approach used to estimate monthly wE production is based on the use of the hourly frequency distribution of wind velocity within each month and an estimate of the power production dependence on wind, based, for instance, on the theoretical power curve or some substitute of it obtained from the observations (Celik, 2004, 2003b,c).

An estimation of the total monthly wind energy (wE) production can be obtained from summing all the power contributions from the various wind classes considering their frequency of occurrence and scaling the sum to the total number of time steps and turbines in the farm:

$$wE = \Delta t N N_t \sum_{i=1}^{n} p_{out}(w_i) f(w_i), \tag{3.1}$$

where $f(w_i)$ is the expected frequency for each of the n wind speed class intervals represented by w_i and $p_{out}(w_i)$ is a transfer function for the wind power *vs.* wind relationship that provides an estimation of the power production for a given w_i; Δt is the time resolution of the input wind speed data (1 hour), N is the total number of hours per month and N_t is the number of wind turbines. In those wind farms with several types of turbines installed, Eq. (3.1) is computed for each group of wind turbines, with different $p_{out}(w_i)$ and N_t and the results are summed to provide a single estimation for the whole wind farm. Consequently, this method produces a cumulative contribution of the frequency of wind in each interval to the total wind power production by multiplying the frequency terms by the corresponding power contribution of each bin, $p_{out}(w_i)$. Many practical cases involve situations in which wE must be estimated without knowing the precise wind frequency distribution, $f(w_i)$, or the exact wind power *vs.* wind

relation, $p_{out}(w_i)$. In such cases, two potential sources of error are involved in the wE estimation through Eq. (3.1): one stems from the use of an approximation for $p_{out}(w_i)$, for instance if the theoretical/manufacturer power curve is used (Akpinar and Akpinar, 2005a; Seguro and Lambert, 2000); the other is associated with the use of a theoretical distribution for $f(w_i)$ (Ramírez and Carta, 2006; Pryor and Schoof, 2005; Li and Li, 2005a).

As previously mentioned, the use of an approximation for $p_{out}(w_i)$ introduces an error related to the fact that the power curve itself is an approach to the more complex actual wind-wind power relation (see Fig. 3.2) which also varies with time (e.g. Fig. 3.4). Due to factors such as turbulence, the effect of wind velocity reduction caused by the shadow between turbines, the variability of wind direction, etc., the actual power production does not coincide exactly with what theoretical power curves predict. Furthermore, the use of a global (spatially averaged in this work) power curve also introduces perturbations with respect to the expected power production since the wind power generation from each individual wind turbine within the site is not identical to the rest (Noorgard and Holttinen, 2004). The use of a theoretical probability distribution instead of the observed wind velocity frequency involves an additional source of error when estimating wE in Eq. (3.1) as much as the specific wind speed frequency distribution of a certain month deviates from the shape of the assumed theoretical probability distribution function.

This chapter is devoted to explore the second source of error through evaluating the extent to which the assumption of a given probability distribution, $f(w_i)$, can contribute to the error in the final monthly wE estimation. A complete evaluation of errors involves analyzing the impacts of selecting a certain $p_{out}(w_i)$ power curve. Thus, some of the results obtained herein do have implications concerning the effect of the $p_{out}(w_i)$ and this source of error will be subject of attention in Chapter 4.

The Weibull probability distribution has been selected for this study in the basis of the arguments provided in Section 3.1. A limitation of the Weibull density function is that it can not estimate with accuracy the probability of calms or very low wind velocities (Weisser and Foxon, 2003). However, this aspect does not produce a considerable impact on the final wE estimation as, for the lowest wind intervals, there is no relevant contribution to the wind power production, i. e., the corresponding $p_{out}(w_i)$ is negligible in comparison to the power associated with the largest wind velocities, see for instance the values in Figs. 3.2 and Fig. 3.4 for low wind speeds. For wind velocities below 4 ms^{-1} the production is 0 kW and for wind speeds smaller than 6 ms^{-1} the power output is under 100 kW. Though the selection of a particular probability distribution such as the Weibull can inevitably narrow the final conclusions to the specific case studies in which

this distribution is used, the following sections will arrive at some implications which attain a broader focus.

The evaluation of the error contribution from the probability terms $f(w_i)$ can be easily done through establishing a maximum benchmark level of predictability with respect to which other errors can be defined. Of all possibilities, the most accurate estimation of wE with Eq. (3.1), would be the one obtained by using the observed frequency histogram in each specific month as $f(w_i)$ and the observed wind power *vs.* wind relation as $p_{out}(w_i)$, within each particular month. The variability in the actual monthly frequency distributions and effective power curves is shown in Figs. 2.2 and 3.4. Such an estimation serves as the most accurate estimation possible and therefore as a benchmark of the upper limit of predictability that can be obtained using Eq. (3.1). This estimate will be denoted as wE_{H-ref}. The error made by this estimation is obtained by calculating the difference between wE_{H-ref} and the observed wE (wE_{obs}), and will be denoted as

$$\xi_1 = wE_{obs} - wE_{H-ref} \tag{3.2}$$

This quantity provides information about the error in the method described by Eq. (3.1), independent on any assumption made on $p_{out}(w_i)$ and $f(w_i)$. This error is derived from the extent to which the EPC is a bad representation of the wind power *vs.* wind relation in the different masts and from the approximation which implies considering a frequency histogram. If, in a limit case, the wind power *vs.* wind transfer function was perfect, when using point values, the estimated and observed wE would converge.

The second control estimation calculated also assumed the corresponding *EPC* for each month as $p_{out}(w_i)$, but in this case, the theoretical Weibull frequencies were employed as $f(w_i)$ in Eq. (3.1). This estimation is denoted as wE_{H-EPCw}. As wE_{H-ref} and wE_{H-EPCw} only differ in the use of the Weibull expected frequencies in one case and the observed ones in the other, the contribution to the error of the frequency terms, under the assumption of a Weibull distribution can be studied from the difference between both previous estimations,

$$\begin{aligned} \xi_2 &= wE_{H-ref} - wE_{H-EPCw} \\ &= \Delta t N N_t \sum_{i=1}^{n} p_{out}(w_i) f_{obs}(w_i) - \Delta t N N_t \sum_{i=1}^{n} p_{out}(w_i) f_{weib}(w_i) \\ &= \Delta t N N_t \sum_{i=1}^{n} p_{out}(w_i) \left[f_{obs}(w_i) - f_{weib}(w_i) \right], \end{aligned} \tag{3.3}$$

This should help to understand qualitatively and quantitatively the effect that discrepancies between the observed and the expected Weibull frequencies produce in the monthly wE estimation at the locations considered. A third error that addresses the combined effect of both kinds of error described above is provided by

$$\xi_3 = wE_{obs} - wE_{H-EPCw} \tag{3.4}$$

This magnitude incorporates the effects of assuming a certain probability function to the method errors in ξ_1.

3.3.1 Fitting to the Weibull probability distribution

The Weibull probability density function (Justus et al., 1977; Takle and Brown, 1978),

$$f(w) = \frac{k}{c}\left(\frac{w}{c}\right)^{k-1} exp\left[-\left(\frac{w}{c}\right)^{k}\right], \tag{3.5}$$

where w is the wind speed, is defined by two parameters, k and c. k is the dimensionless *shape parameter* related to the variability of wind and therefore, provides an approximation of the flatness of the distribution. c is the *scale parameter* in ms^{-1}, and is related to the mean value of the distribution (Pérez et al., 2007). In this work, both parameters defining the Weibull function are calculated using the *method of moments*, which provides a suitable estimation of the parameters (Fawzan, 2000; Seguro and Lambert, 2000; Gove, 2003) and the best result for the higher wind speed values in the distribution according to Tuller and Brett (1984). This method is based on the calculation of the first n sample moments and the use of them as estimators of population parameters of the distribution. The mean Weibull parameters, calculated over the whole period of data, and their corresponding standard deviations are summarized in Table 3.1 (columns 3 to 4). The overall values of the shape parameter distribute close to the value $k = 2$, typical in practice (Biswas et al., 1990) and the limit value in which the Weibull distribution reverts to the Rayleigh distribution. The deviation of k is larger at Aritz and El Perdón, an unsurprising feature in view of the variability of the monthly distributions (points) in Fig. 2.2 and the wind speed standard deviation values in Table 2.2. The scale parameter (c) provides larger values for Aritz and El Perdón, the sites with maximum wind speed; deviations for this parameter are also larger at these sites.

The goodness of fit of the Weibull adjusted distributions to the observed data was established in terms of the χ^2 statistic. This allows to test the null hypothesis

Table 3.1: Mean Weibull parameters ($\overline{k}$, $\overline{c}$), monthly mean estimations using the observed histograms (wE_{H-ref}) and estimations using the Weibull histograms (wE_{H-EPCw}) and their respective standard deviations (S_k, S_c, $S_{wE_{H-ref}}$, $S_{wE_{H-EPCw}}$) at each wind farm.

	$\overline{k} \pm s_k$	$\overline{c} \pm s_c$	$\overline{wE_{H-ref}}$ ($S_{wE_{H-ref}}$)	$\overline{wE_{H-EPCw}}$ ($S_{wE_{H-EPCw}}$)
	(adim.)	(ms^{-1})	(GWh)	(GWh)
Alaiz	2.0 ± 0.3	9.0 ± 1.3	3.4 (0.8)	3.2 (0.8)
Aritz	2.1 ± 0.5	9.4 ± 2.1	2.0 (0.8)	2.0 (0.8)
El Perdón	2.4 ± 0.4	11.4 ± 1.5	3.2 (0.6)	3.1 (0.5)
Leoz	2.1 ± 0.2	8.9 ± 1.0	2.2 (0.5)	2.0 (0.4)
San Martín	2.5 ± 0.2	9.1 ± 1.2	2.8 (0.7)	2.8 (0.7)

that the actual sampled data follow a Weibull function (Akpinar and Akpinar, 2005b; Dorvlo, 2002). The test statistic is defined as:

$$\chi^2 = \sum_{i=1}^{n} \frac{[O(w_i) - E(w_i)]^2}{E(w_i)} = N \sum_{i=1}^{n} \frac{[f_{obs}(w_i) - f_{weib}(w_i)]^2}{f_{weib}(w_i)}, \tag{3.6}$$

with $O(w_i)$ and $f_{obs}(w_i)$ being the absolute and relative observed frequencies for interval i, $E(w_i)$ and $f_{weib}(w_i)$ the absolute and relative expected Weibull frequencies for the same interval and N the total number of observations. The presence of the expected frequency in the denominator in Eq. (3.6) attempts to weight the squared differences between frequencies eliminating the dependence on the specific shape of the distribution. That is, with the expected Weibull frequency in the denominator all intervals have the same weight in the calculation of differences. χ^2 will be used in the next section to analyze the goodness of fit and to illustrate its relationship with the error in the total monthly wE estimation.

One further comment is needed to address the sensitivity of χ^2 test to the number of intervals and the existence of missing data. χ^2 is sensitive to the choice of the number of intervals to calculate histograms and differences in Eq. (3.6). Also Eq. (3.6) is sensitive to small frequency numbers in $f_{weib}(w_i)$ which are often related to the handling of the wind intervals at the tails of the distribution. In order to mitigate this problem, the same conditions were imposed to each monthly histogram, that is, the number of intervals were fixed and the tails of the distribution were forced to contain 3% of the data. The question whether the selection of a specific number of intervals may affect the conclusions met by the analysis of the goodness of fit can be assessed by exploring the sensitivity of the χ^2 values to a varying number of intervals. This is calculated at Leoz as

an example and represented in Fig. 3.5. Monthly χ^2 tend to slightly increase as the number of intervals increases, although the variability of the time series is similar for all cases explored (Fig. 3.5a). This could lead to a situation in which the Weibull null hypothesis may be accepted or rejected, depending on the selection of the number of intervals selected, for some months. Nevertheless, from Fig. 3.5b it can be said that as the number of intervals increases, and so does the mean χ^2 value, the critical value increases accordingly, pointing out that if n is kept constant the number of months that verify the Weibull assumption does not change significantly regardless of the specific value selected for n.

The presence of a varying number of missing data in each month would also affect the results in Eq. (3.6). This could make it difficult to discriminate whether changes in χ^2 correspond to a feature of the methodology or to the varying number of observations in each monthly sample, which could plausibly influence the resulting values obtained in Eq. (3.6). Additionally, final monthly estimations of wE in Eq. (3.1) could be affected by the lack of data at certain months which could lead to an inaccurate result when computing contributions from the available hourly data. This possible perturbation was avoided by randomly selecting a fixed number of 350 hours (ca. 50% of observations in each month) from the available wind-wind power pairs for each month (see section 2.2). This number, as commented in the previous section, represents a balanced decision between using months with a very low number of observations, which might not adequately represent the monthly means and totals and alternatively, selecting only months with a high number of measurements, which would lead to a scarceness of monthly records in original the data set.

3.4 Analysis of results

This section compares the observed and calculated monthly wind energies at the five sites and analyzes the implications of using a Weibull probability function to model wind behavior. Section 3.4.1 presents the errors associated with the use of Eq. (3.1) and evaluates the impact of using the Weibull probability distribution on the energy estimations in terms of the behavior of the errors at each site along the period of observation. Section 3.4.2 explores the relation of the error terms with the quality of the fit through illustrating and discussing systematic biases in the Weibull fit at the various sites.

3.4.1 Errors in wE estimation

The time evolution of the observed total monthly wind energy (wE_{obs}) is compared to the resulting wE_{H-ref} and wE_{H-EPCw} estimations in Fig. 3.6 for

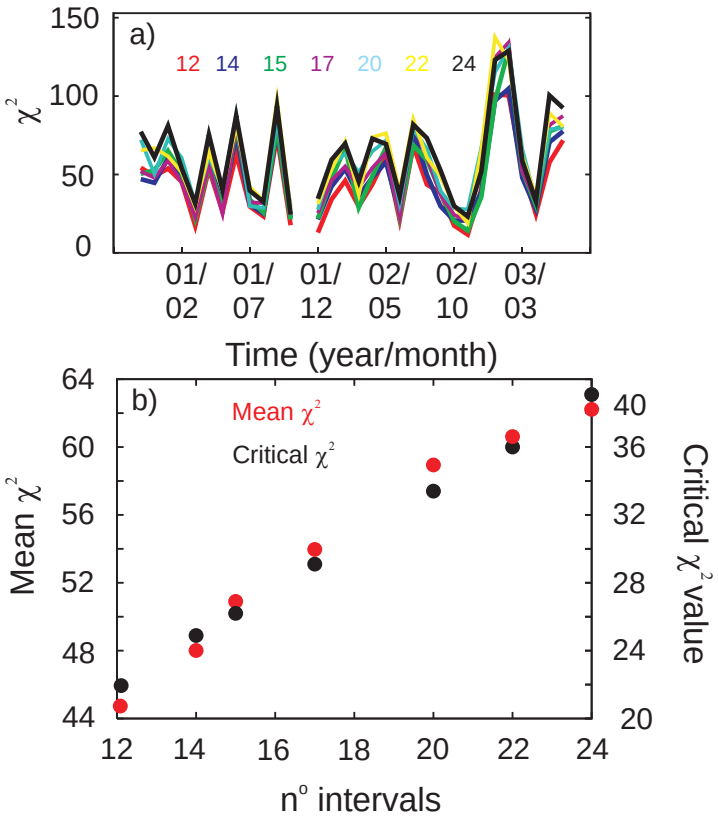

Fig. 3.5: Sensitivity of the χ^2 to the number of intervals considered in the goodness of fit test at Leoz. a) χ^2 time series as a function of the the different number of intervals (see legend), b) Mean χ^2 and critical χ^2 value depending on the number of intervals.

all wind farms. The mean values of the two estimated series (wE_{H-ref} and wE_{H-EPCw}) are shown in Table 3.1 (columns 5 and 6) for all locations. Both estimations are close to the monthly mean observed value (second column in Table 2.2). Fig. 3.6 shows that there is a general agreement between measurements and estimations in all cases analyzed. The estimations using a realistic power curve and actual monthly frequency histograms (wE_{H-ref}) are difficult to distinguish from the observational values (wE_{obs}). Substituting the frequency histograms by the Weibull approximation introduces a slight error that becomes obvious only

at Leoz, i.e., the largest error is found in Leoz for the wE_{H-EPCw} estimation which on average is no greater than 227 MWh (10.3%). It is interesting to note that wE_{obs} displays a considerable amount of intra annual and inter annual variability which wE_{H-ref} and wE_{H-EPCw} are able to capture. Such variability in energy production is likely related to changes in atmospheric circulation and will be dealt with in Chapter 6. As expected from the wind energy production means and standard deviations shown in Table 3.1, Alaiz and El Perdón are the sites reaching higher energy productions in Fig 3.6.

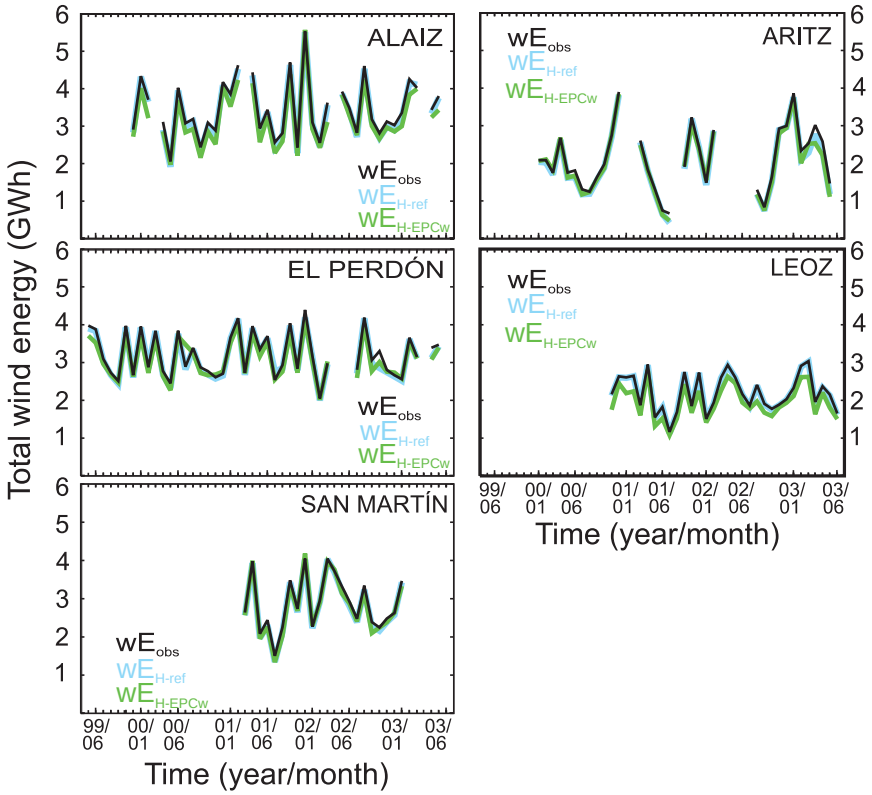

Fig. 3.6: Total monthly observed wind energy (wE_{obs}) and estimations (wE_{H-ref} and wE_{H-EPCw}) at each site.

The monthly evolution of the three types of error, ξ_1, ξ_2 and ξ_3 in the five wind farms, is presented in Fig. 3.7 and allows for some further insight into the error behavior. The errors are expressed in relative terms and they are the result of the division of the average total error by $\overline{wE_{obs}}$ in the case of ξ_1 and ξ_3 and by $\overline{wE_{H-ref}}$ in the case of ξ_2. It can be observed from Fig. 3.7 that most errors are positive, thus suggesting some bias to underestimate wE_{obs}. Celik (2003b) and Biswas et al. (1990) report results showing a tendency of the Weibull energy estimation to underestimate the reference energy in similar approaches. A summary with the averaged errors for the whole period at each site is given in Table 3.2. The smallest mean error corresponds to ξ_1 (wE_{obs}-wE_{H-ref}) at the three of sites (Alaiz, El Perdón and Leoz) and to ξ_2 (wE_{H-ref}-wE_{H-EPCw}) at Aritz and San Martín. Thus, the substitution of the empirical histogram by a fitted distribution does not necessarily lead to larger errors in the energy estimation in spite of introducing additional errors in the probability representation. This feature is also apparent in the time evolution of errors in Fig. 3.7. Though this might appear counter intuitive at first sight, it stems simply from Eq. (3.1) and will be discussed in the next section.

Table 3.2: Averaged relative (total) errors in monthly wE estimation at each wind farm (columns 1 to 3), average χ^2 values (column 4) and correlations (r) between ξ_2 and χ^2 time series at each wind farm (column 5). Columns 6 and 7 show correlations between errors and χ^2 for the wind intervals where the contribution to $Np_{out}(w_i)\,[f_{obs}(w_i) - f_{weib}(w_i)]$ is negative (ξ_2^-) and positive (ξ_2^+) (see text for details).

	$\overline{\xi_1}$	$\overline{\xi_2}$	$\overline{\xi_3}$	$\overline{\chi^2}$	r(ξ_2,χ^2)	r(ξ_2^-,χ^2)	r(ξ_2^+,χ^2)
	%(GWh)	%(GWh)	%(GWh)				
Alaiz	2.6 (0.1)	4.5 (0.2)	7.2 (0.2)	34.8	0.3	-0.5	0.5
Aritz	5.0 (0.1)	0.2 (4.10^{-3})	5.2 (0.1)	48.4	0.2	-0.5	0.6
El Perdón	1.7 (5.10^{-2})	2.4 (0.1)	4.2 (0.1)	36.8	0.5	-0.5	0.6
Leoz	0.9 (2.10^{-2})	10.3 (0.2)	11.3 (0.2)	55.0	0.6	-0.6	0.7
San Martín	2.9 (0.1)	0.3 (0.01)	3.0 (0.1)	29.2	-0.2	0.2	-0.2

The largest impact of introducing the Weibull approximations is found at Leoz where mean relative differences between wE_{H-ref} and wE_{H-EPCw} amount to 10.3% (see Table 3.2). These larger differences are also apparent in Fig. 3.7. Interestingly, the ξ_1 methodological errors at Leoz are considerably smaller than at the other sites, a feature that probably relates to the lower amount of variability

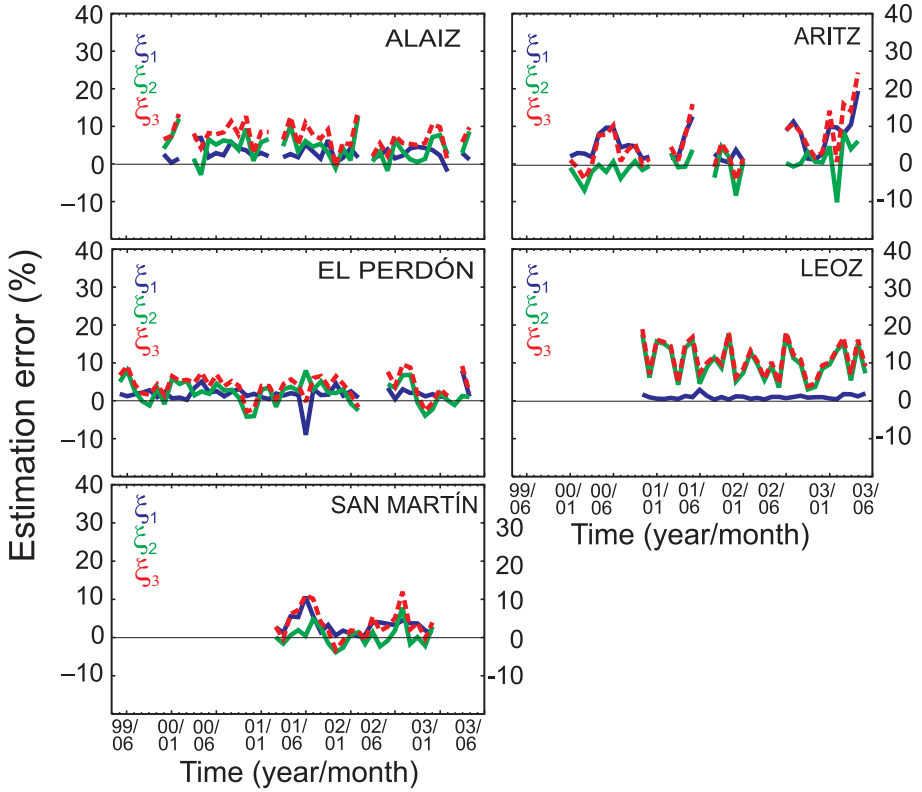

Fig. 3.7: Time series of monthly errors (ξ_1, ξ_2, ξ_3) in wind energy estimation at each site.

in the wind power *vs.* wind relation at this location (see Figs. 3.2 and 3.4), where a spatially averaged wind time series was computed from every wind turbine.

A last comment can be made concerning the behavior of the ξ_3 errors which basically accumulate the ξ_1 errors inherent to the method and ξ_2 related to incorporating a theoretical distribution function as a substitute for the observed histogram. As a result, changes with time in ξ_3 (Fig. 3.7) are coherent with those in ξ_1 and ξ_2 depending on which one has the largest contribution to the error.

3.4.2 Goodness of fit

The ξ_2 errors shown in Fig. 3.7 represent a relatively small part of the variability in wE_{obs} except for Leoz where they stand out amounting to about 10% on average. Even if the impact of *a priori* introducing the Weibull distribution assumption is relatively small, the associated errors still represent a considerable amount of energy and it is interesting to elucidate the reasons for such errors and the potential contribution of the goodness of the fit to them. In addition, it cannot be ruled out that, for other sites not considered here, such contributions may be larger, thus it is relevant to understand the role of the frequency terms in Eq. (3.3). For this reason, the error contribution of the Weibull distribution was evaluated through an exploratory analysis of the relation between ξ_2 and the monthly evolution of the goodness of the fit by means of the χ^2 statistic.

Table 3.2 (column 4) shows the average of all monthly χ^2 values at each site and Fig. 3.8 compares the monthly evolution of ξ_2 and χ^2 along the period of observation. The $\chi^2_{0.01,14}$ critical value, beyond which the null hypothesis is rejected for a 0.01% significance level and 14 degrees of freedom (the analysis uses 17 intervals for every month and 2 fixed parameters, k and c), is also shown. $\overline{\chi^2}$ averages in Table 3.2 show the lowest values for San Martín and the largest ones for Leoz in agreement with the relatively small ξ_2 values in Table 3.2 and Fig. 3.7 for both sites. It is interesting to note though, that Aritz shows a very low $\overline{\xi_2}$ while it displays a comparatively large $\overline{\chi^2}$. This suggests there is not a close correspondence between smaller (larger) ξ_2 and smaller (larger) χ^2. Fig. 3.8 allows for the assessment of this relation at a monthly resolution, studying the time series of χ^2 in comparison with ξ_2. The amount of months that satisfy the null hypothesis is variable from site to site. Though most of the months with available data at all sites register relatively low χ^2, close to or lower than the critical value, the percentage of months strictly respecting the threshold level is smaller, e.g. at Alaiz, El Perdón and San Martín, 29%, 33% and 60% of the months (respectively) show χ^2 values that strictly suggest a Weibull distribution and at Aritz and Leoz lower percentages of 2% and 14% are registered. Thus, according to this test, the initial assumption of using a Weibull distribution is not broadly met at all sites and time steps. To a large extent, San Martín can be considered Weibull distributed or very close to the Weibull distribution in most months, but this assumption is only partially substantiated at the other sites. In spite of this, the replication of the energy production is reasonable in Fig. 3.6 as previously illustrated. As it was argued before, the poorer quality of the fit along the period of observation at Leoz is consistent with the high $\overline{\xi_2}$. However, this link between larger (smaller) errors and worse (better) fit is not evident at every site and time step.

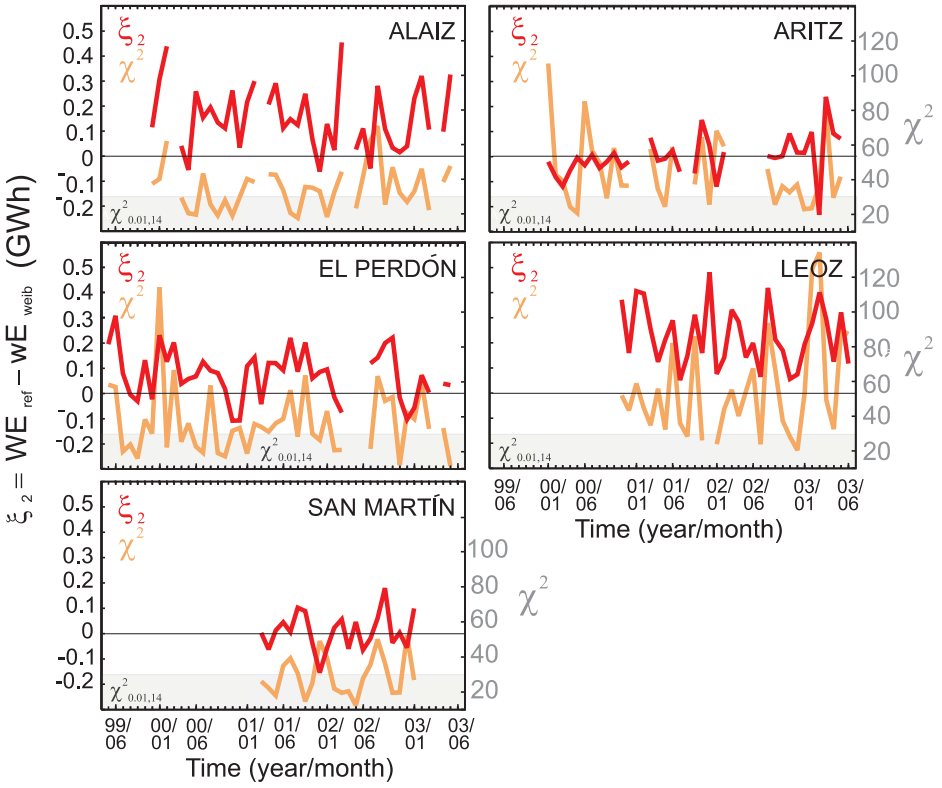

Fig. 3.8: Time series of ξ_2 errors and monthly values of χ^2 at each site.

The temporal variability in χ^2 and ξ_2 at Leoz reveals coherent changes that lead to a correlation of 0.6 linking larger (smaller) distribution errors to larger (smaller) energy errors. Correlations for the other sites are shown in Table 3.2 (column 5) with values of 0.3 at Alaiz and 0.5 at El Perdón and negligible values (0.2) at the remaining sites. Thus, some of the sites show some consistent temporal link between χ^2 and ξ_2, however, as it was argued on the basis of Table 3.2 above, larger (smaller) ξ_2 do not regularly coincide with larger (smaller) ξ_2 values suggesting that a closer Weibull fit does not guarantee smaller ξ_2 errors. For instance if the time series at Aritz is considered, May and June of year 2000 show respectively a low and a high χ^2 value that meets in the first case the critical level and considerably departs from it in the second, while at the same

time similar ξ_2 values are attained for both months; such type of events are not infrequent through the time series in Fig. 3.8. The reasons for this behavior can be found on the error contributions by the $[f_{obs}(w_i) - f_{weib}(w_i)]$ terms in Eq. (3.3).

Fig. 3.9 illustrates the quality of the Weibull fit for various χ^2 levels and provides some insight into their contribution to Eq. 3.3. Two examples of histograms and associated Weibull fits for low and relatively large χ^2 values at Alaiz and Leoz are. The selected months were arbitrarily chosen to be December 2001 and July 2002. For December 2001 deviations of the observed histogram from the Weibull shape produce χ^2 values of 19 (Alaiz) and 22 (Leoz). Larger deviations from the Weibull shape in July 2002 generate χ^2 values of 72 (Alaiz) and 95 (Leoz).

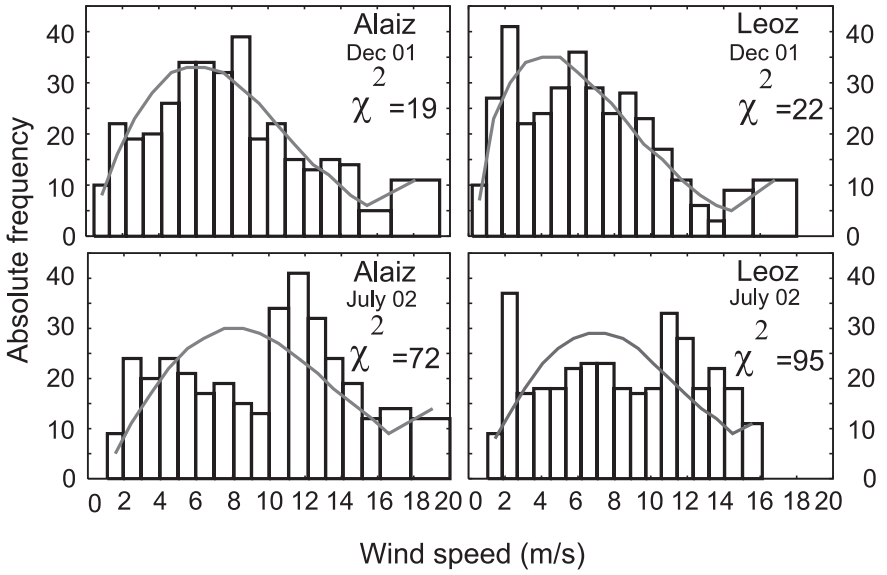

Fig. 3.9: Absolute frequency histograms (bars) and adjusted Weibull probability functions (scaled to absolute frequencies) for December 2001 and July 2001 at Alaiz and Leoz. χ^2 values are indicated for each case.

The larger differences contributing to the error in July are due to the Weibull function overestimating the observed histogram in the intermediate range of wind values and underestimating it in the lower and upper ranges. These discrepancies

between the observed and adjusted distribution seem to often present a similar pattern of over- (under-) estimation in the intermediate (lower and upper) wind ranges, i. e. negative (positive) values of the $[f_{obs}(w_i) - f_{weib}(w_i)]$ terms in Eq. (3.3). In order to illustrate this deformation in the observed histogram a dispersion diagram in which points represent the differences in absolute frequencies, $N\,[f_{obs}(w_i) - f_{weib}(w_i)]$ (observed minus expected absolute frequencies), for all intervals, in every month within the specific wind farm, is represented in Fig. 3.10, together with the line representing the average of all points. It can be appreciated that there is a tendency to under- (over-) estimate the Weibull frequency values in the lower and upper (middle) range of wind speeds, generating positive (negative) results in $N\,[f_{obs}(w_i) - f_{weib}(w_i)]$. This produces therefore positive (negative) contributions in Eq. (3.3) as it is the difference $f_{obs}(w_i) - f_{weib}(w_i)$ that imposes the sign to the error contribution in ξ_2=wE_{H-ref}-wE_{H-EPCw}.

This underestimation (overestimation) is more pronounced at Leoz and it is less noticeable at San Martín and Aritz. At Alaiz and El Perdón such deformation is also apparent in the experimental histogram. The error contributions of different sign tend, therefore, to be systematic in Fig. 3.10 and can be partially averaged out in Eq. (3.3). Thus in spite of having relatively large differences between the theoretical and actual frequency histogram, the impact of them can be at least partially balanced out by their sign, producing relatively small contributions in Figs. 3.6 and 3.7. Additionally, the differences between both distributions are weighted by the factor, $p_{out}(w_i)$ in Eq. (3.3). The most significant production of wE corresponds to the upper intervals of the histogram, that is, to the higher wind speed values, where the power generation is nearly the *rated power* (Fig. 3.2). Thus, the weight applied by the factor $p_{out}(w_i)$ is considerably greater for these intervals than for the rest. This makes their contribution to the errors larger. A dispersion diagram representing all the products, $Np_{out}(w_i)\,[f_{obs}(w_i) - f_{weib}(w_i)]$ is presented in Fig. 3.11. It shows that these products are negligible in the lower range of wind speeds as the energy produced here is also small. In the upper (intermediate) range of wind values the net contribution of the products in Eq. (3.3) becomes positive (negative) as shown in Fig. 3.10. As the contribution to the error is larger for the upper range of wind speeds, the dominant effect is a positive error in ξ_2=wE_{H-ref}-wE_{H-EPCw} and thus an underestimation of the actual energy production as observed in Fig. 3.6 and 3.7 and Table 3.1 (see subsection 3.4.1). The underestimation is larger for the sites where the positive contribution of the upper range of wind speeds is larger in comparison to that of the intermediate speeds. This is the case for Leoz, Alaiz and El Perdón, the sites that displayed larger $\overline{\xi_2}$ averages in Table 3.2. Therefore, a larger level of underestimation of the monthly wE_{obs} is related to

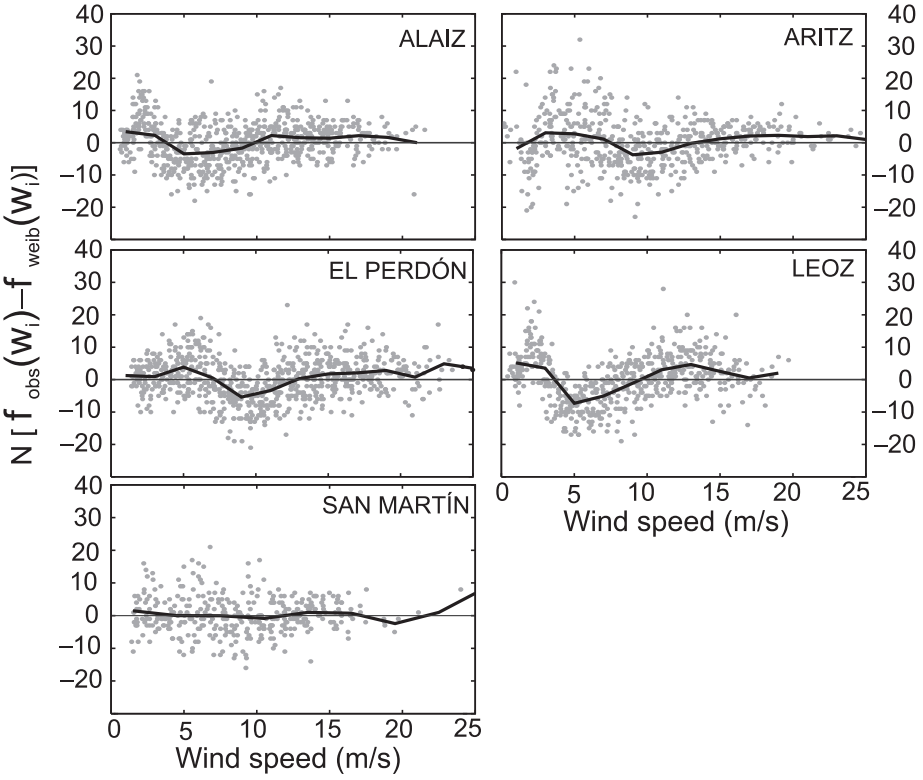

Fig. 3.10: Differences $N\left[f_{obs}(w_i) - f_{weib}(w_i)\right]$ (points) in absolute frequency histograms between observed and Weibull adjusted probability functions (scaled to absolute frequencies). Differences are overlaid for each monthly histogram along the whole period of observations at each site. Averages of differences are calculated for wind speed intervals of 2 ms^{-1} and depicted with lines for each site.

larger discrepancies between the observed and the Weibull modeled distribution for the higher wind speed bins.

The deformation of the wind speed histograms analyzed in the previous paragraphs additionally allows for an understanding of why the time concordance between monthly χ^2 and ξ_2 values is hardly noticeable in Fig. 3.8 for all wind farms, except for the case of Leoz. It could be expected that, as in the case of Leoz, the other locations would evidence links in the χ^2 and ξ_2 changes with

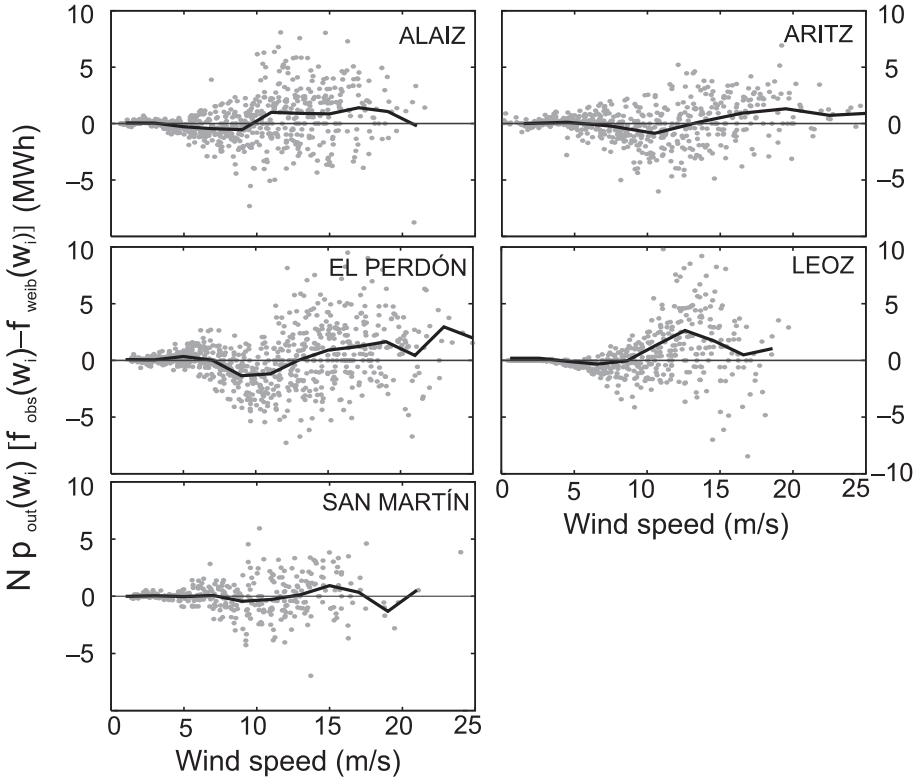

Fig. 3.11: As in Fig. 3.10 but for the terms $Np_{out}(w_i)\,[f_{obs}(w_i) - f_{weib}(w_i)]$.

time. The lack of this clear relation can be easily understood if it is recalled that the differences between observed and Weibull frequencies, $f_{obs}(w_i) - f_{weib}(w_i)$, take part in Eqs. (3.3) and (3.6) in a different way. While in their contribution to χ^2 is always positive, in ξ_2 positive or negative resulting differences can partially cancel their respective contributions. Therefore, it is possible that small ξ_2 values are associated with large χ^2 values. This fact disguises the expected relation between χ^2 and ξ_2. Alternatively, small χ^2 values would be indicative of small frequency differences, but can contribute to the final ξ_2 value differently depending on the w range they are produced at and on the $p_{out}(w_i)$ factor that relatively amplifies or attenuates them.

The absence of concordance between χ^2 and ξ_2, i. e. the partial cancellation of error, would be lessened if the differences $f_{obs}(w_i) - f_{weib}(w_i)$ were mainly positive or mainly negative, that is, if there was a dominant sign in the intermediate, and preferably, in the upper intervals of wind speed, where the production of wP is larger. That is the case of Leoz (Figs. 3.10 and 3.11) where the highest correlations were found (0.6) between χ^2 and ξ_2. Alternatively, the three bands in which Fig. 3.10 and 3.11 conceptually divide the range of wind speed can be considered separately and compared with χ^2, the rationale being the fact that the underestimation and overestimation discrepancies between monthly observed and Weibull adjusted histograms take place in a related way, i.e., the larger underestimation in the lower and upper bands, the larger the overestimation in the intermediate band. This can be argued on the basis that the sum over all relative frequencies is 1, thus, if the probability of occurrence in the Weibull histogram is lower than the observed frequency at the intermediate frequencies, the probabilities in the lower and upper wind ranges must necessarily be larger. Therefore, the ξ_2 errors accumulated within the bands generating positive contributions (lower and upper) and that producing negative contributions (intermediate) in Eq. 3.3 should behave coherently with time and display a more obvious relation respectively with χ^2 than the total ξ_2 added contributions in Eq. (3.3). In order to illustrate this, the positive (negative) error contributions were computed using as boundaries the wind speed intercepts with the axis of the averages lines at each site in Fig. 3.11. The resulting errors were denoted as ξ_2^+ (ξ_2^-) and plotted for comparison in Fig. 3.12. These quantities verify that $\xi_2{=}\xi_2^+{+}\xi_2^-$. Their evolution in Fig. 3.12 shows a much more consistent behavior with changes in χ^2 as highlighted by the correlations values show in Table 3.2 (columns 6 and 7). The improved correlations with the different sign error contributions relative to those with the total ξ_2 (column 5 in Table 3.2) highlight the fact that the lack of a clear association between χ^2 and ξ_2 in Fig. 3.8 stems from the partial cancellation of errors of different sign (ξ_2^+ *vs.* ξ_2^-). In fact, Fig. 3.12 allows for the discrimination of the dominant error contribution at each time step that justifies the occurrence of a large χ^2 value.

3.5 Conclusions

This work compared observed and estimated monthly wind energies. Observations were based on hourly wind velocity and wind power production measurements at five wind farms in the Northeast of the IP (Fig. 2.1).

As a first approach to the estimation of wind energy the best available information for the wind power *vs.* wind relation and for the frequency histogram was considered for each month. This served as a means of quantification of the

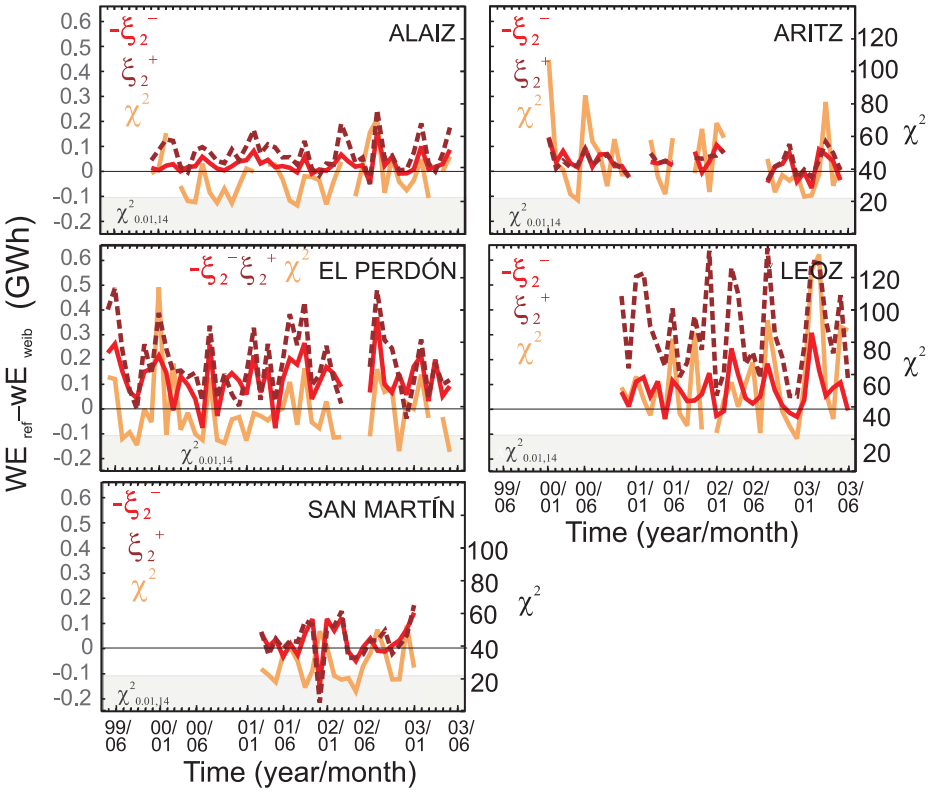

Fig. 3.12: Time series of χ^2 and ξ_2 error contributions to the low and upper (ξ_2^+) and the intermediate (ξ_2^-) wind speed intervals. Boundaries for the definitions of the three bands at each site were established from the intercepts of the error average lines in Fig. 3.11 with the x axis. ξ_2^- is represented with positive sign ($-\xi_2^-$) to help perception of the visual agreement with the other lines.

errors (ξ_1) inherent to the methodology. On average, a slight underestimation resulted which amounted to a maximum of 5.0% of the variability in one of the sites; individual peak error values seldom reached 10% of the target value.

A second approach incorporated the Weibull assumption which contributed only slightly to underestimate target wind energies. Average error (ξ_2) biases ranged from 0.2% at Aritz to a maximum of 10.3% at Leoz. Therefore the assumption of the Weibull probability distribution did not seem to strongly impact

the energy calculation. The reasons for this were not found to be based on a broad high quality of the Weibull fit but on a partial cancellation of error terms in the wind energy calculation.

An analysis of the goodness of the fit to the Weibull distribution based on the χ^2 statistic enabled an exploration of the relation between the quality of the wind speed fit and the discrepancies between observed and estimated wind energy. Such analysis revealed that the Weibull assumption could not be broadly substantiated at all the sites: the representativeness of the Weibull distribution varied from site to site and from month to month.

The relation observed between the χ^2 statistic and the estimated errors suggested that months which can not be strictly considered to be Weibull distributed do not necessarily present higher errors in the wind energy estimation. The lack of an obvious relation between the error and the χ^2 statistic is due to partial cancellations of opposite sign contributions to the error in the calculation of the monthly energy which do not take place in the χ^2 computation.

The error contributions to the energy calculation and to the χ^2 statistic revealed that the Weibull distribution tends to overestimate the observed histograms in the intermediate wind speed range and to systematically underestimate it in the lower and higher wind speed intervals. The effects of these departures from the observed frequency histogram tend to be averaged out due to the differences of sign. However the product by the power terms in the calculation of wind energy weights more over the highest wind speeds, thus underestimation errors in this range tend to dominate and contribute to the systematic observed bias to underestimate total wind energy. It could be expected that sites/months with larger underestimations in the highest wind speed intervals disclose a much more evident relation between the energy estimation error and the performance of the Weibull probability distribution as it is the case of Leoz.

The next chapter is devoted to examine the contribution of the power terms to the errors in the wind energy estimates (Eq. 3.1).

4

A comparison of methodologies for monthly wind energy estimation*

In the previous chapter the agreement between empirical and theoretical wind speed probability distributions was analysed, together with an evaluation of the impacts of assuming a particular theoretical wind PDF on the estimation of monthly wind energy. In the present chapter the effect of selecting certain transfer functions between the wind speed and the wind power is explored. With this aim, monthly wind energy estimations obtained by means of three different methodologies are evaluated. One of the approaches is based on the combined contribution of the hourly wind speed frequency distribution and the corresponding power production. Several alternatives to represent the empirical wind power *vs.* wind speed relationship are considered in this context and their impacts on the error of monthly energy estimations assessed. Two more approaches are used to derive monthly energy estimates directly from monthly wind values: one uses the theoretical power curve to obtain interpolated monthly wind power production values and the other consists in a simple linear regression between the observed wind speed and wind power monthly pairs, which serves as an approximation to the global power curve. It will be shown that linearity is a reasonable assumption for the relation between wind speed and power production at monthly timescales. This result will have relevant implications for regional prediction of wind energy from atmospheric variables as it will prove useful in the identification of connections between the wind power and the large scale circulation in Chapter 6, Part II of this thesis.

* The main contents of this chapter are included in:
García-Bustamante, E., J. F. González-Rouco, P. A. Jiménez, J. Navarro and J. P. Montávez, 2009: A Comparison of Methodologies for Monthly Wind Energy Estimation. *Wind Energ.*, **12**, 640-659.

This chapter is organized as follows. The next section underpins the rationale for exploring the role of the wind-wind power relationship in the estimation of total monthly wind energy. Section 4.2 describes and comments on the approaches employed to estimate wE from wind. Section 4.3 presents and discusses results and finally, main conclusions are summed up in section 4.4.

4.1 The rationale

The wind energy (wE) market (facilities, wind energy conversion systems, energy policies, wind speed prediction, etc.) has experienced a fast and wide development in many regions of the globe, and some of them have been exploiting wind resources since a few decades ago (Ackerman and Soder, 2002; Jager-Waldau and Ossenbrink, 2004; Flowers and Dougherty, 2004; Kenisarin et al., 2006; Faulin et al., 2006; Fairless, 2007). Thus, admissibly long wE production series are now available for many locations and it is possible to use them to accurately validate the empirical relations between wind speed and power production at the various timescales of interest for resource assessments. For instance, in the previous chapter monthly wE was estimated at several wind farms in the Northeast of the IP assuming a theoretical PDF (Weibull) would fit hourly wind speed observations. Using such a technique, the frequency terms are weighted by the corresponding power output, which can be derived from the TPC or some substitute of it. In that particular case, the study was focused on the evaluation of the magnitude and nature of the error that the use of a Weibull distribution introduces in the estimation of monthly wind energy. This was done by using the historical records of power outputs to isolate the effects produced by the theoretical probability distribution. Celik (2003b,c) employed measured wE values generated by a specific type of wind turbine and hourly wind observations to fit a third order polynomial curve that attempts to depict an experimental power curve, alternatively to the TPC. Availability of wE time series allows for a translation between wind speed and wE production for a specific site helping to understand the underlying relation between both variables at every timescale. Such a relation can be used for instance in the assessment of the sustainability and predictability of wind resources (Weisser and Foxon, 2003; Jamil et al., 1995; Mathew et al., 2002; Bechrakis et al., 2004; Weisser, 2003).

The objective of this part of the work is to illustrate the performance of several methodologies in estimating monthly wE production. This is done in an attempt to review some typical approaches for estimating wind power from wind speed and in doing so, exploring and understanding the relation between wind speed an wind power production at monthly timescales. For this aim, wind speed and wE wind production data from five wind farms sited in Northeast IP (see Section 2.2)

are employed. Three methods are compared in their ability to estimate monthly wE (wE_m). The first method examined is a common technique in wind resource evaluation that involves the fit of hourly wind data to a theoretical PDF and the use of a power curve that translates wind speed into wind power. The inspection of this methodology can be regarded as a continuation of the previous chapter where the impact of errors in the wind speed PDF distribution was analyzed. Here the impact of selecting a specific power curve on the estimations and the associated errors of wE_m is included. This method operating in hourly timescales is compared to other approaches that only use monthly resolution data. One of them adopts the strategy of estimating monthly wE by interpolating monthly wind speed values in the TPC. This rough approximation could be useful as a benchmark in the estimation of wE_m in the case that no historical wE production data were available at a particular site. The last procedure is based on the empirical relationship found between wind speed and wind power at monthly time scales and consists in assuming a linear relationship between wE_m and monthly wind velocity. Therefore, the standard approach providing estimations of wE_m from hourly wind speed is compared to even more parsimonious approximations making use of coarser temporal monthly resolution information. This will allow for evaluating to what extent situations in which only monthly data are available could involve a loss of information in the estimation of wE_m.

4.2 Analysis of methodologies

Wind speed and wind power production data for the analyses herein were described in Section 2.2 and are the same as those used in the previous chapter.

Three strategies are compared in their performance to derive estimations of wE_m. The first strategy is based on a standard procedure (Celik, 2003c,b,a; Biswas et al., 1990; Celik, 2004) that takes into account hourly wind velocity data. It considers the observed wind speed frequency histogram, or a viable fit to a theoretical PDF of the frequency terms, and a transfer function representing the relation between wind speed and power production. The other two strategies lean on the use of monthly wind and power production data. The second approach is based on the very rough assumption that the TPC would be valid at monthly timescales and thus, translates monthly wind values into monthly power production through an interpolation in the TPC. Some considerations addressing the validity of such an assumption are discussed in section 4.2.2.

The third approach is based on assuming that the relationship between wind speed and wind power is linear. Their monthly averages, as will be discussed in section 4.2.3 (e.g. Fig. 4.2) fall in the quasi-linear part of the TPC and are suggestive of a simple linear empirical relationship between them.

A more detailed description of the three methodologies is presented in the following subsections.

4.2.1 Estimation based on hourly resolution data

The first approach to estimate the total production of wE_m is based on the use of the hourly distribution of wind speed within each month and an estimate of the wind speed-wind power dependence such as the TPC or some substitute of it. This method has become relatively standard in obtaining wE estimates from high temporal resolution wind speed series (Mathew et al., 2002; Bechrakis et al., 2004; Weisser, 2003; Pryor and Schoof, 2005) and allows to assess to what extent including hourly information refines results in comparison with the other approaches described below that only consider monthly time resolution. The estimation of the wE_m is obtained through:

$$wE_H = \Delta t N N_t \sum_{i=1}^{n} p_{out}(w_i) f(w_i) \tag{4.1}$$

(notation in Eq. 4.1 follows that of Eq. 3.1 in Chapter 3).

Several comments can be made at this point concerning the evaluation of $f(w_i)$ and $p_{out}(w_i)$. As discussed in Section 3.3, of all possibilities, the most precise estimation of wE for a given month should be the one calculated using the observed wind speed frequency, $f(w_i)$, and the observed relationship between power production and wind speed within each particular month, $p_{out}(w_i)$. The wind speed frequencies can be easily obtained from splitting the range of hourly wind observations into wind intervals, whereas the effective relationship between wind speed and generated power can be derived from the observation of the power production at each one of those intervals. This provides an empirical wind power *vs.* wind speed curve that was denoted in Chapter 3 as the EPC and that can be used as $p_{out}(w_i)$.

Such an estimation was already used in Chapter 3 as the reference estimation. There, as in this chapter, it represents a benchmark of the predictability that can be obtained using the procedure explored in the previous chapter (Eq. 3.1) and that here (Eq. 4.1) serves also to provide an idea of the systematic error in the methodology associated with the discretization of the wind speed series into intervals. This estimate will be also denoted herein as wE_{H-ref}.

As discussed in Chapter 3, many practical cases involve situations in which the precise knowledge of $p_{out}(w_i)$ and $f(w_i)$ is not available. In these practical situations, wE_H must be estimated by making approximations to the wind frequency distribution and the corresponding power output. A first approximation in such cases is the use of a specific theoretical PDF, like the Weibull function for

instance (Tuller and Brett, 1984; Palutikof et al., 1987; Celik, 2003b; Pryor and Schoof, 2005; Dorvlo, 2002) as a substitute for the observed wind speed frequency. This constitutes a first source of error when estimating wE_H in Eq. (4.1) to the extent that the specific wind distribution of a certain month deviates from the Weibull shape; the deviation being particularly relevant in the high wind speed range where the largest power production is achieved (recall results in Chapter 3).

A second source of error stems from the assumptions made to estimate $p_{out}(w_i)$. One of the goals in this chapter is the evaluation of the impact of using an approximation to the power terms in Eq. (4.1). With this purpose the observed frequency distribution is employed to provide the $f(w_i)$ terms (as in the case of wE_{H-ref}) and a set of variants for the power outputs terms were considered in order to isolate their influence on the wE_m estimations. These allows for the segregation of the two sources of error as previously done in Chapter 3 but, in this case focused on the impact of the assumptions made about the power curve. Thus, in addition to wE_{H-ref} that provides information about the methodological error in Eq. (4.1), three more estimates of monthly energy production obtained with different versions of the wind speed-power relation are proposed here. The substitutes for the EPCs adopted herein are also considered to be representative of the whole wind farm, in spite of the fact that power production may show changes within the group of wind turbines (Noorgard and Holttinen, 2004).

The first candidate for the $p_{out}(w_i)$ terms is the TPC. This is the simplest and roughest approximation since the TPC does not take into account the global wind farm effects (e.g shading between turbines). However, it has the advantage that historical data are not required. Bechrakis et al. (2004), Jaramillo and Borja (2004) and Bivona et al. (2003) for instance, have used commercial TPCs to obtain energy production. Hereafter the energy estimation produced using the TPC as an estimate of $p_{out}(w_i)$ will be denoted as wE_{H-TPC}.

Two more approximations of the EPC are considered: an *average power curve* (APC) and a third order *polynomial fit curve* (PFC). The APCs are calculated as the average of all the EPCs along the period of observation at each site, calculating for each wind speed interval the corresponding mean power production value. The PFC is the cubic polynomial that better fits the whole ensemble of EPCs. The use of these approximations is intended to explore the potential benefits of developing more elaborated models as substitutes for the EPC and that can be used as a realistic representation of the wind speed-wind power relationship. These approaches can incorporate some effects that are specific to the wind farm location and make use of the already existing information to face situations in which no data for a particular month are available. Even if these two new power

curve models appear to be somewhat more elaborated than the EPC case, they are still conceptually simple since they do not take into account the effects of more complicated features like the dependence on wind direction, the relative position of masts within a wind farm, air density, etc. This will be commented on in Section 4.3.

In order to keep independence between monthly wE_H estimations and the EPC averaging/fitting process through the methodological assessment, the data for the target month (the month for which the wE_H is going to be estimated) are excluded in the calculation of the APC/PFC curves. With this specification, a single APC/PFC is independently obtained for each particular month. This procedure can be compared to a crossvalidation approach through which the temporal robustness of the empirical relation found between sets of predictand and predictor variables is assessed (von Storch and Zwiers, 1999): for each time step the estimation of the target-predictand variable (i.e., wind energy production herein) is obtained from the available predictor (i.e., wind speed) through the use of an empirical model (in this case, APC or PFC) that is built on the basis of the available information from all other time steps. The energy estimation in this case is denoted with wE_{H-APC}/wE_{H-PFC}.

Fig. 4.1 illustrates the three approaches (TPC, APC, PFC) employed to represent the $p_{out}(w_i)$ terms in Eq. (4.1). December 2001 is shown as a particular case example. The TPC generally underestimates the power generated at the lower wind speeds whereas it tends to overestimate it for the higher wind velocities. The weighting effect of the $p_{out}(w_i)$ terms in Eq. (4.1) is stronger for the highest wind speeds and thus, a global overestimation of the final wE_{H-TPC} should be expected. This point is further analyzed through the interpolation method in Section 4.2.2. The APC and PFC are very similar, though the PFC displays generally (not shown) smaller power values than the APC for the same wind.

The dispersion of the hourly wind speed-wind power pairs discussed in Section 2.2 is also evidenced in the representation of the EPCs (Fig. 4.1). Such an effect is, as expected, minimized in Leoz where the set of EPCs displays a much smaller monthly variability. A consequence of the spatial average over the set of turbines to obtain a single power production series at each wind farm can be appreciated in the bended shape of some of the EPCs close to the *cutoff* wind part of the curve in Fig. 4.1; for winds above the cutoff level, some turbines may be stopped leading to a diminished average power production in the whole wind farm (for more details see Section 3.2). An alternative to the PFCs calculation adopted herein could be the implementation of a polynomial fit over all the available hourly wind speed-wind power pairs (Celik, 2003b,a). However the large dispersion of hourly observations leads to low signal to noise ratios that do not statistically support the fit to polynomial functions of orders higher than one. The generation

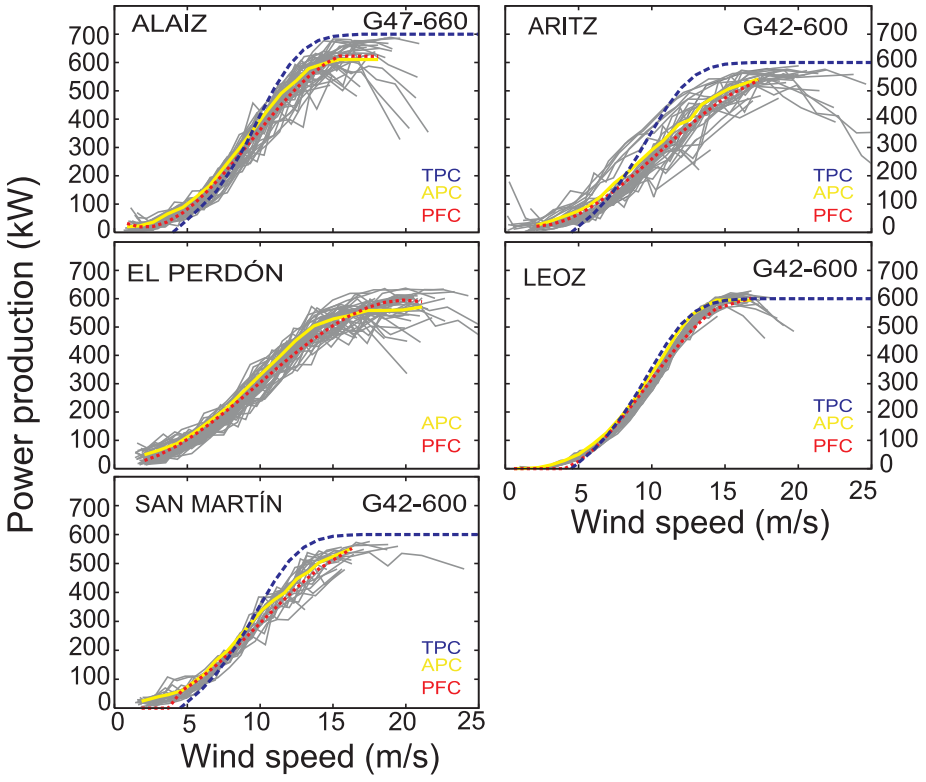

Fig. 4.1: TPC, APC and PFC (see legends) for December 2001 at each of the wind farms; wind turbine types are G47-660 kW in Alaiz and G42-600 kW in Aritz, Leoz and San Martín. In El Perdón no TPC was used (see text).

of monthly EPCs from hourly data enhances signal to noise ratios (Fig. 4.1) and allows for implementing higher polynomial orders that are consistent with the typical shape of a TPC. The TPCs cannot be established properly for El Perdón due to the frequent technical manipulations during the period of measurements and that probably contribute to a large dispersion of the wind speed-wind power pairs at this specific wind farm. Thus, the corresponding curve for this site is not shown in Fig. 4.1.

The comparison of wE_{H-ref} with the energy production calculated using the various estimates of the EPC (wE_{H-XXX}, with $XXX \equiv$ TPC, APC, PFC) al-

lows for an evaluation of the errors associated to the $p_{out}(w_i)$ terms in Eq. (4.1). However, in order to compare the results of this approach to the ones described in Sec. 4.2.2 and 4.2.3 it is desirable to provide an integral error estimation that includes also the effect of the $f(w_i)$ terms discussed above. The evaluation of the error impact of the frequency terms is non trivial since it depends on the theoretical PDF that wind speed is assumed to follow. For the sake of simplicity and consistency with the previous chapter, this study adopts the Weibull distribution. Therefore the $f(w_i)$ terms are substituted by their corresponding Weibull estimates following the same procedure as in Chapter 3. The monthly energy estimations including both types of error will be denoted as wE_{H-XXXw} (with $XXX \equiv$ TPC, APC, PFC).

4.2.2 Interpolation using the theoretical power curve

The TPC is the relationship between wind speed and power production, usually calculated using 10-minute observations, provided by manufacturers and specific for each type of wind turbine.

As expected from basic theoretical considerations of wind kinetic energy, the available power carried by the wind is $P_a = \frac{1}{2}\rho A w^3$ (Chang et al., 2003; Noorgard and Holttinen, 2004), where ρ is the air density and A is the area swept by the rotor. However the power that can be actually produced by a turbine does not increase with the cubic wind speed. Therefore the maximum wind energy that could be generated by an ideal wind turbine (P_w) is P_a, increasing with the cubic wind speed up to the the rated wind speed or the wind over which no increase in power production can happen (Chang et al., 2003). Additionally, P_w is reduced by the rotor presence so that the power that can actually be generated results from balancing out the expected efficiency of the turbine, aerodynamic loads, turbulence, rated power and various other technical aspects. The attenuation can be expressed as a percentage in terms of the *power coefficient*, $C_P(w)$, that depends on wind speed and shows a theoretical upper limit of *ca.* 0.59, given by the *Betz Limit* (Bergey, 1979). Therefore

$$P = \frac{1}{2} C_P(w) \rho A w^3 \tag{4.2}$$

is the actual power produced by a wind turbine as a function of wind speed (Noorgard and Holttinen, 2004).

It could be argued that the actual power production (P) corresponding to monthly wind speeds would not deviate much from the manufacturer's reference value obtained by evaluating the TPC on the specific wind speed monthly averages. Such an assumption can serve as a rough benchmark estimation to be

compared with the results of the somewhat more elaborated approaches described in sections 4.2.1 and 4.2.3. On the basis of assuming the TPC as an appropriate candidate for a monthly power curve, monthly estimations of power production can be obtained by direct interpolation within the TPC:

$$P_{Interp} = P_0 + \frac{(P_1 - P_0)}{(w_m - w_{m_0})}(w_{m_1} - w_{m_0}) \tag{4.3}$$

where w_m is the monthly mean wind, (w_{m_0}, P_0) and (w_{m_1}, P_1) are the two nearest points in the TPC and P_{Interp} is the monthly interpolated power output. From a formal standpoint, Eq. (4.3) cannot be supported since it is tantamount to considering that the nonlinear TPC function that describes power production at high resolution (usually 10 min) timescales can also be used to estimate monthly power production when evaluated over monthly wind speed averages. This assertion would be necessarily incorrect since the monthly average of a nonlinear function (TPC) will not equate the result of evaluating the nonlinear function over monthly values (monthly wind averages herein). The results of applying Eq. (4.3) will illustrate the poorer performance of this assumption. Nevertheless, the estimates obtained can be useful to illustrate the error that can be made with such a crude approximation. In addition, Eq. (4.3) may be useful as a first rough estimate of the potential power production that can be expected in situations with no availability of historical wind power observations and having only monthly power records; this could be the case for instance of downscaling applications where only monthly estimations of wind variables are available (Kaas et al., 1996). An example of this is presented in Chapter 6 where, alternatively to the direct downscaling of wind power, estimations of the wind power will be obtained through the downscaled wind field and some variants of the wind-wind power transfer functions are calculated. On the basis of this rationale, P_{Interp} estimations have been included herein for comparison with the other approaches presented in this chapter.

The P_{Interp} values after interpolating the observed w_m at each wind farm, are shown, together with the corresponding TPC for comparison in Fig. 4.2. Observed monthly averages span within the quasi-linear interval of the TPC. It is worth noting that the slope of the straight line that best fits the monthly observations is lower than that of the TPC, a consequence of the monthly averaging and the perturbations discussed. This larger tilt anticipates that any estimation of wE based on the TPC interpolation will likely overestimate the variance of observations, as was first discussed in Section 4.2.1.

The total monthly interpolated wE (wE_{Interp}) is calculated according to:

$$wE_{Interp} = NN_t P_{Interp} \tag{4.4}$$

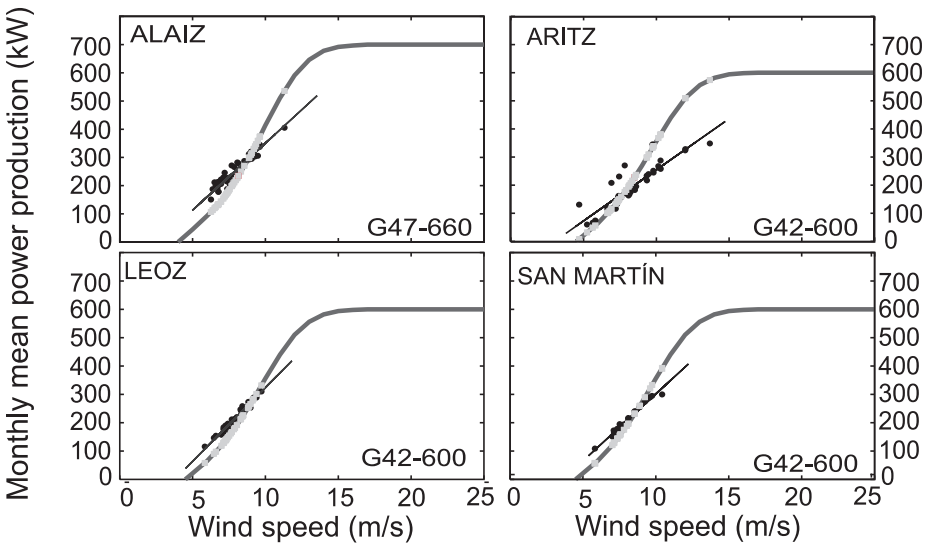

Fig. 4.2: Observed monthly wind speed and wind power pairs (black points) and its linear fit (black solid line), TPC (gray line) and interpolated values of power production from monthly wind velocity in the TPC (light gray points). Notice that the TPC corresponding to turbine type G47-660 kW is shown in Alaiz while for the other sites G42-600 kW is used. El Perdón is excluded since it does not have a well defined TPC.

where N is the number of hours of each month (here 350, see Section 2.2) and N_t is the total number of wind turbines of the same type at the wind farm.

4.2.3 Linear regression

Though the theoretical relation between wind and wind power at shorter timescales shows a cubic dependence of the P_a on the wind, monthly power production values have disclosed a significant linear relation (Fig. 4.2). This linearity can be moreover appreciated in the monthly power and wind velocity standardized time series in Fig. 4.3 at the five sites for which correlations are confined in the interval [0.89,0.99].

In the light of this linear relationship between the monthly power production and wind speed values evidenced through Fig.s 4.2 and 4.3, a third approach based on a simple linear least squares fit between both variables is evaluated using:

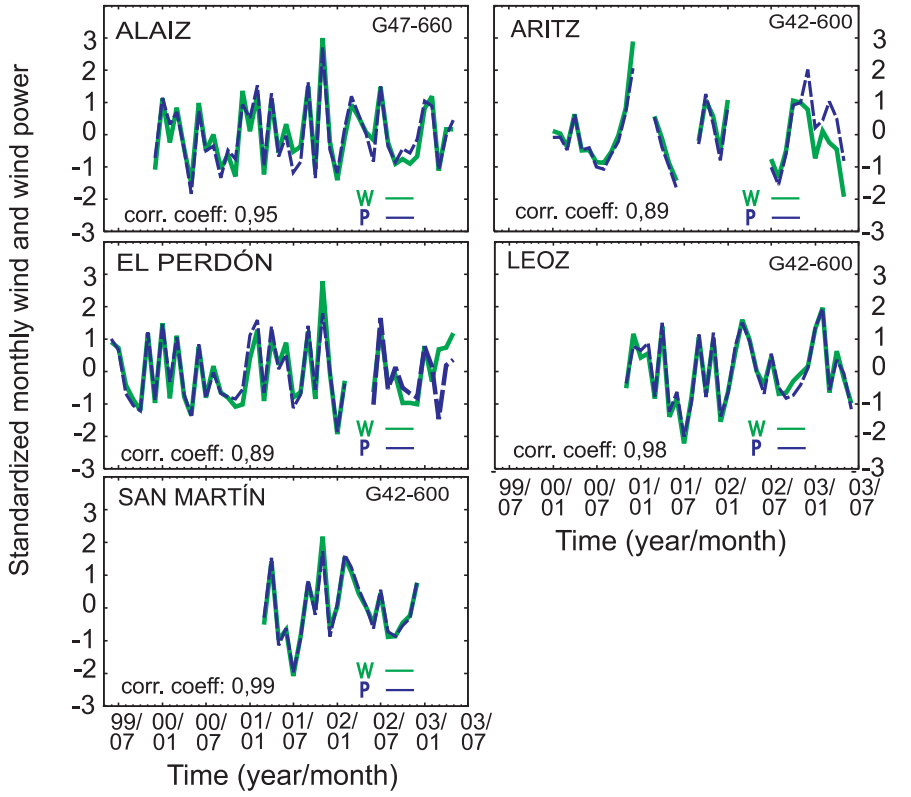

Fig. 4.3: Monthly wind speed (w) and power production (P) time series in all wind farms. The series have been standardized by removing their mean and dividing by their standard deviation. Notice that the TPC corresponding to turbine type G47-660 kW is shown in Alaiz while for the other sites G42-660 kW is used.

$$P_{Linear} = aw_m + b \tag{4.5}$$

where w_m is the observed monthly wind speed and a and b are the regression coefficients.

Additional arguments supporting a linear relation between monthly wind and wind power can be also found in the statistical properties of the Weibull distribution if this was considered to be representative of wind field properties or, from a broader perspective, in the relation between wind speed and its cubic power in Eq. (4.2). If theoretically it was assumed that the Weibull distribution appropriately describes the statistical features of the wind field, the idea of linearity

stems from the properties of this frequency distribution (Conradsen and Nielsen, 1984), for which the n order moments are defined by:

$$E(w^n) = c^n \Gamma(1 + \frac{n}{k}) \tag{4.6}$$

being w the wind speed, c the scale parameter and k the shape parameter. Then, the expected mean value, which would represent the monthly wind velocity, is defined as $E(w) = c\Gamma(1 + \frac{1}{k})$, and the third order moment, that would be representative of the monthly wind energy carried by the wind if assuming a Weibull distribution is $E(w^3) = c^3\Gamma(1+\frac{3}{k})$. The correlation coefficients for the calculated monthly $E(w)$ and $E(w^3)$ series range from 0.94 to 0.97 (not shown). Thus, a good approach to linearity between the wind speed and the energy carried by the wind in the range of monthly values could be also considered if a Weibull distribution was theoretically assumed.

Furthermore, the previous argument can be generalized for any frequency distribution, by calculating the correlations between the monthly wind speed and the available monthly power carried by the wind (P_a), represented by means of the monthly-averaged cubic wind speed. A dispersion diagram of the monthly wind speed and cubic wind speed is plotted in Fig. 4.4. The correlation coefficients between both variables are 0.93 for Alaiz and Leoz, 0.94 for Aritz, 0.92 in El Perdón and 0.95 for San Martín, respectively, thus supporting that linearity can be a parsimonious assumption for the relation between wind speed and P_a for the typical monthly range of values at the various sites.

The difference between P_a and the power generated by an ideal wind turbine (P_w) is that, in the case of P_w, the power production increases with the cubic wind up to the rated wind speed (Chang et al., 2003). Finally, the differences between P_w and the actual power generated are mainly due to the $Cp(w)$ power coefficient in Eq. 4.2. This factor, at the range of values considered at monthly timescales and for the turbine types described above, can be approached as constant (e.g. technical note, 1996). Thus, linearity can be a plausible assumption that is worth testing also from this perspective.

In order to ensure independence in the building of the model in Eq. (4.5) a similar process as in the case of the hourly based method (Eq. 4.1) was performed: each monthly P_{Linear} estimation is obtained by inserting the corresponding w_m value into the linear regression previously calculated incorporating all the remaining monthly wind speed-wind power pairs after excluding that of the target month. This procedure was carried out consecutively for each month and separately for each one of the groups with similar wind turbines at farms with more than one type of turbine. The total monthly wind energy estimation (wE_{Linear}) is computed as in Eq. (4.4), replacing P_{Interp} with P_{Linear}.

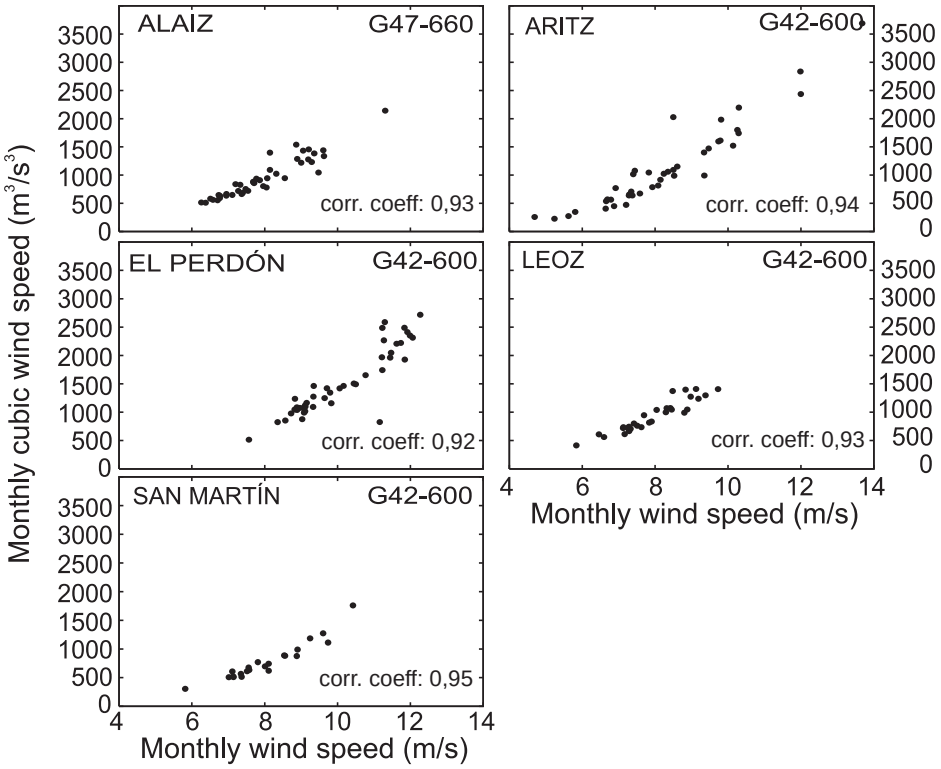

Fig. 4.4: Monthly cubic *vs.* monthly wind speed in all wind farms. Notice that the TPC corresponding to turbine type G47-660 kW is shown in Alaiz while for the other sites G42-600 kW is used.

4.3 Results and discussion

4.3.1 Estimations based on hourly data

Fig. 4.5 (left column) shows the observed temporal evolution of wE_m production at each wind farm and the wE_m estimations obtained from hourly resolution data using the approaches described in Sec. 4.2.1. It is worth noting that months with large production alternate with months with less power generation which is a sign of inter annual variability potentially related to atmospheric circulation (this issue will be assessed in Chapter 6 in the second part of the text). It is apparent that all methodological variants capture the overall structure of

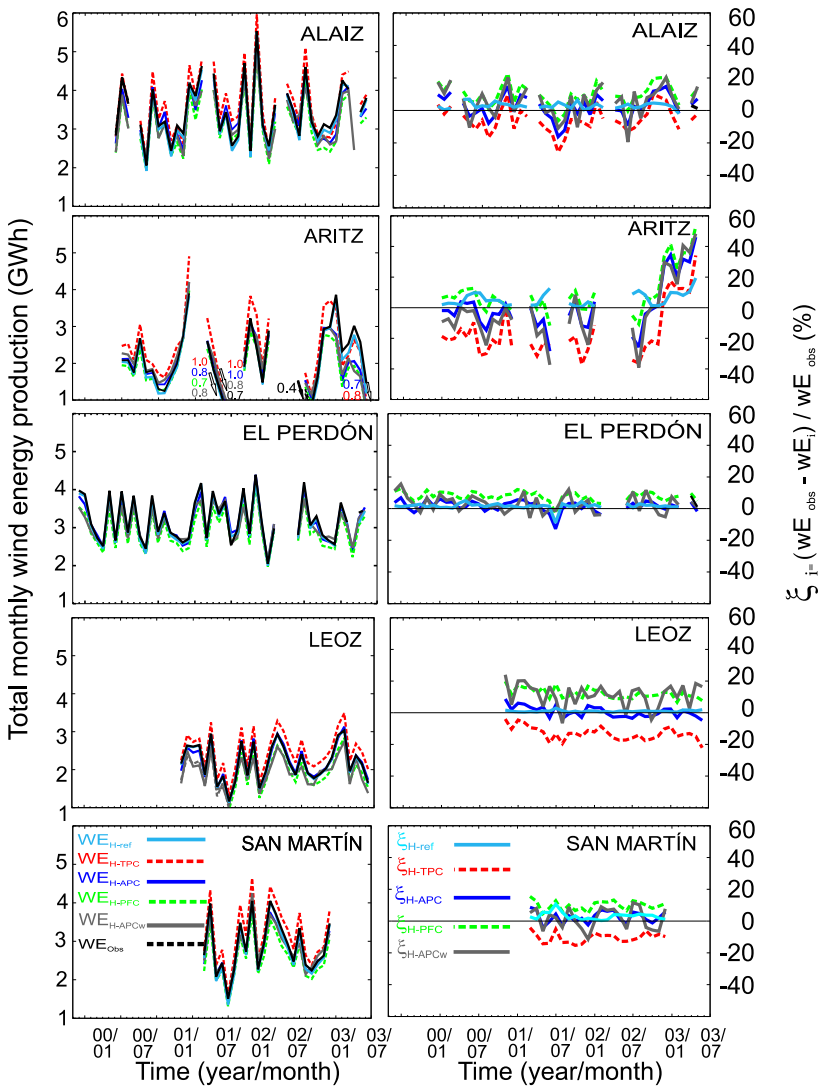

Fig. 4.5: Observed and estimated total monthly wE_m time series (left column) for all wind farms using hourly resolution data as described in Sec. 4.2.1. The optimal methodological estimations using the actual monthly EPC and histogram, wE_{H-ref} are compared to other variants, wE_{H-XXX} ($XXX \equiv TPC, APC, PFC$). wE_{H-APCw} estimations including APC as an estimate of EPC and a Weibull fit for the frequency terms are also shown. The corresponding estimation relative errors are represented in the right column.

the temporal variability at all sites. The differences among the various energy estimations are smaller than the range of intra and inter annual variability. The different power production ranges at each wind farm seem to be also well represented. The two methodological variants that produce the larger discrepancies are the ones incorporating the TPC and the PFC (wE_{H-TPC}, wE_{H-PFC}). The similarity between energy estimations and observations can be quantified with the correlation (ρ) and the Brier skill score (β) statistics in Table 4.1 that measure the concordance between observations and estimations and an estimate of the observational variance that the model accounts for, respectively (von Storch and Zwiers, 1999).

Table 4.1: Correlation (ρ)/Brier (β) skill score for the different methods.

ρ/β	Alaiz	Aritz	El Perdón	Leoz	San Martín
wE_{H-ref}	1.00/0.98	1.00/0.98	1.00/0.98	1.00/1.00	1.00/0.98
wE_{H-TPC}	0.96/0.87	0.90/0.71	-/-	0.99/0.68	0.99/0.83
wE_{H-PFC}	0.96/0.67	0.89/0.60	0.99/0.66	0.99/0.63	0.99/0.72
wE_{H-APC}	0.95/0.88	0.89/0.73	0.98/0.94	0.99/0.98	0.99/0.94
wE_{H-APCw}	0.92/0.76	0.84/0.72	0.96/0.85	0.94/0.59	0.96/0.91
wE_{Interp}	0.94/0.56	0.81/0.52	-/-	0.97/0.82	0.98/0.83
wE_{Linear}	0.94/0.88	0.76/0.47	0.96/0.92	0.98/0.95	0.98/0.96

The wE_{H-ref} estimations show the largest values of ρ and β (Table 4.1) indicating that, as expected, they reproduce best the variability in observations. The methodological variants incorporating the TPC, APC and PFC curves still deliver very high ρ and β values. The performance in terms of the β score is best for the wE_{H-APC} estimations and worst for the wE_{H-PFC} case. This suggests that assuming the TPC as a simple estimate of the relationship between wind speed and power production or the average of all available monthly power curves (APC) can produce as good performance or even better than more elaborated polynomial fits.

The additional use of Weibull estimates for the frequency terms further deteriorates monthly energy estimations and provides a more realistic estimation of the error associated to this approach, due both to the $f(w_i)$ and $p_{out}(w_i)$ terms. For simplicity reasons results in Fig. 4.5 and Table 4.1 are only shown for the case of incorporating the APC power curve (wE_{H-APCw}), which has produced the best results so far. It is noticeable that in general the wE_{H-APCw} estimation falls within the variability of the ensemble of methodological variants, thus

suggesting that incorporating the error in the frequency terms is, in general, of less relevance than changing the estimation used for the power terms. This comparatively smaller impact does not necessarily point out a good quality Weibull fit as argued in Chapter 3.

Fig. 4.5 (right column) illustrates also the different performance of the methodological variants discussed above by showing the temporal evolution of the relative error: $\xi_i = (wE_{obs} - wE_i)/wE_{obs}$. As indicated in Table 4.1 the smallest errors are produced by the reference methodological estimations, wE_{H-ref}. The case of incorporating the APC power terms provides the second best estimations and the TPC and PFC cases tend to present negative (overestimation) and positive biases (underestimation), respectively. This is due to the over- (under-)estimation of $p_{out}(w_i)$ terms by the TPC (PFC) for large monthly wind speeds (see Fig. 4.1). In Fig. 4.5 this reveals a systematic behavior for which specific corrections could be developed at each wind farm, thus improving the performance of these model variants. Some methodologies can be found in the literature regarding potential improvements that could be used to derive more refined estimates of the power curve at each site than the ones used herein. For example, Pinson et al. (2007, 2008) applied nonparametric techniques providing probabilistic estimates of the power production to evaluate the uncertainty associated with the wind power estimates and to derive a more accurate estimation of the power curve. Some other works use nonparametric statistical methodologies for different issues related to the wind speed modeling, as for instance, in wind tunnel experiments (Hwang-Dae et al., 2007) or to correct bias, scattering or inhomogeneities in data coming from a model (Caires and Sterl, 2005).

An overall perspective for the error at each site is provided in Table 4.2 where the average of relative and total errors is shown. For the calculation, absolute values at each time step have been considered to avoid cancellation of errors by changes in sign. The worst estimations are obtained at Aritz for all methods. The average error ranges between 0.9% and 5% for the five wind farms in the best case scenario for the hourly resolution method (wE_{H-ref}) and between 7.8% and 21.7% for the roughest power curve approximation case (wE_{H-TPC}). As discussed above, wE_{H-APC} produces the best results of the three tested approximations with values ranging between 2.9% and 11.8%; these errors increase to values between 4.8% and 14.8% when the Weibull approximation is included. As mentioned above, this comparatively small increase suggests that, in general, the contribution to error of assumptions made in the power terms is more important for the sites studied herein than those concerning the fit to a theoretical probability distribution. Yet, two amendments should be made to this statement. The first one is that a clear exception takes place in Leoz where the average error increases from 2.9% to 10.0% after the introduction of the Weibull approximation.

This is also shown clearly in Fig. 4.5. The reason for this behavior is the poorer quality of the Weibull fit at this site that is due to a large underestimation of observed frequencies at high wind speeds (see Section 3.4 for details).

Table 4.2: Averaged absolute relative ($\overline{|\,\xi_r\,|}$) and total ($\overline{|\,\xi_t\,|}$) errors in monthly wE estimation at each wind farm.

	Alaiz	Aritz	El Perdón	Leoz	San Martín
$\overline{\|\,\xi_r\,\|}$ ($\overline{|\,\xi_t\,|}$)	% (MWh)	% (MWh)	% (MWh)	% (MWh)	% (MWh)
wE_{H-ref}	2.6 (89)	5.0 (102)	1.7 (55)	0.9 (20)	2.9 (80)
wE_{H-TPC}	7.8 (265)	21.7 (434)	- (-)	13.1 (288)	10.5 (294)
wE_{H-PFC}	10.2 (347)	11.9 (238)	8.0 (256)	12.2 (268)	9.9 (277)
wE_{H-APC}	6.2 (211)	11.8 (236)	2.9 (93)	2.9 (64)	3.7 (104)
wE_{H-APCw}	9.2 (313)	14.8 (414)	4.8 (153)	10.0 (264)	6.0 (168)
wE_{Interp}	18.1 (615)	24.3 (486)	- (-)	13.4 (295)	11.8 (330)
wE_{Linear}	6.6 (224)	17.5 (350)	3.5 (112)	4.1 (90	3.9 (110)

The second amendment to the last statement stems from the fact that the errors associated to the frequency terms have been included in wE_{H-APCw} considering the optimal monthly fit to a Weibull distribution as was done in Chapter 3. However, there is a conceptual difference between this approach and the incorporation of errors in the $p_{out}(w_i)$ terms performed in this text. For the latter, the estimation of the power curve for each monthly case involved an independent assessment based on the exclusion of data belonging to the target month whereas for the $f(w_i)$ terms the best fit was developed using the hourly data of the target month. This means that the error associated to the inclusion of the Weibull assumption represents only the contribution of substituting the observed histogram by its Weibull fit and not the impact of estimating the Weibull parameters from information independent of the target month. This issue would expectedly increase in practical situations the error associated to the $f(w_i)$ terms in the wE_{H-APCw} estimations.

A couple of final comments are worth concerning Fig. 4.5. It is apparent that all energy estimations, except for wE_{H-ref}, tend to produce a similar pattern in the temporal evolution of errors, an exception being Leoz, where the impact of errors in the $f(w_i)$ terms is comparatively larger. This suggests that all approaches fail to conveniently reproduce some of the specific features of the monthly variability in the $p_{out}(w_i)$ terms. This common pattern of errors can be understood if it is recalled that the power curve models employed in the different energy

estimations do not consider the influence of several factors like the wind direction or the air density, etc. The elaboration of a power curve that is valid for the whole wind farm can involve many physical and engineering aspects to be taken into account in order to represent in detail the global wind speed-wind power relation (Noorgard and Holttinen, 2004). Previous work has attempted to illustrate for instance the uncertainty in the energy production estimation that arises from the use of a specific wind turbine power curve (Lange, 2005; Lackner et al., 2008). Also, Pinson et al. (2008) employ an advanced nonparametric statistical approach to adequately estimate the conversion function from wind speed to wind power. Such a refinement of the energy estimations or the inclusion of specific corrections for each power curve model is out of the scope of this work and from such perspective the power curve models used herein are parsimonious and all omit a number of complexities that can lead to the common pattern of errors in Fig. 4.5.

It is also interesting to highlight the increase of error produced by all methodological variants, including wE_{H-ref}, in Aritz at the end of the observational period. The causes for this overall failure that produces the largest errors have not been elucidated. This behavior suggests problems with the quality of data as a plausible cause that would deteriorate the performance of the reference estimate wE_{H-ref} and consequently also of the others.

4.3.2 Estimations with monthly data and comparison with the hourly case

Fig. 4.6 allows for extending the assessment to the performance of the two very simple approaches described in Sections. 4.2.2 and 4.2.3 (wE_{Interp} and wE_{Linear}). Results for ρ and β as well as for relative error averages are also shown in Tables 4.1 and 4.2. For clarity purposes only the wE_{H-APCw} variant, which involves the more realistic assessment of errors in Fig. 4.5, is included in Fig. 4.6 for comparison.

It can be appreciated in Fig. 4.6 (left column) that both wE_{Interp} and wE_{Linear} reveal quite a good performance in comparison to wE_{H-APCw} in spite of the rough approximations adopted. The wE_{H-APCw} and wE_{Linear} estimations are very similar in all cases and they are additionally very close to the observed values. This is also evidenced in Fig. 4.6 by the relative errors of the different estimations (wE_{H-APCw}, wE_{Interp} and wE_{Linear}) and in the statistics in Tables 4.1 and 4.2. The interpolation method, although is able to replicate their temporal structure and reasonably captures the variability of observed time series in the wind farms (the explained variance is 89%, 66%, 95% and 96% for Alaiz, Aritz, Leoz and San Martín, respectively), presents the largest errors, as shown in Fig. 4.6 (right column), in the higher error averages of Table 4.2 and in the

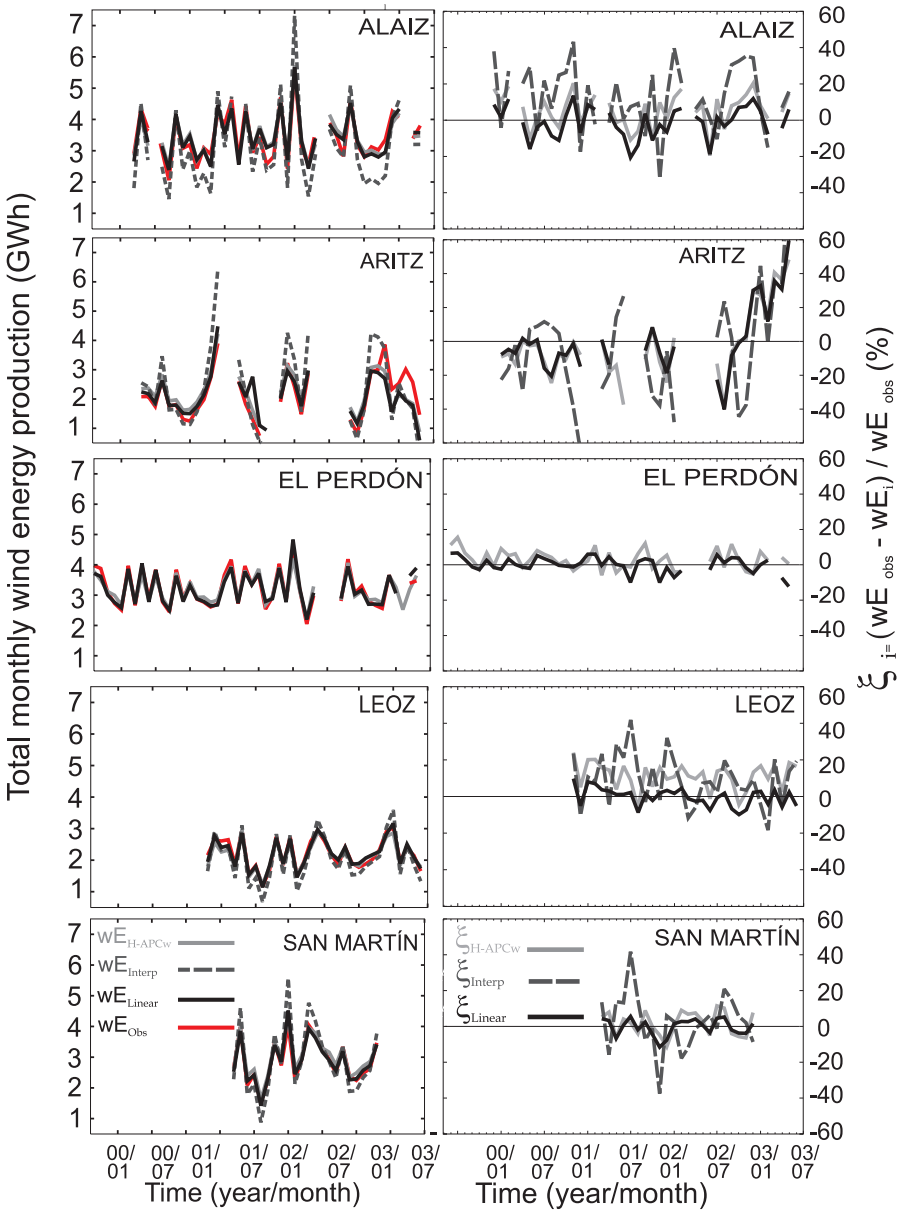

Fig. 4.6: Left: observed and estimated total monthly wE (wE_{H-APCw}, wE_{Interp} and wE_{Linear}) time series for all wind farms. Right: corresponding relative errors.

decrease of the Brier score values in Table 4.1. This is due to an overestimation of variability by this method produced by the larger tilt of the TPC relative to the observed wind speed-wind power relationship at monthly timescales (see Fig. 4.2). It can be argued that the TPC is calculated to represent the relationship between wind speed and wind power for 10-minute resolution data. Its use as an estimation of the EPC in wE_{H-TPC} in an hourly resolution data approach is admissible in view of the results shown in Fig. 4.5 and Tables 4.1 and 4.2. The use of monthly averages involves changes in the relationship between wind speed and wind power (Fig. 4.2) that are not well captured by an interpolation in the TPC. The reason is the use of the averaging operator (which is linear) over a curve that is essentially not linear, except at intermediate range of wind values where it can be approached as a quasi-linear curve (see discussion in section 4.2.2). Nevertheless, wE_{Interp} still captures the temporal variability in the observations (Fig. 4.6) and thus, it may prove useful when monthly wind energy estimations are required in situations of no availability of power production observations (see Chapter 6).

The more interesting feature in Fig. 4.6 is perhaps the fact that wE_{H-APCw} and wE_{Linear} produce a similar performance. wE_{Linear} performs worse in Aritz (see Tables 4.1 and 4.2) and compares well or outperforms wE_{H-APCw} in the rest of the sites. In Leoz, where the impact of the frequency terms produces larger deviations in wE_{H-APCw}, wE_{Linear} does visibly better (Fig. 4.6, right column). In addition, in practical situations the error associated to wE_{H-APCw} could be expected to increase if we recall the fact that these estimations incorporate only a lower limit estimation of the error in the frequency terms (see independence arguments raised above). This argument further endorses the performance of a parsimonious simple linear regression in comparison with more elaborated approaches. Therefore, not only does the linear approach achieve comparably good results, but also it constitutes a simple and robust methodology operating on monthly resolution data.

It is also interesting to notice that the temporal evolution of errors in Fig. 4.6, in particular those of wE_{H-APCw} and wE_{Linear}, is correlated (values not shown). Such changes in wE_{Linear} can only stem from deficiencies in the representation of the monthly variability of the slope in the linear regression. Therefore, this supports the idea that in the case of wE_{H-APCw} and the methodological variants included in Fig. 4.1 the common temporal structure of error derives from common deficiencies in the representation of the tilt of the power curve.

4.4 Conclusions

In this work three methods have been compared in their performance to estimate monthly wind energy. The first strategy makes use of hourly resolution data and builds estimates based on the wind speed frequency distribution and on a transfer function that expresses the relationship between wind speed and wind power at these time scales. Different estimates have been analyzed: the observed monthly power curves (EPCs), the theoretical power curve provided by manufacturers (TPCs), the average of the available EPCs (APCs), or a polynomial fit to them (PFCs). Observed frequency histograms have also been replaced by Weibull estimations to take into account the influence of the frequency terms. The selection of these power and frequency estimates has been done on the basis of their simplicity and/or standard use.

In the second approach, the TPC has been used to obtain monthly values of power production through an interpolation procedure using directly the monthly wind velocity. Some evidences of the linear relationship existing between wind and power production at monthly timescales are shown, in spite of the expected cubic relation between both variables. Thus, the last approach considered here consists in a simple linear regression calculated over the monthly wind speed-wind power pairs.

All methods and methodological variants used pick up the intra and inter annual variability of energy production at all wind farms. The hourly approach produces minimal errors when the EPC and monthly frequency histograms are used in wE_{H-ref} and they are raised most often below 20% (below 15% on average) when power curve and frequency approximations are used. The APC provides a simple and straight forward estimation for the power terms that leads to the best results.

The inclusion of the Weibull approximation raises the error, particularly at sites where the quality of the fit is clearly bad as in the case of Leoz. The results achieved in this work suggest that the choice of a power curve is more critical than the errors stemming from using a Weibull fit to the data.

The interpolation based method provides wE_{Interp} estimations that tend to overestimate monthly wind energy variability due to a larger tilt in the TPC than in the observed relationship between wind speed and wind power at monthly timescales. Nevertheless, monthly energy estimations with this approach may be useful in situations of unavailability of power production data.

The hourly based and linear regression methods perform comparably in spite of the simplicity of the linear regression approach. This supports the use of regression estimates in estimations of energy production from monthly resolution data.

Estimating the wE production from the wind at monthly timescales based on the robust knowledge of the wind speed-wind power relationship can be useful in the medium and long term framework. For instance in an empirical or dynamical downscaling context where the wind speed is derived through its relation with the large scale circulation and afterwards the wind energy is estimated from the wind velocity. Some previous works that assess the past variability of the wind and wind energy density and evaluate possible changes in the wind energy resources in potential climate change scenarios can be found in the literature (Pryor et al., 2005b; Pryor and Schoof, 2005; Kaas et al., 1996; Pryor et al., 2005a, 2006). The empiric linearity between the two variables at monthly timescales involves an additional interesting alternative: the direct estimation of the wind energy production from its relation with the synoptic atmospheric flow. It can be expected that such a relation presents similar properties as the relation between the wind and the atmospheric circulation at monthly timescales due to the empirical linearity observed between wind velocity and power production at these timescales. These issues are explored in the second part of this work where the regional wind variability will investigated in terms of its relationship with the large scale atmospheric circulation and the wind power production will be considered as an impact variable providing a framework to examine its predictability in the basis of changes in the large scale circulation.

Part II

Wind and wind power dependence on large scale atmospheric circulation

5

North Atlantic atmospheric circulation and surface wind in the Northeast of the Iberian Peninsula*

¿Sabe el mar como se llama, que es el mar? ¿Saben los vientos sus apellidos, del Sur y del Norte, por encima del puro soplo que son?.

Pedro Salinas. La voz a ti debida, 1933.

In the first part of this thesis the relationship between wind speed and wind power production was explored. The wind measured at various wind farms in the CFN has been analyzed on the basis of the implications that assuming a certain PDF has on the production of wind energy. A suite of methodologies for the estimation of wind power were investigated leading to disclose a relation between both variables that can be assumed as linear at monthly timescales. This last conclusion will show relevant consequences in the analysis of the wind power variability as a meteorologically-driven variable. In this second part of the work a different perspective is adopted in which both, wind and wind power are analysed through their relation with the large scale atmospheric circulation. Thus, transfer functions translating the large scale information to the regional scale will be derived by applying statistical downscaling techniques.

In this chapter the variability and predictability of the surface wind field at the regional scale over the CFN is explored. A downscaling technique based on Canonical Correlation Analysis (CCA) allows for calibrating and validating a statistical method that elicits the main associations between the large scale atmospheric circulation over the North Atlantic and Mediterranean areas and the regional wind field. In an initial step the downscaling model is designed by

* The main contents of this chapter are included in:
García-Bustamante, E., J. F. González-Rouco, J. Navarro, E. Xoplaki, P. A. Jiménez and J. P. Montávez, 2011: North Atlantic atmospheric circulation and surface wind in the Northeast of the Iberian Peninsula: uncertainty and long term downscaled variability. *Clim. Dyn.*. DOI 10.1007/s00382-010-0969-x.

selecting parameter values from practise. To a large extent, the variability of the wind at monthly timescales is found to be governed by the large scale circulation modulated by the particular orographic features of the area. The sensitivity of the downscaling methodology to the selection of the model parameter values is explored, in a second step, by performing a systematic sampling of the parameter space. The downscaling model is used to extend the estimations several centuries to the past using long datasets of sea level pressure, thereby illustrating the large temporal variability of the regional wind field from inter annual to multicentennial timescales. The analysis will not evidence large long term trends throughout the twentieth century, however anomalous episodes of high/low wind speeds will be identified.

In Section 5.2 the main aspects of the methodology applied are reviewed. Section 5.3 illustrates the results of calibrating and validating the statistical technique applied, showing the pairs of optimally correlated patterns for the synoptic and the local scales, respectively, and the estimations obtained after the method is validated against the available observations. The results within this section will be referred to as the *reference case*, where a certain configuration of the model is selected with illustrative purposes. Section 5 highlights the assessment and implications of the associated uncertainty combining the large scale influence in the estimations with various methodological aspects that could introduce some variance in the results obtained. In Section 6 the long term variability of the wind field over northern Iberia is evaluated in the base of a reconstruction of the wind climatology for approximately the past three centuries. Finally, Section 7 presents and discusses the main conclusions.

5.1 The regional climate problem: the role of the downscaling techniques

The improved understanding of the regional/local wind variability and its relation to the large scale atmospheric circulation, greatly benefits applications targeting the prediction of wind related variables. Assessments of climate variability at the regional scale are mainly based on the application of dynamical or statistical *downscaling* approaches that attempt to bridge the gap between the information provided by large scale datasets as GCMs outputs, reanalysis, etc. and the reliable estimations required at the regional scale by increasing the spatial resolution.

A broad classification of the downscaling techniques divides them into dynamical or statistical (Chapter 1). The dynamical approach involves the use of a RCM that, feeded by large scale boundary conditions, solve the fundamental equations of the atmosphere yielding estimates at refined resolutions. Thus, RCMs are able to provide a coherent response with the large scale boundary conditions and the

physics involved in the cascade of multiple processes to achieve local resolutions. Boundary conditions are usually provided by large scale reanalysis (Hong and Kalnay, 2000; Herrmann and Somot, 2008; Conil and Hall, 2006) or by the outputs of a GCM (Pryor et al., 2005b; Lenderink et al., 2007). Some examples in the context of wind field analysis can be cited: Pryor et al. (2005a) studied the implications of the long term wind variability for the wind energy resources over northern Europe using RCMs; Winterfeldt and Weisse (2009) explored the ability of two RCMs to reproduce instantaneous values and frequency distribution of surface marine winds over the North Atlantic highlighting the added value of RCM simulations compared to reanalysis data and Jiménez et al. (2010b) evaluated the ability of a RCM to identify subregions with similar wind behaviour that was previously found with observations over the same area in the northeast of the Iberian Peninsula (IP).

In turn, the statistical downscaling consists in training a statistical model making use of the empirical relationships observed between the local variables, *predictands* and the large scale atmospheric variables, *predictors* (González-Rouco et al., 2000; Xoplaki et al., 2004; Busuioc et al., 2008). The classification of statistical methods entails a certain degree of subjectivity. In broad terms they can be segregated in analog methods (Zorita and von Storch, 1999), classification techniques (Yarnal, 1993), linear models (Xoplaki et al., 2004) and more sophisticated non-linear approaches, as the neural networks (Hewitson and Crane, 1996), and their use depends on the particularities of the problem. Linear methods, for instance, are widespread used within the context of empirical techniques and the specific method may involve different levels of complexity.

Statistical tools have been widely employed with large scale sea SLP or sea surface temperature (SST) observations to understand the regional precipitation and temperature variations (Zorita et al., 1992; Zorita and von Storch, 1999; Xoplaki et al., 2003a,b, 2004). However such methodologies have not been extensively applied to wind related variables. Some examples can be cited: Kaas et al. (1996) identified the connection between SLP/SST patterns and the local wind field in winter over Scandinavia; Faucher et al. (1999) provided an empirical reconstruction of surface winds using observations from buoys along the western coast of Canada; Pryor and Schoof (2005) proposed an empirical downscaling to estimate variations in the parameters of a typical wind probability distribution at the regional scale in northern Europe; Klink (2007) investigated the relation between the large scale atmospheric circulation and the wind at typical wind turbine heights in central United States (US) using a regression approach and Davy et al. (2010) applied a novel approach based on machine learning strategies combined with a linear regression and a classification scheme to explore the large scale influence on the wind field variability over south-eastern Australia. An

extended application of these methods consists in forcing the statistical model with the conditions in a climate change scenario simulated by a GCM (Denman et al., 2007). Some examples concerning statistical approaches for future climate projections deserve attention: Bogardi and Matyasovszky (1996) combined a circulation classification scheme with multivariate regression to interrelate local wind and large scale atmospheric patterns and studied the impact of a doubling CO_2 scenario in Nebraska; Sailor et al. (2000, 2008) employed neural networks to assess the effects of some climate change scenarios on wind power resources and generation over northwestern US; Najac et al. (2009) applied a statistical downscaling to a multi GCMs ensemble and estimated future changes of the wind field over France in a particular future climate scenario. In this chapter the variability and predictability of the wind field over the CFN is investigated through a statistical downscaling model based on CCA that searches for the associations of large scale predictors in the North Atlantic and Mediterranean areas and the local wind.

Downscaled estimations allow for an understanding of climate variability at the regional scale, but they are also subject to uncertainties that are seldom considered. Uncertainty can be propagated from the global to the regional scale and will be additionally increased in the downscaling step (Mitchell and Hulme, 1999; Schwierz et al., 2006). At the global and large scales, uncertainty permeates through the use of different versions of instrumental datasets reanalysis products or GCMs when, for instance downscaling models are calibrated. All of them produce similar but non-identical representations of climate and will add variability to the downscaled estimations. If experiments in the context of future climate change scenarios are considered, the use of different forcings scenarios and different GCMs will further contribute to this. The use of downscaling models adds to the pool of uncertainty from three main sources. One of them is the specific downscaling scheme selected for the experiment from a variety of dynamical or statistical downscaling approaches (hybrid cases also included) that will produce purportedly similar albeit non-identical results. Once the methodology is selected, there is often a multiplicity of available parameter and configuration options that are based on experience and that also have an impact on the results. Finally, although at the top of the hierarchy of importance, we are subject to our representation of reality by the regional/local observational datasets, that play the role of validation benchmarks for dynamical downscaling or calibration and validation data in the case of statistical downscaling. A proper representation of the cascade of uncertainties would imply a sampling of all possibilities of change at each step of this hierarchy. This would picture the range of all possible estimations attained with the available methods and datasets. This type of assessment can be regarded as a frequentist approach (see Chapter 1)

If we consider the downscaling step, the evaluation of methodological uncertainties stemming from the use of different model configurations is not extensively explored within the statistical downscaling approaches. Here, the uncertainty assessment is based on the examination of the effects that variations of the model parameters can have. These parameters involved in the model configuration that are investigated in this step are for instance the size of the geographical domain of the large scale predictors or the number of canonical patterns retained for the analysis. The uncertainty that arises from the use of different datasets as large scale predictors (reanalysis data, observations or climate field reconstructions) is also evaluated. The combination of both sources of uncertainty will provide a more reliable estimation of the wind field variability. An additional benefit of obtaining a measure of the uncertainties that arise in the downscaling step implies that in subsequent stages of the work they could be compared to those derived from the use of different GCMs in future climate change projections or those coming from the use of different scenarios. In such conditions a representation of the full cascade of uncertainties involved in future regional climate projections would be feasible.

The understanding of the mechanisms responsible for the temporal variations of the regional wind at inter decadal and centennial timescales is hampered by the limited temporal length of the observational series since usually short periods are used for calibrating and validating models. The statistical methodology applied allows for extending the wind estimations several centuries backward in the absence of wind observations using the available datasets of large scale predictor variables. The long term variability of the regional wind is interpreted in terms of the variations in sign and intensity of the main modes of the atmospheric circulation affecting the regional wind that were found during the calibration period. This exercise provides a broader perspective of the regional wind variability in observations that may be of use in the context of comparison with climate change downscaling exercises. To the knowledge of the authors, this approach has not been documented in the literature before.

5.2 Downscaling methodology

The statistical method applied in this study is based on CCA. This is a multivariate statistical technique that isolates linear associations between sets of predictor and predictand variables that are optimally correlated (Hotelling, 1935, 1936; Glahn, 1968; Levine, 1977). The original data are projected onto their principal components (PCs) to remove noise and reduce the number of degrees of freedom. This method was first proposed by Pearson (1902) and applied first to the meteorology context by Lorentz (1955). The CCA selects pairs of spatial

patterns from a set of several space-time dependent fields that have maximum correlation coefficient and generates new pairs of variables from the original fields by linear combination of them. They are called *canonical component vector* or *canonical coordinates*, present maximum correlation and they are normalised to unit variance. The original variables can be expressed as a linear combination of its canonical coordinates and its *canonical correlation patterns*. The last are the result of projecting the original fields onto the *canonical component vectors* space. The *canonical coordinates* or scores represent the intensity of the modes found, that is, they describe the amplitude and sign of the corresponding patterns at each time t. To obtain an estimation of the field of interest, a regression model is designed. It represents the predictand variable as a linear combination of the canonical coordinates and the patterns obtained during the analysis. The methodology is further described in von Storch and Zwiers (1999).

Before calibrating the model, the annual cycle is removed by subtracting the monthly climatological mean to obtain anomaly fields. Time series were also detrended applying a linear least square fit in order to ensure the long-term stationarity (Xoplaki et al., 2003b). In order to account for the latitudinal distortions, anomalies from the large scale fields were weighted at each grid point by multiplying by the square root of the latitude to consider the decreasing size of grid boxes with latitude (North et al., 1982b). Additionally the time series were standardized (dividing by their standard deviation). The size of the matrices allowed for managing the problem in a single step. Eventually, the same number of modes from both predictor EOFs were retained, as they accounted for a similar amount of explained variance, for the posterior combined CCA (Preisendorfer, 1988; von Storch and Zwiers, 1999).

A certain combination of the model parameters was selected in a first step of the analysis. This selection does not correspond to the optimal case, although it generates reasonable estimates of the wind field. This selection, prior to the sensitivity analysis, represents a standard situation (thereafter called *reference case*) to illustrate the potential of the methodology and allows for understanding the emergent associations between predictors and predictands. The choice of parameters for this reference case is exposed in Section 5.3.1. However, variations in this selection and their influence on the results will be explored in the sensitivity analysis in Section 5.4.

After the design of the downscaling model, its skill is verified using a crossvalidation approach. This allows to reduce a possible overfitting of data by the model (Barnett and Preisendorfer, 1987). The crossvalidation is a resamplig technique in which a small number of data is dismissed and the model is trained with the retained data subset. The removed values are then estimated with the calibrated model. This procedure is repeated recursively by sampling subsets of the same

length along the entire observational record in order to obtain a full set of independent estimates that are compared afterwards to the original observations (Michaelsen, 1987). Further details on the size of the sampling subsets are given in the following sections.

The actual extended winter season dataset analysed herein is composed of 91 monthly wind observations at each site (14 yrs x 7 months/year) and thus hardly spans more than a decade. It can be argued this is a limitation for the analysis and should not be forgotten in the interpretation of results since the model is calibrated making use of intraseasonal to decadal crosscovariances and it is assumed to reproduce wind variability at multidecadal and even centennial timescales. This assumption is however not alien to downscaling approaches where the best use of available data has led in some analysis to calibrate models based on comparatively short decadal records (Huth, 2002, 2004; Orlowsky et al., 2008) or, in a more typical approach, to use multidecadal long records to estimate variability on centennial and longer timescales (e.g., González-Rouco et al., 2000; Xoplaki et al., 2003a). On the other hand, the afore mentioned crossvalidation approach contributes to ensure the robustness of the statistical relationships and reduces possible overfitting of data (Barnett and Preisendorfer, 1987).

To evaluate the predicting skill of the method, the correlation coefficient (ρ) and the Brier Skill Score (β) have been used in this work. ρ yields a measure of the temporal concordance between the observations and estimations. β provides a measure of the variance of observations that is accounted for by the model. This coefficient is defined as $\beta = 1 - \left[S^2_{ES}/S^2_{OB}\right]$, were S^2_{ES} represents the variance of the estimations error and S^2_{OB} is the observations variance, provided that the climatology is selected as reference value to evaluate the error. In such conditions $\beta = 0$ represents a prediction not better than climatology. If the estimations error variance is similar to that of the observations a positive β is obtained (the better the prediction, the closer to 1).

5.3 Wind estimations in the CFN: the reference case

In this section results from the calibration of the statistical downscaling model are presented (Section 5.3.1) and evaluated (Section 5.3.2). This will serve as a reference configuration hereafter. Monthly zonal (west-east) and meridional (north-south) components of the wind are employed as predictand fields. These wind field observations were presented in Section 2.3. Additionally, for this exercise, wind data from three wind farms are included to illustrate potential differences in the influence of the large scale circulation on the local wind since in the wind farms data is recorded at heights between 30-40 m and typically on the top of the mountains or hills (recall Section 2.2). Using wind components instead of wind

module introduces directional information that helps to interpret the influence of the large scale circulation and the orography on regional flows. This allows for taking into account the direction of the flow in the search of relations between the regional wind and the large scale circulation since it implies a segregation of large scale circulation patterns that would be merged if the wind module is employed as predictand.

In the reference case two ERA-40 fields (see Section 2.4), ϕ_{850} and $Z_{500-850}$, are used as predictors as they provide a dynamical and thermal description of the atmospheric circulation. The analysis is limited to a geographical area spanning from 35^oN to 65^oN and 40^oW to 10^oE, which includes the western North Atlantic area, the Iberian Peninsula, the British Isles, the westernmost region of the European continent and part of the Mediterranean basin. This spatial window has been used in studies addressing the connections between circulation patterns over a similar Atlantic area and local variables in the IP and Mediterranean areas: temperature (e.g., Xoplaki et al., 2003a,b), precipitation (e.g., Trigo et al., 2004) and solar radiation (e.g., Pozo-Vázquez et al., 2004). 4 predictor $EOFs$ are retained for the analysis, accounting for a 81.5% of the total variance. The same number of $EOFs$ is considered for the predictand that account for a 90.2% of the variance. 2 pairs of canonical modes are retained in the design of the downscaling model. In the reference configuration the size of the crossvalidation sampling subset is one month. This selection does not necessarily correspond to the optimal case. The choice of model parameters is based on a prior heuristic exploration of several model configurations, as a previous step to the sensitivity analysis, to gain some insight about the variance within estimates due to changes in the model parameters. Thus, this configuration was selected for illustration purposes and provides estimations in good agreement with observations. In section 5.4 variations of this reference configuration will be explored.

5.3.1 Canonical patterns and series

The first pair of canonical patterns (CCA1) is represented in Figs. 5.1a,b for the predictor and predictand variables, respectively, together with their amplitude time series or *canonical coordinates* (Fig. 5.1c). The large scale pattern (Fig. 5.1a, shaded for ϕ_{850} and contours for $Z_{500-850}$) depicts a dipole structure with positive anomalies over the North Atlantic area, that reaches the west side of the IP. Negative anomalies are located northeast of the British Isles, centred over the Scandinavian Peninsula. The simultaneous CCA1 pattern for the predictand (regional wind) presents in its positive phase NW-SE wind oriented anomalies which can be related to the well known regional '*Cierzo*'. It should be noticed that the reverse sign of the patterns is also possible since it is determined by the sign of

eigenvalues of the cross-covariance matrix (von Storch and Zwiers, 1999). Therefore, the negative phase of this mode presents contributions to the flow from the SE with relatively warm and moist air advection from the Mediterranean that can be regarded as the typical '*Bochorno*'. The two patterns are physically meaningful provided that the large scale mode induces a pressure gradient that favours a NW-SE (SE-NW) direction for the geostrophic wind. In addition, the axis of the Ebro Valley, aligned with this NW-SE direction, contributes with a strong channeling effect at the surface. Thus, the local wind pattern arises as a result of the large scale atmospheric structure modulated by the orographic configuration of the CFN. This first mode accounts for 18% (22%) of the total variance of the ϕ_{850} ($Z_{500-850}$) predictor field and around 36% of the total predictand variance (see Table 5.1 for summarized information on correlations and explained variances). It is interesting to mention that, in agreement with a more meridional large scale circulation, in this canonical mode the largest amount of explained variance (46%) corresponds to the meridional component of the wind while in the case of the the zonal one, the CCA1 accounts for a smaller portion (25%) of variance. The same large scale regime as found here, that causes a partial blocking of the westerlies, has been associated with the Mistral conditions (Buzzi et al., 2003; Burlando, 2009). Thus, this large scale pattern is broadly responsible for predominant meridional circulations not only in the region under study, but also in wider areas over the European continent.

Table 5.1: Canonical correlations and explained variances by the CCA modes.

	Corr.	$\phi_{850}/Z_{500-850}$ expl. var.(%)	Predictand expl. var. (%)
CCA1	0.87	18/22	36
CCA2	0.86	30/13	36

The corresponding amplitude series for predictor and predictand (Fig. 5.1c) present a canonical correlation of 0.87 and exhibit considerable intra and inter annual variability with extreme values at the end of 1995 and 1999. The variability is higher till 2000 and slightly lower in the following period. As this change in the regional wind variance during the last period is also noticeable in the predictor series, it can be attributed to changes in the large scale circulation variability. The canonical series of the local wind components presents a correlation of 0.92 and -0.83 with the regional time series of the observed zonal and meridional wind components (Fig. 2.6), respectively. Thus, this first canonical mode describes

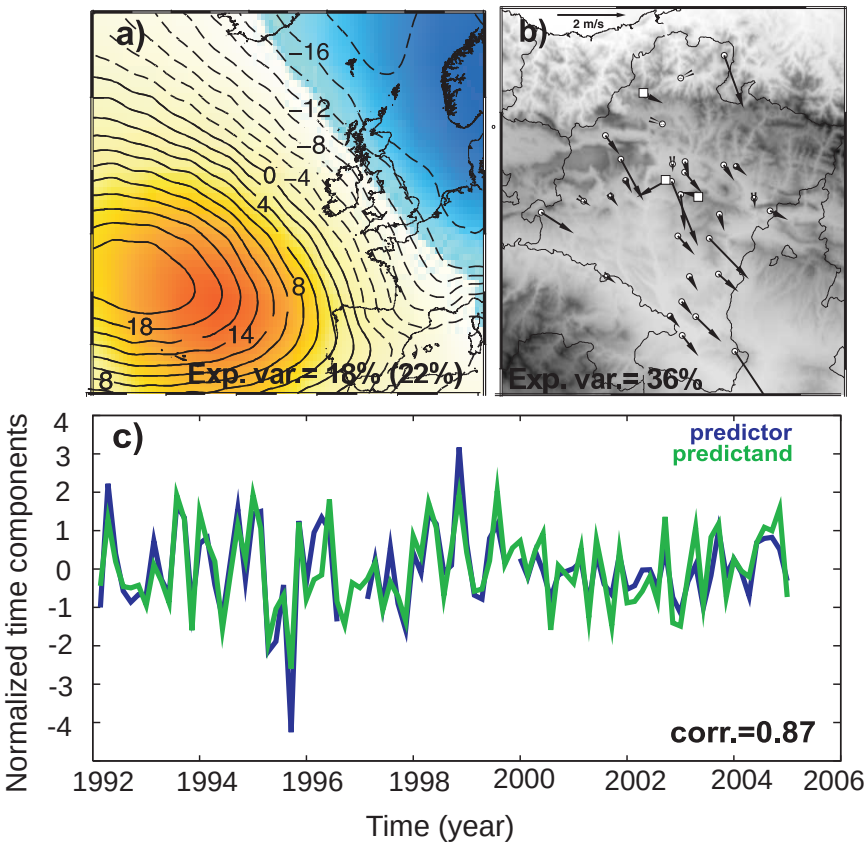

Fig. 5.1: Canonical patterns and series of the first CCA mode (CCA1). **a**) Predictor patterns, ϕ_{850} hPa (shaded) and $Z_{500-850}$ hPa (contours); the explained variance of the ϕ_{850} ($Z_{500-850}$) field is also indicated; **b**) predictand (local wind in the CFN) pattern together with the variance accounted for by this mode; wind farms are represented with white squares. **c**) canonical series for predictor (blue) and predictand (green).

the most important changes in regional monthly wind variability for the period studied.

The second pair of coupled patterns (CCA2) shares 30% (13%) of variance of the ϕ_{850} ($Z_{500-850}$) field and 36% with the regional wind or predictand. Note that this second mode accounts for larger amount of variance of the zonal component (40%) than in the case of the meridional one (33%) which is consistent with a more zonal large scale forcing. In fact, the canonical predictor mode consists of a monopole pattern of negative anomalies centred westward of the British Isles. This pattern in its positive phase indicates a zonally eastward oriented geostrophic flow. The CCA2 wind pattern (Fig. 5.2b) shows a configuration with a more zonal direction at most of the windiest sites over the northern and central part of the region, that coincide with the wind farm locations. These sites are more exposed to quasi-geostrophic circulations and less affected by local scale phenomena. For the rest of stations, the surface wind field displays a SE-NW direction which is coherent with a deflection of the geostrophic wind that tends to balance the horizontal pressure gradient and helps to introduce southern surface flows in the valley mouth. Hence, this mode in its positive (negative) phase evidences contributions to the *Bochorno* (*Cierzo*). This coupled mode shows a decisive impact of the orography, contributing for instance to circulations that are prone to be channeled along the Ebro valley due to the strong orographic constraint. It additionally evidences an important influence of the large scale circulation since some stations in central and northern CFN or the wind farm locations, which are not subject to the channeling effect at the valley, show a more zonal response to that mode. The correlation between the CCA2 time components is 0.86 (see Table 5.1). They show large intensity contributions in 1993 and during the period between 2000 and 2002 and also reveal a considerable intra and interannual variability.

It is well worth to discuss the relation of the canonical large scale modes with the main teleconnection patterns in the Atlantic area. The Iberian Peninsula and especially the CFN, is geographically located at the boundaries of the storm track in the North Atlantic region and potential fluctuations of the different modes over the climate of the region can be expected (Seierstad et al., 2007). The low frequency patterns affecting the European continent are (Barnston and Livezey, 1987): the North Atlantic Oscillation (NAO), this being the preferred mode in this area affecting all seasons and influencing the intensity of zonal and meridional heat and moisture transport; the East Atlantic Pattern (EA), a second predominant mode considered as a southward shift of the NAO and also linked with subtropical low frequency variability; the East Atlantic/Western Russia pattern (EA/WR) -a four-center pattern affecting Eurasia during the

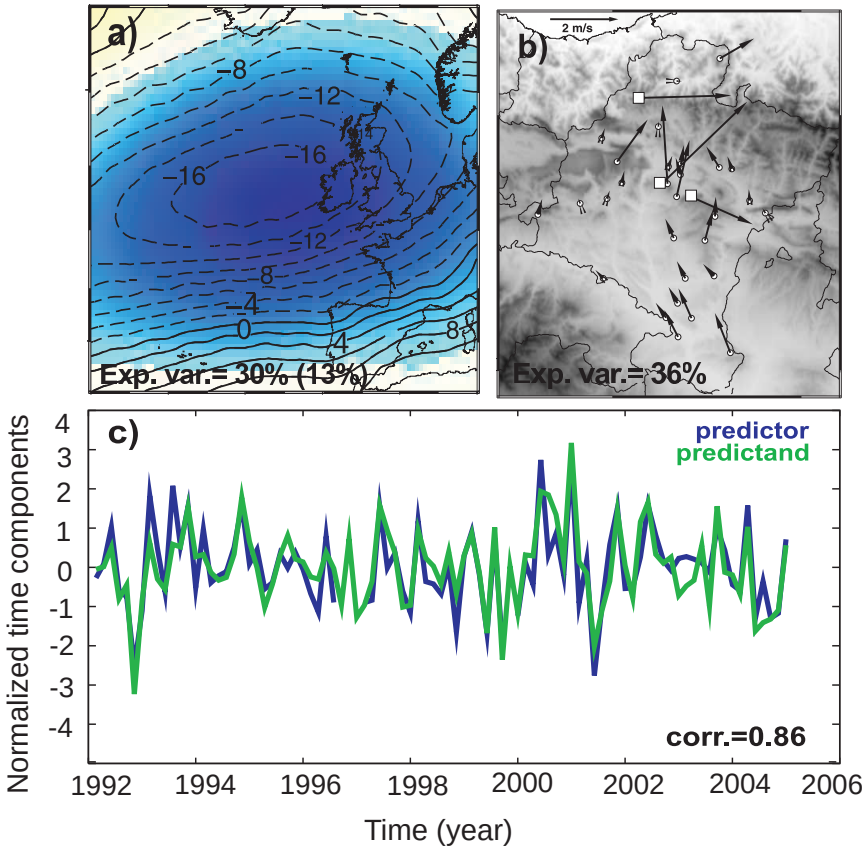

Fig. 5.2: As in Fig. 5.1 but for the second CCA mode (CCA2).

whole year and finally the Scandinavian (SCAN) pattern, which has somewhat weaker centers of opposite sign located over western Europe and western Russia.

In Table 5.2, the correlations between the first two canonical series of the predictor fields and the indexes of the teleconnection patterns are given (Barnston and Livezey, 1987)†. Most of the correlation values are significant at a 0.05 level (in bold). However, the highest correlation with the CCA1 large scale canonical series is found with the East Atlantic/Western Russia mode (EA/WR; Burlando, 2009). In the case of the CCA2, the strongest relation is found for the East Atlantic pattern (EA).

† www.cpc.ncep.noaa.gov/data/teledoc/telecontents.shtml

Table 5.2: Correlation values between the two first canonical series and the main low frequency teleconnection patterns over the Atlantic area: NAO, EA, EA/WR and SCAN.

	NAO	EA	EA/WR	SCAN
CCA1	0.16	**0.28**	**-0.47**	**-0.32**
CCA2	**-0.24**	**0.46**	**0.20**	**0.27**

5.3.2 Validation of wind estimates

The estimated regional anomalies for the zonal and meridional wind components and wind module are compared to their observational counterparts in Fig. 5.3. The correlations between the regional estimations and observations are 0.79 and 0.80 for the zonal and meridional component, respectively and 0.70 for the wind module (all correlations are significant at a 0.05 level). The lower correlation of the wind module can be understood on the basis of the non-linear transformations applied to obtain it from the wind components together with the potential accumulation of the errors from each component. The higher variability of the meridional component becomes evident again. It can be observed that the estimations show also reduced variance with regard to the observations. This loss of variance is inherent to the linear methodologies (von Storch and Zwiers, 1999).

The skill of the method at each station is evaluated through the values of ρ and β represented in Figs. 5.4a,b,c. This inspection allows for a validation of the procedure at the local scale providing an overview of the predictability depending on the specific location. The size of circles is proportional to the correlation (ρ) value and the color is related to the Brier skill score (β). At most locations the correlation values range from 0.85 to 0.50 for both wind components. Also the Brier skill score shows a reasonably good performance of the model in terms of the variance error (values span the interval 0.72 to 0.30). A few locations at the northern areas and some stations at the mainland valleys show a decay of the skill in both their ρ and β values. These stations are located in less windy sites (Fig. 2.5) or in areas with more complex orography that contributes to a decrease of the predictability. Overall, the pattern is very similar for both components but higher scores can be observed along the NW-SE axis of the Ebro Valley for the meridional one. The main differences between them are found in the northern and the mountain stations, where the zonal component predictability is slightly deteriorated. The wind module as in the case of the regionally averaged series shows also slightly worse performance compared to the two wind components.

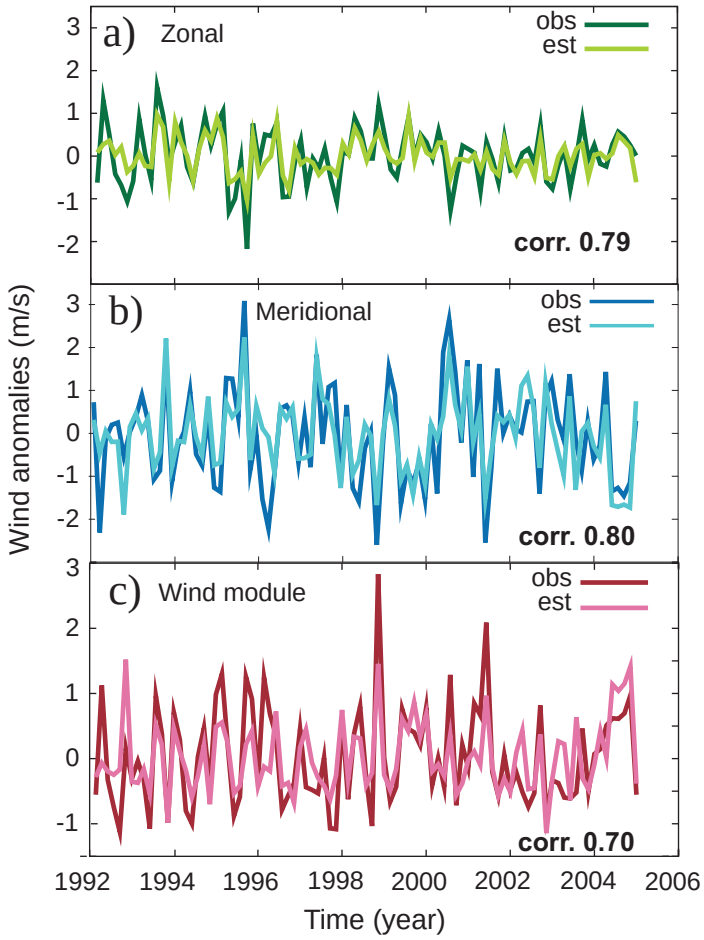

Fig. 5.3: Regional observed and estimated monthly anomalies of zonal (**a**) and meridional (**b**) wind components as well as wind module (**c**).

The Taylor diagram (Taylor, 2001) in Fig. 5.4d illustrates the behavior of the regional estimations compared to the performance of the wind estimates at each location. This is a polar diagram where the angle is indicative of the correlation value and the radial coordinate accounts for the standard deviation between estimations and observations at each location. Green (blue) points correspond to the zonal (meridional) component of the wind for each site whereas the red dots

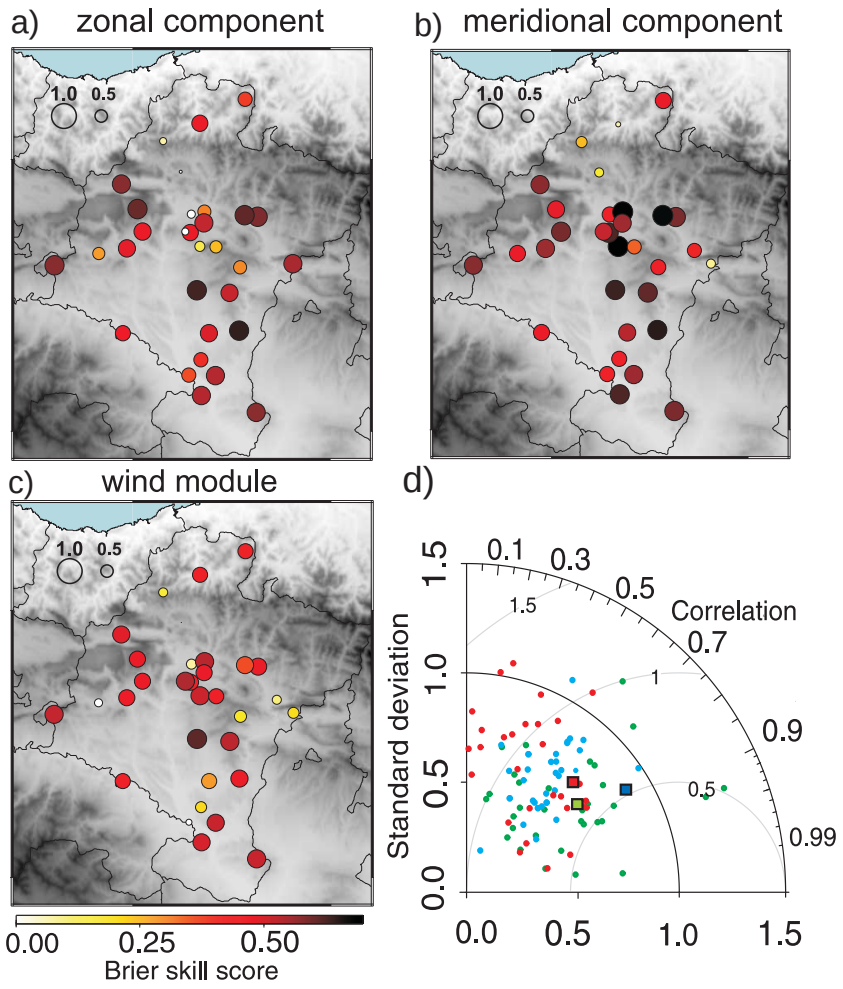

Fig. 5.4: Correlation (circle size) and Brier skill scores (colors) calculated between the wind observations and estimations for **a**) zonal, **b**) meridional wind component and **c**) wind module. **d**) Taylor diagram for each wind component (green is zonal and blue meridional) and for the wind module (red) for each time series (points). The corresponding regional scores are represented with squares.

correspond to the wind module. It is worth noting that the regional average time series (squares) tend to outperform the cloud of points. The regional estimates filter out many local effects that in some cases cannot be well captured by the downscaling model and reinforce the signal to noise ratio. This is especially the case of the meridional component of the wind that is characterized by showing common variability in the whole region of study (Jiménez et al., 2008b).

On the basis of the results above, hereafter, the discussion of the method performance will be restricted to the wind components.

5.4 Uncertainty analysis

In this section an evaluation of the uncertainties associated with the statistical downscaling model is presented. The methodological sensitivity is assessed in order to evaluate to what extent a certain choice of parameters in the set up of the experiment produces an impact in the estimations, thus exploring the robustness of the downscaling strategy. The approach consists in allowing a certain degree of variability in each parameter that is important for the model configuration. The sampling of the parameters space is accomplished in two subsequent steps. First, variations in each parameter with respect to the reference model are allowed keeping the others fixed. This variation of parameters generates a family of estimates that will allow for an assessment of the spatial variability of the method sensitivity to changes in one specific parameter. Second, all parameter values are systematically varied in a large amount of model configurations that allow for any parameter combination (see Table 5.3). By doing so the temporal evolution of the method sensitivity will be studied.

The uncertainty derived from the large scale adds on top of the cascade when evaluating the regional estimations of climate variability. In this context, it is also interesting to evaluate the impacts of using large scale predictors from different datasets. The differences between datasets are connected to their nature, for instance whether they are observations, global model outputs or reconstruction data or to the methodologies applied to obtain these datasets for instance, the quality control procedures, their validation, interpolation schemes, etc. This type of uncertainty is explored in section 5.4.2.

5.4.1 Methodological uncertainty

The parameters of the model configuration that are systematically sampled are: a) the size of the large scale domain, tested by using different windows that cover from smaller areas over the target region to larger windows over the northern

Atlantic and Mediterranean areas; b) the predictor field, considered by examining several dynamical and thermal variables and/or combinations of them; c) the number of EOFs and CCAs retained for the analysis and d) the size of the crossvalidation subsets, exploring cases where this changes from one month to four years (28 months). The crossvalidation option is not a decisive parameter of the downscaling method since it does not affect the associations between the large scale circulation and the regional wind. However changes of the crossvalidation subset length should not affect an assessment of the quality of estimates. Thus, it is interesting to test the robustness of the validation process to variations in the crossvalidation option. The number of options for all parameters is summarized in Table 5.3.

Table 5.3: Parameters of the model configuration and number of options considered for each one. The last two rows correspond to the total number of experiments (note that the penultimate row is the result of the sum of the number of options when a single parameter is allowed to vary and the last row corresponds to the case where changes in all parameters are combined).

Parameter	n^o options
Predictor domain	9
Predictor field	25
n^o EOFs/CCAs	31
Crossval. subset	9
Total n^o experim. 1 param. varying	74
Total n^o experim. all params. varying	62.775

Nine large scale windows (Fig. 5.5; plotted for illustration over the ERA-40 SLP mean field) are analysed with the aim of understanding and illustrating the effect of the spatial domain on the estimations. The window corresponding to the reference case is number 4 in this figure. Regarding the predictor field(s) the variables considered are: SLP, ϕ_{850}, ϕ_{500}, the $Z_{500-850}$ and the UV10 fields together with all possible combinations of two or three of these fields. The number of retained EOFs for the analysis varies between 2 and 6. The maximum (6) was determined by including all the statistically significant correlations between the predictor and predictand principal components (PCs). This can be seen in detail in Fig. 5.6a where the coloured matrix shows the correlation values between the first six predictor and predictand PCs (significant correlations at 0.05 level are marked with a circle). For the minimum number of EOFs a criterion based on the variance that the leading EOFs account for is considered. This minimum is

determined by the presence of a breakpoint in the curves of Fig. 5.6b (explained variance *vs.* number of EOFs/CCAs) which is an indicator of the modes that should be included in all the experiments since they contain the most significant amount of explained variance. In the case of the predictor, the minimum number of EOFs is 2. This implies a 57% of explained variance. For the predictand the breakpoint occurs also at the second EOF (more than 80% of explained variance). The selection of the number of EOFs can be also done with more sophisticated methods although there is no optimal criterion for it (Kaiser, 1960; North et al., 1982a; Preisendorfer, 1988). In the case of the number of CCAs, the maximum is imposed by the maximum number of EOFs retained, since the number of CCA modes must be equal or smaller than the smaller (predictor or predictand) number of EOFs (Barnett and Preisendorfer, 1987). Although the maximum was 6 only the first four canonical patterns presented significant correlations. The minimum is set to 2 with the same criterion of explained variances (see Fig. 5.6b, note that the explained variance of the predictor is that accounted for by the two combined fields, ϕ_{850} and $Z_{500-850}$). Thus, all possible combinations (31) between the number of EOFs and CCAs in the ranges commented are employed. The crossvalidation time step parameter varies between one month and four extended seasons (September to March) so 1, 2, 3, 4, 5, 6, 7 (equivalent to 1 yr),14 (2 yrs) and 28 (4 yrs) months are the crossvalidation subset sizes considered.

Considering the above possibilities, 74 realizations of the model (see Table 5.3) are obtained. The spatial distribution of the methodological variance is represented in Fig.s 5.7a and 5.7b for the zonal and meridional wind component, respectively. The size of the circles at every location is related to the dispersion of the ensemble of estimations: for each time step it is calculated as the difference between the maximum and minimum estimated values and then temporally averaged to obtain a single *sensitivity* value at each site. It can be observed that the circles are larger in the more windy places (the area of the Ebro Valley and the highest mountain sites, see Fig. 2.5) that also correspond to those locations where the wind speed variability is also larger (section 2.3). This is illustrated by plotting the *sensitivity* at each location (size of circles in Figs. 5.7a and 5.7b) against the corresponding observed standard deviation of the wind (Figs. 5.7c and 5.7d, zonal and meridional component, respectively). A linear relationship between them is evident. This leads to the conclusion that the larger the standard deviation and thus, the variability of the wind at the specific location, the larger is the sensitivity or associated uncertainty. In these figures it is also evident that the meridional wind component presents higher levels of variability, thus, also a higher sensitivity, compared to the zonal one.

The respective influence of each model parameter has been further analyzed by separating its individual contribution to the spread of estimations. This is

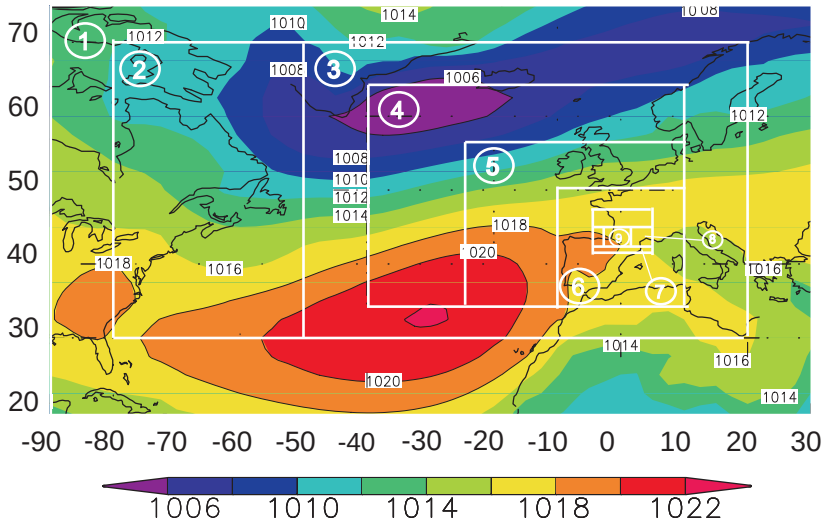

Fig. 5.5: Different large scale domains together with the mean field of one of the predictor variables (ERA-40 SLP) considered for the sensitivity analysis.

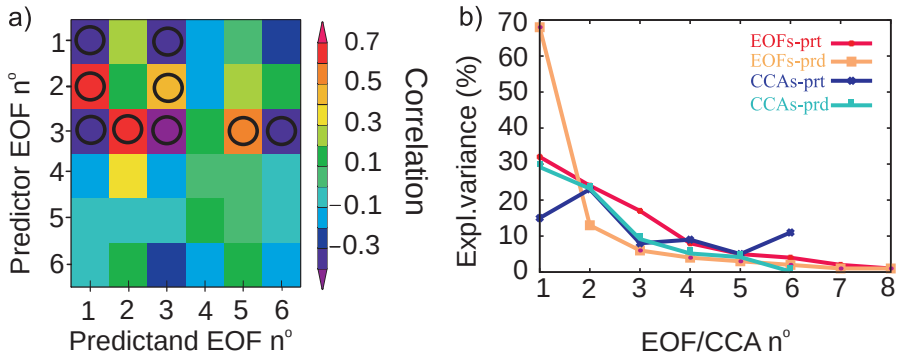

Fig. 5.6: **a**) Correlations between predictor and predictands EOFs. Significant values at a 0.05 level are marked with a circle. **b**) Explained variance as a function of the number of EOF/CCA modes retained for the predictor (red/blue) and predictand (orange/light blue).

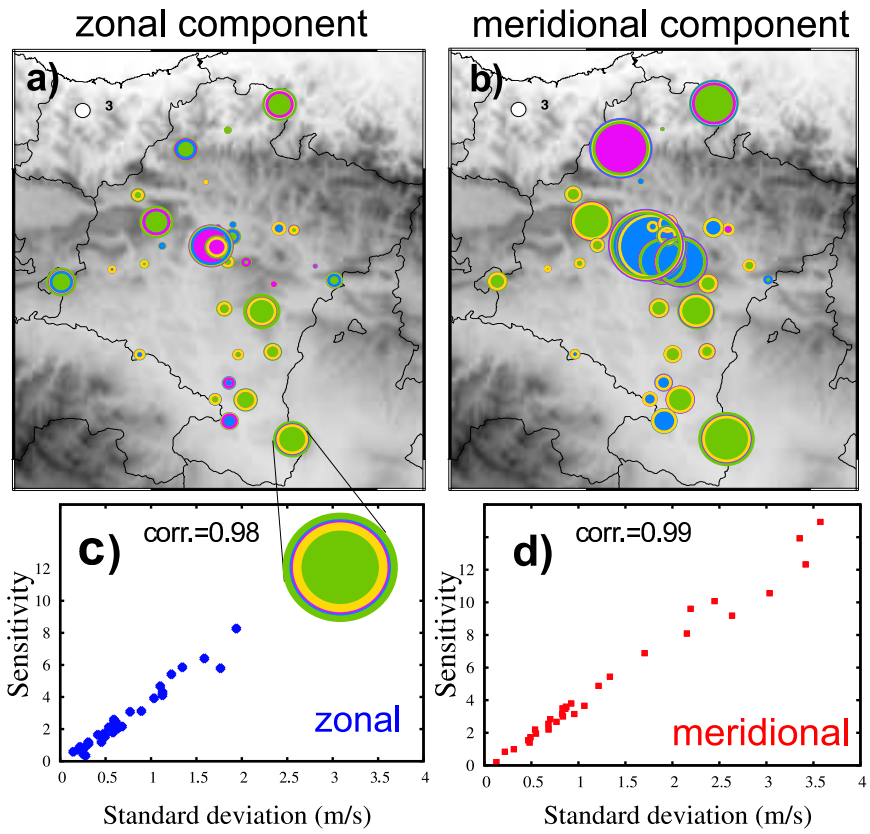

Fig. 5.7: Top: Methodological sensitivity at each location in the CFN for the zonal (**a**) and meridional (**b**) wind component, respectively. The size of circumferences is related to the methodological sensitivity obtained in the first step of the uncertainty analysis (only one parameter is allowed to vary at a time in the model). Colors indicate what parameter produces the largest contribution to the sensitivity at each location (green corresponds to the large scale window, violet to the predictor field, blue is associated with the varying number of EOFs/CCAs retained and yellow corresponds to the crossvalidation subset size). Bottom: *Sensitivity* at each location in the CFN *vs.* the corresponding standard deviation of the wind for the zonal (**c**) and meridional (**d**) component.

done by plotting at each location circumferences with increasing size according to the impact of each parameter in the total uncertainty (Figs. 5.7a,b). A color code is needed to identify the influence of the variable large scale window (green), the change of predictor field (violet), the varying number of retained EOFs/CCAs (blue) and the crossvalidation subset option (yellow). At each site only the largest circumference is filled with the corresponding color to help in the identification of the parameter that produces larger sensitivity. It can be appreciated that in most parts of the region the size of the large scale domain is responsible for generating the largest uncertainties for the two wind components. There are a few places, especially for the meridional component, where the number of EOF/CCA modes included produces a larger contribution to the uncertainty. However, it is also noticeable that the individual contribution of each parameter is very similar in most of the sites of the region (i.e., similar circumference size, see the zoomed circle in Fig. 5.7c as an example). In this line, Huth (2002) reported, that the performance of the different predictors were comparable as long as thermal and dynamic fields were included when applying similarly a statistical downscaling approach to estimate daily temperatures over Central Europe.

The interest is focused now in considering the combination of all possible parameter configurations in the design of the experiments, i.e., the parameters described above are allowed to vary jointly in this second step giving rise to a considerably larger number of estimations (more than 60.000, see Table 5.3). This complements the preliminar methodological sensitivity evaluation in the previous step. The large ensemble obtained is divided in ten groups of equal frequency (deciles) distributed around the median. This is represented for the regional time series in Figures 5.8a and 5.8b (for the zonal and meridional wind component, respectively) together with the observations (black line), the reference estimate (gray, see section 5.3) and the maximum and minimum values (dashed orange line). It is interesting to observe that, qualitatively, the uncertainty area preserves the variability of the observations during the whole period 1992-2005, pointing out the robustness of the methodology in estimating the wind field. Thus, most of the observations are confined within the uncertainty intervals. For illustration, it is shown in the horizontal axis a square-symbol every time the observations exceed the sensitivity area. In the case of the zonal (meridional) component a 15% (9%) of the observations falls out of the area. This percentages agree with the better predictability of the meridional component as explained in section 5.3.

Thus, the uncertainty represented in Figures 5.8a,b evidences that the performance of the model is not largely dependent on the configuration selected and it can be argued that the method is able to reproduce the main features of the surface wind field over the region whatever the selection of the model set up is. The reference estimate maintains to a good degree a centered position within the

spread: i.e., the selection of parameters in this case does not yield estimates biased to the tails of the distribution. This suggests that the associations found between the global circulation and the regional wind exposed through the reference case in section 5.3 are representative of the large number of possible configurations considered in this part of the experiment and also representative of the influence of the synoptic circulation in the regional wind variability.

The deciles distribution of the residuals (estimations minus observations) are shown in Figs. 5.9c (5.9d) for the zonal (meridional) wind component, respectively, for a brief insight into the temporal variation of the errors. No significant trends can be observed neither for the zonal nor the meridional series, pointing that the variance of the residuals is constant along the calibration period, as desired. The structure of the residual series is noisy but still resembles the variability of the observations. As the residuals represent the portion of the observed variance not explained by the model, this points out the existence of a tendency to underestimate the observations variance. A formal residual analysis would include an evaluation of the residual autocorrelation, probability distribution, etc. This is out of the scope of the present study however, a formal treatment of the residuals can be dealt with in future stages of the analysis.

5.4.2 Single and multi-data experiments

To gain insight into the possible impacts of using different datasets as large scale information entering the model, two comparable experiments are considered. For them the SLP is the single predictor since for some of the datasets this is the only variable available. The rest of parameters are allowed to vary freely as in the previous exercise. The first experiment uses the SLP field from ERA-40 and involves a total of 2511 model configurations. This will be referred hereafter as the single-data experiment. In a second experiment SLP fields from the following datasets were employed (see Table 2.5): the observed NCAR SLP (Trenberth and Paolino, 1980), the Hadley Centre historical SLP (Allan and Ansell, 2006) and the SLP reconstruction for the North Atlantic area by Luterbacher et al. (2002). Similarly every parameter, except for the predictor field is varied in this second case implying a total of 5301 realizations. Note that the Luterbacher et al. (2002) dataset allows only for 5 windows since the westernmost longitude is 30^o. This exercise will be referred to as the multi-data experiment through which the effect of using different large scale data resources can be assessed.

The deciles distributions of the ensemble of regional estimates for the single- and multi-data experiments are calculated to account for the sensitivity of estimations to the use of different predictor datasets. The differences between the two deciles distributions is represented in Fig. 5.10. Differences for the zonal component present a certain tendency to lower values at the second half of the

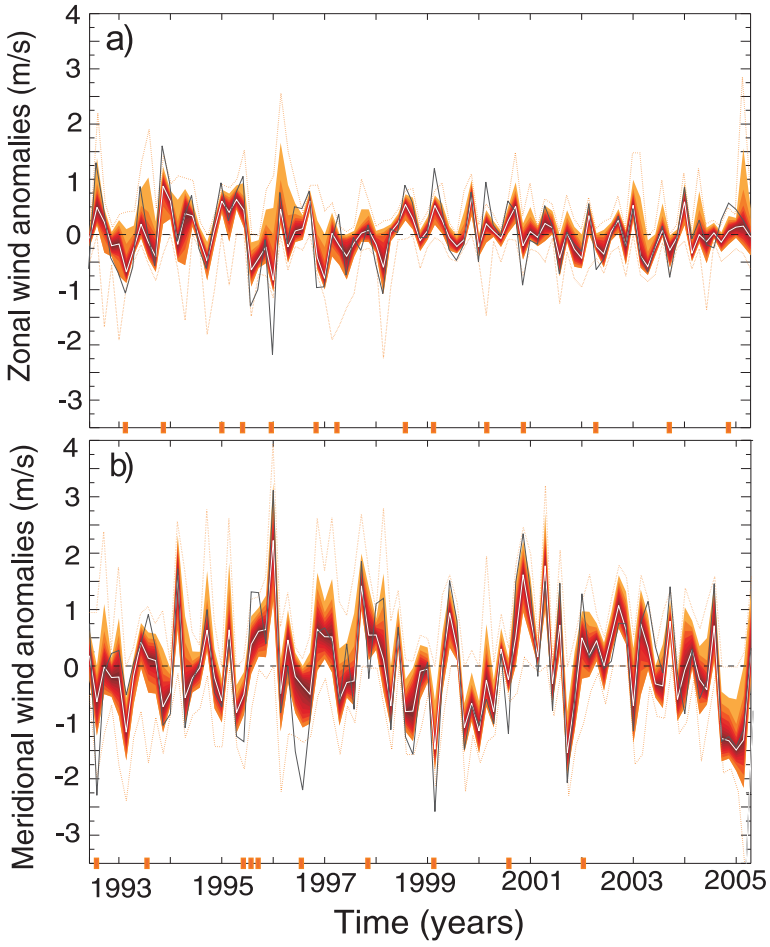

Fig. 5.8: Deciles distribution of the regional estimations (orange) with respect to the median for **a**) the zonal and **b**) the meridional wind component together with the observations (black line), the reference case estimate (gray line, see section 5.3) and the maximum and minimum values (dashed orange line).

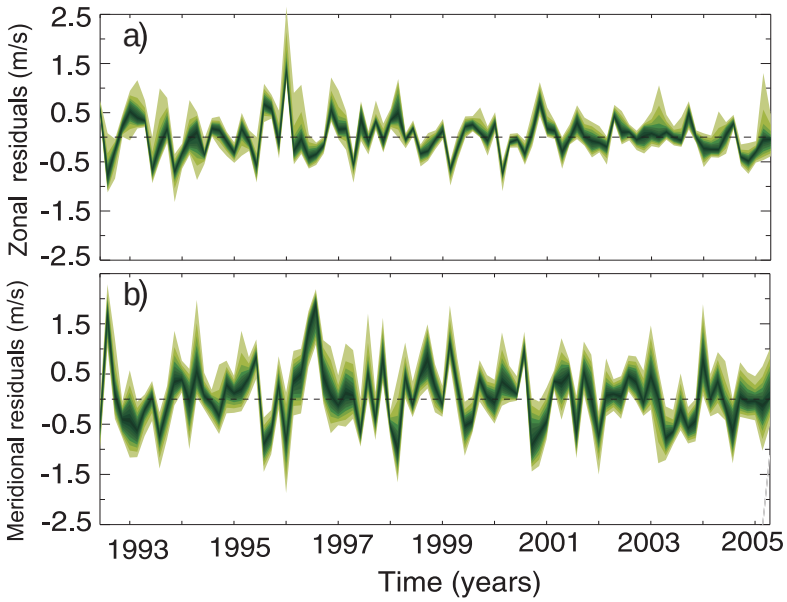

Fig. 5.9: Deciles distribution of the regional residuals (estimations minus observations) for (**a**) the zonal and (**b**) meridional wind component.

calibration period (1998-2005) compared to the levels of variance of the first half. This is to a less degree also apparent in the case of the meridional component. These changes in the variance of the regional wind have been already discussed in the view of the the canonical series of the previous section and they were attributed to changes in the large scale circulation. Therefore it is apparent that all datasets used capture a fluctuation in the variability of the atmospheric circulation around this period. As a result and in agreement with what was hypothesized in subsection 5.4.1, the methodological uncertainties associated with the use of different large scale predictors are larger at the beginning of the observational period since the variability of the regional wind field is also larger during the first years. A closer look at the distribution (see also boxplots in Figs. 5.10b,d; blue for the single and violet for the multi-data cases) evidences that these differences are mainly localized in the upper deciles of the distribution, especially the ninth decile. Then, most of the residuals (approx. 80% of the estimations) are close to zero, denoting that no large differences are found from the fact of using different datasets as predictors. In addition, differences between the single-data percentile distribution (blue in Figs. 5.10b,d) and the first case of including variations in

all parameters (green; recall that identically only ERA-40 but for more predictor variables were used in the previous subsection) are small since the 90% of values are similarly distributed for both wind components. This supports the previous reasoning of Section 5.4.1 where it was argued that the use of one predictor or combinations of various of them did not cause a very strong impact on the methodological uncertainty.

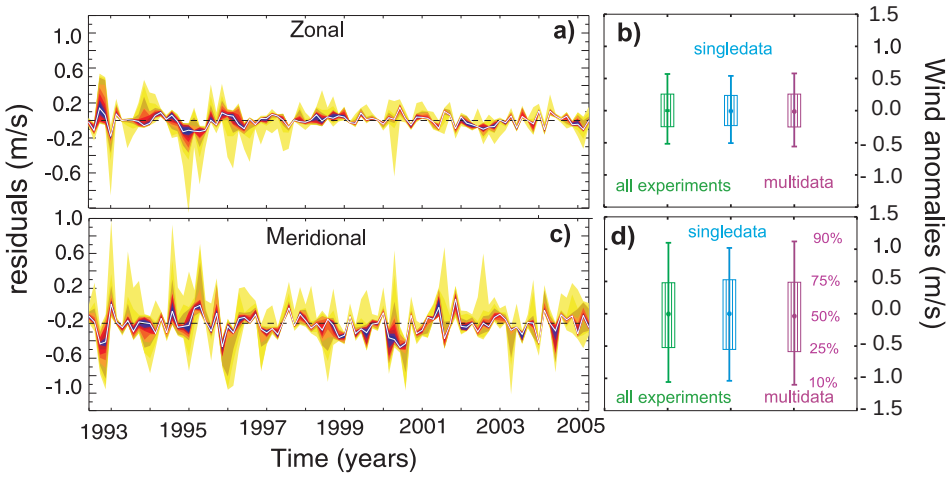

Fig. 5.10: Left: multi-data minus single-data regional residual deciles distribution. Right: frequency distribution for the first experiment (variations of all parameters and ERA-40 predictors, Section 5.4.1, green), the single-data (blue) and the multi-data experiments. **a**) and **b**) is the zonal and **c**) and **d**) the meridional wind component.

5.5 Wind field long term variability: a wind climatology reconstruction

The following paragraphs focus on the assessment of the long term past variability, from inter annual to decadal or centennial timescales, of the regional wind in the area under study together with the estimation of the long term uncertainties associated with the use of multiple model configurations.

The statistical model derived in Section 5.3 allows for obtaining wind speed estimates when no observations are available out of the calibration period. Simi-

larly, as in Section 5.4.2 regarding the multi-data exercise, the SLP from different datasets is used in the present case as single predictor, yielding past estimations with different temporal coverage (recall Table 2.5). First, a reference past estimation with each predictor dataset is calculated. For each reference experiment an equal selection of parameters, as the one described in Section 5.3, is considered. Additionally, to make all the experiments comparable the calibration period is fixed to the period 1992-1999, imposed by the time span of the longest SLP dataset (Luterbacher et al., 2002, reconstruction). Thus, the four reference reconstructions differing in their corresponding length and predictor source are labeled as: R_{era40} for the last five decades, R_{ncar} for the 20^{th} century, R_{had2} covering the period 1850-2004 and R_{Luterb} for estimates back to the 17^{th} century.

The reference reconstructions of the zonal and meridional regional wind component anomalies are shown in Figs. 5.11a,b. The associated projected uncertainties related to all possible variations of the model parameters (as in section 5.4.2, see Table 5.3) are also presented as decile distributions in Fig. 5.11. Some general features of the reconstructed series regarding the long term past variability can be discussed. The meridional component presents again larger variability compared to the zonal one. The negative correlation between the two components also exists at longer time scales as a consequence of the momentum conservation discussed in section 2.3. All reference reconstructions in Fig. 5.11 show a good temporal concordance in their corresponding overlapping periods and also during the calibration period. It is interesting to observe that a slight discrepancy between the reconstructions takes place in the period from 1850 and 1900, where R_{had2} presents a certain tendency to more negative (positive) anomalies for the zonal (meridional) component compared to R_{Luterb}. This fact suggests the existence of differences in the SLP fields from each data source that were not evident during the observational period (Section 5.4.2). A strengthening or weakening of the large scale patterns in one dataset with respect to the others can be responsible for certain discrepancies between the wind estimates. This issue will be further discussed latter in the present section. Another possibility is that these discrepancies are caused by the presence of certain inhomogeneities in the earlier years of the HadSLP2 dataset due to differences in the density of predictor data in the SLP reconstruction procedure (Allan and Ansell, 2006).

Higher anomalous wind velocities can be observed, for instance, in the second half of the 17^{th} and 20^{th} centuries, the first half of the 18^{th} century, the beginning of the 20^{th} century and during the observational period. These larger anomalies (marked with a dashed line in Fig. 5.11) are especially noticeable in the meridional component of the wind. Regarding the high anomalies during 17^{th} century, previous works address interestingly an increase of wind extremes during the colder period of the Little Ice Age and especially during the Maunder

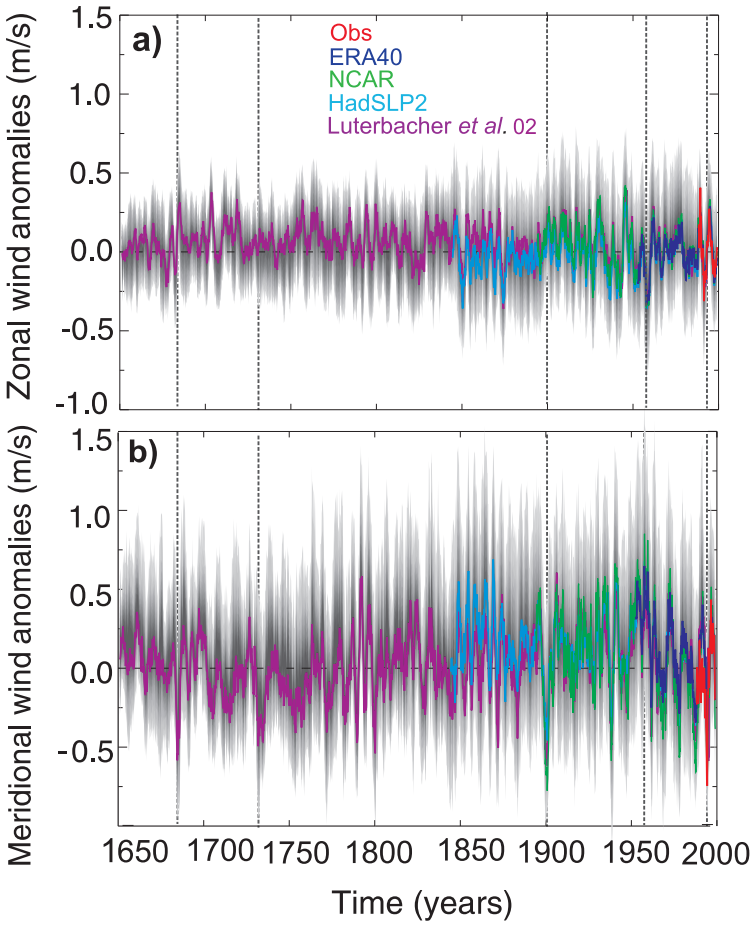

Fig. 5.11: Wind climatology reconstruction and its associated uncertainty for the zonal (**a**) and meridional (**b**) wind component, respectively. The uncertainty is represented in gray. See legends for the colors of each driving dataset. Series present a 2 yr moving-average filter.

Minimum (1640-1715) apparently due to a southward shift of the storm tracks between 20^{o}N and 35^{o}N (Raible et al., 2007). However, no significant trends at multicentennial scales are found for the whole reconstruction period. Despite the former, it is apparent the presence of a certain tendency of the zonal (meridional) wind component to positive (negative) values during the second half of the 20^{th} century till present. This can be interpreted as a strengthening of the first canonical mode (Fig. 5.1a) connected with intensification of northwesterly winds over the region. This reinforcement of the meridional circulation was also found by Davis et al. (1997) who detected a trend indicative of such intensification over the eastern Atlantic and western Europe in the second part of the 20^{th} century while exploring the semi permanent subtropical anticyclone and its spatial and temporal variance structure. The reconstructed climatology as well as the projected uncertainty anomalies (gray-shadowed in Figs. 5.11a,b) reveal the presence of inter annual and decadal variability.

This can be further assessed by means of the wavelet spectra represented in Figs. 5.12a,b for the zonal and meridional wind components. As the reference reconstructions show very similar variances, only the longest reconstruction (R_{Luterb}) has been selected for this analysis. For details on the wavelet spectra calculation the reader is addressed to Torrence and Compo (1998). In Fig. 5.12 the significant variance at the 5% level above a red noise background is given by the thick contours. Additionally, the cone of influence that specifies the region in which the edge effects, due to the finite length of the series, become important, is also represented by the dashed line. It can be seen that both components present some intra annual variability, denoting that changes of the wind field month to month are statistically significant. The presence of seasonal variability is also evident, especially for the meridional component. Although the annual cycle was removed prior to the analysis, a residual variance is still present around the 7 month (= 1 year) band. This could be attributed to the presence of a residual portion of variance from the annual cycle in the anomalies during the calibration period (not shown) that can be propagated through the projections and that manifests itself with special emphasis in the meridional wind component. Although a more sophisticated procedure accounting for the annual cycle goes beyond the aim of the present work, some references in the literature, as Wu et al. (2008) who propose an alternative modulated cycle taking into account the non-stationarity of the cycle could be considered.

Between 1800 and present a few isolated significant regions can be seen in the 3-14 yr bands with a tendency to vanish in the preceding decades, in both the zonal and meridional wind components spectra. For the previous centuries, although some variance is still present in this frequency band it cannot be considered as significant. A potential loss of variance during the first decades of the

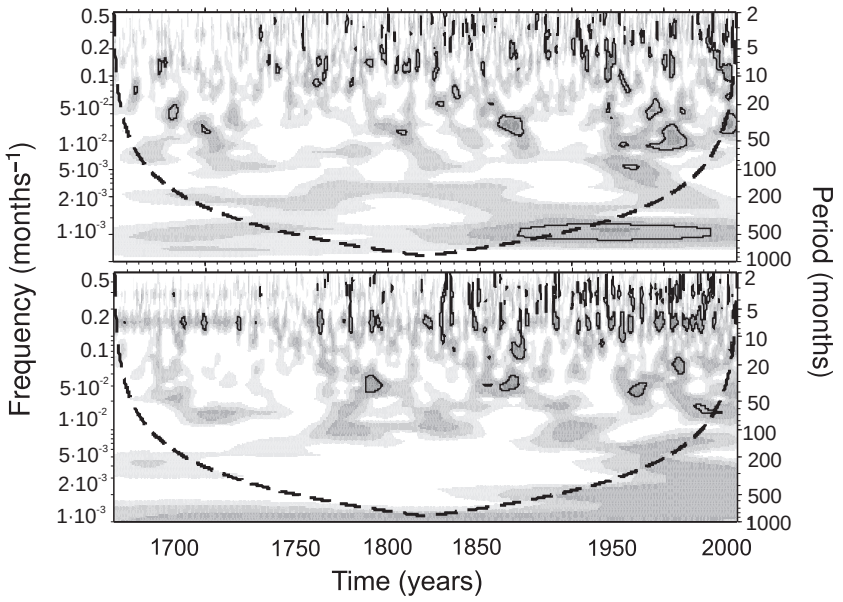

Fig. 5.12: Wavelet spectra of the zonal (top) and meridional (bottom) regional R_{Luterb} estimations.

SLP reconstruction for the Eastern North Atlantic area could be associated with the lack of significant variance in the wind reconstructions, however further analyses would be necessary to understand these changes in the variance along the reconstruction period.

The deciles distribution of the uncertainty, similarly to that of the calibration period (Fig. 5.8) is also represented in Figs. 5.11a,b (gray shadowed). It can be said that the variability of the past projections of the uncertainty remains in reasonable levels of variance compared to the variance of the reference reconstructions. The effect that each parameter produces in the long term methodological uncertainty can also be discussed. During the observational period the relative importance of the different parameters on the estimated wind was tested. Variations in the predictor field(s), the large scale window, etc., have evidenced a comparable influence in the uncertainty (see section 5.4.1). However, the question can be posed whether this argument can be considered plausible also for long term variations, or on the contrary, at longer timescales, any of the model parameters has a particular impact on the estimations. To answer this question the estimations are segregated by isolating all cases with a fixed parameter value

allowing variations in the rest of parameters of the model configuration in order to investigate the specific influence of each parameter in the reconstructed wind. Only results concerning the number of canonical patterns included in the downscaling model are illustrated (Fig. 5.13). The uncertainties associated with the estimated wind components have been separated according to the inclusion (orange) or exclusion (gray) of the third and fourth canonical modes. The first situation produces a visible bias to positive (negative) zonal (meridional) anomalies in the earlier years of the reconstruction, while the opposite is true for the case with only two canonical modes (gray in Fig. 5.13).

The third large scale canonical pattern (CCA3, not shown) consists in a dipole with positive (negative) anomalies over the eastern North Atlantic and a center of opposite sign located to the north of the IP contributing to NE-SW (SW-NE) wind anomalies in the region. This mode is interesting for several reasons. On one hand, the ideal atmospheric situation that generates the Cierzo conditions consists of high surface pressures over England and low ones over the Balearic islands and Italy, as in the CCA3 large scale pattern in its positive phase. However, the strength of the association of this pattern with the regional wind in the northeastern IP is variable. While small canonical correlations (0.2) and predictand explained variances (5%) are found in the observational period between 1992 and 2005, in the reconstruction exercises, where the statistical model was calibrated between 1992 and 1999, the canonical correlation is 0.66 accounting for a 15% of predictand variance. A test on the sensitivity of the estimations to changes in the calibration interval and length along the observed period was conducted. No impacts were detected due to slight variations in the intensity of the associations between the local wind and the large scale circulation modes. Nevertheless the strength of the large to local scale associations may change depending on the time interval considered because of low frequency changes in the modes or in their relative weights (explained variances) throughout the calibration period. This can potentially affect long term estimations of the wind as illustrated in Figure 5.13. Even in the case of having relatively long records for calibration (Kaas et al., 1996; Benestad, 2002; Xoplaki et al., 2003a) there is no means of anticipating the occurrence of temporal changes in the associations between the local and the large scales out of the observational period and in fact, this is usually catalogued as the main drawback of statistical models.

An extended estimation of the large scale CCA3 canonical series calculated applying a regression using Luterbacher et al. (2002) SLP as predictor is represented in the inset in the middle panel of Fig. 5.13. It is apparent the presence of a tendency towards negative scores which is indicative of a change in sign of the third large scale mode (see Section 5.3.1). This tendency can be considered responsible for the reverse of sign in the past wind estimations depending on the

inclusion or not of the third canonical mode, whose contribution to the regional wind is variable. Thus, the apparently negligible impact of selecting a specific number of canonical modes evidenced during the calibration/validation period, turns out to be of importance in the application of the downscaling model outside of the calibration period. This fact highlights the need for assessing and understanding the uncertainties associated to the methodology for obtaining downscaling estimates and illustrates that estimations based on a single configuration of the model must be interpreted with care.

5.6 Conclusions

The analysis of the wind field variability and predictability at the northern Iberian Peninsula is undertaken by applying a statistical downscaling technique, the Canonical Correlation Analysis, to identify the main associations between the regional predictand and the large scale circulation over the North Atlantic area at monthly time scales. To do so, wind measurements from several locations in a complex terrain area at the NE of the IP for the period between 1992 and 2005 has been used.

The two first canonical modes from a certain configuration of the model have been shown as a reference example where the predictor fields (ϕ_{850} and $Z_{500-850}$) are supplied by the ERA-40 reanalysis. The modes of variability found highlight the meridional component of the flow as preferred direction of the regional wind together with the strong influence of the surrounding orography as the Ebro Valley, which serves as a natural channel that accelerates the flow. The wind field is represented as a linear combination of the leading synoptic patterns governing the regional circulation. The approach has proven skillful after comparison of the estimations with the observed wind during the crossvalidation process.

Results evidence a certain underestimation of the variance that can be attributed to the linear constraint imposed by the method in the search of associations between the regional and the synoptic circulations. Thus, there is space for the study of alternative approaches that do not emphasize the linearity in the methodology. In addition, non-linear processes that resolve in shorter than monthly timescales are filtered out here. They may also contribute to some extent to the wind variability underestimation. This calls for the investigation of these type of statistical downscaling methods at, for instance, daily timescales, in order to test their skill in reproducing higher frequency wind variability.

The methodological sensitivity has been evaluated by allowing individual variations of the model parameters values. This exploration illustrates that the uncertainty associated with the method depends on the variability of the wind at each specific location. In a second step multiple experiments are carried out in

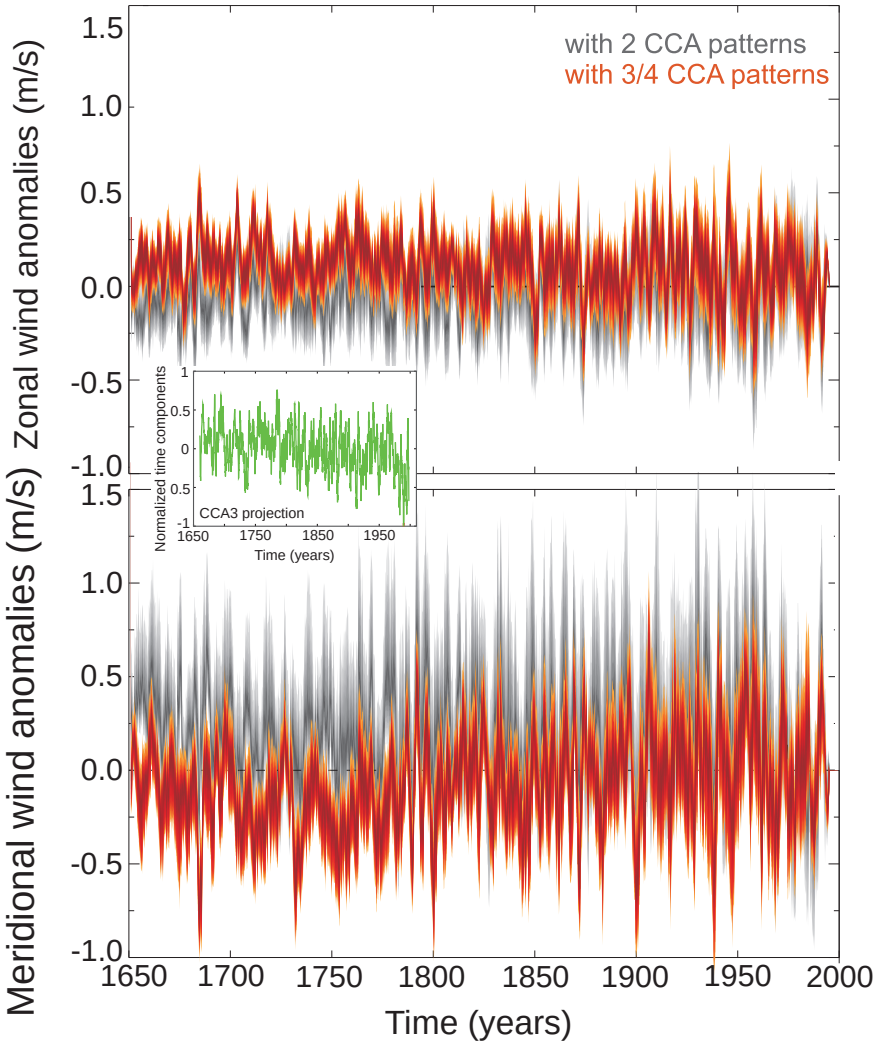

Fig. 5.13: Uncertainty showing the influence of the inclusion of the third and fourth CCA mode obtained using Luterbacher et al. (2002) SLP reconstruction as predictor for zonal (top) and the meridional (bottom) wind component. Gray areas correspond to the case with only two canonical modes while orange stands for the cases including the third and fourth modes. The inset in the middle panel corresponds to the projection on the third canonical series from the middle of 17^{th} century till present obtained using Luterbacher et al. (2002) SLP reconstruction as predictor.

which changes in the different parameters of the model configuration are systematically combined yielding a very large number of estimates (more than 60.000). The uncertainty that is associated to this part of the analysis remains in the range of the variability of the observations and also shows a large dependence on the wind field variance. A full assessment of the uncertainty in the downscaling step is provided by considering the influence in estimations of using different data sources as large scale predictors namely, reanalysis, observations as well as a proxy-based reconstruction. The results are illustrative of a discrete influence of this type of uncertainty showing the largest impacts in the upper deciles of the estimates uncertainty distribution. However, the use of different sources for the large scale predictor introduces further uncertainty which adds to that generated by the variation of the parameters in the downscaling model. In view of the methodological uncertainty analysis presented herein, the statistical method appears as a robust approach to estimate the monthly wind in this region.

The long term past variability of the regional wind has been assessed by a regression-based approach fed by the information from the large scale circulation in the absence of observed measurements out of the calibration period. Different data sources are employed and the comparison between the independent wind estimations revealed a good agreement during the overlapping periods. No overall trends along the approximately 350 years of wind reconstruction are appreciated, though signs of considerable inter annual and inter decadal variability are found. Uncertainties were also projected backward to gain insight into the degree of dispersion of wind estimations in the past due to the methodological variance and to illustrate the potential impact of using different datasets as synoptic circulation predictors. In this context, the long term variability of the regional wind field revealed a special sensitivity to the choice of the method configuration. Specifically, the presence of a trend found in the canonical series of one of the modes produced clear tendencies of opposite sign in the regional estimated wind, depending on the inclusion or not of the third and fourth canonical pattern in the model. This type of exercises allows for the assessment of fluctuations in the regional wind and its main drivers at climatic scales which could be of great value in the context of for instance, wind power production sustainability.

The comparison among the different types of uncertainty associated with regional wind estimates could represent a valuable exercise that can be extended for instance to the context of future climate projections. This would allow for the comparison of the uncertainties obtained in the downscaling step to those associated to a changing of the driving climate model output or the forcing scenario.

The next chapter is devoted to explore the application of the same downscaling technique to investigate the predictability of the wind power production on the basis of its linear relation at monthly timescales evidenced in Chapter 4.2.3.

6

Relationship between wind power production and North Atlantic atmospheric circulation*

Windmills, which are used in the great plains of Holland and North Germany to supply the want of falling water, afford another instance of the actions of velocity. The sails are driven by air in motion -by wind.

H. von Helmholtz. The Conservation Of Force, 1863.

In the previous chapter the predictability of the wind field was investigated by means of the application of a downscaling technique that allowed for an improved understanding of the variability of the regional wind that is connected with the large scale atmospheric circulation. The use of the statistical model was extended to the estimation of regional wind out of the observational period, and thus, the long term variability of the wind was explored for the last centuries together with an assessment of the the methodological uncertainty related to the use of a single model with varying configurations. In the present chapter a similar approach is followed to provide an assessment of the wind power variability at various wind farms within the CFN (see Section 2.2). Two different methodologies will be compared with this aim: on one hand, a direct downscaling with the wind power series as predictand will be performed evidencing the predictability of this non-meteorological variable at monthly timescales that is elicited through its relation to the large scale atmospheric circulation. In a second step the use of transfer functions based on the linearity between wind and wind energy (recall Section 4.2.3) will be used to translate the estimated wind into wind power in

* The main contents of this chapter are included in:
García-Bustamante, E., J. F. González-Rouco, J. Navarro, E. Xoplaki, P. A. Jiménez and J. P. Montávez, 2010: Relationship between wind power production and North Atlantic atmospheric circulation: methods, associated uncertainty and long term downscaled variability. To be submitted.

those locations where no previous observations of wind power production were available.

6.1 The wind power production as an impact variable

The impacts of the climate evolution on a wide range of natural (physical and biological) and human managed systems have been the focus of a large number of studies. Diverse changes on the cryosphere, marine, freshwater and terrestrial ecosystems, water and renewable energy resources, agriculture, human health and other socio-economic schemes has proven to be climatically driven (Reid et al., 1998; Nicholls et al., 2001; Perry et al., 2005; Barnett et al., 2005; Alcamo et al., 2007; Parry et al., 2007).

Climate impact models require information at higher spatial resolutions than those provided by GCMs. Thus, there is an extensive variety of ecosystem and impact oriented applications that call for methodologies providing climatic information at the spatial scales not resolved by the GCMs: river flows and runoff studies (Tisseul et al., 2010; Chiew et al., 2010), meteorological alerts and insurance companies for instance require hurricanes intensity and frequency assessments (Bender et al., 2010), impacts of climate on forests (Fuhrer et al., 2006) and agriculture (Zhang, 2005; Barrow and Semenov, 1995), evaluation of climate variability consequences on health (van Lieshout et al., 2004), air quality (Nolte et al., 2008), floods (Brissette et al., 2006), heatwaves (Toreti et al., 2010) or even fire risk (Carvalho et al., 2000). Statistical downscaling approaches represent a consistent strategy to provide the reliable information about the connection between the large scale atmospheric circulation and the local variables of interest required by the impact models. Alternatively, RCMs may produce climatic fields with sufficient resolution that serve as inputs to those impact oriented models. The analysis that follows in this section illustrates an impact type of case study where the aim is to assess the predictability of the wind power, a non-climatological variable that depends on the evolution of the wind field.

A controversial debate about the conflict between availability and demand of energy stresses the search of *ad hoc* solutions to fulfill the increasing energetic requirements of a growing global population and comfort-demanding societies (DTI, 2006; Dermibas, 2009). Many efforts oriented to obtain and manage alternatives to the classical energy supplies have been made (Hohmeyer and Trittin, 2008). In particular, the wind energy resource has received a special attention during the last decades. This has favoured an emphasis in evaluating its variability and predictability together with an improved understanding of the inherent relation with its primary agent, the wind.

The main purpose of the subsequent paragraphs is to explore the relation between the large scale atmospheric circulation and the wind power production in the CFN following a similar approach to that employed in the previous chapter to analyse the wind field variability. Chapter 4 showed the existence of an empirical linear relation between the wind speed and the wind power at monthly timescales through an evaluation of available wind power data from several wind farms at the same region in the northeastern IP. A linear relation between both variables was evidenced, even if at shorter timescales the expected relation between wind speed and wind power is cubic. Additionally, in Chapter 5 the associations between the large scale atmospheric circulation and the regional wind field were assessed by means of a statistical downscaling method (CCA) that is based on linearity assumptions. Therefore, the question arises whether a direct linear relationship can be established between large scale circulation and the regional non-meteorological predictand (wind power) at monthly timescales. To answer this question a comparable analysis to the case of the wind field (Chapter 5) is applied to the wind power as predictand. Similarly, the assessment herein includes an evaluation of the methodological uncertainties. The monthly temporal resolution allows for filtering other short term fluctuations of the power production that relate to more local effects and other engineering aspects, typically resolved at shorter than monthly timescales and for which the linear assumption between wind speed and wind power might not be applied.

The availability of wind power records favours then the treatment of the power production as an independent variable alternatively to the classical procedures that obtain wind energy density as a wind related variable (Jamil et al., 1995; Weisser and Foxon, 2003; Pryor and Schoof, 2005). This type of strategy that aims at providing direct wind power downscaled estimations has not been yet documented in the literature. Additional to this approach, optional strategies can be proposed based on a first estimation of the wind field (following Chapter 5) and the subsequent translation of downscaled wind into wind power estimations (following Chapter 4). This last *modus operandi* offers some advantages since wind power could be estimated at locations with no availability of wind power data.

Next section presents the application of a CCA to the wind power predictands and large scale circulation predictors. Section 6.3 investigates several variants to estimate wind power production and compares their ability in reproducing the observed wind energy variability to the results from Section 6.2. Section 6.4 includes two inference exercises were the application of the former approaches would imply some benefits regarding the assessment of wind energy availability and sustainability. Finally, Section 6.5 summarizes the main findings in this chapter.

6.2 Statistical downscaling of wind power production

As in Section 5.3 results from applying a statistical downscaling methodology based on CCA are presented here. The predictand variable is the monthly wind power production time series, from September to March, recorded at three wind farms within the dataset (Aritz, El Perdón and Alaiz; squares in Figure 2.1). The time series span the period from June 1999 to June 2003 in the longest case. Due to the shorter observational period, the other two wind farms were not included for this analysis (see Chapter 2).

The predictors employed for this evaluation are, as in the reference case of Chapter 5, the ϕ_{850} and the $Z_{500-850}$ from the ERA-40 fields. Identically, the reference model configuration of Section 5.3 serves to explore the predictability of the wind power production. However, the number of the EOFs for the predictand has been changed with respect to the reference case in Section 5.3 due to the shorter period of observations and the limited spatial coverage (three locations). Thus, only two EOFs of the wind power variable are retained for this analysis. It should be mentioned that the selection of this reference case was made to ease comparison with the analysis of wind speed in Section 5.3, thus, results shown below do not necessarily correspond to the optimal model configuration. In addition, an estimate of the methodological sensitivity is provided by sampling multiple model configurations. This is implemented with a similar procedure as exposed in Section 5.4 where all possible combinations of parameter values were considered generating a large ensemble of estimations.

The two canonical pairs of patterns and amplitude time series obtained with the reference configuration are shown in Figs. 6.1 ($CCA1_{pow}$) and 6.2 ($CCA2_{pow}$). The first large scale pattern consists of a negative (positive) anomaly centre located westward of the British Isles. It resembles to a good degree the second pattern found in the case of the wind speed analysis but with a certain displacement to the northwest that introduces zonal circulations in the region. The corresponding local pattern (Figure 6.1b) shows a dipole with positive anomalies to the north and negative wind power production anomalies to the centre. This is coherent with the local pattern obtained if a comparable CCA set up (the same period -1999 to 2003- and the same number of EOFs/CCAs -422-) is applied to the wind module as predictand. The local wind canonical pattern obtained in such comparable conditions (not shown) coincides to a good degree with the wind power canonical pattern described above, i. e., more windy conditions (equivalent to positive wind power anomalies) in the northern areas and a decelerated flow (equivalent to negative wind power anomalies) to the centre of the region. Thus, in this first association between the atmospheric circulation and the local wind power production, the flow over the northern region seems to be decoupled with

the flow over the central mountains and the Ebro Valley, possibly due to the relative position of the anomaly centre, hardly striking the Cantabrian coast.

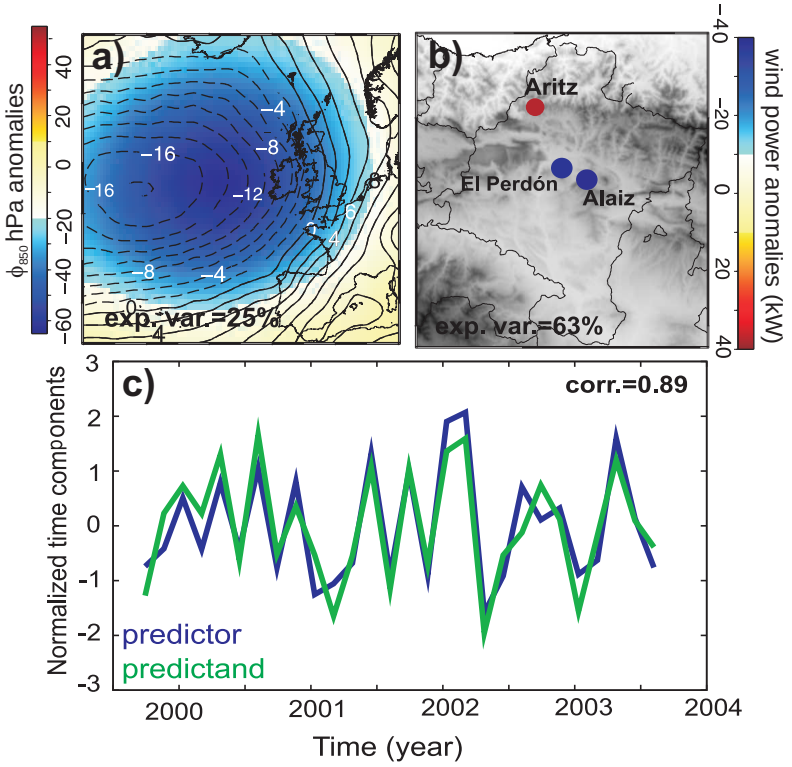

Fig. 6.1: First canonical pair of patterns ($CCA1_{pow}$) of a) the predictor fields (ϕ_{850} hPa, shaded, and $Z_{500-850}$ hPa in contours; b) regional wind power pattern field or predictand and c) amplitude time series.

The second CCA circulation pattern (Figure 6.2a) shows a monopole of negative anomalies less intense but with a deeper penetration into the peninsula compared to that of $CCA1_{pow}$. This implies a similar influence of the large scale flow over both the northern and central parts of the region and thus, it favours the appearance of positive wind power anomalies in the three wind farms which coincides with strong wind conditions over the higher locations of the region, as is represented in Figure 6.2b. The variance that the first (second) canonical mode

accounts for is 25% (24%) in the case of the large scale predictor fields and 63% (34%) in the case of the wind power.

The first canonical mode shows a strong correlation between predictor and predictand amplitude series (0.89) and also a large explained variance of the three predictand sites. This mode is then the main responsible for the wind power monthly variations in the region. The second CCA mode shows a decline in its canonical correlation value (0.31). Thus, the temporal variations of the two coupled canonical patterns will evidence a reduced agreement as it is shown in Fig. 6.2c. It can be considered that with a partial agreement between the two amplitude time series and the smaller, compared to that of $CCA1_{pow}$, correlation value this second CCA mode entails a poorer predictability potential in comparison to the first one. However, the second mode is also kept for the subsequent analyses since at least for one of the locations it shows interesting contributions to the predictability of the wind power. It is noticeable that the canonical series of both CCA modes oscillate between high positive and negative scores pointing out a considerably intra annual variability.

After the calibration of the downscaling model, a crossvalidation is accomplished as in the case of the wind velocity. The correlation (Beta Brier skill score) values, i.e., ρ (β), are 0.70 (0.40), 0.54 (0.15) and 0.35 (-0.10) at Aritz, El Perdón and Alaiz (see Fig. 6.1), respectively. These scores evidence the presence of some predictability for at least two of the wind farms (Aritz and El Perdón) and a poor performance of the third location (Alaiz). However, the main hypothesis is substantiated at two of the locations and this can be considered as indicative of a transfer of the linearity between the large scale and the wind at monthly timescales to the wind power generation. The lower scores in Alaiz will be discussed in the following paragraphs. Thus, the variability of the wind power production over the region can be considered to some extent being governed by the synoptic circulation and this will prove some utility as shown below.

The crossvalidated wind power reference estimations (dash-dot gray) at Aritz, El Perdón and Alaiz are represented in Figs. 6.3, 6.4 and 6.5, respectively. The observed and estimated series show a good agreement through most part of the observational period, especially at Aritz (Fig. 6.3) where the highest correlation between observations and estimations was found. Nonetheless, the concordance between the observed and estimated values is also noticeable at El Perdón, particularly for the periods 1999 to about the middle of the year 2000 (correlation 0.88) and 2001 to 2002 (correlation 0.98). Interestingly and in spite of the difference in the correlation scores at El Perdón and Alaiz, in the latter the agreement between observations and estimates is also perceptible. In fact, the correlation value for the period September 1999 to March 2000 is 0.89 and between February and December 2001 the correlation score amounts to 0.72. In view of these

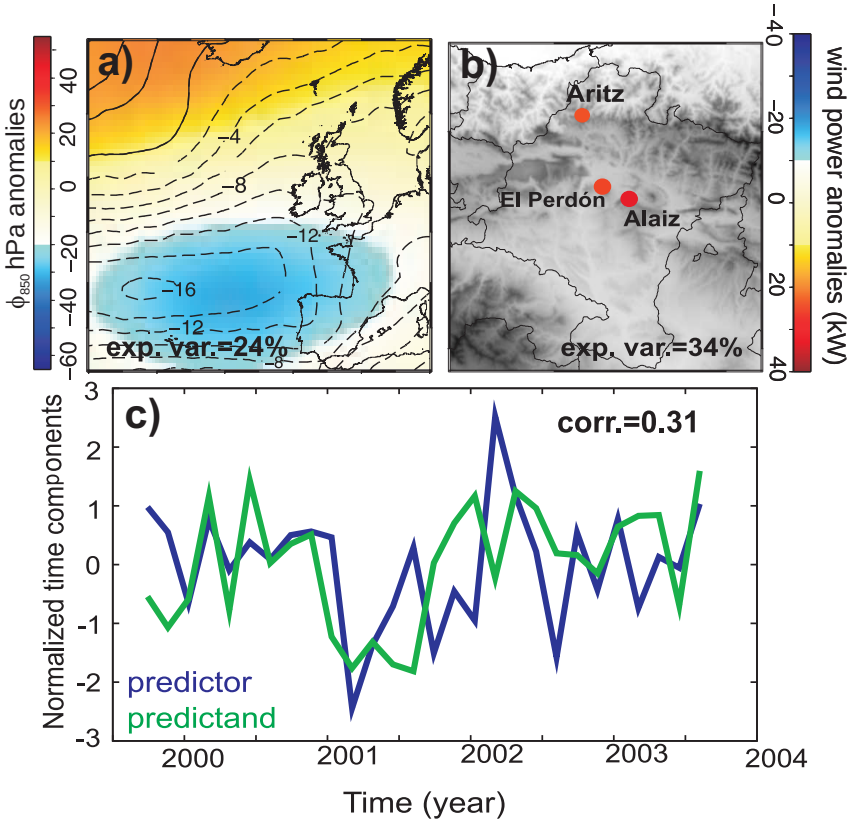

Fig. 6.2: As in Fig. 6.1 but for the $CCA2_{pow}$ canonical mode.

correlations it seems that there are some periods for which the downscaling performs well but there are also other periods (2001-2002 and 2002-2003) that are responsible for a decrease of the agreement between observed and estimated series, particularly at Alaiz. Those periods, that to a great extent are coincident at El Perdón and Alaiz (Figs. 6.4 and 6.5), will show an important contribution to the methodological uncertainty in all wind farms as explained below.

The uncertainty is also represented as the deciles distribution with respect to the median (blue) in Figs. 6.3, 6.4 and 6.5 together with the the observations (black) and the maximum and minimum for illustration. For this assessment the number of estimations generated to provide a measure of the methodological uncertainty is similar to that in Section 5.4.1. In that case all possible combinations

of parameter values were considered. This generated a very large ensemble of estimations (see last row in Table 5.3) based on multiple model configurations. Herein the parameters that are allowed to vary in the configuration of the model are identically the size of the large scale domain, the predictor field(s), the number of EOF/CCA modes retained and the crossvalidation sample size. The only difference lies on the fact that a maximum of two CCA modes was possible due to the limited spatial and temporal coverage of the predictand field. Aritz (Fig. 6.3) shows the narrower uncertainty distribution. Nevertheless, for the other two sites the distribution also replicates reasonably well the variability of the observations and the width of the distribution is comparable to that of the wind field (see Section 5.4). So, it can be said that the methodology is robust in an analogous sense as discussed in the case of wind. A further comment regarding the width of the decile distribution deserves attention. All figures evidence a wider distribution and thus a larger uncertainty in estimations, during the periods where the concordance between observed and estimated series decreases (between the middle and the end of 2001 and from the end of 2002 onwards). This fact is illustrative of the relevance of assessing the methodological sensitivity associated with estimations, especially for those time steps that reveal a decreased predictability. In spite of this, the observations within those periods fall well within the range of the uncertainty intervals produced by the ensemble of downscaling estimates. A 11%, 25% and 18% of the observations fall out of the range of values defined by the uncertainty distribution at Aritz, El Perdón and Alaiz, respectively (time steps are tagged in the horizontal axis of Figs. 6.3, 6.4 and 6.5 for illustration). It is worth noting that even a higher percentage of observations are confined in the uncertainty area in the case of Alaiz with respect to El Perdón. Thus, in view of Figs 6.4 and 6.5, it can be argued that, in spite of the lower skill scores for Alaiz, the performance at this site and at El Perdón is comparable. As it happened in the case of the analysis of wind speed (Chapter 5) the reference estimations (dash-dot lines in Figs. 6.3, 6.4 and 6.5) fall well within the envelope of the uncertainty distribution and thus the reference configuration selected can be considered representative of the whole ensemble of estimations.

6.3 Alternative methods for the estimation of wind power production

The estimation of wind power can be undertaken with some simple variants as substitutes of the direct downscaling explored in the previous section. An alternative technique consists in the downscaling of the wind field followed by the translation of the wind estimates into wind power by using a transfer function as the linear relation found between them (Section 4.2.3). In this line, three variants

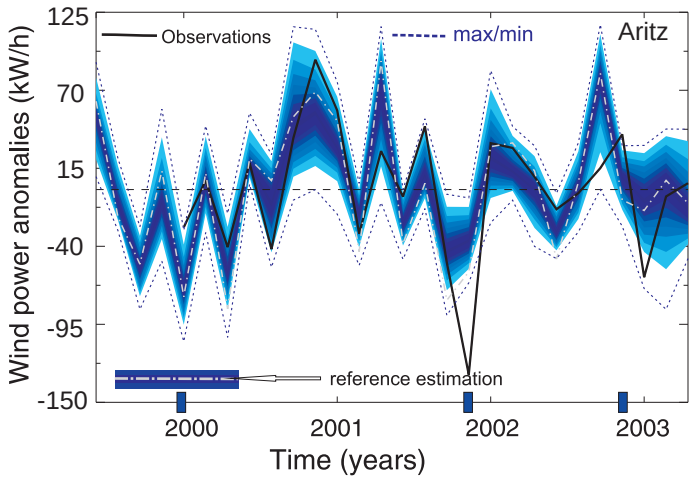

Fig. 6.3: Deciles distribution with respect to the median of the uncertainty associated with the wind power estimates (degraded blue area) together with the observations (black) at Aritz, the reference case estimate (dash-dot white) and the maximum and minimum values (dash blue).

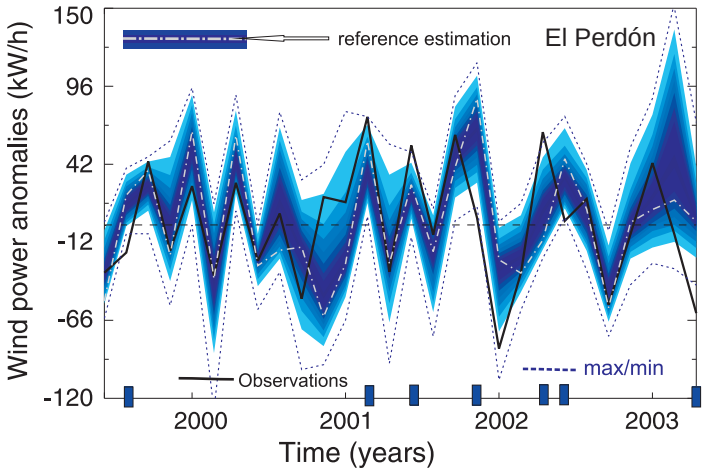

Fig. 6.4: As in Fig. 6.4 but for El Perdón.

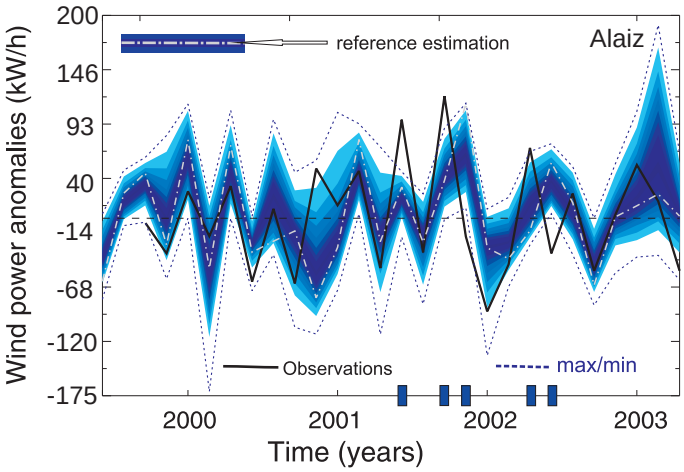

Fig. 6.5: As in Fig. 6.4 but for Alaiz.

have been explored in order to obtain comparable estimations of wind power. These variants could present differential advantages and implications depending on the specific situation, for instance, in the absence of wind power data in certain or in all locations over the CFN.

The first alternative approach, hereafter $CCA_{Pow-mod}$, where *mod* stands for wind module, consists in the downscaling through a CCA of the wind module and the subsequent translation of the wind module estimates into wind power values. The latter thread is carried out by using the linear relation between the standardized observed wind and wind power in the calibration period at each one of the wind farms. Only those months entering the CCA (September to March) in both, wind speed and wind power cases, are considered in the linear regression fit. In order to make estimations independent from the fitted model, a single regression is calculated for each time step by excluding the target month and estimating it from the independent regression over the remaining months in the dataset as in Chapter 4.2.3. The procedure is repeated for every month and also independently for each wind farm. The linear regressions (one per month) are represented in Fig. 6.6 where blue linear fits correspond to Alaiz, green ones to Aritz and red to El Perdón. The standardized monthly wind and wind power observations are represented by crosses with the corresponding color. Interestingly, the worst linear relationship correspond to the wind farm in which the best scores are achieved in the validation of the downscaling method (Aritz, green in Fig. 6.6). Notwithstanding, correlations in the case of Aritz (around 0.85), although

lower that in the other sites, are still indicative of a robust linearity between wind speed and wind power. In the second variant, CCA_{Pow-uv}, uv represents the zonal (u) and meridional (v) wind components respectively and they serve as predictand fields for the CCA calculations. The wind component estimations are then transformed first into wind module and second, the linear regression step (as in $CCA_{Pow-mod}$) provides final wind power estimations. Finally, a third strategy ($CCA_{Pow-reg}$) involves a *regional* linear regression. This implies that, instead of fitting the standardized wind power and wind speed observations individually at each site, a unique regression valid for the three locations is obtained. Additionally, as in the previous cases regressions are calculated for each time step to keep independence between observations and estimations. In standardized conditions (zero mean and unit variance) the linear relation between wind power and wind speed can be expressed as $P = \rho \cdot w$, where P and w are the monthly standardized wind power and wind module, respectively and ρ represents the correlation coefficient between them. Thus, the relation between both variables becomes independent of the particular features of each location as for instance, the type of wind mills installed, that can provide different levels of wind power output according to their dimensions. The assumption involves the use of a single regression model that can be considered valid to describe the linear relation between wind power and wind module at the three locations, and thus it can be considered as a regional linear relationship.

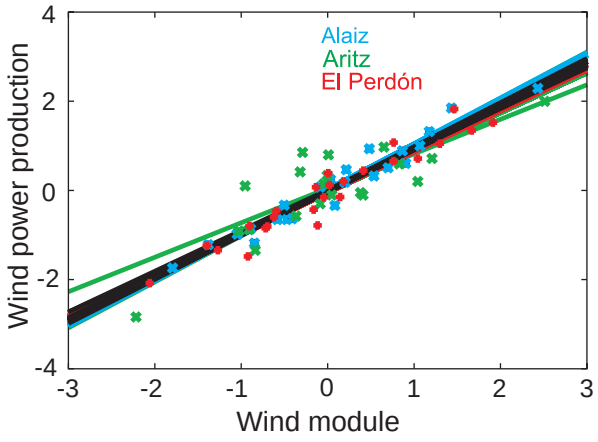

Fig. 6.6: Monthly standardized wind module *vs.* wind power observations. Colors represent each wind farm (see legend). Their corresponding linear fits (one per month) are also shown. Black lines depict the regional fits (one per month).

The basis for this hypothesis is illustrated in Fig. 6.6 by the degree of agreement between the linear fits at the different sites and the *regional* regressions (black, also one per month). In view of the dispersion diagram of wind speed-wind power pairs at each wind farm, the corresponding linear fit and that of the regional case, it can be said that a regional regression model is a reasonable approach to estimate the wind power production in the three sites. Then, this $CCA_{Pow-reg}$ case is comparable to the $CCA_{Pow-mod}$ variant except for using a regional linear model to translate wind into wind power. In all variants the downscaled module and components are based in reference configurations identical to that of Section 6.2.

All estimations of wind power are in the last step re-scaled with the standard deviations of the observed power at the corresponding wind farm. A Taylor diagram (Fig. 6.7) compares the performance of all methodological variants. A different symbol is assigned to each one of the three wind farms within the dataset: circles (Alaiz), stars (El Perdón) and pentagons (Aritz). In addition, colors are representative of the approaches followed to obtain wind power estimations: red symbols indicate that estimations have been obtained through direct downscaling of the wind power production as predictand; blue stand for $CCA_{Pow-mod}$; green correspond to CCA_{Pow-uv} and yellow show the results for the $CCA_{Pow-reg}$ approach.

Correlations are within the range 0.26 to 0.75 (values no significant at the 0.05 level are marked with a cross). The standard deviation ratios are comprised in the interval (0.5,1.1). It can be appreciated that the variance is generally underestimated for all estimations except for one case (Aritz; direct downscaling of wind power). In view of Fig. 6.7 it can be said that the direct downscaling of the wind power production (red symbols) performs generally better than the other three more elaborated approaches. The scores for the rest of variants are grouped, for each site, around similar values of correlation and a slightly larger degree of scattering of the deviation ratios. Thus, the variants employed do not produce a great impact on the resulting variance of estimations nor do they distort the linear relation between wind speed and wind power that has been used in three of the approaches ($CCA_{Pow-mod}$, CCA_{Pow-uv} and $CCA_{Pow-reg}$). In contrast, the differences in the scores observed in Fig. 6.7 depend mostly on the specific location, meaning that the better the results from the direct downscaling, the better the wind power estimations from all the variant approaches. One of the winds farms (Aritz) shows better results than the other two. The difference in the ability of the statistical model to reproduce the observed wind power depending on the site could be indicative of some spatial variability, as discussed in the previous paragraphs and illustrated in $CCA1_{pow}$ (Fig. 6.1). Therein a better predictability in the northern than the central areas of the CFN, both for wind

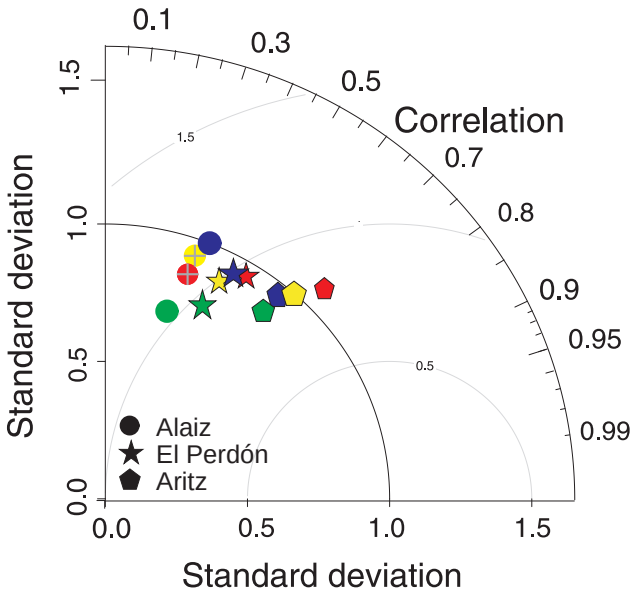

Fig. 6.7: Taylor diagram for the wind power production estimations. Red stands for the direct wind power downscaling, blue for $CCA_{Pow-mod}$, green for CCA_{Pow-uv} and yellow for $CCA_{Pow-reg}$.

and wind power, was argued. This is consistent to a great extent with results in Chapter 5, where it was shown that the Ebro Valley and the northern areas show better predictability that some stations around the central part of the region. This argument together with the resemblance of the canonical patterns in Section 6.2 to the second CCA mode of the wind (Chapter 5) provide consistency to the conclusions met in this chapter regarding the application of the CCA and thus, are aligned with the idea of validation of the relationship between wind and the atmospheric circulation that is propagated to the wind power through its linear relation with the wind speed.

6.4 Applications: estimating wind power in the absence of observations

This section aims at illustrating potential uses of the predictability of the wind power production either based on the direct downscaling of wind power as predictand or through the downscaling of the wind field and the subsequent use of

the linear relation between the wind speed and the turbine outputs. These aplications allow for obtaining wind energy estimations at locations or for periods with no availability of observed records.

As it has been shown, the downscaling procedure applied to the wind field through the use of the regional linear relation as transfer function between the wind estimations and wind power ($CCA_{Pow-reg}$) can be assumed as a sound approach to obtain wind energy estimates at monthly timescale since the extent to which the wind power estimations reproduce the observations has proven to depend mainly on the skill of the downscaling. Thus, an interesting application of the latter is the estimation of the wind power production also in those sites where no power production records are available. Wind power production estimates in the following case study are obtained by first applying CCA_{Pow-uv}, the calculation of the wind module values from the estimated wind components and finally, wind power estimations are obtained via the regional linear transfer function. An example of this is represented in Fig. 6.8. September 2001 has been randomly selected with the only requirement of being illustrative of windy conditions over the CFN. The spatial distribution of the wind field for the selected month is plotted in Fig. 6.8a. It can be observed that this month shows in fact high wind velocities in most of the locations within the dataset, except for the stations more northernly located, where lower winds can be appreciated. This month stand as representative for the decoupling of the wind circulation between the northern areas and the rest of the CFN (Jiménez et al., 2008b). Additionally, there is a reasonable agreement between observations and estimations, not only in the direction but also in the longitude of vectors, representative of the intensity of the wind. As explained above, if it is assumed that a regional linear fit conveniently represents the relationship between wind speed and wind power at each location, then it is reasonable to obtain local wind power estimates by applying the regional linear transfer function to both, observed and downscaled, wind field. The wind power estimations are rescaled to finally obtain absolute wind power values values by multiplying by a factor (the average, over the three wind farms, standard deviation of the power production) and by adding the mean wind power also over the three wind farms. This is represented in Fig. 6.8b, where circles stand for power production calculated from the observed wind and diamonds represent the production obtained from the estimated wind. As expected, there is a good agreement between both wind power values in most of the sites. Some locations in central CFN evidence worse concordance between observations and estimations related to a poorer performance of the downscaling approach in those locations as it was discussed in the previous chapter. A final comment is worth concerning Fig. 6.8b. Estimations of wind power in this inference exercise are obtained from wind speed values at the typical hub heights (around 30-45 m

in this case study). Wind speed values were extrapolated by using the power law (Pryor and Schoof, 2005). A more elaborated approach to the extrapolation of the wind values with height would requiere information about the surface roughness at each location, as for instance the application of the logarithmic wind profile (Stull, 1990). However the purpose of the present exercise is to illustrate potential applications of the wind-wind power relation in a simple fashion rather than presenting more refined approaches for the estimation of accurate wind power production. Thus, this can be considered a potential straightforward application of the wind power downscaling even in the absence of power production records, which could be of some help to explore the wind energy availability over a wider region, provided that the variability of the wind field at monthly timescales is dominated by the large scale circulation.

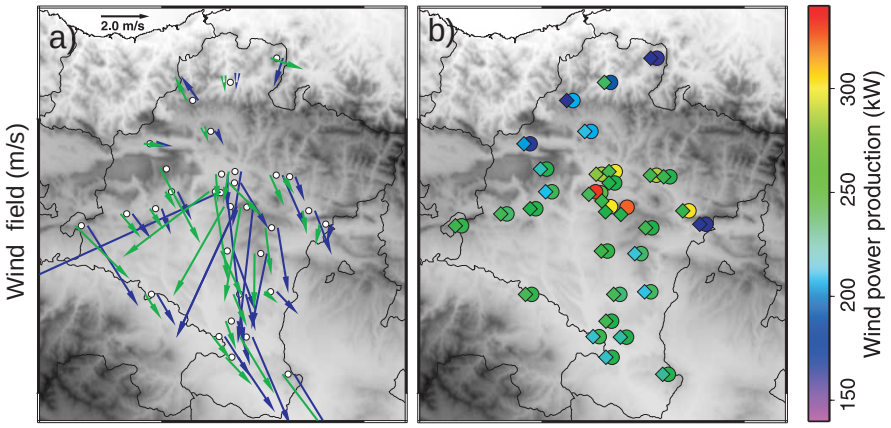

Fig. 6.8: Estimation of wind power production in the CFN. **a**) Observed (blue) and estimated (green) wind field for September 2001 and **b**) observed (circles) and estimated (diamonds) wind power production for the same month.

In addition, there are some interesting questions related to the long term variability of the wind power production. For instance, whether independent wind speed and power production downscaled estimates maintain the linear relation over monthly time scales. Another interesting question relates to the long term trends of wind power production or the presence of periods with higher/lower anomalies of power generation. An inspection of the long term variability of the wind power production benefits the evaluation of the wind resource sustainability and the identification of the temporal variations that the wind farm could be

subject to throughout the typical lifetime of facilities. In order to shed some light on these aspects, a reconstruction of the wind power climatology has been calculated using the relation found between the predictand at El Perdón, as an example, and the large scale circulation during the calibration period (1999-2003).

The reference reconstruction (identical to that of Section 6.2, i.e., CCA_{pow}), at El Perdón is represented in Fig. 6.9. Wind power estimates are extended backward to the beginning of the 20th century. As in the case of wind speed (Section 5.5), several predictor (SLP) datasets are employed to obtain past estimations of the wind power: the ERA-40 SLP (1957-2005; light blue in Fig. 6.9, $R_{Pow-era40}$), the NCAR SLP (1899 to 2005; in green, $R_{Pow-ncar}$) and the HadSLP2 database from 1850 (in violet, $R_{Pow-had2}$). A good agreement between the three reconstructions can be appreciated. Additionally, the comparable reference reconstructions for the wind module (dashed lines) have been also represented. All series are standardized to allow for a better comparison and they are represented with a 2-year moving average filter. It is evident from the graph that both variables conserve their linear relation through the whole recostruction period (correlation values are 0.98 in the three cases). They reveal no overall trends during the 150 years of reconstruction, althoug a marked tendency to decreased power production is apparent between 1960 and 1990, approximately after a period of power increase between 1925 and 1960, in agreement with what is observed in the wind reconstruction of the previous chapter (see Fig. 5.11b). As in that case, interesting intra and inter annual variability can be appreciated in Fig. 6.9.

The uncertainties in the regional wind power reconstruction related to variations of the parameters in the model configuration (as in the previous Section 6.3) have been also calculated and represented in Fig. 6.10. The three wind power reference reconstructions (see legend) are also represented. Series present a 2-year moving average filter. The area defined by the deciles distribution (gray) that account for the dispersion of estimates due to the multiple model configurations explored is comparable to that of the wind field. This is an expected feature since the methodological uncertainty together with that arriving from the large scale (different data sources) have proven to be independent on the ability of the CCA model to reproduce the observations (Section 6.3). Instead it was shown the dependence of the uncertainty on the observed variability. However, estimating the uncertainty can still be considered important. For instance, anomalies of some tens of kW implies a large gap between the real generation and the estimation of power production that could be of great importance for manufacturers, promotors or electricity markets.

This type of exercise allows for having some insight into the potential variability of local wind power production at longer timescales. Typically, a single year of observations is considered sufficient for the evaluation of a specific location on

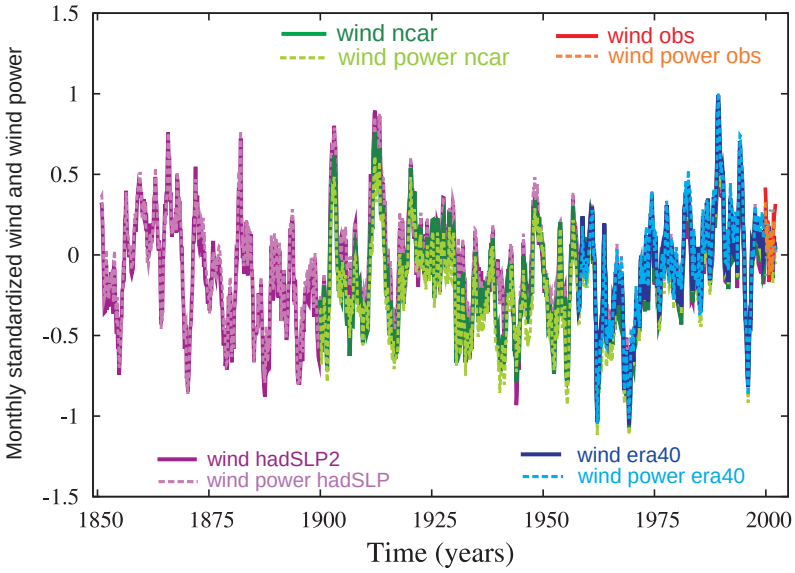

Fig. 6.9: Reference monthly wind and wind power past estimates at El Perdón. See legend for color an line type assignment. All series present a 2 year moving average filter.

its suitability as a wind energy resource (Barbour and Walker, 2008). However, neither a single year nor a few of them can offer sufficient information to decide an investment at a certain location since the natural variability of the resource has been evidenced to be large and consequently the projected production could significantly vary from one year to another and through decades. Analogously, regarding the uncertainty associated to estimations, it can be said that a single estimation does not provide the robust level of confidence that would be desirable in order to, for instance, participate in the pull of the electricity market maintaining reasonable margins of risk (Zeineldin et al., 2009).

6.5 Conclusions

Some insight into the relation of the wind power generated at three wind farms in the region between 1999-2003 and the large scale circulation is provided, as a climatic impact-oriented analysis. Different approaches have been tested rendering wind power estimations. A direct downscaling of the wind power production

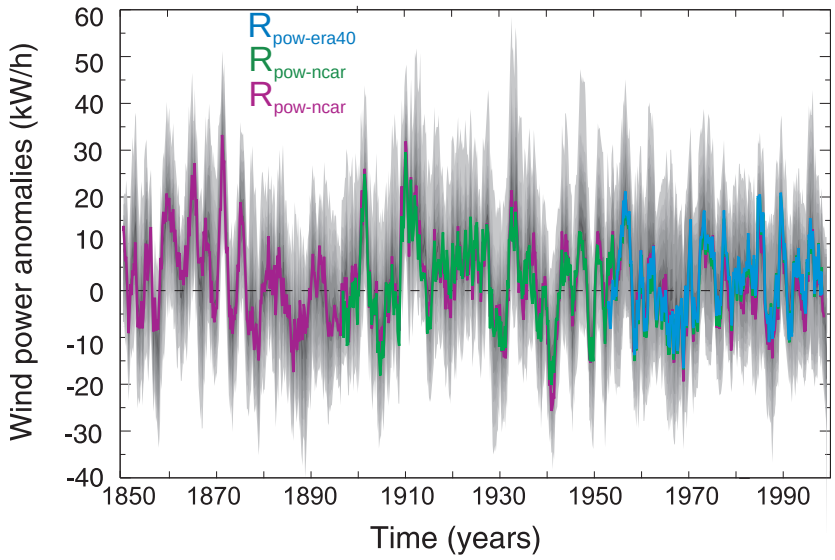

Fig. 6.10: Wind power reference reconstructions and their associated uncertainty at El Perdón. In gray the deciles distribution (with respect to the median) of the uncertainty is represented. See legend for colors.

as predictand variable was explored at those sites with turbine outputs availability. This exercise showed the existence of predictability through the application of a CCA at the wind farms. The main canonical mode resembles the second mode found while exploring the performance of the CCA over the wind field in the previous chapter. Other variants for the estimation of wind power based on a downscaling of the wind field through a CCA followed by a linear transfer to obtain final wind power values were also tested. The different methodologies evidenced a large dependence on the ability of the downscaling model to provide reasonable estimations of wind. Locations with a relative worse performance at some periods or time steps of the downscaling approach for the wind power coincide to a good degree with those where the downscaling of the wind field suffers also a decrease in the ability to reproduce the variability of the predictand.

Two inference analyses are presented as an example of potential applications of the wind power production estimations. In one case, the wind field at every location over the CFN was used to obtain power production estimates through the use of a regional linear relation between wind and wind power. The assumptions for such an approach were based on the suitability of a linear fit between regional

wind and wind power at the three different wind farms to represent the relation between both variables. The added value of this approach lies in the possibility of estimating wind power at sites where no wind power series are available, providing thus an idea of the wind power generation that would be feasible over the region.

Additionally, an estimation of the past variability of the wind power out of the observational period allowed for an insight into the long term changes of the power production at one of the wind farms. It has been shown that the generation of wind energy presents considerable variability and interannual at interdecadal timescales. This evaluation of wind power production at long timescales may be relevant for the sustainability of a wind power facility

The application of this kind of methodologies to non-meteorological variables shape a framework for ecosystem-like climate related impact analyses. The basis for this is that evidences of the large scale circulation governing monthly variations of the wind power production have been found. This allows for the application of simple strategies to assess the spatial and temporal variability of the wind power together with its associated uncertainty over the region under study. Such evaluations could be of relevance to assess the impact on wind energy resources of potential changes in wind and wind power variability due to the the expected evolution of the climate in the future.

The next chapter is devoted to explore the uncertainties that are asssociated with downscaling estimations via the application of a probabilistic approach that attempts to provide an objective and complementary assessment of the frequentist methodological sensitiviy explored in previous chapters.

7

Bayesian uncertainty in downscaled wind field estimations*

It is a truth very certain that when it is not in our power to determine what is true we ought to follow what is most probable.

R. Descartes, Discours de la Methode, 1637.

In the previous chapters the assessment of the regional variability and predictability of the wind and wind power fields encompassed an evaluation of the uncertainties associated to a varying configuration of an statistical downscaling model. Thus, multiple variations on the parameters that are important for the model set up were investigated. This last uncertainty analysis can be ascribed to the frequentist approaches based on the exploration of plausible values for the parameters, the selection of which can be affected however by a certain degree of subjectivity. In this chapter an approach based on a Bayesian probabilistic assessment is presented in order to provide a complementary and more objective evaluation of such a selection. The technique is based on objective criteria for the selection of the model parameter values. Through this probabilistic approach prior knowledge is combined with the observations to provide posterior inferences about the relevant parameters of the method configuration. Consequently, the analysis that follows expands the evaluation of the uncertainties of Chapters 5 and 6 through a different conceptual approach that aims at further constrain the parameter values selection based on probabilistic arguments.

Next section presents the motivation for this analysis. In section 7.2 the fundamentals of the Bayesian methodology are presented. Section 7.3 is devoted to

* The main contents of this chapter are included in:
García-Bustamante, E., J. F. González-Rouco, J. Sáenz, E. Xoplaki, J. Navarro, P. A. Jiménez and J. P. Montávez, 2010: Bayesian uncertainty in downscaled wind field estimations. In preparation.

expose and discuss results found in the assessment of the uncertainty associated with parameters of the statistical model. Finally Section 7.4 summarizes the more relevant points and conclusions of the analysis.

7.1 Motivation

The previous chapters have provided an assessment of regional wind and wind power providing some understanding of the mechanisms involved in their climate variability at regional scales. Such assessment requires the application of downscaling strategies to overcome the cross-scales problem for a reliable representation of the regional climate. Different sources of uncertainty can affect the estimation of a climatological variable and it can be increased during the downscaling step (Mitchell and Hulme, 1999). This calls for a quantification and understanding of the uncertainty that stems from the application of any given downscaling technique. Specifically, in the case of statistical methods it is relevant to assess the implications of the assumptions made in the design of the model (Benestad, 2002).

However, evaluating downscaling models from a perspective that considers these models as essential components of the uncertainty involved in the regional estimations of any specific variable, as well as the implementation of methodologies for such an evaluation can be still considered a challenge (Denman et al., 2007). Traditional methods oriented to the evaluation of the uncertainty usually present a non negligible heuristic component (Giorgi and Mearns, 1991) and are based in the systematic sampling of the properties of the model configuration that can potentially produce an impact in the regional estimations. In the case of RCMs sensitivity analyses to changes in the physical parametrizations (Weisse and Feser, 2003) or for the statistical downscaling methods, an inspection of the influence of changes in model configurations (Huth, 2004) can be considered classic approaches to the problem of evaluating the degree of uncertainty that arises in the downscaling step. This type of strategies are usually denoted as frequentist analyses of the uncertainty (O'Hagan and Oakley, 2004) since they consider multiple possibilities in the attempt of evaluating the extent to which sampling the parameter space in the model produces effects in the estimations. The use of an ensemble of various GCMs providing the information to feed the regional models also pertains to this type of approaches as the driving climatic fields that change from one model to other have proven to generate considerable impacts on the regional estimates (Greene et al., 2006).

Consequently, the treatment of the uncertainties associated to wind and wind power estimation in Chapters 5 and 6 contributes to a frequentist exploration of the possible model configurations providing a measure of sensitivity attached to

the methodology. Notwithstanding the arguments for the selection of the different combinations therein were based on several assumptions that attempted to ameliorate the subjectivity involved in the choice of the parameter values. More formal conceptual approaches, although still not fully developed in the literature, may be explored by pursuing an objective probabilistic assessment of the probability distribution of the model parameters and thus, of the uncertainty distribution inherent to any estimation. For instance, an assessment of uncertainties based on probability distribution functions (PDFs) presents interesting attributes like the possibility of assigning relative weights to the different models used, the various configurations of the model or the different parametrizations investigated (Räisänen et al., 2001). In this line, some constraints can be imposed for instance to the parameters of the model, accounting for their relative ability to provide skillful estimations. Hence, one of the assets of the probabilistic approaches is that they can discriminate the parameter values of the model set up that provide more realistic estimations from those that generate larger uncertainty in the estimates, which is one of the foremost purposes in this part of the work.

Bayesian methods belong to the core of such probabilistic approaches and have been widely used in statistical inference analyses. Epstein (1962) first discussed their utility in meteorological applications. Recently, Bayesian based techniques have experienced an extended use in the estimation of the probability associated to some important properties of the climate system as a measure of the uncertainty within long term climate projections (Forest et al., 2000, 2002; Hegerl et al., 2006). Giorgi and Mearns (2003) and Tebaldi et al. (2004a,b) followed a Bayesian analysis to evaluate the uncertainty that arrived from the use of a multimodel simulation approach for regional climate change estimations. Another possibility for the use of the Bayesian formulation is the calibration of model simulations on the basis of empirical constraints as done by Coelho et al. (2004) who combined simulated and observed ENSO variability in order to provide more skillful estimations. The same techniques were previously applied in climate change detection and attribution methodologies (Hegerl et al., 1997; Allen and Tett, 1999). However its use in the context of regional wind field estimations has not been explored.

Nonetheless, the Bayesian handling on the uncertainties is still at a preliminary stage and further investigation would be necessary to incorporate precise expert judgement in the method through the use of prior distributions and also to understand the impact of the various assumptions made in the selection of the penalizing function. The prior distributions encompass the actual knowledge of the system and thus provide a first ranking to the various competing hypothesis. The limited information comprised in the prior distributions is afterwards combined with observational evidences through the likelihood function aiming at an

update of the system knowledge by penalizing or rewarding the various competing model configurations. The combination of prior knowledge and the likelihood function arises in the form of a probability distribution known as the posterior distribution, that allows for inferences on the initial hypothesis being tested.

In this chapter, an alternative and completing to the classic frequentist approach for the assessment of the methodological uncertainty is presented, based on a Bayesian analysis of the parameters that are important for the configuration of the statistical downscaling model. This offers a new perspective through a more formal treatment of the parameter uncertainties allowing for a discrimination of those parameters that produce higher impact on estimations and those values of each parameter that provide more robust estimates. This analysis can be considered as an extension of the evaluation of the methodological sensitivity of wind and wind power estimations proposed in the previous chapters.

7.2 Methodology: the Bayesian framework

In general, the Bayesian method is a probabilistic approach that consists in the update of the *a priori* knowledge of the hypothesis to be tested (prior probability) using the available observations. Then, the likelihood function plays the role of constraining the initial information by assigning weights to what is more likely on the basis of the observed data. The posterior probability depends thus, on some prior knowledge about the system conditioned to the probability of the observations given the hypothesis of interest. Here an hypothesis is made assuming a range of values of any of the parameters that are involved in the model set up. The observations play the role of constraining the prior probability by penalizing the responses of the model that fall far from the observed one.

The *Bayes's theorem* can be written as:

$$p(H_i|D) = \frac{p(D|H_i) \cdot p(H_i)}{p(D)} \tag{7.1}$$

where, H_i is the prior hypothesis or assertion, it constitutes for instance, the space of the model parameter i; D stands for the data or observations; $p(H_i)$ represents the prior probability of the hypothesis (prior probability of parameter i); $p(D|H_i)$ designates the probability of obtaining the value D in the data, supposed H_i is true and is also known as the likelihood function; $p(H_i|D)$ denotes the marginal posterior probability of H_i and $p(D) = \sum_i p(D|H_i) \cdot p(H_i)$ is a normalization factor that ensures $\sum_i p(H_i|D) = 1$.

This formulation can be applied to multiple statistical inference exercises where the aim is to obtain a probabilistic representation of the uncertainty associated to any hypothesis. This is achieved by assigning probabilities to the set of competing hypothesis. In our case the interest is focused on the classical parameter estimation problem (Gregory, 2005). Then D will stand for the wind observations during the calibration period and H_i represents the model parameter space. H_i will be denoted as: μ_i that stands for the size of the large scale domain, with i=1,..,9 (1 corresponds to largest size of the window while 9 is the smallest, see Section 5.4); σ_j designates the predictor field, with j=1,..,25 (as j increases more large scale fields and combinations of them are included as predictors); κ_k denotes the number of EOF/CCA modes to be retained, with k=1,..,31 (larger k implies that a lower number of EOFs/CCAs are included) and θ_l is the crossvalidation subset size, with l=1,..,9 (1 stands for 1 month and 9 corresponds to 2 years, each year comprising 7 months from September to March). The multiple combinations of these parameters options constitute the hypothesis parameter space. All parameter combinations are specified in Appendix A.

7.2.1 Prior probabilities

The prior distribution represents the *a priori* knowledge about the parameters given in terms of probabilities. The probability distributions, P(μ), P(σ), P(κ) and P(θ), are here assumed as uniform since for each parameter all values are supposed to have equal probability of producing reasonable estimations of wind. It can be said that the uniform distribution is an *uninformative* distribution, in the sense that it provides only general information about the variable and it assigns equal probabilities to each possible value of the parameters (Gregory, 2005). Given this, the major responsible of assigning the probabilities to each parameter values will be the likelihood function.

A posterior distribution of each model parameter will be obtained through marginalization over the joint posterior distribution providing a more realistic estimation of the probabilities of the parameters involved. The aim is therefore to discriminate whether any option of each parameter of the model involves a differentiated skill to provide estimations of the wind field. The frequentist exploration of the methodological sensitivity in Chapters 5 and 6 allowed for a quantification of the uncertainty in estimations and a brief insight into the relative importance of each parameter within the ensemble of estimations, i.e., whether any of the parameters has a more decisive impact in the set up of the model to generate skillful estimations. The Bayesian analysis herein aims at responding to a different question: which options or values among all possibilities considered for a certain parameter are more realistic in terms of providing robust estimations of

wind. The selection of the range of values for each parameter was based on the experience (some prior knowledge) in Chapters 5 and 6. In this chapter we attempt to objectively constrain such a selection by conditioning the prior knowledge in the basis of observational evidences.

In the results section the impact on the posterior distributions of each parameter due to the use of different prior distributions based on expert practice will be also shown.

7.2.2 Likelihood function

In the Bayes's theorem this is the probability of the data conditioned to the hypothesis, $p(D|H_i)$. Its importance relies on the fact that it implies a penalty for those parameter values that are less probable. Here is where the observations play the fundamental role of determining what is more likely. A typical approach consists in assigning a probability that depends on the relative importance of the corresponding residuals (Forest et al., 2002; Hegerl et al., 2006).

The residuals of the downscaling estimations are denoted:

$$r(\mu, \sigma, \kappa, \theta) = \overline{w_{obs}}(t) - \overline{w_{est}}(t; \mu, \sigma, \kappa, \theta) \tag{7.2}$$

with $r(\mu, \sigma, \kappa, \theta)$ being the residual for the combination of parameters μ, σ, κ and θ; $\overline{w_{obs}}$ is the spatial average of the observed wind and $\overline{w_{est}}(t; \mu, \sigma, \kappa, \theta)$ represent the corresponding spatial average wind estimation.

The approach followed here considers the normalized distance of every sum of square residuals to a reference one. The reference residual is obtained from the combination of parameters that generates the minimum sum of square residuals (corresponding to the best combination of parameters) and is denoted as $||r_{min}||^2$, where $||r||^2 = \sum_t r(t, \mu, \sigma, \kappa, \theta)^2$

The difference between any $||r||^2$ and $||r_{min}||^2$, normalized by the variance of the minimum residual ($\sigma^2_{r_{min}} = \frac{||r_{min}||^2}{n-1}$, n being the length of time series), is F-distributed:

$$\frac{||r||^2 - ||r_{min}||^2}{\sigma^2_{r_{min}}} \propto n_1 \cdot F(n_1, n_2) \tag{7.3}$$

where F is the Fisher distribution with n_1 and n_2 degrees of freedom. In this exercise the degrees of freedom are $n_1 = 4$, the number of free parameters in the model and n_2=n - 4 (the length of the time series minus the number of free parameters). The numerator represents the residual variance of estimations and

the denominator is the variance of the error. The arguments for this assumption are provided in Appendix A.

The minimum sum of squared residuals was selected as the mean value of the 10% series with minimum residuals to ensure that the minimum values were not obtained by chance. Different percentages of values to define the set of minimum values were tested and no significant changes were obtained.

It can be appreciated from the Fisher probabilities calculated as the area under the PDF curve for values larger than the one of interest (Figs. 7.1a,b for the zonal component and meridional component, respectively) that the resulting likelihood function appears to be very restrictive, i.e., the shape of the probability distribution is considerably narrow and it can be said in advance that this penalty will likely reject a great amount of parameter combinations just by visual inspection of the Fisher probability distribution.

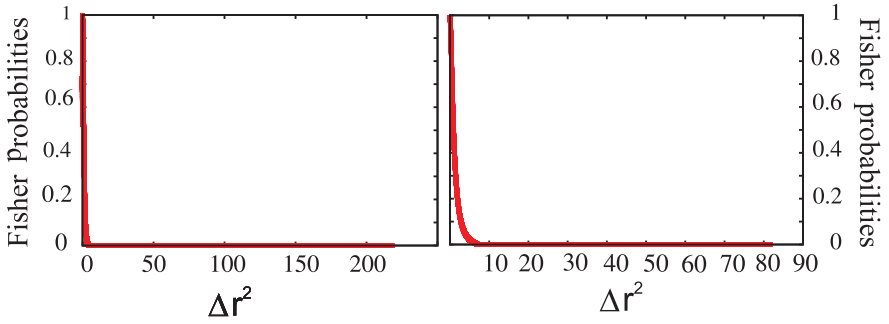

Fig. 7.1: Zonal (a) and meridional (b) Fisher probabilities for each possible combination of the model parameters.

7.2.3 Marginal posterior distribution

The posterior distribution is the joint distribution of the parameters conditioned to the data. It represents the update of the prior information on the parameters given the information provided by the available observations. So we write:

$$p(\mu,\sigma,\kappa,\theta \mid D) = \frac{p(\mu,\sigma,\kappa,\theta)\cdot p(D \mid \mu,\sigma,\kappa,\theta)}{\int\int\int\int p(\mu)\cdot p(\sigma)\cdot p(\kappa)\cdot p(\theta)\cdot p(D \mid \mu,\sigma,\kappa,\theta)} \tag{7.4}$$

The denominator of the ratio is the normalization factor. In terms of discrete functions, Eq. 7.4 can be also written

$$p(\mu,\sigma,\kappa,\theta|D) = \frac{p(\mu,\sigma,\kappa,\theta)\cdot p(D \mid \mu,\sigma,\kappa,\theta)}{\sum_i\sum_j\sum_k\sum_l p(\mu_i)\cdot p(\sigma_j)\cdot p(\kappa_k)\cdot p(\theta_l)\cdot p(D \mid \mu_i,\sigma_j,\kappa_k,\theta_l)} \quad (7.5)$$

$\forall$ i=1,..,n_μ; $\forall$ j=1,..,n_σ; $\forall$ k=1,..,n_κ; $\forall$ l=1,..,n_θ

However, we are interested in the marginal posterior distributions in order to obtain probability information about the values of each parameter to elucidate which ones are more probable. We consider the parameter μ as an example to show how its marginal distribution can be calculated:

$$p(\mu \mid D) = \frac{p(\mu)\int p(\sigma)\cdot\int p(\kappa)\cdot\int p(\theta)\cdot p(D \mid \mu,\sigma,\kappa,\theta)\cdot d\theta d\kappa d\sigma}{\int p(\mu)\int p(\sigma)\cdot\int p(\kappa)\cdot\int p(\theta)\cdot p(D \mid \mu,\sigma,\kappa,\theta)d\theta d\kappa d\sigma d\mu} \quad (7.6)$$

$$p(\mu_i|D) = \frac{p(\mu_i)\cdot\sum_j\cdot p(\sigma_j)\cdot[\sum_k p(\rho_k)\cdot(\sum_l p(\theta_l)\cdot p(D|\mu_i,\sigma_j,\rho_k,\theta_l))]}{\sum_i p(\mu_i)\{\sum_j\cdot p(\sigma_j)\cdot[\sum_k p(\rho_k)\cdot(\sum_l p(\theta_l)\cdot p(D|\mu_i,\sigma_j,\rho_k,\theta_l))]\}} \quad (7.7)$$

$\forall$ i=1,..,n_μ, $\forall$ j=1,..,n_σ; $\forall$ k=1,..,n_κ; $\forall$ l=1,..,n_θ

7.2.4 Autocorrelation

The residual series with minimum variance was used to explore the autocorrelation of the residuals (Hegerl et al., 2006). This is important as the number of degrees of freedom, the effective length of the time series, is affected by the serial autocorrelation in Eq. 7.3. A test based on the variance of an estimator of the autocorrelation function was applied, determining the number of lags that include significant autocorrelation values. The null hypothesis to be tested assumes that for a certain lag L the autocorrelation value does not significantly differ from zero. This is performed by defining the ratio between the correlation at a particular lag and the corresponding standard deviation of the autocorrelation function for the same lag. Each of the ratios are compared with the critical values of a normal distribution (von Storch and Zwiers, 1999). The effective length of the series was calculated as:

$$n_{effec} = n\frac{\Delta t}{T_o} \quad (7.8)$$

being n the length of the time series, $\Delta t = 1$ and T_0:

$$T_0 = 1 + 2\sum_{l=1}^{n}(1 - \frac{L}{n})r_L \tag{7.9}$$

where r_L is the autocorrelation value for the lag L (Trenberth, 1984).

The autocorrelation functions for the zonal and meridional component are represented in Fig. 7.2 together with the critical values based on the variance of the autocorrelation function estimator. The lags for which the autocorrelation can be considered significant are those for which the autocorrelation values (red) are larger than the corresponding critical value (blue).

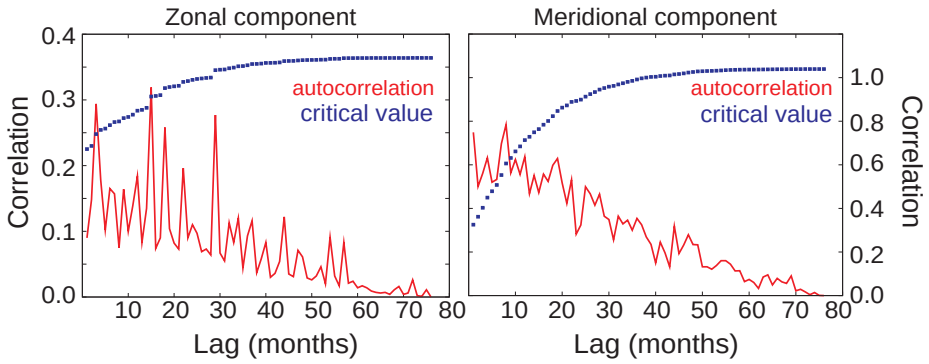

Fig. 7.2: Autocorrelation series and critical values for the zonal (a) and meridional (b) component.

The number of lags with significant autocorrelation values is 3 (9) for the zonal (meridional) component of the wind and the resulting effective length of the time series that needs to be determined to obtain the Fisher probabilities is 37 (7) for the zonal (meridional) component. It should be noticed that n is fixed to 76 time steps, focusing over the period between September 1993 and March 2004, where most of the stations present a large amount of data availability.

7.3 Results and discussion

7.3.1 Some insight into the parameter rejection areas

Before obtaining the marginal posterior PDFs a previous inspection of the constraints that each parameter imposes on the rest is provided (Forest et al., 2000,

2002). With this aim a statistic R^2 is calculated as the sum of squared residuals for each estimated series weighted by the inverse of the minimum residual variance (the estimations that show minimum variance of its residuals are selected among the whole set of estimations, see Appendix A). Then, the average R^2 obtained for each pair of parameter values is represented for every combination of two parameters. The surface generated is suitable for discriminating which regions of the parameters space may be rejected based on the ability of each pair of parameters to provide estimations with small residuals. Parameter rejection areas are plotted in Figures 7.3 and 7.4 for the zonal and meridional component of the wind, respectively. Thus, as explained each map represents the $||r||^2/\sigma^2_{r_{min}}$ of every pair of parameters values.

The pattern in Fig. 7.3a represents for the zonal wind component the rejection areas based on the R^2 statistic of μ *vs.* κ, i. e., the large scale domain (x axis) *vs.* the number of EOFs/CCAs retained (y axis: numbers in the κ triplets stand for the number of predictor EOFs, the number of predictand EOFs and the number of CCA modes, respectively). It indicates that smaller values of R^2 appear in the region of middle sized windows, that implies a better performance of those model configurations that consider a medium size domain. The minimum is located along the domain number 5 (see Fig. 5.5). It can be appreciated that poor constraints are placed by the parameter κ, since R^2 reaches similar values for all κ possibilities. This is obvious for the larger domains (1-3). However, for the smaller sizes of μ, some options of the number of EOF/CCA modes behave comparatively worse. These values correspond to those cases where two CCAs are included in the model. It seems that the worst combination of κ is 222, the one that incorporates less number of EOFs and CCAs.

Similar behaviour could be observed when combining μ with σ (predictor field) in Fig. 7.3b. Middle size windows perform better and larger windows perform worse showing similar R^2 values for all combinations of predictors. Smaller windows ($\mu \in$ [7,9]) perform better only with some combinations: those including the wind components, U10 and V10 as predictors.

In the combination of σ and κ (Fig. 7.4c), those options of σ comprising U10 and V10 present smaller values of R^2, for all possibilities of κ. In addition, those predictor fields that generate small residuals maintain this tendency with every combination of number of patterns, except with κ=222 that has larger residuals for all cases. Then, it seems that is the predictor field who imposes stronger constraints on the number of modes included in the model.

In the case of the combination of σ and θ (crossvalidation subset size) it can be appreciated (Fig. 7.3d) that the latter does not produce constraints on the predictor options. The cases that preset smaller residuals coincide with those cases where the wind components are included as predictors. Thus if the predic-

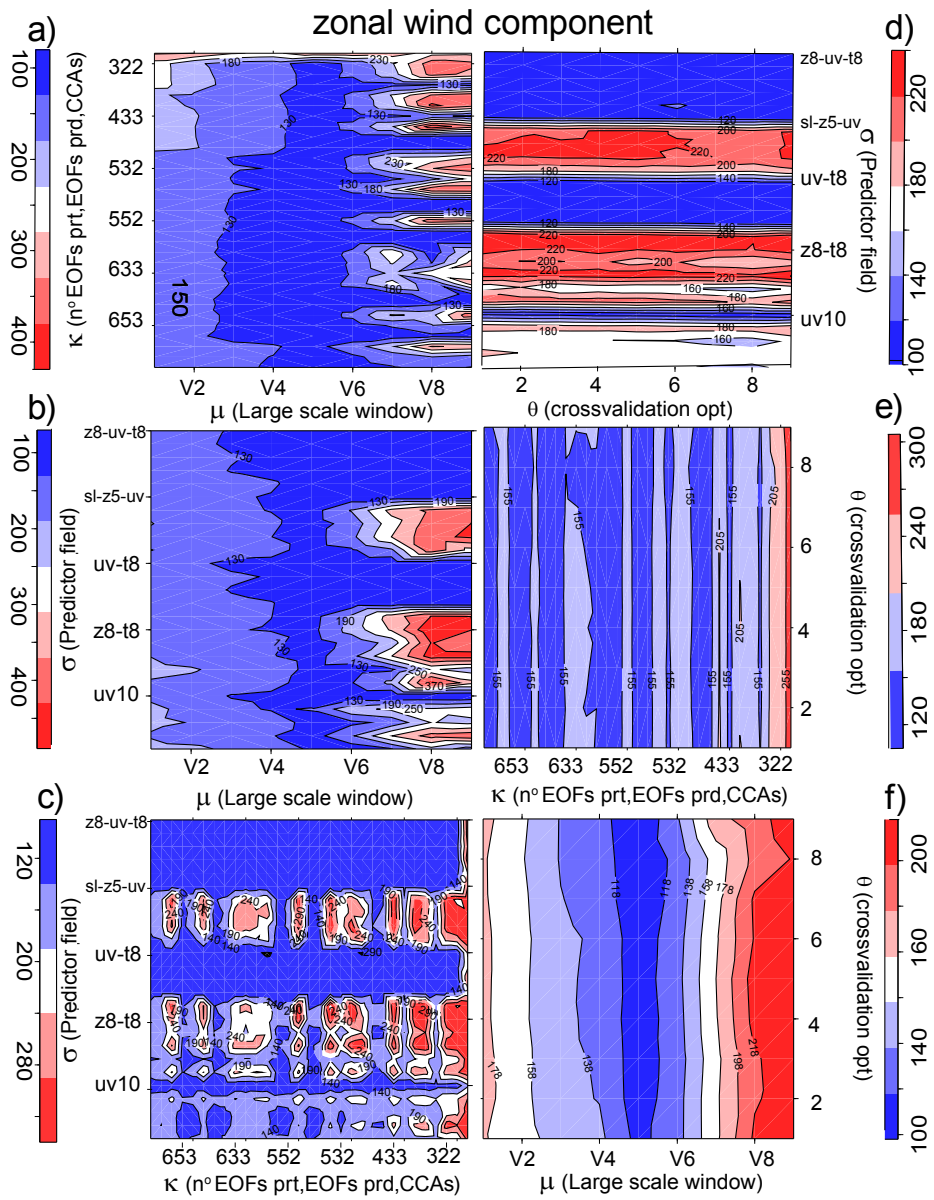

Fig. 7.3: Rejection maps for each pair of parameters: a) domain-number of modes, b) domain-predictor, c) number of modes-predictor, d) crossvalidation subset-predictor, e) number of modes-crossvalidation subset and f) domain-crossvalidation subset.

tor field generates small residuals, any option of the crossvalidation parameter performs well.

The comparison between the number of modes (κ) and the crossvalidation option (θ) indicates (Fig. 7.3e), as in the previous case, that the latter does not produce constraints on other parameters. It can be appreciated that the number of patterns presenting smaller residuals are those with four CCA patterns included, starting from those with the largest number of EOF patterns. The combinations presenting larger residuals are those that include only two CCA modes.

The crossvalidation subset values do not generate constrains on the large scale domain parameter as can be seen in Figure 7.3f. In general the performance of the method is better with the middle size windows and the quality of the estimations decreases as the large scale domain enlarges or decreases.

For the case of the meridional component similar comments can be made. Additionally it is interesting to mention that the variability of residuals is larger (Figs. 7.4a-f). In the case of the number of patterns retained, there is a clear division of residuals, being smaller the cases with four CCA modes, followed by the cases with three CCA modes and being the worst cases those with only two CCA modes included (Fig. 7.4e). The stratification in the cases with 4 and 3 modes was not so clear for the zonal component. The relation between domain and crossvalidation subset, reveals that the central windows perform generally better.

Thus, the analysis of parameter rejection areas based on the average residuals of each pair of parameter values allows to identify what parameter combinations generate estimations with smaller residuals. In general, medium size domains, predictor field combinations including the 10 m wind components or the inclusion of more than two CCA modes seem to best fit the observed records. Overall the crossvalidation parameter has little influence on the final statistics. This is a desirable result given the fact that θ is an exogenous parameter of the model. Stating that it does not have a discernible impact on the residuals is tantamount to saying that we are not modifying the evaluation of model skill by our decisions on the selected crossvalidation set up.

In the view of the constraints that each parameter imposes on the rest, it can be said that the more relevant parameter is the size of the large scale window, followed by the predictor field and the number of EOFs/CCAs included. The crossvalidation parameter does not seem to be relevant for the skill of the model. These results are in agreement with those in Section 5.4.1. However the more interesting comment here is that this analysis has allowed for discriminating which values of each parameter produces better estimations in terms of their residuals. This involves then further knowledge with respect to the frequentist

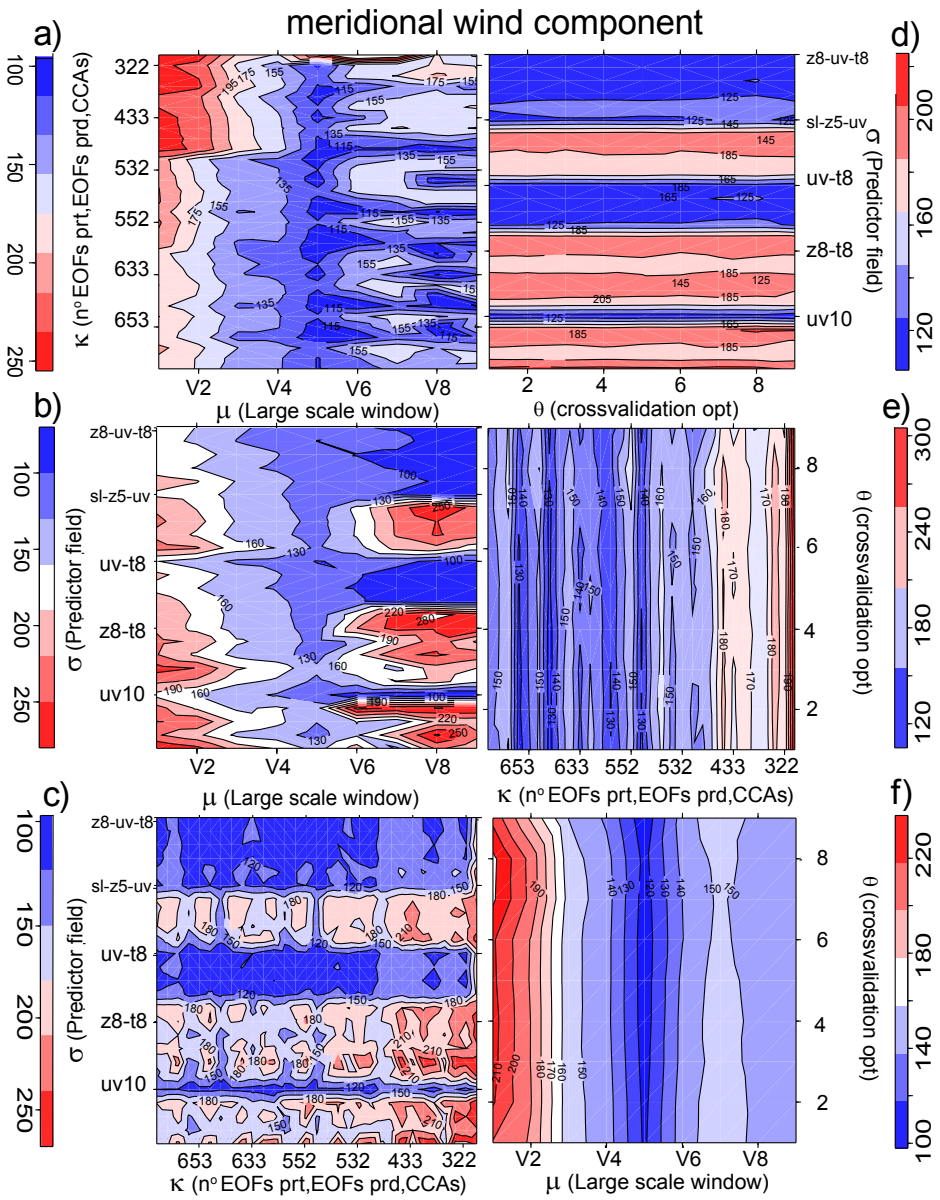

Fig. 7.4: As in Figure 7.3 but for the meridional component.

analysis as it provides an insight into the differentiated ability of each parameter value of the downscaling model. These preliminary results are contrasted with the more elaborated Bayesian approach in the following section.

7.3.2 Posterior distributions

The joint PDF of the data conditioned to the parameters (likelihood function) was calculated on the basis of a Fisher distribution, combined with the corresponding prior uniforms to obtain a joint posterior distribution of each parameter. They are represented in Figs. 7.5 (Fig. 7.6) for the zonal (meridional) wind component. The posterior PDF for the large scale domain (μ) assigns the highest probabilities to the smallest windows sizes (μ=7-9, Fig. 7.5a and 7.6a), and penalizes the rest with lower probabilities in the case of the domain number 5 and 6 and close to zero for larger windows. Thus the Bayesian analysis identifies as suitable those domains that cover smaller areas and rejects the rest. The marginal posterior for the predictor field (σ, Fig. 7.5b and 7.6b) selects those combinations of parameters that include the U10 and V10 wind components of the wind (from ERA-40 fields) as predictors, specifying for them the highest probabilities, specially for the cases with less number of fields included. Probabilities decrease as more fields are incorporated as can be appreciated in Figs. 7.5b and 7.6b. The PDFs for the number of EOF/CCA modes (κ) show a bimodal appearance (Figs. 7.5c and 7.6c). The probabilities assigned to the parameters have been divided into two groups, those combinations of parameters with only two CCAs included are labeled in the x axis with the numbers 1-15 and the rest (those including three or three and four CCA modes) are designated with numbers between 16 to 31. The probability distribution indicates that in general the combinations of parameters with only two CCAs receive lower probabilities. Higher probability values are shown for the combinations with four CCA patterns followed by those with three. However there is a subgroup of combinations in the area of only two CCAs (12-15) that show probabilities comparable to the cases with four CCAs. The zonal and meridional component PDFs show very similar information with the exception of a division between three and four CCAs not so clear in the zonal component as with the meridional one. The marginal PDF for the crossvalidation subset size (θ) reveals very similar probabilities for all parameter values, with the only exception of the subset 5 (5 months) of the zonal component (Fig. 7.5d) and the last two options corresponding to the subsets 8 (14 months = 2 years) and 9 (28 months = 4 years) of the meridional component (Fig. 7.6d), which show very low probability.

Through the Bayesian inference on the model parameters based on the marginal posterior distributions we have arrived at two different situations. On

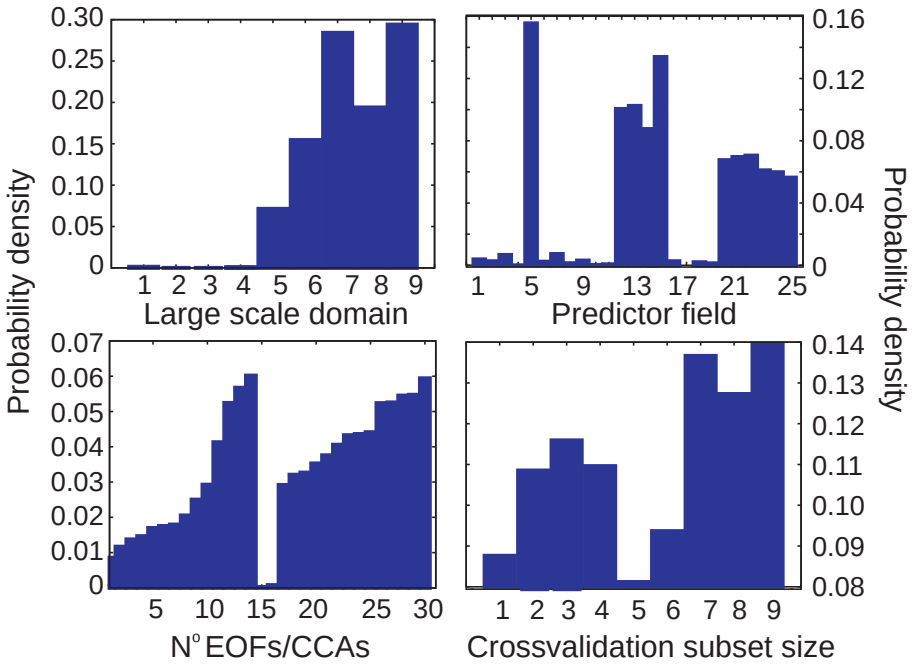

Fig. 7.5: Marginal posterior distributions of the zonal component of the wind for a) the large scale domain (μ), b) the predictor field (σ), c) the number of EOF/CCA patterns (κ) and d) the crossvalidation subset size (θ).

one hand we have found consistency with results from the parameter area rejection analysis in the case of the crossvalidation subset: both indicates that there are little differences between the various options considered for this parameters in terms of the residuals of estimations, except for the case 5 (8 and 9) of the zonal (meridional) wind component. In addition for the predictor field, both analyses resolve that there is a positive impact on estimations when including as predictor the wind components, U10 and V10. However, the marginal PDF penalizes considerably the rest of combinations, pointing out that the rest of parameters combinations should be rejected. On the other hand a lack of agreement is evident for the other two parameters: the marginal PDF of the large scale domain evidences penalization for the middle size windows being the smaller ones rewarded. For the number of EOF/CCA modes although smaller probabilities also correspond to the case with only two CCAs, a high score is shown in three cases (κ=622, 522, 422).

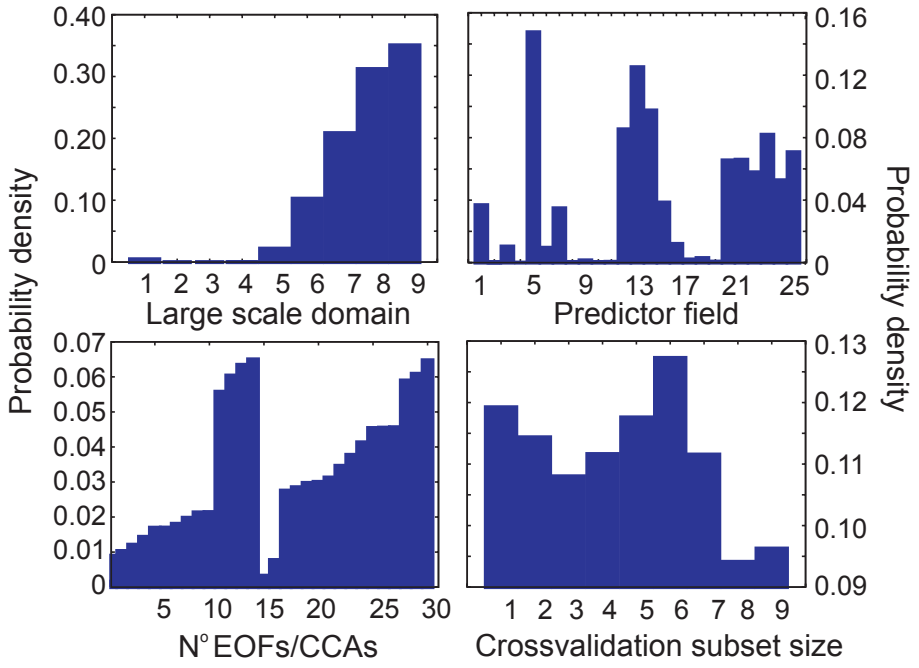

Fig. 7.6: As in Fig. 7.5 but for the meridional component of the wind.

The previous disagreement between results based on the Bayesian probabilities and the residuals behavior is illustrated on the following paragraphs by using one of the parameters, the large scale domain, for the case of the meridional component as an example. Similar conclusions can be met for the zonal one. The sum of squared residuals of each estimated series, segregated according to the large scale window are plotted in Fig. 7.7 (colors stand for each domain). For a given curve (given domain size), each point represents the sum of squared residuals for each combination of the rest of the 3 parameters. To represent this figure residuals are prior ordered from smallest to largest values. Thus, notice that the x axis in Fig. 7.7 only assigns a number to each combination of parameters with the purpose of illustrating the total number of possible combinations for each large scale domain. Then, in the design of Fig. 7.7, the value in the x axis does not help in the identification of the particular parameter combination. As can be appreciated the residuals present a large variability with values oscillating between 0 and 80.

In such conditions the shape of the Fisher distribution becomes of relevance since a narrow distribution allows only for a few valid residual values, penalizing the rest with lower or close to zero probabilities. Such a case corresponds to a very strict likelihood function which focuses on (assigns a high probability to) those combinations of parameters that produce the smallest residuals, i. e., those cases for which the sum of squared residuals is very close to the minimum (see likelihood function design in the Appendix A). The latter situation can be appreciated in Fig. 7.1 where the likelihood function based on the Fisher distribution assigns close to zero or zero probabilities to most sum of squared residuals, and thus, to most of the parameter combinations. On the contrary, a wider distribution would assign a probability different from zero to several sum of squared residuals allowing for the corresponding parameter combinations to be considered as suitable configurations of the statistical model.

The shape of the Fisher distribution depends on its number of degrees of freedom. This is determined by the number of parameters that needs to be tested and the effective length of the estimated time series (specifically the estimate with minimum residual variance, see Section 7.2 and Appendix A). Some authors propose a correction based on the serial autocorrelation in the attempt of generating wider Fisher distributions (Hegerl et al., 2006). However, even with the correction due to the autocorrelation, here the Fisher PDF or likelihood function is considerably slim as appears in Fig. 7.1. Nevertheless, in the view of the disagreement between results through posterior PDFs and parameters rejection in Section 7.3.1, the question arises whether the large amount of parameter combinations with low or very low probabilities should indeed be rejected as inadequate or less appropriate model set ups.

Two different behaviors deserve a comment in Fig. 7.7. On one hand, for the approximately 3.000 parameter combinations with the smallest residuals of each large scale domain, it is possible to identify that systematically the larger windows (see legend) generate larger residuals while for the medium and small windows residuals are smaller. Additionally, for the larger domains residuals are more sparsely distributed whereas intermediate/small domains are less scattered and concentrated around similar residual values. Still it can be appreciated that residuals for windows 7-9 are slightly lower than the corresponding to the cases 5 and 6. On the other hand, the rest of parameter combinations (those with $x > 3.000$) depict a more complicated behavior: the four smallest domains (numbers 9, 8, 7 and 6, see Section 5.4.1) show a sudden increase of residual values for the rest of combinations of parameters while residuals for domains 1 to 5 remain fairly stable or show a slight monotonous increase through the whole range of combinations.

In view of the latter it can be said that larger windows produce the largest residuals between observed and estimated series while the small and intermediate domains produce smaller residuals. However, only the middle sized windows evidence a stable behavior: they show similar residuals for almost all possible combinations. In contrast, the smallest windows behave inadequately (very large residual values) for a large amount of parameters combinations. Nevertheless, even though it only happens for very few combinations of the statistical model, the minimum squared residual sums are attained when using the smallest domains number 8 and 9.

Consequently, the suitability of the different possible model configurations can be then thought of in terms of two possibilities: either identifying the optimal cases, i.e., those with residual values close to the minimum whatever the behavior with the rest of parameter combination is (smallest window sizes) or recognizing the cases with reasonably small residual values that systematically maintain this behavior with the greatest amount of model parameter combinations. The latter is not discriminated by the Bayesian approach that instead tends to identify the cases whose residuals are very near to the minimum (optimal cases) rejecting the rest. The reasons for this are connected with the arguments given above about the width of the likelihood function and its tendency to severely penalize combinations of model parameters that generate residuals not rigorously close to the minimum.

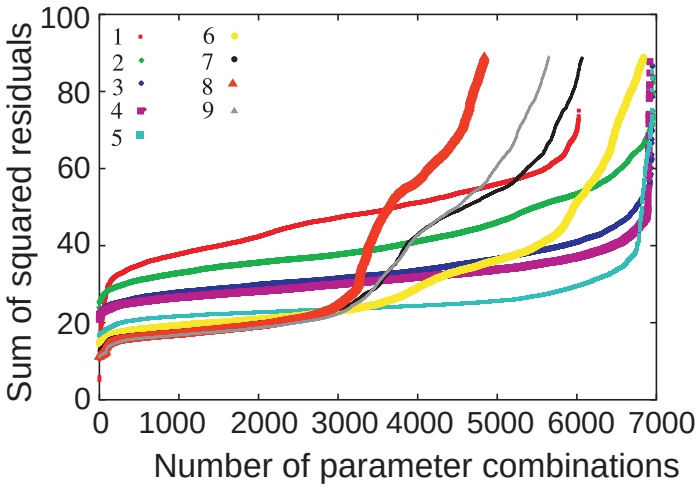

Fig. 7.7: Sum of square residuals segregated according to the large scale domain for the meridional component of the wind.

A similar argument can be used to explain why some cases including only two CCAs have obtained a high probability (not shown): for a few combinations of the rest of parameters, the smallest residuals are achieved by these three options mentioned: κ=622, 522, 422. As in the case of the large scale domain, this behavior is not stable for all the combinations of the rest of parameters and the residuals increase considerable for many other combinations, especially for the smallest predictor windows (7, 8 and 9; not shown).

These results hint a discussion about the interpretation of the Bayesian inference regarding the degree of subjectivity that may be involved in every methodology. The Bayesian method applied to the particular issue of determining the suitability of the parameters in the model configuration is able to recognize some optimal parameter combinations based on the residuals obtained between estimations and observations. However it failed in recognizing those parameters that perform adequately with most of the combinations. The identification of those cases is a desirable feature of the methodology since it would evidence those model configurations that are more robust to changes in any of the other parameter options. Thus, the Bayesian methodology may evidence skill depending on the specific purposes of the analysis: for the detection of optimal cases with smaller residuals, this method has shown efficiency in isolating the particular cases that minimize the error. If the aim is to determine stable combinations of the parameters for the identification of configurations that perform reasonably well in most cases, the Bayesian approach as implemented here is partly limited.

Summarizing, the large scale windows that have shown a reasonable good performance with the rest of the parameters are the medium size ones which include the large scale gradients that bring predictability for the regional wind. Too small windows, although not systematically, as we have seen for some combinations of parameters, can involve a loss of information regarding the large scale atmospheric structure. The number of EOF/CCA modes has shown a segregation of cases based on including or not the third and/or the fourth CCA mode in the analysis (recall probabilities in posterior PDFs in Figs. 7.5c and 7.6c, for the zonal and meridional wind component, respectively). Such a performance of this parameter is more evident in the cases based on using the smaller large scale domains (see parameter rejection maps of Figs. 7.3a and 7.4a). Then, it can be concluded that small windows with the minimum number of CCAs lead to a poor representation of the relations between the large scale flow and the regional features of the wind field. For the predictors there are clear advantages of using the wind components (posterior probabilities in Figs. 7.5b and 7.6b) although it cannot be said that the cases which do not incorporate U10 and V10 fail in reproducing the regional wind variability (Figs. 7.3b and 7.4b).

One more comment deserves attention at this stage. In Chapter 5 it was shown that combinations of model parameters including only two CCAs produced estimations with a different tendency and sign (anomalies) than those that included three or more CCA. In this chapter both, the assessment based on the parameter rejection areas and the Bayesian inference, agree in considering a better fit (smaller residuals for most of the parameter combinations) and a more robust behavior (higher probabilities) in the cases including more than two CCAs. Although the reasons for this are still not clear and further investigation would be needed to provide a physically meaningful argument, there are some evidences pointing out that the most suitable number of CCA modes in the downscaling model are those generating positive (negative) zonal (meridional) wind anomalies in the reconstructions of Fig. 5.13. It is interesting to notice that the frequentist approach for the uncertainties in Chapter 5 was not able to identify such differentiated performance of this parameter options (nor in the case of the other parameters). This fact then illustrates to some extent the added value of the alternative approach proposed in this chapter.

An analysis encompassing the study of parameter-rejection areas and the Bayesian posterior probabilities, has served as a mean to illustrate the adequacy of the different parameter values of the model set up. The former is based on the average behavior of the residuals of each combination of parameters while the latter combines prior knowledge with a penalizing function (likelihood). The following subsection is devoted to discuss the role of the prior knowledge in the performance of the Bayesian methodology. Thus, another question arises regarding the sensitivity of the Bayesian method to changes in the assumptions made for the prior distributions. The robustness of the method is also assessed in the next subsection by exploring the spatial variability of the results from the Bayesian analysis.

7.3.3 Sensitivity to prior knowledge

To gain insight into in the results achieved or to further learn about possible critical aspects of the methodology there is a need for examining also the ability of the model to generate robust posterior inference when different prior distributions are used. For every parameter, the uniform PDF was substituted by another prior PDF, where the probabilities were assigned by weighting the different parameter values according to the residuals they generate: the larger the sum of squared residuals, the lower the probability, being this case representative of a more realistic assignment of probabilities. With this the analysis starts at a different state of knowledge that could have implications in the final posteriors. Nonetheless, after the change of the prior distributions no variations in the final posteriors distribution are appreciated. This is illustrated in Figs. 7.8b and 7.8g.

In this figure left panels correspond to the sequence of different prior distributions tested and right panels show the resulting marginal posterior of the large scale domain for the zonal component of the wind (similar results were found for the meridional one). The first pair of plots (Fig. 7.8a and 7.8f) corresponds to the case explored in the previous paragraphs where the prior distribution of all parameters was assumed as uniform. Further, various subjective priors have been additionally included in this sensitivity analysis to illustrate what are the thresholds in the prior information that are able to modify the posterior probabilities (Figs 7.8c-e). This is shown only for one parameter (the large scale domain) and for the zonal wind component as an example. The prior distributions sequentially attach a higher probability to the medium size windows while the probability of the larger ones decreases. This sensitivity check illustrates how the posterior PDF is only able to show a change in the 'winner' values of the parameter when the prior designates nearly zero probabilities to the smaller windows. As it can be appreciated in Fig.7.8 the changes in the prior assumptions only produce an impact in the posterior PDF when the probability assigned to the medium size windows are close to 1 and subsequently the other probabilities are close to 0.

The latter implies that the determinant factor in the analysis is the likelihood function which ultimately decides the posterior probabilities. Other authors use different approaches for the modelling of the likelihood function, employing Gaussian distributions to penalize the residuals (Jackson et al., 2004), or in other studies, some more sophisticated diagnostics of the goodness of the fit by the model (Coelho et al., 2004). However, apart from an examination of the technical details of the approach, the interesting point here is to notice that an objective approach like the Bayesian one as exposed here, also needs a detailed analysis of its performance and a thorough review of the various assumptions made in the design of the strategy in order to interpret the results obtained.

To finish, an additional test is carried out with the twofold aim of understanding more on the robustness of the method and to discern some aspects regarding the spatial variability of the methodology. Thus a similar Bayesian analysis as implemented for the regional wind estimations is accomplished at every location within the dataset and for each one of parameters. The large scale domain posterior PDFs at every site in the CFN are represented in Fig. 7.9 for the meridional component of the wind. In view of the posterior distributions it can be said that in most of the locations there is a tendency for assigning the highest probabilities to the smaller windows and lowest (nearly zero) to the medium (large) domain sizes. In this sense the method is robust. However, it can also be appreciated that at a few sites the dominant contribution to the PDF is given by windows number 5 or 6 revealing a partial disagreement between the different time series. However no spatial pattern can be associated to the fact that some of the stations

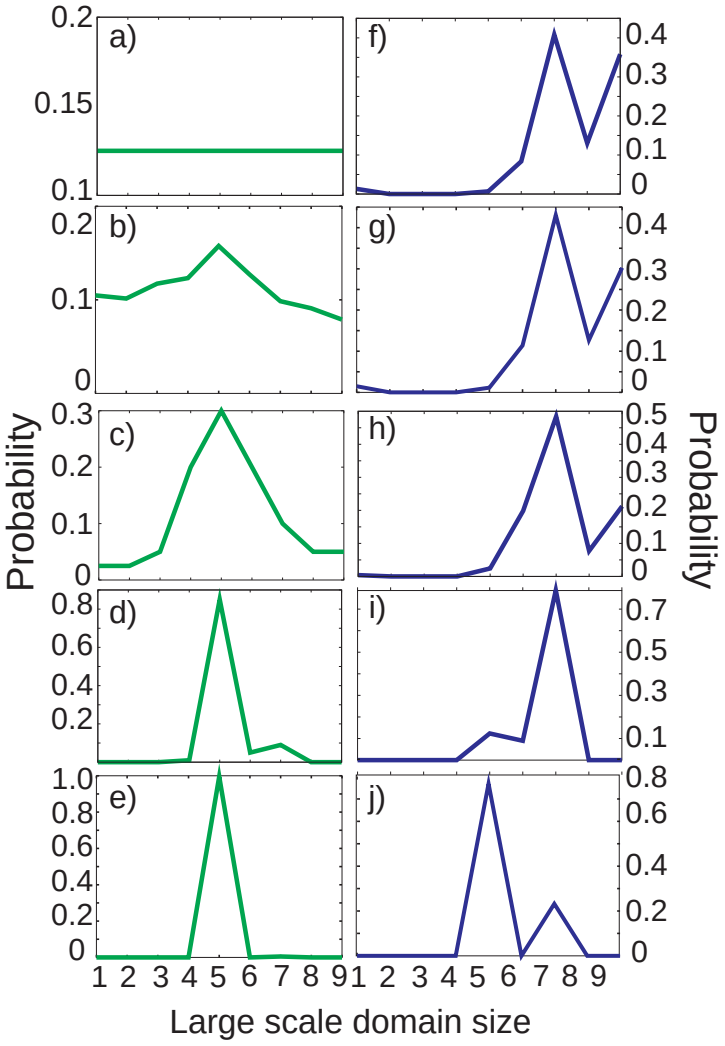

Fig. 7.8: Left: Different μ prior distribution tested for the estimations of the zonal wind component. The weights that are assigned to the medium size large scale domains are progressively increased while the corresponding to the other windows sizes are decreased. Right: marginal posterior μ PDFs obtained by applying the corresponding prior PDF.

present a differentiated behavior of the posterior PDFs: the sites whose marginal PDF assigns higher probabilities to the middle windows cannot be segregated according to a division in subregions, nor they can be divided depending on the ability of the method at each station to generate reliable estimations (see Fig. 5.4). It can only be mentioned that some of those specific stations are located along the Ebro Valley or in mountainous sites. This hints a good exposure to the circulations, not intensively affected by the local features that could be associated with the fact of detecting as more appropriate the medium size domains to provide a suitable representation of the atmospheric structure and the large scale gradients that are important for the regional wind predictability. For the case of the predictor field (not shown) apparently all the locations tend to show a predominant influence of the combinations including the U10 and V10 components of the wind. In the case of the number of modes a spatial distribution cannot be found neither, as in the case of the parameter μ. The map shows a similar tendency as in the regional case exposed in Figs. 7.6 and 7.7. Thus, it seems that a change of the time series that are the inputs of the method (i. e., whether they are the regional or the local estimates) does not produce a great impact in the results.

7.4 Conclusions

In this chapter a complementary approach to the frequentist evaluation of the methodological uncertainty associated with the use of a single downscaling model and multiple configurations has been presented. This is done by exploring the properties of the model parameter probability distributions. Thus, the assessment of the methodological sensitivity presented herein was focused on providing a probabilistic analysis on the suitability of parameter values to yield wind field estimations in good agreement with the observations, rather than presenting a measure of the methodological variability of wind estimates as in Chapters 5 and 6. The methodology raised is based on a Bayesian probabilistic analysis through which prior knowledge on the parameter population is combined with the available observations to generate posterior distributions. This posterior PDFs allow for making inferences about the ability of the different parameter options to produce skillful estimations.

The parameters of the model set up that were tested through this methodology are the size of the large scale domain, the predictor field(s), the number of EOF/CCA modes to be retained and the crossvalidation subset size. Uniform prior distributions were used in a first step allowing for equal probabilities to each parameter value. In addition, a likelihood function responsible for penalizing those configurations that generate estimations with large residuals was

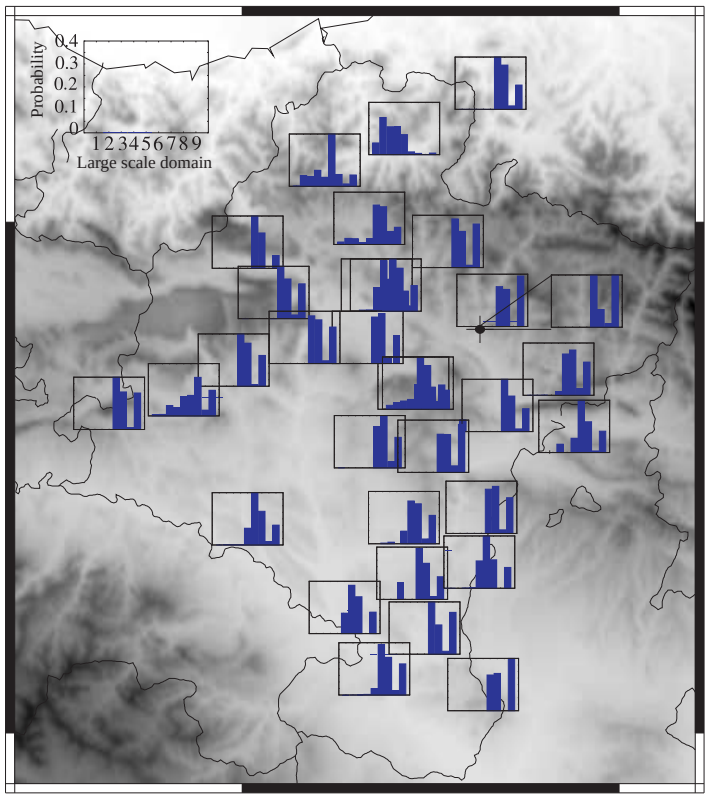

Fig. 7.9: Marginal posterior PDF of the large scale domain at each location within the CFN for the meridional component of the wind.

calculated based on the Fisher distribution. The formulation of the approach exposed in this chapter can be considered an interesting contribution since a full elaboration of the theoretical aspects leading to a likelihood function based on the Fisher distribution selection is not totally documented in the literature.

Previous to the analysis of the marginal posterior PDFs of each parameter, the constraints that a parameter imposes on the others were evaluated by calculating the parameter rejection areas, where a statistic R^2 was calculated, for every pair of values of each two parameters, based on the residuals. This examination allowed for a segregation of the model parameter options that on average provide more skilled wind estimates. It was found that using 10 m wind components as predictor fields, including more than 2 canonical modes in the downscaling model

or selecting the intermediate sized large scale windows rendered estimates with smaller residuals with respect to the observations and thus, those can be considered the more suitable parameters in the model set up. However, the results found in such an approach are not substantiated for the posterior marginal distribution of all parameters. Disagreements were found in the case of the large scale domain, for which the rejection areas suggested that the medium size windows were the most suitable for the downscaling exercise whereas the Bayesian inference rejected this domain sizes in favour of the smaller ones. In the case of the predictor fields both assessments agreed in considering as better configurations those cases that incorporate the components of the large scale wind field. However, the Bayesian analysis assigns a very low probability to the rest of predictor field options although estimations of quality are also found in those cases. The number of EOFs/CCAs in both cases evidences a better skill in generating estimations of those combinations of parameters incorporating more than two CCA modes. However, also a few cases with only two CCAs receive high probabilities in posterior distributions of the Bayesian analysis. In the case of the crossvalidation options both, rejection areas and Bayesian posteriors hint to similar probabilities for all possible values.

The disagreement between both types of analysis has been found to be related to the average behaviour of the residuals (that is calculated in the parameter rejection areas approach) in contrast with the tendency of the Bayesian approach to assign high probabilities to the optimum configurations (residuals close to the minimum) and rejecting the rest of the configurations. The reasons for this were found to be related to a narrow and thus, strict Fisher distribution that served as the likelihood function in the Bayesian approach.

Different prior distributions were tested for the case of the large scale domain parameter in order to understand the sensitivity of the Bayesian method to variations in the prior knowledge. Priors were successively modified by increasing the probabilities of those options that showed a reasonable performance in terms of residuals for most of the combinations of parameters. No influence in the marginal posterior PDFs were detected unless the prior were forced to overweight some cases, for instance intermediate sized windows, with very high probabilities. Thus, the responsible for such a severe judgement of the performance of the different model configurations in the Bayesian approach is apparently the likelihood function that focuses on the optimal cases and assigns close to zero probabilities to the rest.

The focus of applying this Bayesian formal technique was to isolate the robustness of some model configurations in generating realistic estimations in order to further constrain the previous frequentist selection of possible parameter values, that was based on more heuristics arguments (Chapters 5 and 6). However,

the methodology returns solely the optimal configurations based on the minimum residuals, i.e., instead of identifying the more robust model set ups, the probabilistic model detected rather a few optimal configurations. In contrast, the evaluation of the parameter rejection areas, based on the behavior of the average residuals, provides in this particular case an appropriate response to the main question: the search of the parameter options that produce estimations in good agreement with observations and are robust to changes in any of the rest of parameter values of the model configuration.

8

Conclusions and discussion

Humanity needs practical men, who get the most out of their work, and, without forgetting the general good, safeguard their own interests. But humanity also needs dreamers, for whom the disinterested development of an enterprise is so captivating that it becomes impossible for them to devote their care to their own material profit. Without doubt, these dreamers do not deserve wealth, because they do not desire it. Even so, a well-organized society should assure to such workers the efficient means of accomplishing their task, in a life freed from material care and freely consecrated to research. [...] Nothing in life is to be feared. It is only to be understood.

M. Curie, Autobiographical Notes, 1867-1934

This work aimed at providing an improved understanding of the variability of the wind field, and its derivative, the wind power production, at regional scales 0n the basis of their connection with the large scale atmospheric variability. Thus, two different, though related lines have been explored in this work. In the first part of the study the relationships between the wind speed and the wind power generated at various wind farms over a complex terrain region in the northeastern Iberian Peninsula have been examined. In the second part of the text the variability of the wind field measured at some stations in the same region has been investigated by identifying the main connections between the local wind at the CFN and the large scale atmospheric circulation over the North Atlantic area. Finally, the two parts have been assembled by exploring the link between the wind power production variability and North Atlantic atmospheric circulation in the basis of the wind-wind power relation evidenced in the first part. The methodological uncertainty associated with wind and wind power estimations has been explored throughout the various chapters of the second part of the manuscript.

The specific conclusions found in the different analyses of this work were detailed in the corresponding section at each chapter. From a broader perspective, the main conclusions of this Thesis are summarized and discussed in Section 8.1. An insight into the open questions and a brief discussion about some concerns related to different aspects within the Thesis are discussed in Section 8.2 and Section 8.3.

8.1 Conclusions

The theoretical PDF traditionally used to represent the wind speed population (Weibull distribution) does not reproduce at every location the properties of the observed wind. This lack of agreement between theoretical and observed wind distributions does not produce however a severe impact on the Weibull based wind energy estimations due to a partial cancellation of errors in the calculation of the wind power estimation. This exploration was raised on the basis of a critical evaluation of classical assumptions in the representation of the wind speed empirical distributions at hourly timescales and allowed for a quantification and understanding of the errors in the wind power estimations arising from the assumptions made on the probability distribution of the wind speed.

A linear empirical relation was evidenced between the wind speed and the wind power at monthly timescales while at shorter timescales the wind power is a function of the cubic wind speed. This evidence has proven a decisive bearing in the evaluation of the relations between the wind energy variability and the atmospheric circulation at monthly time scales in the second part of the work and is derived from the comparison of several methods that made use of hourly or monthly resolution to estimate wind energy production. Simpler methods generally perform well in comparison with more elaborated strategies that require higher temporal resolution data. Notwithstanding, all methods reproduce to a large extent the temporal variability of the observed wind power. Additionally, the quantification of errors in wind power estimations led to identify a larger contribution to these errors due to the assumptions in the wind-wind power relationship compared to that related to the representation of the wind by the Weibull probability distribution.

A considerable fraction of variance of the regional wind field over the CFN can be attributed to the large scale atmospheric variability over the North Atlantic area. The main modes of covariability between the local wind and the predictor fields, found by means of the application of a statistical downscaling technique

(CCA), showed substantial contributions from the East Atlantic/Western Russian and East Atlantic teleconnection patterns. The analysis also evidenced the role of the orography in the region that gives raise to the regional circulations found: typical up and down Ebro Valley regimes and more complicated circulations in the central and northern areas of the region. To our knowledge no references in the literature could be previously found regarding a statistical downscaling of the wind field over the IP. Results have supported the inspection, in a subsequent part of the study, of links between the North Atlantic atmospheric variability and the regional wind power production at the CFN. The foundations for such an exploration are based on the linearity between the wind power and the wind field, and between the latter and the large scale circulation changes.

The uncertainty in the wind field estimations associated with the methodological variance reasonably preserved the variability of wind observations and thus, the statistical method proved robust to changes in the model configuration. The analysis showed that the methodological sensitivity is largely dependent on the variability of the wind: those locations with larger variate evidenced a large sensitivity to variations in the model configuration. In addition, no differential impacts on the estimations of any of the parameters involved in the model set up were identified at this step. This circumstance motivated, in the last part of the work, a probabilistic assessment of the methodological uncertainty that aimed at imposing further constraints to the multiple model configurations in order to identify those with a superior skill in generating suitable wind estimations.

Large interannual as well as interdecadal variability was evidenced in the reconstruction of the wind field during the last centuries. The assessment of the methodological uncertainty at long timescales showed an interesting impact on past wind estimations due to changes in the model set up: the inclusion/exclusion of a certain canonical mode produced a bias to positive/negative estimates. This implication of the model configuration choice was not detectable during the observational period and then it contributed to stress the need of considering with caution estimations from any single model configuration. For this period, no centennial trends were appreciable although some episodes of anomalous large wind speeds were identified connected with low frequency changes of the relevant large scale modes over the North Atlantic region. Knowledge regarding variability from a broader perspective of past long term changes may have relevant applications in the understanding of, for instance, future variations of the wind field in the context of climate change regional projections.

The linearity between the monthly wind and the large scale circulation can be extended to the wind power. Thus, the regional variability of the wind power generated at several wind farms within the CFN can be partly attributed to variations of the relevant large scale modes in the region, as in the case of the wind field. The main mode of covariability between predictand and large scale predictors is similar to the second principal canonical pattern found during the downscaling of the wind field. Hence, results from the downscaling of wind power production were robust with those obtained for the case of the wind speed. Results from comparisons among a set of methodological variants that made use of the downscaled wind field and transfer linear functions to obtain final wind energy estimates, revealed that the direct downscaling performs generally better than the rest. These approaches proved useful to provide wind power production estimates in areas with no availability of power data and also for periods out of the observational one. This served as illustration of potential and simple applications providing information of the available wind power over a wider region and for longer than the observed periods with low computational efforts. The spread of the ensemble of estimations obtained in the methodological uncertainty inspection comprised most of the wind power observations, showing a comparable sensitivity as the wind field to changes of the model parameters.

Certain parameters of the downscaling model configuration evidenced a comparatively larger ability with respect to the rest within the parameter space to provide reliable wind estimations. A procedure that imposed constraints to the parameters performance based on the residuals identified that including the wind components at 10 m as predictor fields or more that two CCA patterns in the downscaling model and using the middle size large scale domains implies some benefits for obtaining estimations in good agreement with observations. However, the subsequent Bayesian analysis, that allowed for inferences on the posterior probability distributions of the parameters of the statistical model, exhibited some discrepancies with the previous result. The arguments for this discrepancy pointed to the ability of the Bayesian analysis for discriminating the optimal configurations but its difficulty to identify those parameter values that provide reliable estimations with most of the possible model configurations, whatever the values of the rest of parameters are. Such a difficulty was directly connected with the extremely narrow likelihood function that penalizes with nearly zero or very low posterior probabilities all cases whose residuals were not very close to the minimum. This approach has not yet been extensively applied for the estimations of regional climate variability and further investigations would be required to understand the implications of the various assumptions in the methodology.

8.2 *Quo Vadis?*

The statistical downscaling approach considered for this work is focused on monthly timescales. This allowed for concentrating on the variations of the wind field that to a great extent are related to variations of the large scale atmospheric circulation. Thus, the local processes that typically are resolved at shorter timescales are not considered for this analysis that focuses mostly on the regional signal. However, increasing the temporal resolution may be of use for instance, in the context of impact studies and extreme events assessment that may require higher spatial and temporal resolution (Maurer and Hidalgo, 2007).

An evaluation of the daily wind field predictability would provide insight into the ability of the statistical downscaling technique applied here for reproducing the observed daily variability. References in the literature regarding statistical downscaling of daily temperature and precipitation related variables are frequent (Wilby, 1998; Huth, 2002; Huth et al., 2008; Hundecha and Bardossy, 2008; Wetterhall et al., 2009), but the topic has been less addressed within a focus on the wind field. Then, such an analysis would deserve special attention.

A related issue regards the question whether other methodologies (i. e., non linear methodologies) would reproduce the regional wind variability comparatively with the CCA. A survey of methods that can empirically relate local to global climate variables can be cited so far: analog methods, fuzzy logic, weather generators, compositing, neural networks, etc. (Wilby and Wigley, 1997; Wilby et al., 1998). Analog methods, for instance have proven efficiency in reproducing the daily and monthly local precipitation picking up the proper level of observed variance (Zorita and von Storch, 1999; Fernández and Saenz, 2003) while performing as well as more elaborated multivariate approaches like the technique applied in this work. In contrast, the last type of approaches can provide a clear physical interpretation of the cross-scale relationships found. Further investigations on these issue would involve an understanding of the drawbacks and advantages of methodologies in the field of statistical downscaling approaches, that, to a great extent remain a challenge in the case of wind related variables.

In this line, a pertinent question can be posed regarding the comparison of both statistical *vs.* dynamical downscaling models applied to reproduce the regional wind field variability. The study by Jiménez et al. (2010b) produced a RCM simulation over the same target region as in this work. The WRF (Skamarock et al., 2005) model simulation covered the whole observational period (1992-2005) at 2 km of horizontal resolution. The evaluation of the model ability to reproduce the variability of the wind field was carried out at daily timescales. Here the regional simulated time series from WRF and CCA estimations are compared at monthly timescales. Series are represented in Fig. 8.1a,b for the zonal

and meridional component of the wind, respectively, together with the observations.

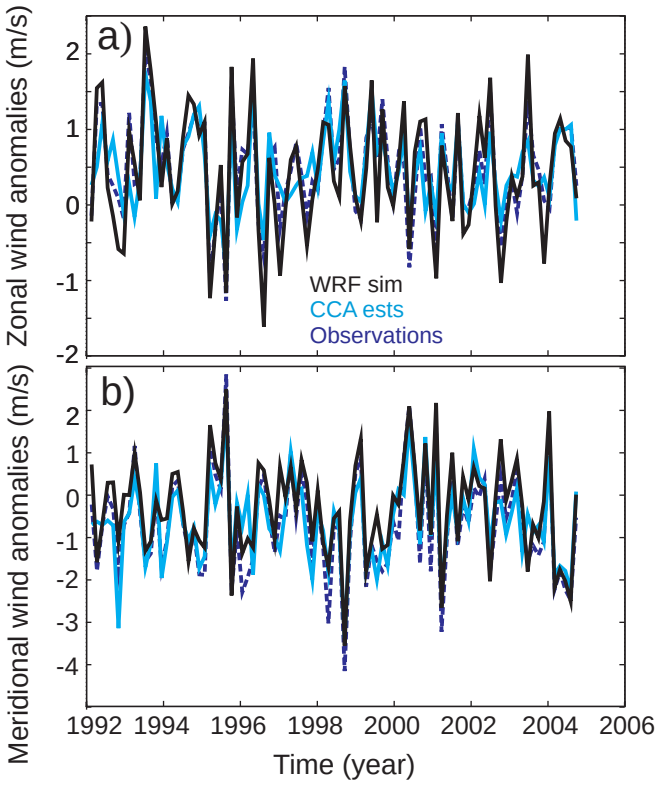

Fig. 8.1: Regional series of the observed (dashed blue) zonal (a) and meridional (b) wind components at the CFN compared to the CCA estimates (light blue) and the WRF simulation at 10 m (black).

As it can be observed in the plot, both estimations reproduce the regional variability of the wind components. In general the WRF simulation tends to return higher variance than the CCA estimations, but it is also noticeable that for some time steps the WRF model overestimates the observed variance. There are also situations in which neither the CCA nor the WRF can simulate the correct variability. Notwithstanding the main issue here is to provide a first approximation to the relative performance of both methodologies that reproduce

with similar ability the observed regional wind field. This a preliminary insight into the relative skill of each method to obtain estimations of the wind field over a complex terrain region. Further analyses would be necessary to evaluate the drawbacks and advantages of each approach.

In fact, one of the main concerns when applying empirical methods, in comparison with dynamical ones, for the downscaling of climate variables is the non-stationarity of the relation between spatial scales. An important assumption of the empirical downscaling methods is that the relation between the global circulation and the regional scales holds in a perturbed climate (Benestad, 2002). The later cannot be guaranteed and thus, this is also catalogued as the main drawback of these models. Some studies have assessed the presence of non-stationarities in the empirical relations between the atmospheric dynamics and the local climate variability. They have found evidences in both directions: while, for instance, Hewitson and Crane (2006) and Schmith (2008) identified signals of non-stationarity over the training period of the model, others, as Murphy (1999) and Hanssen-Bauer et al. (2003), found no indications of significant non-stationarities. To a great extent a reasonable expectation for altered future states of the climate is that they will involve changes in the intensity, frequency of occurrence and persistence of the large scale atmospheric patterns (Hewitson and Crane, 1996). Under this logic, further uncertainty will arrive to regional future projections but this would not necessarily invalidate the conceptual approach that aims at identifying the empirical relations between large and regional/local scales.

Through the assessment of the long term variability of the regional wind field in this work it has been evidenced that there are signs of an influence of the non-stationarities in the intensity of the associations between the large and the local scales on the variability of the wind at decadal and centennial timescales. This finding was based on assessment of the methodological sensitivity involved in the downscaling procedure. This fact highlights the importance of exploring the sources of uncertainty which is crucial for evaluating the reliability of estimations. An interesting assessment would involve a sensitivity analysis to variations in the intensity of the associations between global and regional scales and their impact on wind estimations during the calibration period. The approach can be put in the context of the generation of regional climate change scenarios. The intensity of the associations found during the observational time interval may be artificially increased/decreased creating an ensemble of potential situations and their impact on the estimations uncertainty could be evaluated. Subsequently this could be extended to the past and future estimated variability of the regional wind to examine the importance of this variations in periods different to the observational one.

Regarding the long term regional variability, the question that naturally arises from the analysis carried out here would regard the estimations of the wind field and the wind power production in future climate change scenarios. The main issues to address in this context are the comparative variability of the wind field in the future with respect to that during the last centuries. An assessment of the estimated future changes of wind speed and wind power variables could be feasible by using the different available GCM simulations over the twenty first century. Whether long term trends may appear or the agreement between estimations based on different GCM simulations leads to reliable projections are some of the interesting issues to focus on. Moreover, changes in the frequency of occurrence or intensity of those large scale circulation modes that are responsible for the observed wind and wind power regional variability and the impact in future regional projections of focusing in different climate change scenarios can be explored. Further, this exercise poses the interesting comparison of the uncertainty associated to the use of a specific downscaling method (as examined in this work) with that related to the use of different scenarios and/or GCM simulations. This would provide a wider perspective on the uncertainty that regional estimations should deal with. Besides the last conceptual approach, more formal treatments would be necessary to illustrate a path for the comparison between the different methodologies assessing the uncertainties (for instance, the frequentist *vs.* Bayesian methods).

Finally, one more issue deserves attention. A linear relationship between the wind speed and the wind power at monthly timescales was empirically observed at the various wind farms within the dataset. This relation is not obvious since the relationship between the two variables is not linear by definition (see Sections 4.2.2 and 4.2.3), but it can be assumed as linear for monthly timescales. The arguments for that were exposed in Chapter 4 of this work: the monthly averaging filters out higher and lower wind speed values that distribute around the non-linear parts of the theoretical power curve; in addition, the comparatively better performance of the linear transfer function with respect to rest of approaches explored to obtain wind power from monthly wind values, further supports the assumption of linearity between both variables. It was also shown (Section 6.4) that for longer than monthly timescales this relation also holds between wind and wind power. The question that arises is whether such a linear relationship can be reproduced in other regions, for other time periods apart from those explored in this work or in climate change scenarios. The scarceness of historical turbine outputs hampers this exploration as typically companies, promotors, etc. are not keen on releasing their production archives as it may involve unveiling profit and loss information.

8.3 A discourse on related topics

8.3.1 Need of observations

It has already been stressed in this manuscript that the availability of climate data is crucial for addressing any question regarding the regional or global climate variability. Efforts oriented to improve models and techniques to understand climate changes and their impacts in ecosystems and societies would be ill-founded if they do not run parallel to the endeavor of a global observational network. The term global applies here as the impact of climate variability is far from being uniform across the different regions of the planet.

Mankind started to systematically collect meteorological data by the seventeenth century. The first international meteorological network dates from 1654, established by Ferdinand II of Tuscany and it consisted of 11 stations over northern Italy and some locations in Poland, France, Austria and Germany. The first international meteorological conference had to wait until 1853 to be celebrated in Brussels. Since that time countless advances in technologies have been incorporated to the conventional weather stations. Remote sensing, satellite data and automatic stations have progressively come to scene helping in the task of collecting huge amounts of meteorological information. However, observations for operational forecast requirements do not necessarily coincide with those needed for climate research.

Observations at the different regions around the globe are imperative for any climate related assessment. Models need observational information to be initialized, validated and thus, improved. From the latter it is unquestionable that without observed meteorological and secondary related variables no possible understanding might arrive from the use of models or whatever strategy conceived. Further, observing the evolution of the climate is mandatory for detection and attribution studies. Natural disaster mitigation, risk assessment and reduction as well as adaption for developing and least developed countries are societal needs related to the regional climate evolvement, naturally or anthropogenically induced. Decision makers demand climate observations without which guidelines oriented to a safe and sustainable living cannot be dictaminated. Specifically, water availability and management, public health, agriculture, natural hazards, assessment of vulnerability, etc. are some societal issues that cannot be addressed in the absence of reliable and long enough observed records.

Long datasets (at least 30 years) are needed for the assessments of the climate system. Additionally, data should be free from significant discontinuities, errors and inhomogeneities with a robust quality assurance and availability of metadata. Observations of critical variables, apart from classical measurements of temperature or precipitation, would also be necessary for a whole picture of changes in

climate variability and the understanding of the reasons behind. Thus, sea ice extent, hydrology measurements, marine observations, clouds dynamics, ozone depletion, aerosols and atmospheric emissions, etc. are required at this stage. All this necessarily implies extra efforts in resources and coordination for the design of homogeneous, globe-distributed and robust observational acquisition systems (Trenberth, 2008; Wright, 2008). For the case of regional wind field assessments, the availability of observations becomes particularly important, due to its vectorial nature and the large spatio-temporal variability that it is subject to, in order to attain an improved understanding of the wind circulation particularities over a certain area and to adequately evaluate the ability of downscaling models in reproducing them.

8.3.2 Energy: sources and demand

The basic component of the economic growth of societies and the guarantee of a respectable living standards for population all around the globe is the availability, accessibility and quality of energy. It is clear that there exists a need for ensuring reliable and cost competitive energy supplies. However, it is also apparent that the society approaches a conflict between sources and demands of energy. As an example to quantify this conflict, it can be said that over the last 30 years the global economy growth was a 3.3% while the electricity demand increased a 3.6% (Saidur et al., 2010). Further, the Energy Outlook 2009 (WEO, 2009) estimates that the global energy consumption will increase by a 44% in the period between 2006 and 2030.

In the view of these ciphers, it seems pretty obvious that the energy challenge is too rigid to exclude from the debate any potential supply of energy for the future. However, more than bringing about arguments regarding the controversial renewable *vs.* carbon-based/fossil/nuclear debate, the interest here is to highlight the importance of the progress in renewable energies exploitation.

The interests in renewable energy supplies have considerably increased over the last decades on the basis of the scarceness of conventional fossil fuels and the general conviction that future generations cannot count on unlimited availability of fossils to meet the economical and societal needs; the oil crisis during the mid-seventies promoted a wider view of the use of energies and their associated sources; in addition, concerns about a severe damage to the environment produced by the extensive emissions of contaminants and greenhouses gases to the atmosphere are also the drivers for an increasing interest in favouring renewable energies supplies (hydropower, solar, wind, biomass, geothermal, etc., energies).

Overall, wind energy has experimented the fastest growing and commercialization with little R&D since the 90's. Significant progress in the wind turbines technology and many incentives from local and/or national governments are the

factors contributing to boost the wind energy market, especially in Europe and recently also in the United States.

It is believed that the wind energy may contribute with likely a 15%-20% of annual electricity production without many exceptional arrangements. Some interesting comments in this line can still be made: apparently, the wind energy market can generate a larger number of jobs per TWh than any other energy technology (Worldwatch Institute; USA), in addition, the *energy payback time* for the wind energy is shorter than that for the rest of energies. This implies than when a turbine has been operated for this time period (in the order of a month to a maximum of a year, depending on the turbine) it has already generated an amount of energy enough for manufacturing another turbine of the same type.

Potentially all countries have locations with average wind speeds of more than 5 m/s at 10 m. This implies a global availability of wind energy resources for exploitation. Nonetheless, the design of wind power plants has to overcome difficulties related to geographic and orographic constraints, environmental limitations and technical and financial requests (Sesto and Casale, 2010). In addition, the high spatial and temporal variability of the resource makes it difficult to rely on poor evaluations (not validated model simulations, a single year of records at a specific site, etc.,) of the wind energy availability. The path for overwhelming these restraints goes through measuring wind speed and direction at every potential location for more than one year, to pick the interannual variability of the wind field that has proven to contribute to large wind energy production oscillations.

In general and not only for the case of the wind energy, there are manifest needs for creating policies, also at the global scale, to organize the use and generation of energy. Better technologies may stretch the limited energy resources and maybe reduce the environmental impacts. But the most essential and perhaps difficult issue is to find the path for driving countries, industries and individuals to a more responsible usage of energy.

8.3.3 Science and society

Some aspects of the relationship between the scientific activity and its effects on quotidian life of society deserve a brief insight. In the first line of arguments that defend a close connection between both, lies the fact that no independent development of neither science nor society can be conceived. Thus, it is assumed that such a relation should be profitable in both directions. Leaving apart the discussion about the unequal distribution of means and resources for an acceptable development (unfortunately, a 85% of the global population has already been moved out from this discussion, Ziegler, 2005), there are many examples that illustrate this flow of benefits in both directions. Society has received contributions

from science in countless fields allowing for a progressive increase of the well-being levels and providing many solutions for the everyday life of citizens: medical advances, industrial development, telecommunications and computational progress, knowledge about environmental adaptation and preservation, energy solutions. et. This is a broad enumeration of the different fields that constitute the foundations of a gradual improvement of life conditions throughout the history and science lies in the ground of each one. Whenever it has been possible, society has rewarded the scientific successful activity by recognizing efforts and supporting advances in research. Marie Curie in her autobiographical notes points to this fact claiming that *[...] a well-organized society should assure to such workers the efficient means of accomplishing their task, in a life freed from material care and freely consecrated to research.*

Hence, it can be said that the effective contributions from both sides have been a requirement for a parallel evolution of science and society. Nevertheless, not everything in the relation between sciences and societies is so direct. At any time a clear need comes to scene, society affords a plan for finding a solution. For instance, if a new disease appears (in a developed country), all means in hand are directed to obtain a cure for it. Pharmaceuticals are provided with fundings, laboratories, etc. to guarantee the success of the research. But, what happens when the relation between research and society's needs is not in the form problem-solution? (as disease-cure) What happens when instead, science is in principle solely oriented to acquire further knowledge, an understanding of some field, as for instance the climate sciences? Then such a relation may be obscured due the appearance of some obstacles in the communication. A fluent language and clear communication channels are essential for a healthy science-society relation. Unfortunately, nor media nor scientists are always prepared to understand each other. On the one hand, media has a certain responsibility in disseminating the messages, avoiding their selection or filtering according to any interest and in eluding manipulations. But this seems not so simple. On the other hand, to be easily understood, the scientific language must be clear and adapted to a certain level accessible for the general public. The researcher should have some skill in contextualizing the question and provide understandable answers. Neither of them seems simple.

First of all, it would be desirable that researchers have or acquire certain ability to expose ideas and arguments, i.e., some skill in communicating. However this communication may have different implications depending on the audience (scientific circles or the general public) and could involve differentiated levels of rigor and depth and distinct transparency and simplicity requirements. The question that arises is to what extent any person professionally devoted to science should assume the responsibility of informing the general public about his/her/others

investigations and findings. To some extent it is hard to believe that all scientists are equally qualified to convey reliable and clear messages. It is maybe reasonable to argue that the communication effort requires especial capabilities and perhaps appropriate training. An example of this is explained in Bray and von Storch (2009) where a language confusion (*prediction* instead or *projection* is frequently used when referring to future climate estimates) is clearly detected in the scientific community.

Second, there is an inherent aspect of the communication between science and society that seems to obscure or, at least difficult it: the uncertainty. Oscar Wilde had a perception of this: *Man can believe the impossible, but can never believe the improbable.* Uncertainty is however involved in most of everyday human life: medical diagnoses, stock-market transactions and financial risks, insurance companies activity, the weather bulletin informs about the 'probability' of precipitation, playing lottery, etc.). Nonetheless, when dealing with scientific issues, uncertainty is frequently a synonym of ignorance. Uncertainty is not well received if it is associated with knowledge. It seems that according to public judgement, knowledge must be certain, there is no space for hesitating.

We often hear or read in the media that *the temperature will increase in 2* ^0C *during the course of this century.* In contrast, it is very uncommon to read in the newspaper that the projected changes in the global mean temperature for the next 100 years oscillate between 2 ^{0}C and 6 ^{0}C. The last implies a measure of uncertainty, the first statement does not. But the second one is closer to the truth because the current state of knowledge and the scientific efforts oriented to determine the magnitude of the potential global climate change cannot delimit the projected changes to answer this question with a number. Instead, it can provide a possible range of temperature values and arguments about plausibility. In avoiding references to the uncertainty in climate science for instance, messages to society may generate confusion. Could it be that scientists elude this controversy in front of the general public by explicitly removing the references to the uncertainty involved? or do the media re-interpret and re-formulate the ideas in a deterministic and easier way to explain?

Uncertainty is uncomfortable because we are not used to it, at least in a context where we are supposed to assimilate concepts and ideas, where we are supposed to learn something. This is noticeable in the academic education we receive in schools and universities. Pollack (2006) comments that textbooks in primary and secondary education put an emphasis in 'what we do know' and 'what we do not know', but there are no stimulus for the curiosity of students. The uncertainty is tied to the curiosity and then, it constitutes the engine for the exploration of new ideas, for the investigation of alternatives for an unresolved problem, for science.

Thus, it is reasonable to consider that the education plays a crucial role to overcome the difficulties of coexisting with 'probability' and uncertainty in many aspects of quotidian life, not only what relates to science. Additionally, science could greatly benefit from an alternative attitude to *what is not certain* but still implies knowledge. At least, it would help to resolve the problems derived from the lack of understanding (the absence of a common language) between scientists and citizens by incorporating in public discourses probabilistic assessments as part part of a well founded research.

8.3.4 A case study?

In this inter relation between education and communication and going back to the main argument of this discussion, the feedbacks between science and society in terms of utility, there is a personal experience that deserves a little attention. Some years ago CIEMAT suggested to the Wind Energy department to create a spin-off company. The original idea of a spin-off is to serve as a vector in the transfer of knowledge between the research centers/universities and companies. This appears then as an interesting and challenging example of connection between science and society, a potential direct channel of communication between them that includes all the above mentioned difficulties and thus, deserve to be explored, a testing bench where various *lessons* about the interaction between these two different frameworks may be learnt. The section of this small spin-off company (Globalforecasters S.L.) where I belong to is devoted to evaluate the climatology of the wind energy resource. We have participated in different projects with small and big companies. The first exciting aspect was the interesting questions raised by the people working for those companies. This implied a further motivation for the spin-off team since this entails the opportunity of learning something new from them. We also found that, although academic research and markets have very different time requirements, there were options for coordination. Those options were founded in persistent explanations about how a specific project demands a different treatment to answer the particular questions involved. Arguments were needed to stress that this necessarily implies time and effort to arrive to a rigorous study (observations acquirement, suitable experiments design, validation of results and interpretations). All this is not always easy to implement within the typical hurries of companies. Fortunately, most of the times we found acceptance and understanding in this lines from the companies side. Summarizing, for a project to be accomplished and matured with academic rigour arriving at a common understanding of the work from both sides is fundamental. This little experience in the industry market serves as an example to illustrate and believe that multiple fields in science may be of real service to society and that a common language between them is possible.

In addition, in the philosophy behind the 'wind resource climatology' section of this spin-off example resides the idea of the *self-funded* research. The projects accomplished during these few years served to generate more projects, they have contributed to present studies in international conferences and some publications will be soon submitted to peer reviewed scientific journals. Also, computational resources could be acquired and they were offered to the university (UCM) with the aim that other research groups can also take advantage of it. The fruits of this effort allowed for hiring people to continue new projects (at this time a Ph Dr. is full time employed to coordinate and to work in present and future projects).

This case study may well represent a compendium of the different issues addressed herein, from the efforts in a careful design of strategies for the wind field assessment that incorporates sufficient observational evidences and exhaustive models validation, to the continuous attempts to identify common channels that science and society together can go through, including the belief that renewable energies may contribute with interesting solutions to the unbalanced increase of energy demand. The personal and working experiences during the elaboration of this Thesis encompass a valuable learning process associated to the set up of this spin-off project. My sincere gratitude and admiration to the people committed to this endeavor: Fidel González and Jorge Navarro (supervisors of this Thesis) Pedro Jiménez, Angela Hidalgo and Juanpe Montávez.

Appendix A

The Fisher distribution and the estimation of degrees of freedom

The approach presented in section 7.1 for the likelihood function is based on the comparison of residual variances between models (here, different configurations of the same model depending on the combination of parameters selected in each case). The objective is to test whether the normalized variance of residuals of each model configuration is considerably different from that corresponding to the best model or in the contrary, they are similar. Thus, the target of the likelihood function is to assign low or high probabilities to each model respectively.

To understand how this can be accomplished by using the Fisher distribution and to provide an explanation on the corresponding number of degrees of freedom we will start assuming that the models to be compared are simple linear regression models. This will be extended afterwards to the case of any type of model comparison.

The two regression models to be compared are:

$$M_1 : y = a + b \cdot x$$

$$M_0 : y = a + \beta \cdot x$$

M_0 is the best model fit and β is known. M_1 is a more complex model in the sense that it has a larger number of unknown parameters. Rewriting M_1 as $y = a + (\beta + b') \cdot x$ it can be said that M_1 is contained in the model M_0 and the effect of adding b' is the effect of changing the slope of the best linear fit (

from β to b, supposed identical intercepts a) as it is illustrated if Figure 8.2. We want to test how significant is the difference $\beta - b = b'$, i. e., the change of slope, similarly as in a stepwise regression where the null hypothesis of $b' = 0$ is tested by means of a likelihood ratio that follows a Fisher distribution (Hinckley, 1969, 1971; Solow, 1987).

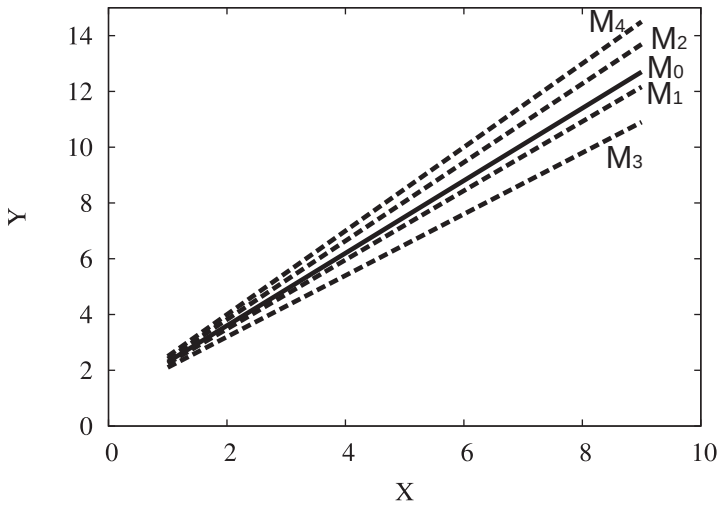

Fig. 8.2: Linear regression models: best fit model (M_0) and a series of alternative models with a change of the slope (M_1, M_2, M_3 and M_4).

Based on the comparison of two models where one of them (M_1) is contained in the other (M_0) this ratio can be written like in Yu et al. (2008):

$$\frac{res(M_1 - M_0)^2/\nu_1 - \nu_0}{res(M_0)^2/n - \nu_o} \sim F \tag{8.1}$$

where $res(M_1 - M_0)^2$ is the sum of squared residual differences of the estimations with M_0 and M_1, $res(M_0)^2$ is the sum of squared residuals obtained with the reference model M_0, ν_1 and ν_0 are the degrees of freedom of M_1 and M_0, respectively and n is the length of the time series; $\nu_1 - \nu_0 = 1$ in the case of the simplified models M_0 and M_1.

In order to further understand the relation to the F distribution, a classical analysis of variance, ANOVA (von Storch and Zwiers, 1999; Sánchez et al., 1996), is applied in order to test what is the effect of changing the parameter from β

to b. For the shake of simplicity we will suppose that the models are $M_1 : y = a + b' \cdot x + \epsilon$ and $M_0 : y = a + \epsilon$ being ϵ an error due to the regression. With this simplification the difference in unknown parameters, and thus, in degrees of freedom, is identically 1. The null hypothesis H_0 is $b' = 0$ which implies that adding the extra term b' has no effect in the estimations. The decomposition of the variance of the estimations can then be written:

$$\sum_i^n (y_i - \bar{y})^2 = \sum_i^n (y_i - \hat{a} + \hat{b'} \cdot x_i)^2 + \sum_i^n (\hat{a} + \hat{b'} \cdot x_i - \bar{y})^2 \tag{8.2}$$

where $\hat{a}$ can be substituted by $\bar{y} - b' \cdot \bar{x}$ and $\hat{b'}$ by S_{yx}/S_x^2 where S_{yx} is the covariance between x and y, and S_x^2 is the variance of x (Sánchez et al., 1996). Then, we can write

$$\sum_i^n (y_i - \bar{y})^2 = n \cdot S_y^2 \tag{8.3}$$

$$\sum_i^n (y_i - \hat{a} + \hat{b'} \cdot x_i)^2 = \sum_i^n (y_i - \bar{y} - \hat{b'}(x_i - \bar{x}))^2 \tag{8.4}$$

$$= \sum_i^n (y_i - \bar{y})^2 - 2 \cdot \hat{b'} \sum_i^n (y_i - \bar{y}) \cdot (x_i - \bar{x}) + \hat{b'}^2 \cdot \sum_i^n (x_i - \bar{x})^2$$

$$= n \cdot S_y^2 - 2n \cdot \frac{S_{yx}}{S_x^2} \cdot S_{yx} + n \cdot \frac{S_{yx}^2}{S_x^4} \cdot S_x^2$$

$$= n \cdot (S_y^2 - \frac{S_{yx}^2}{S_x^2}) = n \cdot S_y^2 \cdot (1 - r_{xy}^2)$$

being $r_{xy} = S_{yx}/S_y S_x$ the regression coefficient and

$$\sum_i^n (\hat{a} + \hat{b} \cdot x_i - \bar{y})^2 = \sum_i^n (\bar{y} - \hat{b} \cdot \bar{x} + \hat{b} \cdot x_i - \bar{y})^2 \tag{8.5}$$

$$= n \cdot \hat{b}^2 (x_i - \bar{x})^2 = n \cdot S_y^2 \cdot r_{xy}^2$$

We have assumed that the errors ϵ_i are normally distributed with mean zero and uncorrelated.

For the term of Eq. 8.3, the total variance of estimations, we write

$$\frac{1}{\sigma^2} \cdot n \cdot S_y^2 \sim \chi_{n-1}^2 \tag{8.6}$$

where σ^2 is the variance of the population. Identically, for the term of Eq. 8.4

$$\frac{1}{\sigma^2} \cdot n \cdot S_y^2 (1 - r_{xy}^2) \sim \chi_{n-2}^2 \tag{8.7}$$

which is an unbiased estimate of the residual or error variance and for the term of Eq. 8.5.

$$\frac{1}{\sigma^2} \cdot n \cdot S_y^2 \cdot r_{xy}^2 \sim \chi_1^2 \tag{8.8}$$

which is an estimate of the variance of the estimated values. Each part of the decomposed variance follows a χ^2 distribution with a number of degrees of freedom equal to the number of unknown parameters respectively (Gregory, 2005).

As we want to know the effect of the term b' in the regression equation the procedure is to compare the contribution to the total variance of each term: the error variance (Eq. 8.4) and the one derived from the regressed values with the term in b' (Eq. 8.5). For this aim the F statistic is defined as

$$F = \frac{\chi_1^2}{\chi_{n-2}^2/(n-2)} \tag{8.9}$$

that follows the Fisher distribution (Gregory, 2005). Thus, to accept the null hypothesis ($H_0 : b' = 0$) with a significance α, the value of the statistic must be minor or equal that the tabulated $F_{1,n-2}(\alpha)$, that is, with 1 and n-2 degrees of freedom. In general, the classical ANOVA denotes the variance of the estimated values as the variance due to the different treatments (the variance of k + 1 different treatments will follow a χ_k^2) and compares this variance with that of the residuals (that follow a χ_{n-k}^2). In our regression context this is equivalent to compare two regression models where the best model presents k unknown parameters less than the alternative model and thus, k degrees of freedom less. In these conditions the statistic is

$$F = \frac{\chi_k^2}{\chi_{n-k}^2/(n-k)^1}^* \tag{8.10}$$

Hotelling (1940) and Atkinson (1969) postulated the same approach to compare any type of models where one of them is the model that best fits the observations or generates the smallest residual (Y_B) and it is compared with the residuals of an alternative model (Y_A). The comparison is also done through the F statistic: $Y_A^2 - Y_B^2/Y_B^2 \sim F(df_B - df_A, n - df_B)$. Thus, the explanation given above can be extended to our ensemble of downscaling models. The null hypothesis is that the model M_1 with m unknown parameters is the best model. Then its residuals will follow a χ^2 distribution

$$\chi_\nu^2 = \sum_i^n \frac{||r||^2}{\sigma^2} \tag{8.11}$$

with $\nu = n - m$. As in the regression example, we add k new terms whose parameters are known to generate the model M_0. Then the number of degrees of freedom decreases in k. The effect of adding k known terms is like reducing the length of the time series in k. The associated χ^2 distribution will have $\nu - k = n - m - k$ degrees of freedom. The objective is to compare the previous residuals with the new ones. The new χ^2 distribution ($\Delta\chi^2$, that represents an estimate of the difference of variance of residuals) must fulfill

$$\chi_\nu^2 = \chi_{\nu-k} + \Delta\chi^2 \tag{8.12}$$

so $\Delta\chi^2$ has k degrees of freedom (Gregory, 2005). It can be also said that $\Delta\chi^2$ represents the effect of applying k different treatments as in an ANOVA analysis. Finally the test consists in comparing the difference between models M_0 and M_1, then:

$$F = \frac{\frac{\Delta\chi_k^2}{k}}{\frac{\chi_{\nu-1}^2}{\nu-1}} \tag{8.13}$$

where the numerator is the difference of the estimations residual variance and the denominator is the estimator of the error variance. Thus, we have finally end up with the same the formulation as in section 7.1 (Eq. 7.3).

Combinations of the statistical downscaling model parameters

Table 8.1: Large scale domain (μ in Chapter 7, see Fig. 5.5).

Window	Latitude	Longitude
1	75^o N-20^o N	90^o W-30^o E
2	70^o N-30^o N	80^o W-20^o E
3	70^o N-30^o N	50^o W-20^o E
4	65^o N-35^o N	40^o W-10^o E
5	55^o N-35^o N	25^o W-10^o E
6	50^o N-35^o N	10^o W-10^o E
7	47.5^o N-37.5^o N	5^o W-5^o E
8	45^o N-40^o N	5^o W-5^o E
9	45^o N-40^o N	2.5^o W-2.5^o E

Table 8.2: Crossvalidation subset size (θ in Chapter 7).

Option	Crossval. subset size (months)
1	1
2	2
3	3
4	4
5	5
6	6
7	7 (= 1 year)
8	14 (= 2 years)
9	28 (= 4 years)

Table 8.3: Predictor field (σ in Chapter 7). Notation: SLP= Sea Level Pressure, ϕ_{850}=850 hPa geopotential height; ϕ500=500 hPa geopotential height, UV10=10-m height zonal and meridional wind components and$Z_{500-850}$=500-850 hPa thickness data.

Option	Predictor field(s)
01	SLP
02	ϕ500
03	ϕ_{850}
04	$Z_{500-850}$
05	UV10
06	SLP-ϕ500
07	SLP-ϕ_{850}
08	SLP-$Z_{500-850}$
09	ϕ500-ϕ_{850}
10	ϕ500-$Z_{500-850}$
11	ϕ_{850}-$Z_{500-850}$
12	SLP-UV10
13	ϕ500-UV10
14	ϕ_{850}-UV10
15	UV10-$Z_{500-850}$
16	SLP-ϕ500-ϕ_{850}
17	SLP-ϕ500-$Z_{500-850}$
18	SLP-ϕ_{850}-thk58
19	ϕ500-ϕ_{850}-$Z_{500-850}$
20	SLP-ϕ500-UV10
21	SLP-ϕ_{850}-UV10
22	SLP-UV10-$Z_{500-850}$
23	ϕ500-ϕ_{850}-UV10
24	ϕ500-UV10-$Z_{500-850}$
25	ϕ_{850}-UV10-$Z_{500-850}$

Table 8.4: Number of EOF/CCA modes (κ in Chapter 7).

Option	Predictor EOFs n^o	Predictand EOFs	n^o	CCAs n^o
01	6	6	4
02	6	6	3
03	6	6	2
04	6	5	4
05	6	5	3
06	6	5	2
07	6	4	4
08	6	4	3
09	6	4	2
10	6	3	3
11	6	3	2
12	6	2	2
13	5	5	4
14	5	5	3
15	5	5	2
16	5	4	4
17	5	4	3
18	5	4	2
19	5	3	3
20	5	3	2
21	5	2	2
22	4	4	4
23	4	4	3
24	4	4	2
25	4	3	3
26	4	3	2
27	4	2	2
28	3	3	3
29	3	3	2
30	3	2	2
31	2	2	2

References

2009: World energy outlook 2009. Technical report, International Energy Agency.

Ackerman, T. and L. Soder, 2002: An overview of wind energy-status 2002. *Renewable and Sustainable Energy Reviews*, **6**, 67–128.

Akpinar, E. and S. Akpinar, 2005a: An assessment on seasonal analysis of wind energy characteristics and wind turbine characteristics. *Energy Conversion and Management*, **46**, 1848–1867.

— 2005b: A statistical analysis of wind speed data used in installation of wind energy conversion systems. *Ener. Conv. Management*, **46**, 515–532.

Alcamo, J., M. Florke, and M. Marker, 2007: Future long term changes in global water resources driven by socio-economic and climatic change. *Hydrological Sci. J.*, **52**, 247–275.

Allan, R. and T. Ansell, 2006: A new globally complete monthly historical gridded mean sea level pressure dataset (HadSLP2): 18502004. *J. Climate*, **19**, 5816–5842.

Allen, M. and S. Tett, 1999: Checking for model consistency in optimal fingerprint. *Clim. Dyn.*, **15**, 419–434.

Archer, C. and M. Jacobson, 2003: Spatial and temporal distributions of U.S. winds and wind power at 80 m derived from measurements. *J. Geophys. Res.*, **108(D9)**, doi:10.1029/2002JD002076.

— 2004: Correction to "spatial and temporal distributions of U.S. winds and wind power at 80 m derived from measurements". *J. Geophys. Res.*, **109**, D20116, doi:10.1029/2004jd005099.

— 2005: Evaluation of global wind power. *J. Geophys. Res.*, **110**, D12110, doi:10.1029/2004JD005462.

Arcimis, A., 1897: La torre de los vientos. *La Ilustración Española y Americana*, **38**.

Atkinson, A., 1969: A test for discriminating between models. *Biometrika*, **56**, 337–347.

Aubrun, S., R. Koppman, B. Leitl, M. Mollman-Coers, and A. Schaub, 2005: Physical modelling of a complex forest area in a wind tunnel-comparison with field data. *Agricultural and Forest Meteorology*, **129 (3-4)**, 121–135.

Bahn, O., L. Drouet, N. Edwards, A. Haurie, R. Knutti, S. Kypreos, and T. Stocker, 2006: The coupling of optimal economic growth and climated dynamics. *Clim. Change.*, **79**, 103–119.

Balouktsis, A., D. Chassapis, and T. Karapantsios, 2002: A nomogram method for estimating the energy produced by wind turbine generators. *Sol. Ener.*, **72 (3)**, 251–259.

Barbour, P. and S. Walker, 2008: Wind resource evaluation: Eola hills. Technical report, Energy Resources Research Laboratory. Department of Mechanical Engineering. Oregon State University, Corvallis, OR 97331.

Barnett, T. P., J. Adam, and D. Lettenmaier, 2005: Potential impacts of a warming climate on water availability in snow-dominated regions. *Nature*, **438**, 303–309.

Barnett, T. P. and R. W. Preisendorfer, 1987: Origin and levels of monthly and seasonal forecast skill for United States air temperature determined by canonical correlation analysis. *Mon. Wea. Rev.*, **115**, 1825–1850.

Barnston, A. and R. Livezey, 1987: Classification, seasonality and persistence of low-frequency atmospheric circulation patterns. *Mon. Wea. Rev.*, **115 (6)**, 1083–1116.

Barrow, E. and M. Semenov, 1995: Climate-change scenarios with high spatial and temporal resolution for agricultural applications. *Forestry*, **68 (4)**, 349–360.

Barry, R. and A. Perry, 1973: *Synoptic climatology: methods and applications*. Methuen and Co. Ltd. London.

Barthelmie, R., S. Frandsen, M. Nielsen, S. Pryor, P. Rethore, and H. Jorgensen, 2007: Modelling and measurements of power losses and turbulence intensity in wind turbine wakes at Middelgrunden offshore wind farm. *Wind Energy*, **10 (6)**, 517–528.

Baynes, C., 1974: The statistics of strong winds for engineering applications. *Res. Rep. BLWT-4-197. Faculty of Engineering Science, University of Western Ontario*.

Bechrakis, D., J. Deane, and E. McKeogh, 2004: Wind resource assessment of an area using short term data correlated to a long term data set. *Solar Energy.*, **76**, 725–732.

Beljaars, A., 1987: On the memory of wind standard-deviation for upstream roughness. *Boundary-Layer Meteorol.*, **38(1-2)**, 95–101.

Bender, M., T. Knutson, R. Tuleya, J. Sirutis, G. Vecchi, S. Garner, and I. Held, 2010: Modeled impact of anthropogenic warming on the frequency of intense atlantic hurricanes. *Science*, **327**, 454–458.

Benestad, R., 2002: Empirical downscaled temperature scenarios for northern Europe based on a multi-model ensemble. *Cli. Res.*, **21**, 105–125.

Bergey, K. H., 1979: Lanchester-betz limit. *J. Ener.*.

Bianco, L., E. Tomassetti, E. Coppola, A. Fracassi, M. Verdecchia, and G. Visconti, 2006: Thermally driven circulation in a region of complex topography: comparison of wind-profiling radar measurements and MM5 numerical predictions. *Ann. Geophys.*, **24**, 1537–1549.

Biel, A., 1952: El clima en zaragoza. serie A (memorias). *S.M.N. Madrid*, **36**.

Biswas, S., B. Sraedhar, and Y. Singh, 1990: A simplified statistical technique for wind turbine energy output estimation. *Wind Engineer.*, **19(3)**, 147–155.

Bivona, S., R. Burlo, and C. Leone, 2003: Hourly wind speed analysis in Sicily. *Renew. Ener.*, **28**, 1371–1382.

Black, T. L., 1994: The new NMC mesoscale Eta Model: Description and forecast examples. **9**, 265–278.

Bogardi, I. and I. Matyasovszky, 1996: Estimating daily wind speed under climate change. *Solar Energy*, **57 (3)**, 239–248.

Bray, D. and H. von Storch, 2009: Prediction or projection?: The nomenclature of climate science. *Science Communication*, **30 (4)**, 534–543.

Brissette, F., R. Leconte, M. Minville, and R. Roy, 2006: Can we adequately quantify the increase/decrease of flooding due to climate change? *IEEE EIC Climate Change Conference*, **Vols. 1 and 2**, 711–716.

Brunt, D., 1934: *Physical and Dynamical Meteorology*. Cambridge Univ. Press edition.

Burlando, M., 2009: The synoptic-scale surface wind climate regimes of the Mediterranean sea according to the cluster analysis of ERA-40 wind fields. *Theor. Appl. Climatol.*, **96**, 69–83.

Busuioc, A., R. Tomozeieu, and C. Cacciamani, 2008: Statistical downscaling model based on canonical correlation analysis for winter extreme precipitation events in the Emilia-Romagna region. *Int. J. Climatol.*, **28 (4)**, 449–464.

Buzzi, A., M. $D'Isidoro$, and S. Davolio, 2003: A case study of an orographic cyclone south of the Alps during the mAP SOP. *Q. J. Roy. Meteor. Soc.*, **129**, 1795–1818.

Caires, S. and A. Sterl, 2004: 100-year return value estimates for ocean wind speed and significant wave height from the ERA-40 data. *J. Climate*, **18**, 1032–1048.

— 2005: A new nonparametric method to correct model data: application to significant wave height from the ERA-40 Re-analysis. *J. Atmos. Oceanic Technol.*, **22 (4)**, 443–459.

Carta, J. and P. Ramírez, 2007: Use of finite mixture distribution models in the analysis of wind energy in the Canarian Archipielago. *Ener. Conv. Management*, **48**, 281–291.

Carvalho, A., A. Carvalho, A. Miranda, C. Borrego, and A. Rocha, 2000: Climate change and fire weather risk. *Int. Sci. Meet. Detect. Model. recent Clim. Change*, 555–56.

Celik, A., 2003a: Assessing the suitability of wind speed probability distribution functions based on wind power density. *Renewable Energy*, **28**, 1563–1574.

— 2003b: Energy output estimation for small-scale wind power generators using weibull-representative wind data. *J. Wind Indust. Aerodyn.*, **91**, 693–707.

— 2003c: Weibull representative compressed wind speed data for energy and performance calculations of wind energy systems. *Ren. Ener.*, **44**, 3057–3072.

— 2004: On the distributional parameters used in assessment of the suitability of wind speed probability density functions. *Ener. Conv. Management*, **45**, 1735–1747.

Chang, T., Y. Wu, H. Hsu, C. Chu, and C. Liao, 2003: Assessment of wind characteristics and wind turbine characteristics in Taiwan. *Renew. Ener.*, **28**, 851–871.

Chiew, F., D. Kirono, D. Kent, A. Frost, S. Charles, B. Timbal, K. Nguyen, and G. Fu, 2010: Comparison of runoff modelled using rainfall from different downscaling methods for historical and future climates. *J. Hydrol.*, **38 (1-2)**, 10–23.

Coelho, C., S. Pezzulli, M. Balmaseda, F. Doblas-Reyes, and D. Stephenson, 2004: Forecast calibration and combination: A simple bayesian approach for ENSO. *J. Clim.*, **17**, 1504–1516.

Conil, S. and A. Hall, 2006: Local regimes of atmospheric variability: a case study of Southern California. *J. Clim.*, **19-17**, 4308–4325.

Conradsen, K. and L. Nielsen, 1984: Review of weibull statistics for estimation of wind speed. *J. Clim. App. Meteorol.*, **23**, 1173–1183.

Coriolis, G., 1835: Sur les èquations du mouvement relatif des systèmes de corps. *J. De l'Ecole royale polytechnique*, **15**, 144154.

Dalton, J., 1837: Notice relative to the Theory of Winds. *Phil. Mag.*, **11**, 390.

Davenport, A., 1963: The relationship of wind structure to wind loading. *Prof. Conf. Wind Effects on Structures. Nat. Phys. Lab.: London, England*, 19–82.

Davis, R., B. Hayden, D. Gay, W. Phillips, and G. Jones, 1997: The North Atlantic subtropical anticyclone. *J. Climate*, **10**, 1788–1806.

Davy, R., M. Woods, C. Russell, and P. Coppin, 2010: Statistical downscaling of wind variability from meteorological fields. *Boundary-Layer Meteorol*, **135**, 161–175.

de Pedraza, L. G., 1985: La predicción del Tiempo en el Valle del Ebro. Technical Report Serie A. Technical Report 38, INM.

de Rooy, W. and K. Kok, 2004: A combined physical-statistical approach for the downscaling of model wind speed. *Weather Forecast.*, **19**, 485–495.

Deaves, D. and I. Lines, 1997: On the fitting of low mean wind speed data to the weibull distribution. *J. Wind Engineer. Ind. Aerodyn.*, **66**, 169–178.

Denman, K., G. Brasseur, A. Chidthaisong, P. Ciais, P. Cox, R. Dickinson, D. Hauglustaine, C. Heinze, E. Holland, D. Jacob, U. Lohmann, S. Ramachandran, P. da Silva Dias, S. Wofsy, and X. Zhang, 2007: *Couplings Between Changes in the Climate System. In: Climate Change 2007: The physical science basis. Contribution of Working Group I to the Fourth Assessment Report of the Intergovernmental Panel on Climate Change [Solomon S. et al. (eds.)]*. Cambridge University Press., Cambridge, United Kingdom and New York, NY, USA.

Dermibas, A., 2009: Global Renewable Energy Projections. *Energy Sources Part B-Economics Planning and Policy*, **4**, 212–224.

Dibike, Y., P. Gachon, A. St-Hilaire, T. Ouarda, and V. T.-V. Nguyen, 2008: Uncertainty analysis of statistically temperature and precipitation regimes in northern Canada. *Theor. Appl. Climatol.*, **91**, 149–170.

Dorvlo, A., 2002: Estimating wind speed distribution. *Ener. Conv. Management*, **43(17)**, 2311–2318.

Dove, H., 1837: Über die verschiedenen Theorien des Windes, als Erwiederung auf vorstehende Bemerkung. *Ann. d. Phys.*, **42**, 316–324.

DTI, H. G., 2006: The Energy Challenge Energy Review report 2006. Technical report, Department of Trade and Industry. United Kingdom.

Epstein, E., 1962: A Bayesian approach to decision making in applied meteorology. *J. App. Meteorol.*, **1**, 169–176.

Fairless, D., 2007: Renewable energy: Energy-go-round. How did a little Spanish province become one of the world's wind-energy giants? *Nature*, **447**, 1031–1142.

Faucher, M., W. R. Burrows, and L. Pandolfo, 1999: Empirical-statistical reconstruction of surface marine winds along the western coast of Canada. *Clim. Res.*, **11**, 173190.

Faulin, J., F. Lera, J.M.Pintor, and J. García, 2006: The outlook for renewable energy in navarre: an economic profile. *Energy Policy*, **34**, 2201–2216.

Fawzan, M., 2000: Methods for estimating the parameters of the Weibull distribution. *INTER STAT*, **http://interstat.statjournals.net/**.

Fernández, J. and J. Saenz, 2003: Improved field reconstruction with the analog method: Searching the cca space. *Cli. Res.*, **24**, 199–213.

Ferrel, W., 1856: An essay on winds and the currents of the Ocean. *Nashville Journ. Medicine Surgery*, **11**, 287–230.

Fisher, E., I. Seneviratne, D. Lüthi, and C. Schär, 2007: Contribution of land-atmosphere coupling to recent European summer heat waves. *GEophys. REs. Lett.*, **34**, L06707.

Flowers, L. and P. Dougherty, 2004: Wind powering america: goals, approach perspectives and prospects. *SAMPE Journals*, **40**, 44–46.

Font, I., 2000: *Climatología de España y Portugal*. Ediciones Universidad de Salamanca, second edition, 422 pp edition.

Forest, C., M. Allen, P. Stone, and A. Sokolov, 2000: Constraining uncertainties in climate models using climate change detection techniques. *Geophys. Res. Lett.*, **27 (4)**, 569–572.

Forest, C., P. Stone, A. Sokolov, M. Allen, and M. Webster, 2002: Quantifying uncertainties in climate system properties with the use of recent observations. *Sci.*, **295**, 113–117.

Frandsen, S., I. Antoniou, J. Hansen, L. Kristensen, H. Madsen, B. Chaviaropoulos, D. Douvikas, J. Dahlberg, A. Derrick, P. Dunbabin, R. Hunter, R. Ruffle, D. Kanellopoulos, and G. Kapsalis, 2000: Redefinition power curve for more accurate performance assessment of wind farms. *Wind Ener.*, **3(2)**, 81–111.

Fuhrer, J., M. Beniston, A. Fischlin, C. Frei, S. Goyette, K. Jasper, and C. Pfister, 2006: Climate risks and their impact on agriculture and forest in Switzerland. *Cli. Change.*, **79 (1-2)**, 79–102.

Furrer, R., S. Sain, D. Nychka, and G. Meehl, 2007: Multivariate bayesian analysis of atmosphere-ocean general circulation models. *Environ. Scol. Stat.*, **14**, 249–266.

Gandin, L., 1988: Complex quality control of meteorological observations. *Mon. Wea. Rev.*, **116**, 1137–1156.

García, A., J. Torres, E. Prieto, and A. D. Francisco, 1998: Fitting wind speed distributions: a case study. *Sol. Ener.*, **62 (2)**, 139–144.

García, L. and A. Reija, 1994: *Tiempo y clima en España. Meteorología de las autonomías*. Dossat 2000, 410 pp.

García-Bustamante, E., J. F. González-Rouco, P. A. Jiménez, J. Navarro, and J. P. Montávez, 2008: The influence of the Weibull assumption in monthly wind. *Wind Ener.*, **11**, 483–502.

— 2009: A comparison of methodologies for monthly wind energy estimations. *Wind Ener.*, **12**, 640–659.

García-Bustamante, E., J. F. González-Rouco, J. Navarro, E. Xoplaki, P. A. Jiménez, and J. P. Montávez, 2010a: North Atlantic atmospheric circulation and surface wind in the Northeast of the Iberian Peninsula: uncertainty and long term downscaled variability. *Cli. Dyn.*, **Under review**.

— 2010b: Relationship between wind power production and North Atlantic atmospheric circulation: methods, associated uncertainty and long term downscaled variability. *To be submitted*.

García-Bustamante, E., J. F. González-Rouco, J. Saenz, E. Xoplaki, J. Navarro, P. A. Jiménez, and J. P. Montávez, 2010c: Bayesian uncertainty in downscaled wind field estimations. in preparation. *To be submitted*.

García-Herrera, R., J. Díaz, R. Trigo, and E. Hernández, 2005: Extreme summer temperatures in Iberia: health impacts and associated synoptic conditions. *Ann. Geophys.*, **23**, 239–251.

Gates, W., 1985: The use of general circulation models in the analysis of ecosystem impacts of climate change. *Clim. Change*, **7**, 267–284.

Gelman, A., J. Carlin, H. Stern, and D. Rubin, 2004: *Bayesian Data Analysis*. Boca Raton, Florida, USA, chapman & hall/crc, 2nd. ed. edition.

Giorgi, F. and G. Bates, 1989: The climatological skill of a regional model over complex terrain. *Mon. Wea. Rev.*, **117**, 2325–2347.

Giorgi, F. and L. Mearns, 1991: Approaches to the simulation of regional climate change: A review. *Rev. Geophys.*, **29**, 191–216.

— 2003: Probability of regional climate change based on the Realiability Ensemble Averaging (REA) method. *Geophys. Res. Lett.*, **30 (12)**, doi:10.1029/2003GL017130.

Glahn, H., 1968: Canonical correlation and its relationship to discriminant analysis and multiple regression. *J. Atmos. Sci.*, **25**, 23–31.

González-Rouco, J., H. Heyen, E. Zorita, and F. Valero, 2000: Agreement between observed rainfall trends and climate change simulations in the southwest of Europe. *J. Climate*, **13**, 3057–3065.

Gove, J., 2003: Moment and maximum likelihood estimators for Weibull distributions under length-and-area-biased sampling. *Env. Ecol. Stat.*, **10**, 455–467.

Graybeal, D., 2006: Relationship among daily mean and maximum wind speeds, with application to data qualitu assurance. *Int. J. Climatol*, **26**, 29–43.

Greene, A., L. Goddard, and U. Lall, 2006: Probabilistic multimodel regional temperature change projections. *J. Clim.*, **19**, 43264343.

Gregory, P., 2005: *Bayesian logical data analysis for the physical sciences*. Cambridge, United Kingdom and New York, NY, USA.

Grimenes, A. and V. Thue-Hansen, 2004: Annual variation of surface roughness obtained from wind profiles measurements. *Theor. App. Climatol.*, **79(1-2)**, 93–102.

Hadley, G., 1735: On the cause of the general trade winds. *Phil. Trans. Roy. Soc.*, **34**, 58–62.

Hanssen-Bauer, I., C. Achberger, R. Benestad, D. Chen, and E. Førland, 2005: Statistical downscaling of climate scenarios over Scandinavia. *Clim. Res.*, **29**, 255–268.

Hanssen-Bauer, I., E. Førland, J. Haugen, and O. Tveito, 2003: Temperature and precipitation scenarios for Norway: comparison of results from dynamical and empirical downscaling. *Clim. Res.*, **25 (1)**, 15–27.

Hau, E., 2006: *Wind turbines*. Springer, isbn:3540242406; 1-738 edition.

Haylock, M., G. Cawley, C. Harpham, R. L. Wilby, and C. Goodess, 2006: Downscaling heavy precipitation over UK: a comparison of methods and their future scenarios. *Int. J. Climatol.*, **26 (10)**, 1397–1415.

Hegerl, G., T. Crowley, W. Hyde, and D. Frame, 2006: Climate sensitivity constrained by temperature reconstructions over the past seven centuries. *Nature*, **440**, 1029–1032.

Hegerl, G., K. Hasselmann, U. Cubasch, J. Mitchell, E. Roeckner, R. Voss, and J. Waskewitz, 1997: Multi-fingerprint detection and attribution of greenhouse gas and aerosol forced climate change. *Cli. Dyn.*, **13**, 613–634.

Hennesey, J., 1977: Some aspects of wind power statistics. *J. App. Meteorol.*, **16(2)**, 119–128.

Herrmann, M. and S. Somot, 2008: Relevance of ERA40 dynamical downscaling for modeling deep convection in the Mediterranean Sea. *Geophys. Res. Lett.*, **35 (4)**, doi: 10.1029/2007GL032442.

Hewitson, B. and R. Crane, 1996: Climate downscaling: techniques and application. *Cli. Res.*, **7**, 85–95.

— 2006: Climate downscaling: techniques and application. *Cli. Res.*, **26**, 1315–1337.

Hinckley, D. V., 1969: Inference about the intersection in two-phase regression. *Biometrika*, **56**, 495–504.

— 1971: Inference in two-phase regression. *Journal of the American Statistical Association*, **66**, 736–743.

Hohmeyer, O. and T. Trittin, eds., 2008: *IPCC Scoping Meeting on Renewable Energy Sources*, Intergovernmental Panel on Climate Change.

Holmes, J., 2002: Effective static load distributions in wind engineering. *J. Wind Engineering Ind. Aerod.*, **90(2)**, 91–109.

Holton, J., 2004: *An Introduction to Dynamic Meteorology*. Elsevier Academic Press., 4th ed. edition.

Hong, S. and E. Kalnay, 2000: Role of sea surface temperature and soil-moisture feedback in the Oklahoma-Texas drought. *Nature*, **408 (6814)**, 842–844.

Hotelling, H., 1935: The most predictable criterion. *J. Educ. Psych*, **26**, 139–142.

— 1936: Relations between two sets of variables. *Biometrika*, **28**, 321–377.

— 1940: The selection of variates for use in prediction with some comments on the general problem of nuisance parameters. *The Annals of Mathematical Statistics*, **11 (3)**, 271–283.

Houghton, J., Y. Ding, D. Griggs, M. Noguer, P. van der Linden, X. Dai, K. Maskell, and C. J. (Eds.), 2001: *Climate Change, 2001: The scientific basis. Contribution of Working Group I to Third Assessment Report of the Intergovernmental Panel on Climate Change*. Cambridge University Press., Cambridge, United Kingdom and New York, NY, USA.

Hundecha, Y. and A. Bardossy, 2008: Statistical downscaling of extremes of daily precipitation and temperature and construction of their future scenarios. *Int. J. Climatol.*, **28**, 589–610.

Huth, R., 2000: Statistical downscaling in Central Europe: evaluation of methods and potential predictors. *Clim. Res.*, **13**, 91–101.

— 2002: Statistical downscaling of daily temperature in Central Europe. *J. Climate*, **1**, 1731–1742.

— 2004: Sensitivity of local daily temperature change estimates to the selection of downscaling models and predictors. *J. Climate*, **17**, 640–652.

Huth, R., S. Kliegrova, and L. Metelka, 2008: Non-linearity in statistical downscaling: does it bring an improvement for daily temperature in Europe? *Int. J. Climatol.*, **28**, 465–477.

Huth, R. and J. Kyselý, 2000: Constructing site-specific climate change scenarios on a monthly scale using statistical downscaling. *Theor. Appl. Climatol.*, **66**, 13–27.

Hwang-Dae, K., T. Robinson, S. Wulff, and P. Parker, 2007: Comparison of parametric, nonparametric and semiparametric modeling of wind tunnel data. *Quality Engineering*, **19 (3)**, 179–190.

Jackson, C., M. Sen, and P. Stoffa, 2004: An efficient stochastic bayesian approach to optimal parameter and uncertainty estimation for climate model predictions. *J. Climate*, **17**, 2828–2841.

Jager-Waldau, A. and H. Ossenbrink, 2004: Progress of electricity from biomass, wind and photovoltaics in the European Union. *Renewable and Sustainable Energy Reviews*, **8**, 157–182.

Jakobs, H., H. Feldman, and H. Hass, 1995: The use of nested models for air-pollution studies - an application of the EURAD model to a SANA episode. *J. Appl. Meteor.*, **34 (6)**, 1301–1319.

Jamil, M., S. Parsa, and M. Majidi, 1995: Wind power statistics and an evaluation of wind energy density. *Ren. Ener.*, **6 (5-6)**, 623–628.

Jaramillo, O. and M. Borja, 2004: Wind speed analysis in La Ventosa, Mexico: a bimodal probability distribution case. *Renew. Ener.*, **29**, 1613–1630.

Jiménez, P. A., J. F. González-Rouco, E. García, J. P. Montávez, E. García-Bustamante, and J. Navarro, 2010a: Quality-control and bias correction of high resolution surface wind observations from automated weather stations. *J. Atmos. Oceanic Tech.-A*, **27**, 1101–1122.

Jiménez, P. A., J. F. González-Rouco, E. García-Bustamante, J. Navarro, J. P. Montávez, J. V.-G. de Arellano, J. Dudhia, and A. Roldán, 2010b: Surface wind regionalization over complex terrain: evaluation and analysis of a high resolution wrf numerical simulation. *J. Appl Meteor. Climatol.*, **49**, 268–287.

Jiménez, P. A., J. F. González-Rouco, J. P. Montávez, E. García-Bustamante, and J. Navarro, 2008a: Climatology of wind patterns in the Northeast of the Iberian Peninsula. *Int. J. Climatol.*, **29**, 501–525.

Jiménez, P. A., J. F. González-Rouco, J. P. Montávez, J. Navarro, E. García-Bustamante, and F. Valero, 2008b: Surface wind regionalization in a complex terrain region. *J. Appl. Meteor. Clim.*, **47**, 308–325, doi: 10.1175/2007JAMC1483.1.

Johannessen, K. and T. M. S. Haver, 2002: Joint distribution for wind and waves in the northern sea. *Int. J. Offshore Polar Eng.*, **31(2)**, 450–460.

Justus, C., W. Hargraves, A. Mikhail, and D. Graber, 1977: Methods for estimating wind speed frequency distributions. *J. App. Meteorol.*, **17**, 350–353.

Kaas, E., T. Li, and T. Schmith, 1996: Statistical hindcast of wind climatology in the North Atlantic and northwestern European region. *Clim. Res.*, **7**, 97–110.

Kaiser, H., 1960: The application of electronic computers to factor analysis. *Educational and psychological mesurement*, **20**, 141–151.

Kant, I., 1756: Neue Anmerkungen zur Erläuterung der Theorie der Winde. *Königsberg*.

Kariniotakis, G., P. Pinson, N. Siebert, G. Giebel, and R. Barthelmie, 2004: The state of the art in short-term prediction of wind power-from an offshore perspective. *Proc. 2004 SeaTech Week*.

Kenisarin, M., V. Karsli, and M. Caglar, 2006: Wind power engineering in the world and perspectives of its development in turkey. *Renewable and Sustainable Energy Reviews*, **10**, 341–369.

Klink, K., 2002: Trends and interannual variability of wind speed distributions in Minesota. *Int. J. Climatol.*, **15**, 3311–3317.

— 2007: Atmospheric circulation effects on wind speed variability at turbine height. *J. App. Meteorol. Clim.*, **46**, 445–456.

Klink, K. and C. Willmott, 1989: Principal components analysis of the surface wind field in the United States: a comparison of analyses based upon wind velocity, direction and speed. *Int. J. Climatol.*, **9**, 293–308.

Koukidis, E. N. and A. A. Berg, 2009: Sensitivity of the statistical downscaling model (SDSM) to reanalysis products. *Atmos-Ocean*, **doi: 10.3137/AO924.2009**.

Lackner, M., A. Rogers, and J. Manwell, 2008: Uncertainty analysis in MCP-based wind resource assessment and energy production estimation. *J. Sol. Ener. Engineer.*, **031006**, 1–10.

Lange, M., 2005: On the uncertainty of wind power predictions: Analysis of the forecast accuracy and statistical distribution of errors. *J. Sol. Ener. Engineer.*, **27 (2)**, 177–184.

Latif, M., 1998: Dynamics of interdecadal variability in coupled ocean-atmosphere models. *J. Clim.*, **11**, 602–624.

Lenderink, G., A. van Ulden, B. van den Hurk, and F. Keller, 2007: A study on combining global and regional climate model results for generating climate scenarios of temperature and precipitation for the Netherlands. *Clim. Dyn.*, **32**, 157–176.

Levine, M., 1977: *Canonical analysis and factor comparison*. Sage University Publications.

Li, M. and X. Li, 2005a: Investigation of wind characteristics and assessment of wind energy potential for Waterloo region, Canada. *Ener. Conv. Management*, **46**, 3014–3033.

— 2005b: Mep-type distribution function: a better alternative to Weibull function for wind speed distribution. *Renew. Ener*, **30**, 1221–1240.

Lorentz, E., 1955: Available potential energy and the maintenance of the general circulation. *Tellus*, **7**, 157–167.

— 1967: The nature and theory of the general circulation of atmosphere. *World Meteorological Organization*, **218**.

Lun, I. and J. Lam, 2000: A study of Weibull parameters using long-term wind observations. *Renew. Ener.*, **20**, 145–153.

Luterbacher, J., E. Xoplaki, D. Dietrich, R. Rickli, J. Jacobeit, C. Beck, D. Gyalistras, C. Schmutz, and H. Wanner, 2002: Sea level pressure fields over the eastern North Atlantic and Europe back to 1500. *Clim. Dyn.*, **18**, 545–561.

Mathew, S., K. Pandey, and A. Kumar, 2002: Analysis of wind regimes for energy estimation. *Renew. Ener.*, **25**, 381–399.

Matulla, C., H. Scheifinger, A. Menzel, and E. Koch, 2003: Exploring two methods for statistical downscaling of Central Europe phenological time series. *Int. J. Biometeorol.*, **48**, 56–64.

Maurer, E. P. and H. G. Hidalgo, 2007: Utility of daily vs. monthly large-scale climate data: an intercomparison of two statistical downscaling methods. *Hydrol. Earth Syst. Sci. Discuss.*, **4**, 3413–3440.

McKendry, I., K. Stahl, and R. Moore, 2006: Synoptic sea-level pressure patterns generated by a general circulation model: Comparison with types derived from NCEP/NCAR re-analysis and implications for downscaling. *Int. J. Climatol.*, **26**, 1727–1736.

McVicar, T., T. V. Niel, L. Li, M. Roderick, D. Rayner, L.Ricciardulli, and R. Donahue, 2008: Wind speed climatology and trends for Australia, 1975-2006: capturing the stilling phenomenon and comparison with near-suface reanalysis output. *Geophys. Res. Lett.*, **35**, L20403, doi:10.1029/2008GL035627.

M*ü*ller, P. and H. von Storch, 2004: *Computer modeling in atmospheric and oceanic sciences - on the building of knowledge*. Springer verlag: Heidelberg, p. 304, isn 1437028x edition.

Mengelkamp, H., 1999: Wind climate simulation over complex terrain and wind turbine energy output estimation. *Theor. Appl. Climatol.*, **63**, 129–139.

Michaelsen, J., 1987: Cross-validation in statistical climate forecast models. *J. Clim. App. Meteor.*, **26**, 1589–1600.

Mitchell, T. and M. Hulme, 1999: Predicting regional climate change: living with uncertainty. *Prog. Phys. Geograph.*, **23 (1)**, 57–78.

Murphy, J., 1999: An evaluation of statistical and dynamical techniques for downscaling local climate. *J. Clim.*, **12**, 2256–2284.

Najac, J., J. Boé, and L. Terray, 2009: A multi-model ensemble approach for assessment of climate change impact on surface winds in France. *Cli. Dyn.*, **32**, 615–634.

Nakicenovic, N., J. Alcamo, G. Davis, B. de Vries, J. Fenhann, S. Gaffin, K. Gregory, and A. G. ant et al., eds., 2000: *Special Report on Emissions Scenarios, Working Group III, Intergovernmental Panel on Climate Change (IPCC)*, Cambridge University Press.

Nicholls, M., M. Oquist, A. Rounsevell, and J. Szolgay, 2001: *Climate Change 2001: Impacts, Adaptation and Vulnerability. Contribution of Working Group II to the Third Assessment Report of the Intergovernmental Panel on Climate Change.*. University Press, Cambridge, UK, 641-692 pp.

Noguer, M., 1994: Using statistical techniques to deduce local climate distributions. an appplication for model validation. *Meteorol. Appl.*, **1**, 277–287.

Nolte, C., A. Gilliland, C. Hogrefe, and L. Mickley, 2008: Linking global to regional models to asses future climate impacts on surface ozono levels in the United States. *J. Geophys. Res.-Atmos.*, **113**, D144307.

Noorgard, P. and H. Holttinen, 2004: A multi-turbine power curve approach. *Nordic Wind Power Conference. Chalmers University of Technology*.

North, G., T. Bell, R. Calahan, and F. Moeng, 1982a: Sampling errors in the estimation of empirical orthogonal functions. *Mon. Wea. Rev.*, **110**, 699–706.

North, G., F. Moeng, T. Bell, and R. Calahan, 1982b: The latitude dependence of the variance of zonally averaged quantities. *Mon. Wea. Rev.*, **110**, 319–326.

O'Hagan, A. and E. Oakley, 2004: Probability is perfect, but we can't elicit it perfectly. *Reliab. Engineer. Sys. Safet.*, **85**, 239–248.

Orlowsky, B., F. Gerstengarbe, and P. Werner, 2008: A resampling scheme for regional climate simulations and its performance compared to a dynamical RCM. *Theor. Appl. Climatol.*, **92**, 209–223.

Palutikof, J., P. Davies, T. Davies, and J. Halliday, 1987: Impacts of spatial and temporal windspeed variability on wind energy output. *J. Climate Appl. Meteorol.*, **26**, 1124–1133.

Parish, T., D. Rahn, and D. Leon, 2008: Aircraft observations of a coastally trapped wind reversal off the California coast. *Mon, Wea. Rev.*, **136**, 644–662.

Parry, M., O. Canziani, J. Palutikof, P. van der Linden, and C. Hanson, 2007: *Climate Change 2007: Impacts, Adapatation and Vulnerability. Contribution of Working Group II to the Fourth Assessment Report of the Intergovernmental Panel on Climate Change.*. University Press, Cambridge, UK.

Pavia, E. and J. Orien, 1986: Weibull statistics of wind speed over the ocean. *J. Clim. App. Meteorol.*, **25**, 1324–1332.

Pearson, K., 1902: On the systematic fitting of curves to observations and measurements. *Biometrika*, **1(3)**, 265.

Pérez, I., M. S. M.A., and García, 2007: Weibull wind speed distribution: Numerical considerations and use with sodar data. *J. Geophys. Res.*, **112**, doi: 10.1029/2006JD008278.

Perry, A., P. Low, J. Ellis, and J. Reynolds, 2005: Climate change and distribution shifts in marine fishes. *Science*, **308**, 1912–1915.

Pinson, P., H. Nielsen, H. Madsen, and T. Nielsen, 2008: Local linear regression with adaptive orthogonal fitting for the wind power application. *Statis. Comput.*, **18 (1)**, 59–71.

Pinson, P., H. Nielsen, J. Moller, H. Madsen, and G. Kariniotakis, 2007: Nonparametric probabilistic forecasts of wind power: required properties and evaluation. *Wind Ener.*, **10 (6)**, 497–516.

Pollack, H., 2006: *Uncertain Science... Uncertain world*. Cambridge University Press, w YorkN.

Powell, M., P. Dodge, and M. Black, 1991: The landfall of hurricane hugo in the Carolinas-surface wind distribution. *Wea. Forecast.*, **6(3)**, 379–399.

Pozo-Vázquez, D., J. Tovar-Pescador, and S. Gamiz-Fortis, 2004: NAO and solar radiation variability in the European North Atlantic region. *Geophys. Res. Lett.*, **31 (5)**, L05201.

Preisendorfer, R., 1988: *Principal component analysis in meteorology and oceanography*. Elsevier edition.

Pryor, S. and R. Barthelmie, 2003: Long-term trends in near-surface flow over the Baltic. *Int. J. Climatol.*, **23**, 271–289.

Pryor, S., R. Barthelmie, and E. Kjellström, 2005a: Potencial climate change impact on wind energy resources in northern Europe: analyses using a regional climate model. *Clim. Dyn.*, **25**, 815–835.

Pryor, S., R. Barthelmie, and G. Tackle, 2009: Wind speed trends over the contiguos USA. *IOP Conference Series: Earth and Environmental Science*, **6**, 10.1088/1755–1307/6/9/092023.

Pryor, S. and J. Schoof, 2005: Empirical downscaling of wind speed probability distributions. *J. Geophys. Res.*, **110**, D19109.

Pryor, S., J. Schoof, and R. Barthelmie, 2006: Winds of change?: Projections of near-surface winds under climate change scenarios. *Geophys. Res. Lett.*, **33**, L11702, doi:10.1029/2006GL026000.

Pryor, S., J. Schoof, and R. J. Barthelmie, 2005b: Climate change impacts on wind speeds and wind energy density in northern Europe: empirical downscaling of multiple AOGCMs. *Clim. Res.*, **29**, 183–198.

Raible, C., M. Yoshimori, T. Stocker, and C. Casty, 2007: Extreme midlatitude cyclones and their implications for precipitation and wind extremes in simulations of the Maunder Minimum versus present day conditions. *Clim. Dyn.*, **28**, 409–423.

Ramírez, P. and J. Carta, 2005: Influence of the data sampling interval in the estimation of the parameters of the Weibull wind speed probability density distribution: a case study. *Ener. Conv. Management*, **46**, 2419–2438.

— 2006: The use of wind probability distributions derived from the maximum entropy principle in the analysis of wind energy. a case study. *Ener. Conv. Management*, **47**, 2564–2577.

Räisänen, J., U. Hansson, A. Ullerstig, R. Döscher, L. Graham, C. Jones, H. Meier, P. Samuelsson, and U. Willén, 2001: European climate in the late 21st century: regional simulations with two driving global models and two forcing scenarios. *Clim. Dyn*, **22**, 13–31.

Reid, P., M. Edwards, H. Hunt, and A. Warner, 1998: Phytoplankton change in the North Atlantic. *Nature*, **391**, 546.

Richardson, L., 1946: The geostrophic wind. *Unpublished notes*.

Robinson, P. and P. Finkelstein, 1991: The development of impact-oriented climate scenarios. *Bull. Amer. Meteorol. Soc.*, **72**, 481–490.

Rosenzweig, C., G. Casassa, D. Karoly, A. Imeson, C. Liu, A. Menzel, S. Rawlins, T. Root, B. Seguin, and P. Tryjanowski, 2007: *Assessment of observed changes and responses in natural and mangaed systems. Climate Change 2007: Impacts, Adaptation and Vulnerability. ¡contribution of Working Group II to the Fourth Assessment Report of the Intergovernmental Panel on Climate Change. M.L*

Parry, O.F. Canziani, J.P. Palutikof, van der Linden and C.E. Hanson, Eds.. Cambridge University Press., Cambridge, UK.

Sahsamanoglou, H., 1990: A contribution to the study of action centres in the North Atlantic. *Int. J. Climatology*, **10**, 247–261.

Saidur, R., M. Islam, N. Rahim, and K. Solangi, 2010: A review on global wind energy policy. *Ren. Sustain. Ener. Rew.*, **14**, 1744–1762.

Sailor, D., T. Hu, X. Li, and J. Rosen, 2000: A neural network approach to local downscaling of GCM output for assessing wind power implications of climate change. *Renewable Energy*, **19**, 359–378.

Sailor, D., M. Smith, and M. Heart, 2008: Climate change implications for wind power resources in the northwest United States. *Renewable Energy*, **33**, 23932406.

Sánchez, M., G. Frutos, and P. Cuesta, 1996: *Estadística y matemáticas aplicadas*. Ed. Síntesis S. A. Madrid, Spain.

Schmidli, J., C. Frei, and P. Vidale, 2006: Downscaling from GCM precipitation: a benchmark for dynamical and statistical downscaling. *Int. J. Climatol.*, **26**, 679–689.

Schmith, T., 2008: Stationarity of regression relationships: application to empirical downscaling. *J. Climate*, **21**, 4529–4537.

Schwierz, C., C. Appenzeller, H. Davies, M. Liniger, W. Muller, T. Stocker, and M. Yoshimori, 2006: Challenges posed by and approaches to the study of seasonal-to-decadal climate variability. *Clim. Change*, **79**, 31–63.

Seguro, J. and T. Lambert, 2000: Modern estimation of the parameters of the Weibull wind speed distribution for wind energy analysis. *J. Wind Engine. Ind. Aerodyn.*, **85**, 75–84.

Seierstad, I. A., D. Stephenson, and N. Kvamstö, 2007: How useful are teleconnection patterns for explaining variability in extratropical storminess? *Tellus*, **59A**, 170–181.

Sesto, E. and C. Casale, 2010: Exploitation of wind as an energy resource to meet the world's electricity demand. *J. Wind Engineer. Ind. Aerodyn.*, **74-76**, 375–387.

Sherlock, R., 1951: Analyzing wind for frequency and duration. *Meteor. Monogr. Amer. Meteoro. Soc.*, **4**, 72–79.

Simpson, J., 1994: *Sea breezes and local winds*. Cambridge University Press, Cambridge, United Kingdom and New York, NY, USA.

Skamarock, W. C., J. B. Klemp, J. Dudhia, D. O. Gill, D. M. Barker, W. Wang, and J. G. Powers, 2005: A description of the advanced research WRF Version 2. Technical Report TN-468+STR, NCAR.

Smith, R., 1979: The influence of mountains in the atmosphere. *Adv. Geophys.*, **21**, 1401–1405.

Solow, A. R., 1987: Testing for climate change: an application of the two-phase regression model. *J. Climate Appl. Meteorol.*, **26**, 1401–1405.

Stocker, T., D. Wright, and L. Mysak, 1992: A zonally averaged, coupled atmosphere-ocean model for paleoclimate studies. *J. Clim.*, **5**, 773–797.

Stull, R., 1990: *An Introduction to Boundary Layer Meteorology*. Springer.

Takle, E. and J. Brown, 1978: Note on the use of Weibull statistics to characterize wind-speed data. *J. App. Meteorol.*, **17**, 556–559.

Taylor, K., 2001: Summarizing multiple aspects of model performance in single diagram. *J. Geophys. Res.*, **106**, 7183–7192.

Tebaldi, C., L. Mearns, D. Nychka, and R. Smith, 2004a: Regional probabilities of precipitation change: a bayesian analysis of multimodel simulations. *Geophys. Res. Lett.*, **31**, L24213, doi: 10.1029/2004GL021276.

Tebaldi, C., R. Smith, D. Nychka, and L. Mearns, 2004b: Quantifying uncertainty in projections of regional climate change: a bayesian approach. *J. Climate*, **18 (10)**, 1524–1540.

technical note, V.-A. W. T., 1996: General specifications 600 kw variable slip wind turbines. Technical Report 941615.R3 25pp, Department of Trade and Industry. United Kingdom.

Tisseul, C., M. Vrac, S. Lek, A. Wade, and W. Andrew, 2010: Statistical downscaling of river flows. *J. Hydrol.*, **385 (1-4)**, 279–291.

Toreti, A., E. Xoplaki, D. Maraun, F. Kuglitsch, H. Wanner, and J. Luterbacher, 2010: Characterisation of extreme winter precipitation in Mediterranean coastal sites and associated anomalous atmospheric circulation patterns. *Nat. Hazards Earth Syst. Sci.*, **10**, 1037–1050.

Torrence, C. and G. Compo, 1998: A practical guide to wavelet analysis. *Bull. Amer. Meteorol. Soc.*, **79**, 61–78.

Torres, J., A. García, E. Prieto, and A. D. Francisco, 1992: Characterization of wind speed data according to wind direction. *Solar Energy*, **66 (1)**, 57–64.

Trenberth, K., 1984: Some effects of finite sample size and persistence on meteorological statistics. part I: autocorrelations. *Mon. Wea. Rev.*, **112**, 2359–2368.

— 2008: Observational needs for climate prediction and adaptation. *WMO Bulletin*, **57 (1)**, 29–35.

Trenberth, K. and D. Paolino, 1980: The northern hemisphere sea level pressure dataset: Trends, errors and discontinuities. *Mon. Wea. Rev.*, **108**, 856–872.

Trigo, R. and J. Palutikof, 2001: Precipitation scenarios for Iberia: a comparison between direct GCM output and different downscaling techniques. *J. Climate*, **14**, 4422–4446.

Trigo, R., D. Pozo-Vázquez, T. Osborn, Y. Castro-Diez, S. Gamiz-Fortis, and M. Esteban-Parra, 2004: North Atlantic Oscillation influence on precipitation,

river flow and water resources in the Iberian Peninsula. *Int. J. Climatol.*, **79**, 1–7.

Tuller, S. and C. Brett, 1984: The characteristics of wind velocity that favor the fitting of a Weibull distribution in wind speed analysis. *J. Clim. Appl. Meteorol.*, **23**, 124–134.

Uppala, S., P. Kallberg, A. Simmons, U. Andra, V. da Costa Bechtold, M. Fiorino, J. Gibson, J. Haseler, A. Hernandez, G. Kelly, X. Li, K. Onogi, S. Saarinen, N. Sokka, R. Allan, E. Andersson, K. Arpe, M. Balmaseda, A. Beljaars, L. van de Berg, J. Bidlot, N. Bormann, S. Caires, F. Chevallier, A. Dethof, M. Dragosavac, M. Fisher, M. Fuentes, S.Hagemann, E. H. E, B. Hoskins, L. Isaksen, P. Janssen, R.Jenne, A. McNally, J. Mahfouf, J. Morcrette, N. Rayner, R. Saunders, P. Simon, A. Sterl, K. Trenberth, A. U. A, D. Vasiljevic, P. Viterbo, and J. Woollen, 2005: The era-40 re-analysis. *Q. J. Roy. Meteor. Soc.*, **131**, 2961–3012.

van Lieshout, M., R. Kovats, M. Livermore, and P. Martens, 2004: Climate change and malaria: analysis of the SRES climate and socio-economic scenarios. *Global Environmental Change-Human and Policy Dimensions*, **14 (1)**, 87–99.

van Loon, H. and J. Rogers, 1978: The seesaw in winter temperatures between Greenland and Northern Europe. *Mon. Wea. Rev.*, **106**, 296–310.

von Storch, H., 1995: Inconsistencies at the interface of climate impact studies and global climate research. *Meteorol. Zeitschrift*, **4**, 71–80.

von Storch, H., E. Zorita, and U. Cubasch, 1993: Downscaling of global climate change estimates to regional scales: an application to Iberian rainfall in wintertime. *J. Climate*, **6**, 1161–1171.

von Storch, H. and F. Zwiers, 1999: *Statistical analysis in climate research*. Cambridge University Press.

Wagner, A., 1938: Theorie und Beobachtung der periodischen Gebirgswinde. *Gerl. Beitr. Geophys.*, **52**, 408–449.

Weisse, R. and F. Feser, 2003: Evaluation of a method to reduce uncertainty in wind hindcasts performed with regional atmosphere models. *Coast. Eng.*, **48**, 211–225.

Weisser, D., 2003: A wind energy analysis of grenada: an estimation using the Weibull density function. *Renew. Ener.*, **28**, 1803–1812.

Weisser, D. and T. Foxon, 2003: Implications of seasonal and diurnal variations of wind velocity for power output estimation of a turbine: a case study of grenada. *Int. J. Ener. Res.*, **27**, 1165–1179.

Wentink, J., 1974: Wind power potential of Alaska; part I. *Sci. Rep. Geophysical Institute, University of Alaska*, 238–507.

Wetterhall, F., A. BArdossy, D. Chen, and S. Halldin, 2009: Statistical downscaling of daily precipitation over Sweden using GCM output. *Theor. Appl. Climatol.*, **96**, 95–103.

Whiteman, C. and J. Doran, 1993: The relationship between overlying synoptic-scale flows and winds within a valley. *J. App. Meteorol.*, **32**, 1670–1680.

Wieringa, J., 1993: Representative roughness parameters for homogeneus terrain. *Boundary-Layer Meterolo.*, **63**, 323–363.

Wilby, R., 1998: Statistical downscaling of daily precipitation using daily airflow and seasonal teleconnection indices. *Cli. Res.*.

Wilby, R. L. and T. M. L. Wigley, 1997: Downscaling of general circulation model output: a review of methods and limitations. *Prog. Phys. Geograph.*, **21,4**, 530–548.

Wilby, R. L., T. M. L. Wigley, D. Conway, P. D. Jones, B. C. Hewitson, J. Main, and D. S. Wilks, 1998: Statistical downscaling of general circulation model output: a comparison of methods. *Water Resour. Res.*, **34**, 2995–3038.

Winterfeldt, J. and R. Weisse, 2009: Assessment of value added for surface marine wind speed obtained from two regional climate models (rcm). *Mon. Wea. Rev.*, **137(9)**, 29552965. Doi:10.1175/2009MWR2704.1.

Wood, A., L. Leung, V. Sridhar, and D. Lettenmaier, 2004: Hydrological implications of dynamical and statistical approaches to downscaling climate model outputs. *Clim. Change*, **62**, 189–216.

Wright, W., 2008: Observing the climate-challenges for the 21^{st} century. *WMO Bulletin*, **57(1)**, 29–34.

Wu, Z., E. Schneider, B. Kirtman, E. Sarachik, N. Huang, and C. Tucker, 2008: The modulated annual cycle: an alternative reference frame for climate anomalies. *Clim. Dyn.*, **31**, 823–841.

Xoplaki, E., J. González-Rouco, D. Gyalistras, J. Luterbacher, R. Rickli, and H. Wanner, 2003a: Interannual summer air temperature variability over Greece and its connection to the large-scale atmospheric circulation and Mediterranean SSTs 1950-1999. *Clim. Dyn.*, **20**, 537–554.

Xoplaki, E., J. González-Rouco, and J. Luterbacher, 2003b: Mediterranean summer air temperature variability and its connection to the large-scale atmospheric circulation and SSTs. *Clim. Dyn.*, **20**, 723–739.

Xoplaki, E., J. F. González-Rouco, J. Luterbacher, and H. Wanner, 2004: Wet season Mediterranean precipitation variability: influence of large-scale dynamics and predictability. *Clim. Dyn.*, **23**, 63–78.

Yarnal, B., 1993: *Synoptic climatology in environmental analysis*. Belhaven Press, 195 pp.

Yu, S., O. G. Clark, and J. Leonard, 2008: A statistical method for the analysis of nonlinear temperature time series from compost. *Bioresource Technology*, **99**, 1886–1895.

Zeineldin, H., T. E. Fouly, E. E. Saadany, and M. Salama, 2009: Impact of wind farm integration on electricity market prices. *IET Renew. Pow. Generat.*, **3(1)**, 84–95.

Zhang, D. and W. Zheng, 2004: Dyurnal cycles of surface winds and temperatures as simulated by five boundary layer parametrizations. *J. Appl. Meteor.*, **43**, 157–169.

Zhang, N., W. Jiang, and S. Miao, 2006: A large eddy simulation on the effect of buildings on urban flows. *Wind Struct.*, **9(1)**, 23–25.

Zhang, X., 2005: Spatial downscaling of global climate model output for site-specific assessment of crop production and soil erosion. *Agricultural and Forest Meteorology*, **135 (1-4)**, 215–229.

Zhou, M., Z. Zhang, S. Zhong, D. Lenschow, H. m. Hsu, B. Sun, Z. Gao, S. Li, X. Bian, and L. Yu, 2009: Observations of near-surface wind and temperature structures and their variations with topography and latitude in East Antarctica. *J. Geophys. Res.*, **114**, D17115, doi:10.1029/2008JD011611.

Ziegler, J., 2005: *L'Empire de la honte*. Santillana edition.

Zorita, E., K. Viacheslav, and H. von Storch, 1992: The atmospheric circulation and sea surface temperature in the North Atlantic area in winter: their interaction and relevance for Iberian precipitation. *J. Clim.*, **5**, 1097–1108.

Zorita, E. and H. von Storch, 1999: The analog method as a simple statistical downscaling technique: comparison with more complicated methods. *J. Clim.*, **12**, 2474–2489.

Glossary

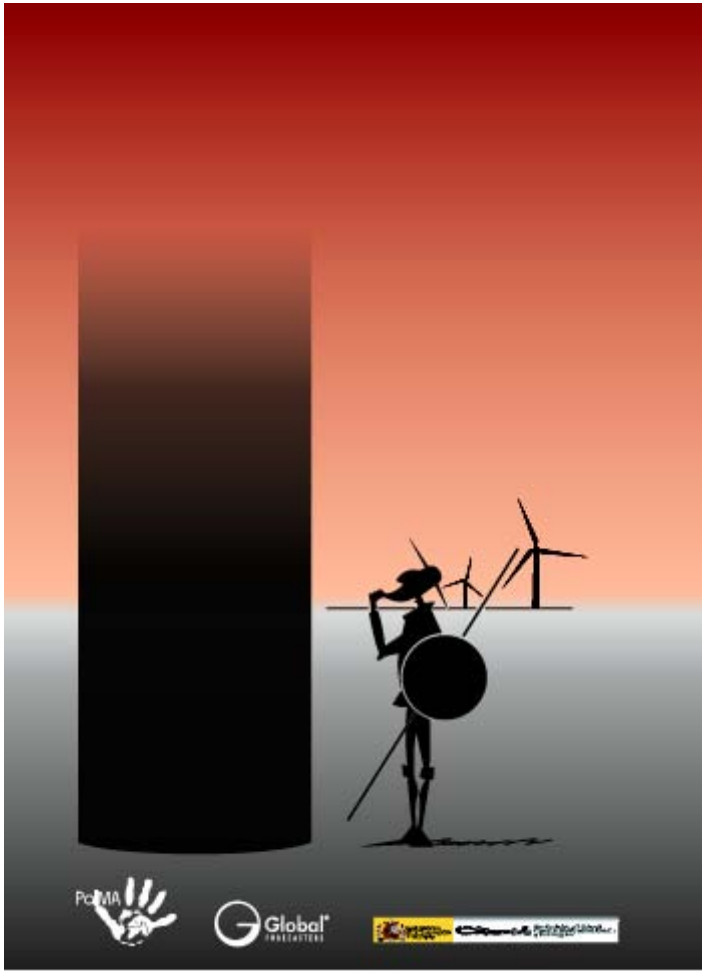
PoMA
Global